Investigating the Roles of Cell Identity Regulation and Eph/ephrin Signalling in Early Hindbrain Segmentation

Megan Elizabeth Addison

University College London
and
The Francis Crick Institute
PhD Supervisor: Dr. David Wilkinson

A thesis submitted for the degree of
Doctor of Philosophy
University College London
November 2016

Declaration

I, Megan Elizabeth Addison, confirm that the work presented in this thesis is my own. Where information has been derived from other sources, I confirm that this has been indicated in the thesis.

Abstract

During development of the vertebrate hindbrain, the neuroepithelium becomes subdivided into seven morphological units, known as rhombomeres. It is necessary that rhombomeres have sharp, well-defined boundaries, which are established from initially rough gene expression domains during early hindbrain segmentation. The mechanisms involved in early hindbrain segmentation that create sharp segment borders are not well understood. There is evidence to suggest that both regulation of cell identity and Eph/ephrin-mediated cell sorting are required for establishing sharp interfaces between rhombomeres.

This thesis investigates the extent to which identity regulation contributes to hindbrain border sharpening in zebrafish. I created a new zebrafish reporter line by CRISPR/Cas9-mediated reporter integration at the *egr2b* locus, which enables cell identity and cell intermingling to be visualised in live embryos during border sharpening. This new reporter line indicates a contribution of cell identity regulation to border sharpening. I also demonstrate that the contribution of cell identity switching to border refinement is greater in cases where cell intermingling is increased by perturbed Eph/ephrin signalling. To help study the role of Eph/ephrin signalling in border sharpening, I have also created a novel EphrinB3b mutant.

The thesis also investigates the mechanisms of identity regulation by community effects and discusses their contribution to border refinement by identity respecification; community effects are suspected to help overcome noise in early gene induction through spatial averaging and thus help establish regions of homogeneous gene expression. The ability of candidate genes to non cell-autonomously regulate the identity of neighbouring cells in the hindbrain is investigated. Of particular focus is the potential involvement of retinoic acid (a morphogen involved in specification of anteroposterior identity) and segmentally-expressed Cyp26 enzymes involved in its metabolism. Analysis of mosaic embryos is used to compare the ability of isolated cells and clustered groups of cells to maintain a different identity to their surroundings. Results presented here are consistent with segmental regulation of retinoic acid signalling contributing to border sharpening.

Acknowledgements

I would like to thank my supervisor, David Wilkinson, for the opportunity to carry out this PhD project in his laboratory, and for his invaluable help and guidance throughout the project. I am also grateful to past and present members of the Wilkinson laboratory for their teaching, advice, support and friendship. In particular, to Qiling, for teaching me so much about zebrafish and related techniques; Jordi for imparting his wealth of knowledge regarding the CRISPR/Cas9 system, and to Sean for help and advice with TALENs.

I would like to thank my thesis committee: Jean-Paul Vincent, Greg Elgar and Andy Oates for their feedback and advice. I am also indebted to the aquatics staff at Mill Hill for taking care of all my fish. Finally, I would like to thank my family and my friends for their support and encouragement throughout.

Table of Contents

Table of figures

List of tables

Abbreviations

4-OHT – 4-hydroxytamoxifen

ACR – α-crystallin promoter driving RFP

AP – anterior-posterior

BAC – bacterial artificial chromosome

CNE – conserved non-coding element

CRISPR- clustered regularly interspaced short palindromic repeats

DEAB – 4-(diethylamino)benzaldehyde

dpf – days post-fertilisation

DSB – double-stranded DNA break

DV – dorsal-ventral

ECM – extracellular matrix

ENU – N-ethyl-N-nitrosourea

FRET – Förster resonance energy transfer

GEPRA – genetically-encoded probe of retinoic acid

GFP – green fluorescent protein

hpf - hours post-fertilisation

HR – homologous recombination

HRM – high resolution melt curve analysis

IHC – immunohistochemistry

ISH – *in situ* hybridisation

MHB – midbrain-hindbrain boundary

MMEJ – microhomology-mediated end joining

MO – Morpholino oligonucleotide

NHEJ – non-homologous end joining

PAM – protospacer activator motif

r1-7 – rhombomere 1-7

RA – retinoic acid

RAR – retinoic acid receptor

RFP – red fluorescent protein

RFLP – restriction fragment length polymorphism

RVD – repeat variable di-residue

SNP – single nucleotide polymorphism

ss – somite stage

SSC – saline-sodium citrate

TALEN – transcription activator-like effector nuclease

TILLING – targeting induced local lesions in genomes

UAS – upstream activating sequence

UTR – untranslated region

WT – wildtype

ZFN – zinc finger nuclease

Chapter 1. Introduction

The main aim of my PhD has been to study the mechanisms involved in hindbrain border sharpening, making use of zebrafish as a model organism. In this chapter, I will introduce the background to my project, focusing primarily on hindbrain development in zebrafish. Some ideas discussed in this introduction have been previously published (Addison & Wilkinson, 2016).

1.1 Patterning and segmentation in development

Development of multi-cellular organisms involves the temporally and spatially regulated generation of many different functional cell types and structures. An evolutionarily-conserved strategy sometimes used to create distinct tissues and structures in the embryo involves the subdivision of an initially equivalent field of cells. This can create a series of repeating units in a process known as segmentation, and mediates the separation of cells with different molecular identities. These segments can subsequently develop independently and acquire distinct features and future functions. A key aspect of segmentation is the prevention of mixing of cells from adjacent segments; for example, between adjacent parasegments in *Drosophila* (Martinez-Arias & Lawrence, 1985), which maintains segments as coherent units with sharp and well-defined interfaces. At the boundaries of adjacent compartments, specialised cells can be created and function as secondary organising centres to help pattern the adjacent territories (Irvine & Rauskolb, 2001).

An important aspect of segmentation is the acquisition of different positional identity by different segments. This positional information can be conferred by a class of signalling molecules known as morphogens. The term “morphogen” was first used by Turing to describe diffusible biochemical substances that act in a concentration-dependent manner (Turing, 1952). Wolpert’s “French Flag” model of translation of gradients into spatial patterns of cell identity can provide a framework to understand how morphogens and their interpretation can provide spatial information (Wolpert, 1969). Morphogens are typically secreted signalling factors

that form concentration gradients by diffusion, and confer positional information to cells by specifying different cell fates in a concentration-dependent manner.

1.2 Studying segmentation in the vertebrate hindbrain

This thesis studies mechanisms involved in the early segmentation of the vertebrate hindbrain, which is an important model of segmentation in vertebrates. The hindbrain, or rhombencephalon, is the posterior region of the brain and has vital unconscious functions such as controlling blood circulation, breathing, and reflexes such as vomiting, coughing and sneezing. The hindbrain is also important for coordination of motor activity and organisation of head development. Because the segmentation of the vertebrate hindbrain into rhombomeres is highly conserved at morphological and molecular levels, studies in amenable model organisms can provide applicable insights into processes in other vertebrate species. Our current understanding of vertebrate hindbrain development has been achieved through studies in a variety of model organisms. The work described in this thesis utilises the advantages of zebrafish (*Danio rerio*) as a model organism, including its fast development, transparency and suitability for live imaging.

The initial step of development of the central nervous system (CNS) is the specification of the neuroectoderm. In zebrafish, neural induction occurs from the onset of gastrulation (6 hours post-fertilisation (hpf)), involving complex interactions between various signalling factors, including BMP, Wnt and Fgf signals (Wilson *et al*, 2001; Streit *et al*, 2000). Neural ectoderm specification also involves SoxB family transcription factors (Pevny & Placzek, 2005). Once the neuroectoderm has been specified, these cells form the neural plate, which is morphologically apparent from the tailbud stage (10 hpf) in zebrafish. From the 6-10 somite stages (ss) (12-14 hpf), the neural plate condenses, forming the neural keel. At 15 ss, the neural keel rounds to become the cylindrical neural rod, which subsequently forms the hollow neural tube via cavitation at 17 ss (16 hpf) (Papan & Campos-Ortega, 1994; Kimmel *et al*, 1995). This process of neurulation is illustrated in Figure 1-1.

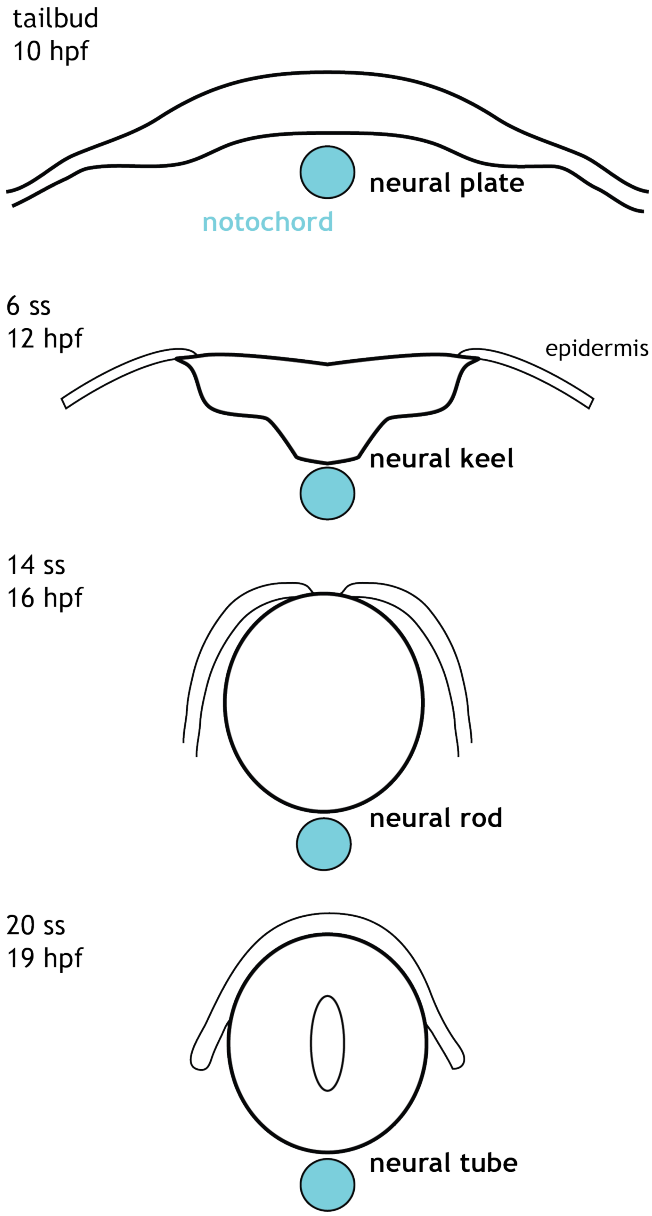

Figure 1-1 Neurulation in zebrafish

Diagrammatic transverse sections through the neuroepithelium. The neural plate undergoes morphogenesis to form the neural keel by infolding at the midline. The neural keel rounds up to form the neural rod, which then cavitates to form the hollow neural tube. Based on (Kimmel *et al*, 1995).

Cells of the neural plate initially have an anterior fate, which is subsequently transformed by posteriorising signals, including retinoic acid (RA) and Fgfs (Kudoh *et al*, 2002). The anterior region of the CNS consists of the forebrain, midbrain and hindbrain, while the posterior region of the neural tube forms the spinal cord.

During development of the vertebrate hindbrain, the neuroepithelium becomes transiently subdivided along the anteroposterior (AP) axis into seven distinct territories, known as rhombomeres, as shown in Figure 1-2. Rhombomeres are morphologically and molecularly distinct segments and become lineage-restricted once morphological boundaries have formed, as shown in chick and mouse (Fraser *et al*, 1990; Jimenez-Guri *et al*, 2010). The segmentation of the hindbrain is non-sequential, in contrast to some other vertebrate segmentation processes, such as somitogenesis, where adjacent segments arise sequentially and rhythmically (Pourquié, 2003).

The segmentation of the hindbrain into rhombomeres underlies several subsequent patterning events. The boundaries that form between rhombomeres are important for positioning and separating populations of neurons in the hindbrain (Cooke *et al*, 2005; Terriente *et al*, 2012). Interneurons and motor neurons are derived from specific rhombomeres, and have important roles in various processes including taste, hearing and balance. For example, in chick, the cell bodies of the trigeminal (V^{th}) nerve are initially found exclusively in r2, and later in r2 and r3, while the motor neurons of the facial (VII^{th}) nerve are initially found exclusively in r4, and later in r4 and r5 (Lumsden & Keynes, 1989), as shown in Figure 1-3.

In addition to neuronal organisation, the segmentation of the hindbrain into rhombomeres is also important for specification of cranial neural crest cells and establishment of their migratory pathways (Lumsden *et al*, 1991; Birgbauer *et al*, 1995; Trainor & Krumlauf, 2000a). Rhombomere-derived cranial neural crest cells have important roles in craniofacial development, and give rise to multiple cell types, including peripheral nerves and glia and connective tissue. As shown in Figure 1-3, streams of neural crest cells arise adjacent to r2, r4 and r6, and migrate into the first, second and third branchial arches, respectively. Neural crest cells derived from different rhombomeres maintain distinct identities from each other and if these are intermixed, they will form sharp borders, which highlights the importance of their rhombomeric origins for their identity (Köntges & Lumsden, 1996).

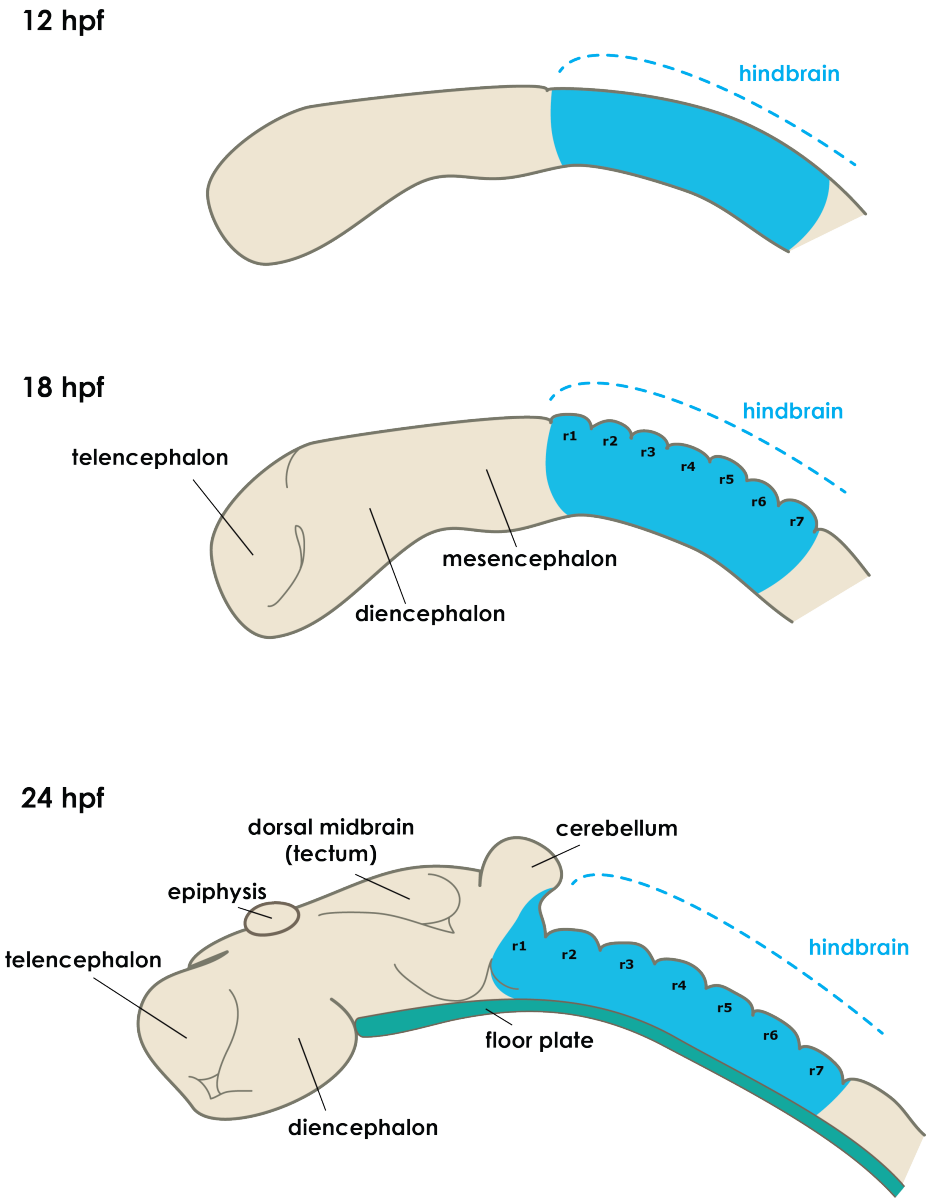

Figure 1-2 The zebrafish hindbrain

Cartoon depicting a lateral view of the zebrafish brain, with hindbrain highlighted (blue). At 12 hpf (6 ss) morphological subdivisions are not yet evident along the AP axis. By 18 and 24 hpf, the seven rhombomeres (r1-7) are morphologically distinct. Based on (Kimmel *et al*, 1995).

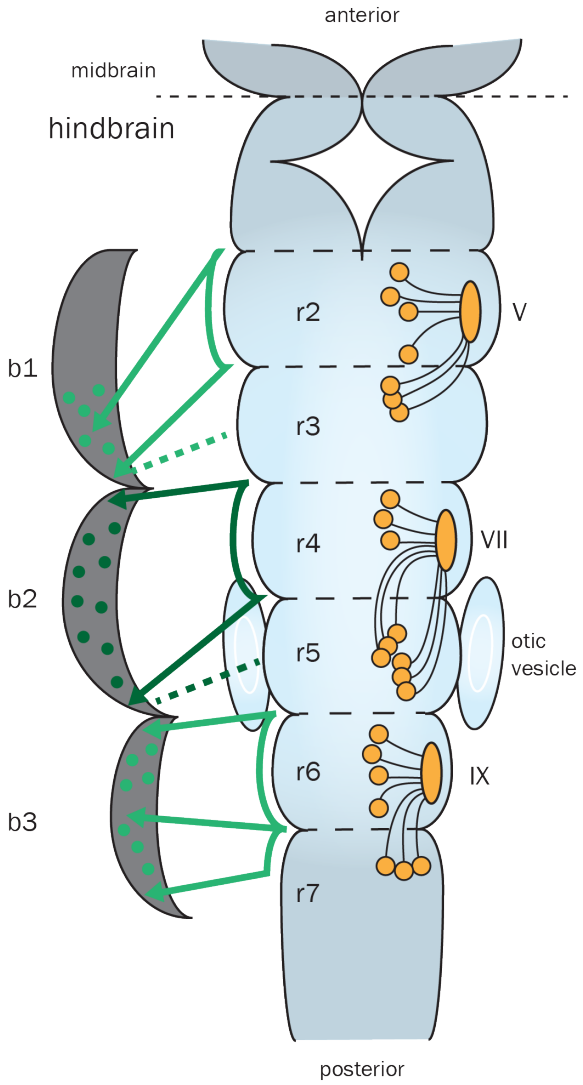

Figure 1-3 The segmentation of the hindbrain underlies subsequent patterning
Schematic representation of segmented hindbrain in chick, from a dorsal view. Rhombomere boundaries are shown as dashed lines between segments. Neural crest cells (green) are derived from specific rhombomeres and migrate into the adjacent branchial arches (b1 – b3). The rhombomeric origins of specific nerves (V, VII, IX) are shown in orange. Figure partially based on (Kiecker & Lumsden, 2005)

1.3 Specification of specialised boundary cells at rhombomere interfaces

Once rhombomeres are molecularly defined, inter-rhombomeric boundaries, which are visible as morphological constrictions, arise at borders (Guthrie & Lumsden,

1991). Throughout this thesis, the interfaces of gene expression domains in the hindbrain are referred to as borders, in contrast to the specialised boundary cells that are subsequently formed at these borders. Rhombomere boundary cells consist of a specialised population of progenitor cells, with distinct histology, gene expression and behaviour from cells within rhombomeres (Heyman *et al*, 1993, 1995). In chick, boundary cells have a larger, more elongated morphology, with enlarged intercellular spaces and proliferate slower than cells within rhombomere centres (Heyman *et al*, 1993; Lumsden & Keynes, 1989; Guthrie & Lumsden, 1991). In chick, boundary cells have reduced gap junction permeability compared to cells within rhombomeres (Martinez *et al*, 1992).

Several functions of these specialised boundary cells have been suggested. Boundaries between tissues can act as local signalling centres and provide positional information to the adjacent compartments. Several *wnt* genes are upregulated at rhombomere boundaries and can contribute to patterning the neighbouring rhombomeres (Riley *et al*, 2004). Signalling from rhombomere boundaries has been shown to contribute to patterning of neurogenesis, by regulating the clustering of Fgf20 neurons at rhombomere centres (Terriente *et al*, 2012), which induce formation of a non-neurogenic zone of neural progenitors in the mantle region at the centre of rhombomeres (Gonzalez-Quevedo *et al*, 2011).

Boundary cells do not appear to directly prevent cell mixing between rhombomeres: several different methods of removing rhombomere boundaries do not appear to affect cell intermingling between rhombomeres, either by surgical ablation of boundaries (Guthrie & Lumsden, 1991) or by prevention of boundary cell specification by RA treatment (Nittenberg *et al*, 1997). Because boundary cells divide slower than non-boundary cells, they may however reduce the potential for cell intermingling between rhombomeres, as cell divisions have been shown to constitute a significant challenge to border sharpness (Calzolari *et al*, 2014).

1.4 Patterning anteroposterior identity in the vertebrate hindbrain

The segmented architecture of the hindbrain along the anteroposterior (AP) axis is established by differential expression of transcription factors that underlie segmentation and/or confer segmental identity, as shown in Figure 1-4.

1.4.1 Segmental gene expression in the hindbrain

Important factors that confer AP identity to segments of the hindbrain are members of the homeobox (Hox) family of transcription factors. *Hox* genes constitute a large family of related genes that encode helix-turn-helix transcription factors, and contribute to specification of AP identity in all animal species along with their Pbx/Meis co-factors. Within the genome, *hox* genes are organised into clusters, in which all genes are transcribed in the same orientation and display co-linearity of their expression pattern and chromosomal arrangement, whereby genes located more 3' within clusters tend to be expressed more anteriorly and earlier than those at the 5' regions of clusters. In the hindbrain, the borders of *hox* expression domains correspond to rhombomere borders (Wilkinson *et al*, 1989b; Hunt *et al*, 1991), and *hox* genes have overlapping and nested expression domains (Tümpel *et al*, 2009). The expression patterns of hox genes in the hindbrain mean that each rhombomere expresses a unique combination of *hox* genes, which determine segmental identity via a combinatorial "*hox* code". In the absence of Hox/Pbx activity, the entire hindbrain undergoes a transformation to an r1-like identity, highlighting the importance of Hox factors for segmental identity (Waskiewicz *et al*, 2002).

The importance of individual Hox factors in specifying segmental identity is illustrated by the consequences of their loss- or gain-of function for rhombomere identity, which has been particularly well-studied in mouse models. In Hoxa1 mutant mice (which is functionally equivalent to zebrafish Hoxb1b), r5 is absent, and r4 and r6 become fused together (Carpenter, 1993; Mark 1993). Hoxb1 mutant mice (functionally equivalent to zebrafish Hoxb1a) fail to maintain an r4 identity,

instead becoming r2-like (Studer *et al*, 1996). Together, Hoxa1 and Hoxb1 function to establish and maintain r4 identity, and in their absence, r4 markers are absent from its AP position (Studer *et al*, 1998). Similar consequences for loss of Hoxb1a and Hoxb1b have been reported in zebrafish (McClintock *et al*, 2001, 2002). Consistent with the roles of these factors in regulating r4 identity, ectopic expression of Hoxa1 or Hoxb1 in mouse and chick causes r2 to transform to an r4-like character (Zhang *et al*, 1994; Bell *et al*, 1999). Additionally, Hoxa2, which is expressed in r2 and r3, is required for maintenance of the identity of these rhombomeres; in Hoxa2 mouse mutants, motor axon guidance is altered in these rhombomeres, while r2 is reduced in size and there is a corresponding expansion of r1 (Gavalas *et al*, 1997). There are multiple cross-regulatory interactions between *hox* factors that contribute to regulation of segmental identity by Hox factors. For example, in mouse and zebrafish, Hoxa1 (Hoxb1b) upregulates Hoxb1 (Hoxb1a) in r4 (Barrow *et al*, 2000; McClintock *et al*, 2002). Hoxa2 and Hoxb2 are also directly regulated in r4 by Hoxb1 and, in turn, reinforce expression of Hoxb1 here (Gavalas *et al*, 2003; Studer *et al*, 1998; Tümpel *et al*, 2007).

In addition to Hox factors, other transcription factors also have segment-restricted expression in the hindbrain and are important for the correct segmentation of specific rhombomeres. The first identified of these was Egr2 (formerly known as Krox20 and referred to as Egr2b in zebrafish) (Wilkinson *et al*, 1989a). Egr2 is a zinc finger transcription factor that is expressed in and required for the segmentation of r3 and r5. Egr2 also upregulates expression of several *hox* genes, including *hoxa2* (Nonchev *et al*, 1996b) and *hoxb2* (Sham *et al*, 1993) in r3 and r5, and *hoxb3* in r5 (Seitanidou *et al*, 1997). In mice that lack functional Egr2, r3 and r5 are specified as normal, but not maintained, causing a complete loss of these territories by later stages; in the absence of Egr2, r3 becomes like r2/r4, while r5 becomes r6-like (Schneider-Maunoury *et al*, 1997, 1993; Swiatek & Gridley, 1993; Voiculescu *et al*, 2001). In line with its role in segmentation of r3 and r5, ectopic overexpression of Egr2 in chick can confer odd-numbered rhombomere identity to other segments of the hindbrain (Giudicelli *et al*, 2001).

Another transcription factor required for the segmentation of specific rhombomeres is vHnf1 (variant hepatocyte nuclear factor 1), which is expressed in and required

for the segmentation of r5 and r6 (Aragón *et al*, 2005). In zebrafish, vHnf1 synergises with Fgfs to activate expression of *valentino* (known as *MafB/Kreisler* in other species) in r5 and r6 and expression of *egr2b* in r5, while also repressing expression of *hoxb1a* in r5 (Wiellette & Sive, 2003). Consistently, in chick, loss of vHnf1 causes a posterior expansion of *hoxb1* expression from r4, reduced expression of *Egr2* r5 and loss of *MafB* expression in r5 and r6. Ectopic expression of vHnf1 causes an anterior expansion of *MafB* expression into r4 (Aragón *et al*, 2005). In zebrafish, Valentino also contributes to correct segmentation, in part through upregulation of *egr2b* in r5 (Moens *et al*, 1996; Wiellette & Sive, 2003).

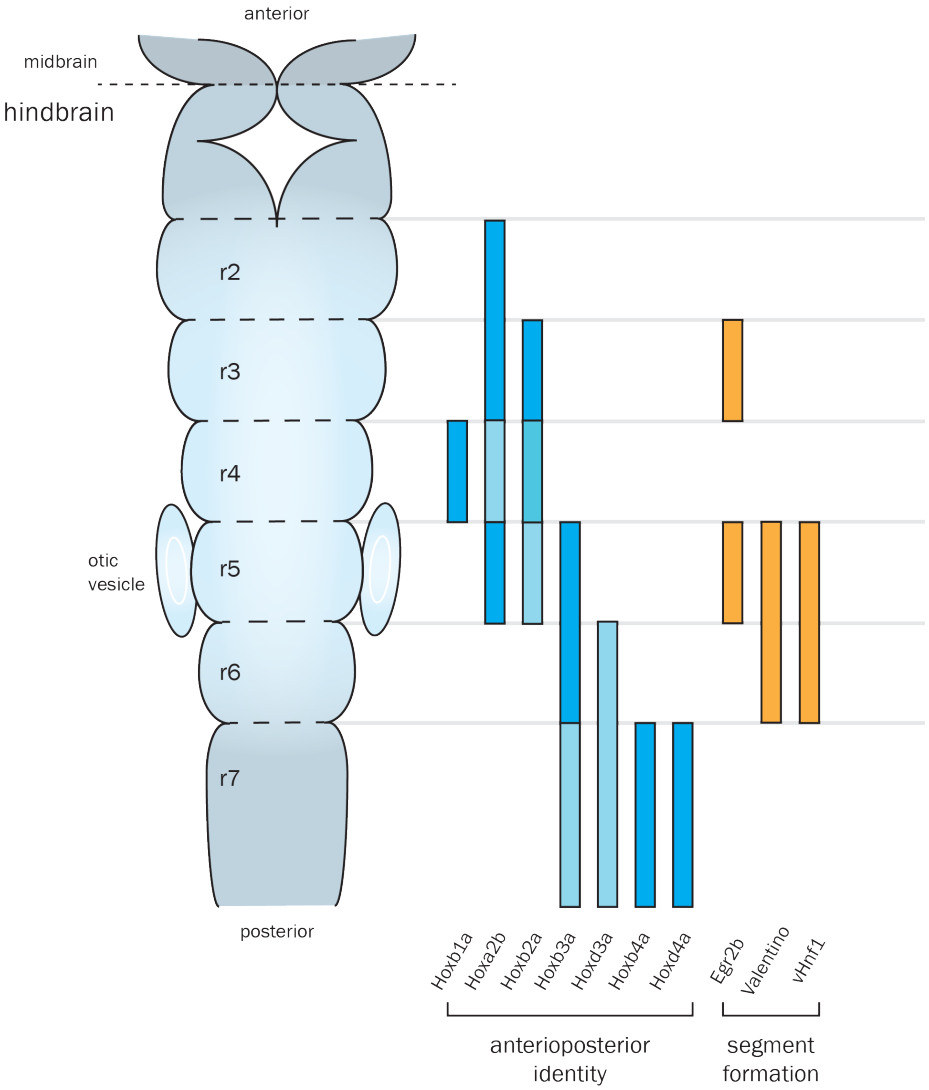

Figure 1-4 Segmented expression patterns of Hox factors and transcription factors required for segment formation

A depiction of the zebrafish hindbrain from a dorsal view. The segmentally-restricted expression patterns of various Hox factors (blue) and transcription factors required for segmentation (orange) are shown. Expression patterns based on (Prince *et al*, 1998) and (Moens & Prince, 2002)

1.4.2 Retinoic acid and AP identity

Several posteriorising factors contribute to the induction and regulation of genes that confer segmental identity to the hindbrain. One important posteriorising factor involved in hindbrain patterning is retinoic acid (RA), a vitamin A-derived non-

peptidic, lipophilic molecule that functions as a ligand for nuclear RA receptors (RARs). RA is synthesised in the paraxial mesoderm posterior to the hindbrain and specifies the identity of hindbrain segments posterior to the r3/4 border, where domains of *hox* expression are patterned by differential responses to varied levels of RA along the anteroposterior axis.

Several different *hox* genes are known to contain RA-responsive elements (RAREs) in their regulatory regions. RA can induce the expression of these *hox* genes directly by activating RAR/RXR heterodimers at RAREs. Accordingly, increased RA signalling during hindbrain patterning causes expansion of posterior hindbrain at the expense of anterior territories, while reducing RA availability or blocking RA signalling causes anterior segments to become expanded into more posterior regions (Gale *et al*, 1996a; Begemann *et al*, 2001, 2004; Linville *et al*, 2004; Niederreither *et al*, 2000; Strate *et al*, 2009). For example, in mouse, Hoxb1 is directly regulated by RA (Marshall *et al*, 1994; Studer *et al*, 1998), while Hoxa4, Hoxb4 and Hoxd4 also require RARE activity for their expression (Packer *et al*, 1998; Gould *et al*, 1998; Zhang *et al*, 2000). The expression of other posterior RA-responsive *hox* genes, including hox-PG3 genes, is regulated indirectly by RA; in zebrafish, for example, *hoxa3* expression in rhombomeres 5 and 6 is regulated by Valentino, which is itself regulated in part by RA-mediated induction of *vhnf1* (Manzanares *et al*, 1999; Hernandez *et al*, 2004; Pouilhe *et al*, 2007).

1.4.3 RA as a morphogen in the hindbrain and regulation of RA signalling

There has been some controversy over whether RA does strictly function as a classic morphogen during hindbrain patterning. This would require that RA forms a concentration gradient and activates expression of different target genes in a concentration-dependent manner. There is evidence to suggest that RA does not necessarily form a simple, static, linear gradient and that regulation of genes by RA is not purely concentration-dependent.

The mechanisms by which the levels of RA activity required for hindbrain patterning are regulated are not completely understood. During hindbrain segmentation, the

RA gradient is shaped through a combination of localised synthesis and degradation. Because RA is small and lipophilic, it is able to diffuse across cell membranes and between cells. Since RA is also soluble in water at physiological concentrations, it can form concentration gradients within the extracellular space. RA can bind intracellular RA-binding proteins, such as a CRABPs (cellular RA binding proteins), which facilitate its delivery to the nucleus. RA is synthesised posterior to the hindbrain in the paraxial mesoderm, where retinaldehyde dehydrogenase 2 (Raldh2) catalyses the final step in RA synthesis from its precursor, Vitamin A. RA can be locally degraded into polar metabolites by the action of Cyp26 cytochrome p450 enzymes, and these polar metabolites are then rapidly excreted, removing RA from cells. Of these enzymes, Cyp26a1 has an important role in the early shaping of the RA gradient across the hindbrain; Cyp26a1 is expressed in the future forebrain/midbrain, where localised degradation of RA is thought to result in a posterior-to-anterior gradient of RA, in addition to being expressed in a shallow gradient throughout the hindbrain (White *et al*, 2007). In addition, RA directly upregulates expression of *cyp26a1*; this self-enhanced receptor-mediated degradation allows RA-induced patterning to be robust despite fluctuations in RA levels, which can result from dietary fluctuations in the RA precursor, vitamin A.

Additional Cyp26 enzymes – Cyp26b1 and Cyp26c1 – also influence the concentration of RA across the hindbrain. Cyp26b1 and Cyp26c1 are segmentally and dynamically expressed during hindbrain segmentation and affect RA responsiveness within the hindbrain through localised RA degradation (White & Schilling, 2008). Exogenous RA applied over a 20-fold range of concentrations and at a variety of developmental stages is sufficient to correctly pattern the hindbrain of embryos that are depleted of endogenous RA (Dupé & Lumsden, 2001; Maves & Kimmel, 2005). Cyp26 enzymes have been shown to be required for this rescue, highlighting their importance in shaping the RA gradient to correctly pattern the hindbrain (Hernandez *et al*, 2007). In the absence of Cyp26 enzymes, the anteroposterior patterning of the hindbrain is disrupted, causing phenotypes comparable to exposure to exogenous RA, (Hernandez *et al*, 2007).
Given the segmentally-restricted expression of Cyp26b1 and Cyp26c1 during hindbrain patterning, it might be expected that rather than being a smooth, linear

gradient, RA forms a step-wise gradient across the hindbrain, due to localised degradation.

Due to various technical difficulties, it is challenging to visualise and measure levels of RA across the hindbrain. RA has a low abundance in cells and has wide absorption and emission spectra, making it difficult to detect using traditional microscopy methods. In mouse, use of a RARE-lacZ reporter has indicated distinct boundaries of RA responsiveness, which move during hindbrain segmentation (Rossant *et al*, 1991; Sirbu *et al*, 2005). However, a RARE-eYFP transgenic zebrafish line has revealed a smoother gradient of RA responsiveness, though only at later stages of hindbrain segmentation, and no more anterior than r7 due to poor sensitivity to RA (Perz-Edwards *et al*, 2001). A smooth gradient of RA in the zebrafish hindbrain has however been observed by visualisation of unbound intracellular RA using FRET-based genetically-encoded probes of RA (GEPRAs) (Shimozono *et al*, 2013). These detect RA through an RA-binding domain fused to a pair of FRET donors and acceptors; binding of RA causes a conformational change within the fusion protein, which alters the level of FRET, thus enabling visualisation of free RA, as bound by the probe. More recently, measurements of endogenous RA in the zebrafish hindbrain have been made using fluorescence lifetime imaging microscopy (FLIM), exploiting the unique fluorescence lifetime of RA, in combination with phasor plot-based analysis. This technique has also indicated a smooth gradient of RA across the hindbrain (Sosnik *et al*, 2016). However, in this study the RA gradient was not measured during the stages when Cyp26b1 and Cyp26c1 are segmentally-expressed in the hindbrain, so the shape of the RA gradient at these stages is still unclear.

Morphogens have been found to regulate different target genes in a duration- and concentration-dependent manner (Dessaud *et al*, 2007, 2010). In the hindbrain, it appears that a combination of the level, timing and duration of exposure to RA is important in determining cellular responses. Use of RAR antagonists has shown that more posterior RA-responsive *hox* genes require higher levels of RA for their induction and are expressed later than more anterior RA-responsive *hox* genes, which are induced at lower levels of RA (Dupé & Lumsden, 2001; Maves & Kimmel, 2005). However, the spatial patterning of *hox* gene expression along the AP axis by

RA is not purely achieved by differential sensitivities of RAREs to RA, as different *hox* RAREs have been found to have comparable sensitivities to RA (Nolte *et al*, 2003). It is possible that the duration of RA exposure also influences *hox* expression. However, while induction of *hox* genes by RA occurs sequentially, more posterior *hox* genes do not require longer exposures to RA for their induction (Maves & Kimmel, 2005; Hernandez *et al*, 2007). Several models for how differential exposure to RA patterns the hindbrain, which are not mutually-exclusive, have been proposed. As shown in Figure 1-5A, one explanation for these observations is that over time, the RA gradient increases, and sufficient levels of RA signalling are only reached in posterior territories at later stages (Maves & Kimmel, 2005). An alternative model has been proposed, focusing on the importance of localised degradation of RA by Cyp26b1 and Cyp26c1. In this model, shifting boundaries of RA, created by localised and dynamic Cyp26 expression, permit step-wise specification of increasingly posterior segments, by regulating the time at which particular regions are exposed to RA (Sirbu *et al*, 2005) (Figure 1-5 B). In this "gradient free" model, the time at which cells are exposed to RA is more important for patterning than the level of RA exposure. Alternatively, it has been suggested that due to the importance of feedback in RA signalling mediated by Cyp26a1, that modulation of RA signalling and feedback via Cyp26a1 and the resulting gradient is sufficient to explain RA-induced hindbrain patterning (Figure 1-5 C) (White *et al*, 2007; Schilling *et al*, 2012, 2016).

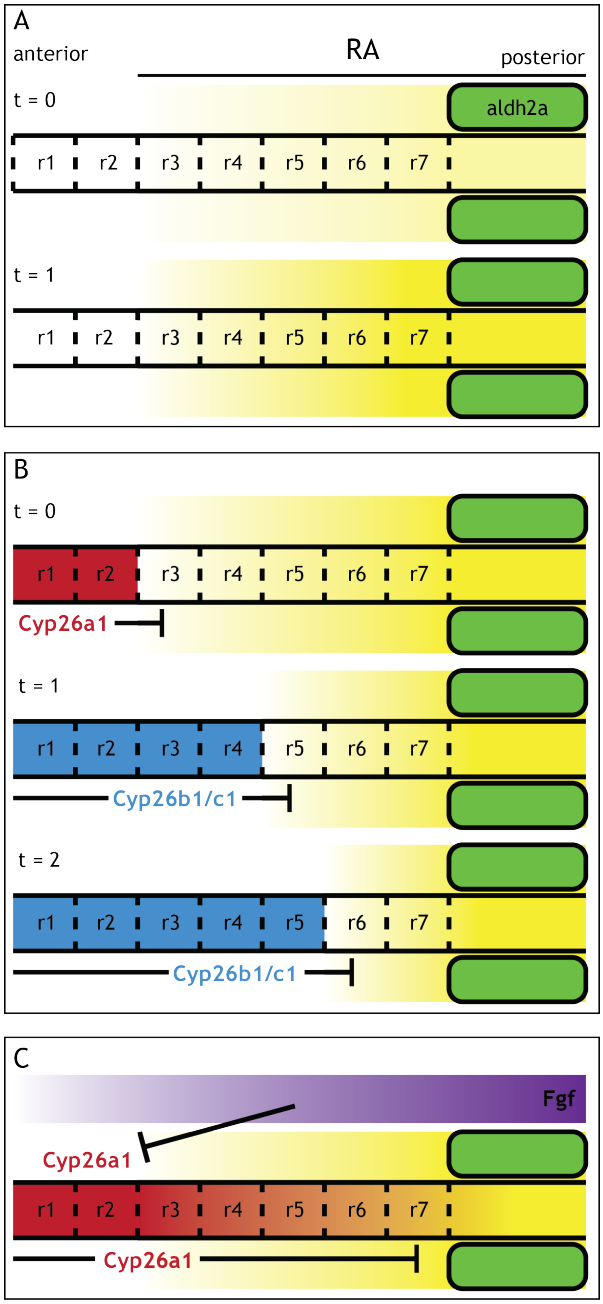

Figure 1-5 Proposed models of regulation of RA signalling and specification of AP identity

The hindbrain (r1-r7) is depicted with pre-segmented borders between adjacent prospective rhombomeres. RA (depicted via a yellow gradient) is produced posterior to the hindbrain in a paraxial mesoderm (green) by Aldh2a.

A: The “increasing gradient” model of RA signalling suggests that over time, the magnitude of the RA gradient increases; this causes more posterior regions, which require higher levels of RA for their induction, to receive appropriate levels of RA for their induction at later stages than more anterior segments. Based on Maves & Kimmel, 2005.

B: The “shifting boundaries” model of RA-induced patterning involves degradation of RA over time, mediated by Cyp26 enzymes (blue). This localised degradation controls the time at which different regions are exposed to RA. Based on Sirbu *et al*, 2005.
C: Integrated inputs of RA and Fgf signalling to Cyp26a1 regulation (red) shapes the resulting RA gradient. RA induces expression of Cyp26a1, whilst Fgfs (purple) inhibit Cyp26a1. Based on White *et al*, 2007 and Schilling *et al*, 2012.

1.4.4 Other morphogens and regulation of AP identity in the hindbrain

During early hindbrain segmentation, posteriorising Fgf and Wnt signals suppress the expression of anterior genes, including *cyp26a1*, in the future posterior hindbrain, in a RA-independent manner. In combination with RA, Fgfs and Wnts also initiate the expression of certain posterior genes, including *hoxb1b* (posteriorly from pre-r4) and *vhnf1*, (in pre-r5/r6) (Kudoh *et al*, 2002). Fgfs also regulate the expression of *cyp26a1*, by inhibiting RA-mediated *cyp26a1* upregulation (White *et al*, 2007). This enables Fgfs to influence the RA gradient within the hindbrain, which has been suggested to help couple growth of the hindbrain with a corresponding expansion of the RA gradient (White *et al*, 2007; Schilling *et al*, 2012) (Figure 1-5(C). Later in segmentation, following induction of segmental gene expression, an Fgf signalling centre is established in r4 (Maves *et al*, 2002). Fgf3 and Fgf8 are induced by Hox-PG1 factors and contribute to patterning the adjacent rhombomeres (Waskiewicz *et al*, 2002; Wiellette & Sive, 2003; Hernandez *et al*, 2004). For example, Fgf signals from r4 cooperate with vHnf1 and RA to drive initiation of *valentino* (*Maf-B/Kreisler*) in r5 and r6 (Hernandez *et al*, 2004), while Fgf8 also contributes to induction of *egr2b* expression in r3. Reduced expression of *fgf3* and *fgf8* causes alterations in gene expression, including loss of hoxa2 expression in r2-r5 and loss of *valentino* and *egr2b* expression in r5.

1.5 Challenges to border sharpness in the developing hindbrain

It is necessary that rhombomeres have a homogeneous identity in order that the derived cell types are correctly specified and patterned. It is therefore important that sharp interfaces between rhombomeres are established and maintained.

However, the expression domains of genes specified in the hindbrain are initially jagged, and subsequently sharpen (Oxtoby & Jowett, 1993; Irving *et al*, 1996; Cooke & Moens, 2002). Two features of hindbrain segmentation are thought to contribute to the initial roughness of gene expression borders: firstly, intrinsic noise and imprecision in the interpretation of morphogen gradients that specify cell identity, and secondly, the intermingling of cells within the hindbrain during early segmentation, driven by cell movement and division.

1.5.1 Intermingling and cell divisions within the hindbrain challenge border sharpness

Morphogenesis and tissue growth that occurs during hindbrain segmentation causes the potential for intermingling of cells between adjacent segments. Lineage analysis in chick shows that the progeny of cells labelled prior to border sharpening can be extensively dispersed among unlabelled cells and across prospective borders, sometimes almost across the entire length of a segment (Fraser *et al*, 1990). Convergent extension cell movements and cell intercalation occur during early hindbrain patterning, and during these movements cells may move between adjacent segments. Intermingling of cells between rhombomeres is also caused by the cell divisions which, at gastrulation and early segmentation stages, are oriented along the AP axis, and can cause dispersal of progeny along this axis and potentially between prospective rhombomeres (Kimmel *et al*, 1994). At later stages, cell divisions become progressively oriented, so the progeny are bilaterally distributed on each side of the neural tube, with less cell intermingling (Kimmel *et al*, 1994). However, it has been recently demonstrated by monitoring border sharpening in live transgenic zebrafish that cell divisions at prospective borders do constitute a significant challenge to border sharpness (Calzolari *et al*, 2014). Evidence indicating that cells do intermingle between rhombomeres has also come from cell lineage analysis in chick. Here, it has been demonstrated that prior to the formation of morphological boundaries, the progeny of cells from one presumptive rhombomere are able to contribute to adjacent segments, and that intermingling and dispersal of clonally-related cells can occur (Fraser *et al*, 1990). In contrast,

once distinct boundaries are established between rhombomeres, cell lineage is restricted to specific rhombomeres (Fraser *et al*, 1990).

1.5.2 Noise in generation and interpretation of the RA gradient

An additional challenge to border sharpness in the hindbrain is thought to arise from the intrinsic limitations of precision of the morphogens that initially pattern the hindbrain. In order for these signals to specify multiple discrete domains of gene expression, cells must be sufficiently sensitive, and significant changes in gene expression are required in response to subtle differences in signal strength. This is particularly a challenge in regions further from the signal source, where gradients are shallower and more susceptible to stochastic fluctuations. The intrinsic stochasticity of various biochemical processes can impose challenges on morphogen-induced patterning. Noise in morphogen-derived patterning can arise at multiple levels, including signal synthesis and transport, as well as in the response to the signal through availability of receptors and variation in downstream target gene expression. There is also the potential for noise to arise in feedback regulation downstream of signalling (Kepler & Elston, 2001; Elowitz *et al*, 2002; Kaern *et al*, 2005).

Due to the aforementioned technical difficulties in measuring RA levels in the hindbrain, the extent of noise in RA levels during hindbrain patterning has been difficult to determine. However, recent measurements of RA fluctuations in the zebrafish hindbrain during patterning, using Phasor-FLIM, have shown that there is substantial noise in RA levels across the hindbrain during early patterning (Sosnik *et al*, 2016). Crucially, these results demonstrated that fluctuations in RA levels occur at a frequency consistent with having an impact on downstream target gene expression, rather than occurring quick enough to be averaged out, without consequences for target gene transcription. In support of this, during early hindbrain segmentation, prior to border sharpening, some cells at segment borders transiently co-express factors that confer opposing identities and thus have an intermediate identity (Zhang *et al*, 2012). Cells' interpretations of morphogen levels

may also be challenged by the movement and intermingling of cells during specification, affecting their perception of RA along the AP axis.

Despite the noise in inductive signals and the movement of cells within the hindbrain, exquisitely sharp borders of gene expression are still formed and maintained. Two main mechanisms, which may operate in concert, have been proposed to contribute to sharpening of gene expression borders in the hindbrain: the regulation of identity of cells that find themselves on the wrong side of a prospective boundary, and the rhombomere-specific sorting of cells by their distinct surface properties, enabling cells of different identities to become segregated from one another. The extent to which these mechanisms are involved in sharpening of borders during early hindbrain segmentation remains unclear.

1.6 Mechanisms of sharpening: regulation of cell identity

One way in which sharpening of rhombomere borders may be achieved is by regulation of the identity of cells at rhombomere borders and ectopic cells within rhombomeres, as shown in Figure 1-6 (1,2).

1.6.1 Gene regulatory networks enable establishment of mutually-exclusive segment identity

In part, due to the previously mentioned noise in signals that specify rhombomere identity, during early segmentation some cells of the hindbrain co-express conflicting factors and thus have an intermediate identity. In zebrafish, cells at the interfaces between rhombomeres 3 and 4 and rhombomeres 4 and 5 can express both *egr2b* and *hoxb1a*, which confer opposing identities. Downstream of gene induction by RA and other morphogens, there are various genetic interactions between factors involved in identity specification that can help resolve overlapping identities, and which have been suggested to contribute to border sharpening (Zhang *et al*, 2012).

There are several instances of segmentally-expressed transcription factors autoregulating their own expression in the hindbrain, which can transform a transient input in gene expression into a cell fate commitment. For example, Egr2 is known to drive its own expression though an autoregulatory loop that is necessary for amplification and maintenance of *egr2* expression in rhombomeres 3 and 5 (Giudicelli *et al*, 2001; Chomette *et al*, 2006; Bouchoucha *et al*, 2013). In r4, Hoxb1a (or Hoxb1 in mouse) also regulates its own expression (Pöpperl *et al*, 1995; McClintock *et al*, 2001), while autoregulation of Hoxa3 and Hoxb3 reinforces their expression downstream of their transient activation by Valentino (Manzanares, 2001). Cross-inhibitory interactions between conflicting transcription factors are also critical for resolving uncertainty of identity at a single cell level. For example, Egr2 and Hoxb1 are able to mutually repress each other. In chick, ectopic overexpression of Egr2 in rhombomere 4 has been shown to cause downregulation of *Hoxb1* expression (Giudicelli *et al*, 2001), while in zebrafish, Hoxb1a represses *egr2b* expression indirectly via activation of Nlz factors (Labalette *et al*, 2015).

One case where it has been suggested that mutual inhibition and auto-activation of conflicting factors can contribute to sharpening is between Egr2b and Hoxb1a at the r3/4 and r4/5 borders. As discussed, Egr2b and Hoxb1a both autoactivate their own expression and mutually repress each other, which creates a bistable switch, whereby only each discrete identity is a favourable state. This enables cells to commit to a single particular fate, generating sharp spatial transitions in identity despite shallow morphogen gradients (Zhang *et al*, 2012; Bouchoucha *et al*, 2013). Computational modelling has demonstrated that such a bistable switch, in combination with noise in the RA gradient, can contribute to border sharpening in the hindbrain by driving the refinement of gene expression domains via noise-induced switching of cell identity (Zhang *et al*, 2012; Schilling *et al*, 2012). Noise-induced switching of identity has been suggested to enable cells to resolve their identity to better reflect their actual AP position and thus sharpen borders (Zhang *et al*, 2012). *In vivo* quantification of actual levels of both spatial and temporal noise in RA during hindbrain patterning has indicated that the level of noise in RA is consistent with this model of noise-induced switching and border sharpening (Sosnik *et al*, 2016).

Modulation of RA noise also contributes to border sharpening, presumably via resolution of overlapping cell identities. Increasing or decreasing the expression of the RA binding protein, Crabp2a, increases noise in RA, as directly measured *in vivo* (Sosnik *et al*, 2016). Consequently, these perturbations also cause increased noise and reduced sharpness of early *egr2b* expression (Sosnik *et al*, 2016). Altered expression of the RA-degrading enzyme, Cyp26a1, also increased variation in and reduced sharpness of *egr2b* expression, though this didn't have a noticeable impact on levels of noise in RA itself.

1.6.2 Plasticity of cell fate in the hindbrain

In addition to resolving dual identities, which may contribute to border sharpening, evidence suggests that cells of the hindbrain are also capable of completely switching their fate from one identity to another, evidently overcoming any autoregulatory feedback mechanisms that may be in place. This may contribute to border sharpening as illustrated in Figure 1-6 (3B). Some evidence that cells of the hindbrain are capable of switching their identity has come from cell transplantation studies. In mouse embryos, transpositions of small numbers of rhombomere cells and neural crest cells along the AP axis have demonstrated plasticity in *hox* expression at stages when border sharpening occurs (Trainor & Krumlauf, 2000b). In zebrafish, it has also been demonstrated that cells within the hindbrain are capable of altering their *hox* expression status following transplantation between rhombomeres during early segmentation (Schilling *et al*, 2001; Kemp *et al*, 2009). Transplantations at later stages have shown that cells progressively lose this plasticity, with increasing percentages of cells' identities becoming irreversibly committed. This suggests that there is a temporal window in which cells remain capable of assessing their environment and adapting their identity accordingly, before becoming committed to a particular identity. Once cells' fates are committed, there is no significant intermingling of cells between rhombomeres.

The mechanisms by which cells can detect and respond to their new AP position following transplantation are not clear. There are two possible mechanisms by which this may be achieved. Firstly, transplanted cells may detect and respond to

new levels of global signals (such as morphogen concentration) that specify cell identity; supporting this, cells transplanted from anterior to more posterior regions of the hindbrain exhibit increased plasticity compared to reciprocal transplantations (Grapin-Botton *et al*, 1995; Itasaki *et al*, 1996; Schilling *et al*, 2001). This suggests that posteriorising signals, such as RA, have roles in maintaining *hox* expression status and contribute to identity switching. Alternatively, transplanted cells may receive local signals from cells in their immediate vicinity that induce the transplanted cells to change their identity. In support of the second mechanism, larger coherent groups of 10 – 30 transplanted cells are also able to maintain their original *hox* expression status, independently of their altered position along the AP axis (Trainor & Krumlauf, 2000b; Schilling *et al*, 2001). Cells within the centre of these groups always maintained their original identity, while cells within 2 diameters from the edge of the group still exhibited some plasticity of hox expression (Schilling *et al*, 2001). This observation suggests that mutually-inductive interactions within these groups of cells enable them to maintain their gene expression status independently of their global environment and that there is a non cell-autonomous mechanism involved in regulation of cell identity during segmentation, which is capable of functioning over several cell diameters. These two different mechanisms are not mutually exclusive.

Evidence for cell identity switching from transplantation experiments does not indicate whether cells switch identity to establish sharp borders in normal hindbrain development. In chick, prior to boundary formation, clones of cells can spread across borders and contribute to adjacent rhombomeres (Fraser *et al*, 1990). This indicates that intermingling and switching of cell identity can occur early in hindbrain segmentation, though the extent to which this occurs is not known. Use of Cre-mediated recombination in mouse to permanently label cells of the hindbrain that have expressed *Egr2* has indicated presence of some labelled cells in even-numbered rhombomeres, where *Egr2* is not ultimately expressed (Voiculescu *et al*, 2001). Again, this is consistent with cells dynamically expressing *Egr2*, and suggests that switching of cell identity can occur *in vivo*, although the extent to which this occurs is still not clear. In zebrafish, stable reporters of cell identity that remain fluorescent beyond the timescale of border sharpening have not been detected outside of the expected territory once sharpening of gene expression

domains is complete (Calzolari *et al*, 2014). This suggests that cells expressing the reporter do not switch their identity in normal development. However, cells do not upregulate expression of the reporter used in this study until some time after border sharpening has occurred; it is therefore possible that the reporter is expressed too late to be present in cells that have intermingled.

1.7 Mechanisms of sharpening: Eph/ephrin-mediated cell segregation

1.7.1 Overview of Eph/ephrin signalling

One mechanism of border sharpening during hindbrain patterning is Eph/ephrin-mediated cell sorting. Eph/ephrin signalling involves interactions between members of the Eph family of receptor tyrosine kinases and their ephrin ligands, which can cause segregation of cells based on their Eph/ephrin expression status. Differential expression of Ephs and ephrins occurs at segment interfaces.

Eph receptors are divided into two different classes based on their binding preferences for ephrins: EphA receptors preferentially bind to GPI-anchored ephrinA ligands, while EphB proteins bind to transmembrane ephrinB ligands. However, there are exceptions to this: EphA4, for example, binds both A- and B-class ephrins (Gale *et al*, 1996b). Upon ephrin binding to an Eph receptor, downstream “forward” signalling occurs in the Eph receptor-expressing cell, which can involve both the tyrosine kinase activity of the Eph receptor with resulting recruitment of SH2 domain-containing proteins, as well as recruitment of PDZ domain-containing proteins. “Reverse” signal transduction can also occur in the ephrin-expressing cell, following the binding of Eph receptors, and also involves both tyrosine phosphorylation and recruitment of PDZ domain-containing proteins in the case of ephrinB proteins.

Ephs and ephrins are both membrane-bound, such that interactions between them require cell-to-cell contact. Since Eph receptors and their ephrin binding partners are often expressed in reciprocal domains they have adjacent borders where Eph/ephrin interactions can occur (Gale *et al*, 1996b). Within the hindbrain, Eph

receptors and ephrins are generally expressed in complementary domains, leading to Eph/ephrin interactions at segment interfaces. This segmented expression is achieved by regulation of Eph and ephrin expression downstream of transcription factors that confer rhombomeric identity. Eph/ephrin interactions at rhombomere borders prevent intermingling between adjacent rhombomeres and drive segregation of cells to contribute to sharpening.

1.7.2 Regulation of segmental expression of Ephs and ephrins in the hindbrain

In order for Eph/ephrin signalling to mediate border sharpening, Eph/ephrin interactions must occur at the interfaces of adjacent rhombomeres, and therefore, segment-restricted expression of Ephs and ephrins is important. For example, in zebrafish, *epha4a* is expressed in r3 and r5, while *efnb3b* is expressed in r2, r4 and r6; *ephB4a* is expressed in r5 and r6, while *efnb2a* is expressed in r1, r4 and r7 (Chan *et al*, 2001; Xu *et al*, 1994, 1995; Cooke *et al*, 2001). This segmental regulation of Eph and ephrin expression is achieved through regulation of expression of Ephs and ephrins downstream of genes that confer rhombomere identity. For example, in r3 and r5, Egr2 directly regulates expression of *ephA4* in r3 and r5 (Theil *et al*, 1998). In zebrafish, Valentino upregulates expression of *ephB4a* and represses *ephrinB2a* in r5 and r6 (Cooke *et al*, 2001; Hernandez *et al*, 2004). In mouse, Hoxa2 is required for *EphA7* expression in r3 (Taneja *et al*, 1996), while Hoxa1 and Hoxb1 upregulate *EphA2* in r4, although it is not clear whether EphA2 contributes to border sharpening (Chen & Ruley, 1998; Studer *et al*, 1998).

1.7.3 Evidence that Eph/ephrin-mediated cell sorting contributes to rhombomere border sharpening

Knockdown of EphA4 and EphrinB2 reduces the sharpness of rhombomere borders at stages when they are usually sharp (Cooke *et al*, 2005). In addition, dominant negative EphA4 causes misplaced cells expressing *egr2b* to occur in even-numbered rhombomeres and disrupts border sharpness by stages when borders are usually sharp, indicating that when Eph/ephrin signalling is

compromised, cells are capable of intermingling between segments (Xu *et al*, 1995).

There is additional evidence that Eph/ephrin signalling can mediate cell segregation and drive sharpening, both in the hindbrain and *in vitro*. Mosaic overexpression of full-length or truncated EphA4 or EphrinB2 causes the sorting of overexpressing cells to the edges of odd- or even-numbered rhombomeres, respectively (Xu *et al*, 1999). Similarly, mosaic knock down of EphA4 or EphrinB2 causes segregation of cells within rhombomeres where these factors are usually expressed (Cooke *et al*, 2005; Kemp *et al*, 2009). Cell culture experiments have demonstrated that Eph/ephrin-mediated cell interactions can cause segregation of Eph- and ephrin-expressing zebrafish cells (Mellitzer *et al*, 1999). More recently, live imaging of border sharpening in zebrafish has indicated that misplaced cells can become sorted into the correct segments, which was suggested to involve Eph/ephrin signalling (Calzolari *et al*, 2014).

1.7.4 Mechanisms of Eph/ephrin-mediated cell sorting

The mechanisms by which Eph/ephrin-signalling drives and maintains border sharpness are not clear. Cell segregation at interfaces can be achieved through differential cell-cell adhesion, cell repulsion and cortical tension, and it is known that Eph/ephrin signalling can regulate these processes (Cayuso *et al*, 2015).

Differential cell adhesion between two populations of cells can sharpen a jagged border through cells of each population rearranging to increase their interactions with cells of similar adhesive strength. In some contexts, Eph/ephrin signalling regulates cell adhesion molecules such as Cadherins to influence cell adhesion (Fagotto *et al*, 2013). Eph/ephrin signalling may also drive cell sorting by mediating cell repulsion, causing cells to become sorted out from the incorrect territory. For Eph/ephrin interactions to cause cell repulsion, it is necessary to overcome the Eph/ephrin interaction itself; this can be achieved by proteolytic cleavage of Eph or ephrin (Hattori *et al*, 2000), or by endocytosis of the Eph/ephrin complex (Marston *et al*, 2003; Zimmer, 2003). This endocytosis is required for cytoskeletal collapse,

resulting in cell repulsion (Poliakov *et al*, 2004). Eph/ephrin signalling can regulate Rho-family GTPases, which are involved in regulating actin assembly (Pasquale, 2008).

An additional mechanism by which Eph/ephrin interactions may contribute to border sharpness in the hindbrain is through increasing cortical tension, and accumulation of actomyosin cables at rhombomere interfaces. Actomyosin-enriched boundaries can prevent cell mixing between compartments and there are well-established roles of cortical tension in boundary establishment and maintenance between *Drosophila* compartments (Major & Irvine, 2005, 2006; Landsberg *et al*, 2009; Monier *et al*, 2010; Aliee *et al*, 2012). In mouse, unidirectional signalling downstream of mosaic EphrinB1 has been reported to drive cell segregation in the neuroepithelium, involving the generation of a cortical actin differential between ephrinB1- and EphB-expressing cells (Neill *et al*, 2016). In zebrafish, Ephs and ephrins interact at the border between the eye field and telencephalon and maintain eye field segregation by accumulation of actomyosin (Cavodeassi *et al*, 2013). In the zebrafish hindbrain, enrichment of actomyosin has also been observed at rhombomere borders, and this accumulation is promoted by EphA/ephrin interactions, although not until a substantial amount of border sharpening has already occurred (Calzolari *et al*, 2014). This mechanism may therefore play a role in preventing cell intermingling once borders are sharp, rather than directly contributing to the process of border sharpening in the zebrafish hindbrain.

1.8 Mechanisms of sharpening: selective cell death

An alternative mechanism by which mis-specified cells may be refined to contribute to border sharpening is the selective elimination of ectopic cells that are in the incorrect territory. Mis-specified epithelial cells can be eliminated from *Drosophila* imaginal discs by increased actomyosin contractility and tension at the interface between mis-specified cells and surrounding cells (Bielmeier *et al*, 2016). This contractility and elimination could be mediated via mis-expression of cell surface cues, such as Ephs and ephrins (Fagotto *et al*, 2014). In the mouse cerebral

cortex, ectopic expression of EphrinA5 in EphA7-expressing neuroepithelial cells causes severe apoptotic death, while loss of EphA7 reduces endogenous levels of apoptosis and results in increased cortical size (Depaepe *et al*, 2005). However, there is no evidence of increased markers of cell death at rhombomere borders during sharpening, suggesting that this mechanism does not significantly contribute to border sharpening, although it remains possible that low numbers of isolated, ectopic cells are refined by a cell-death based mechanism.

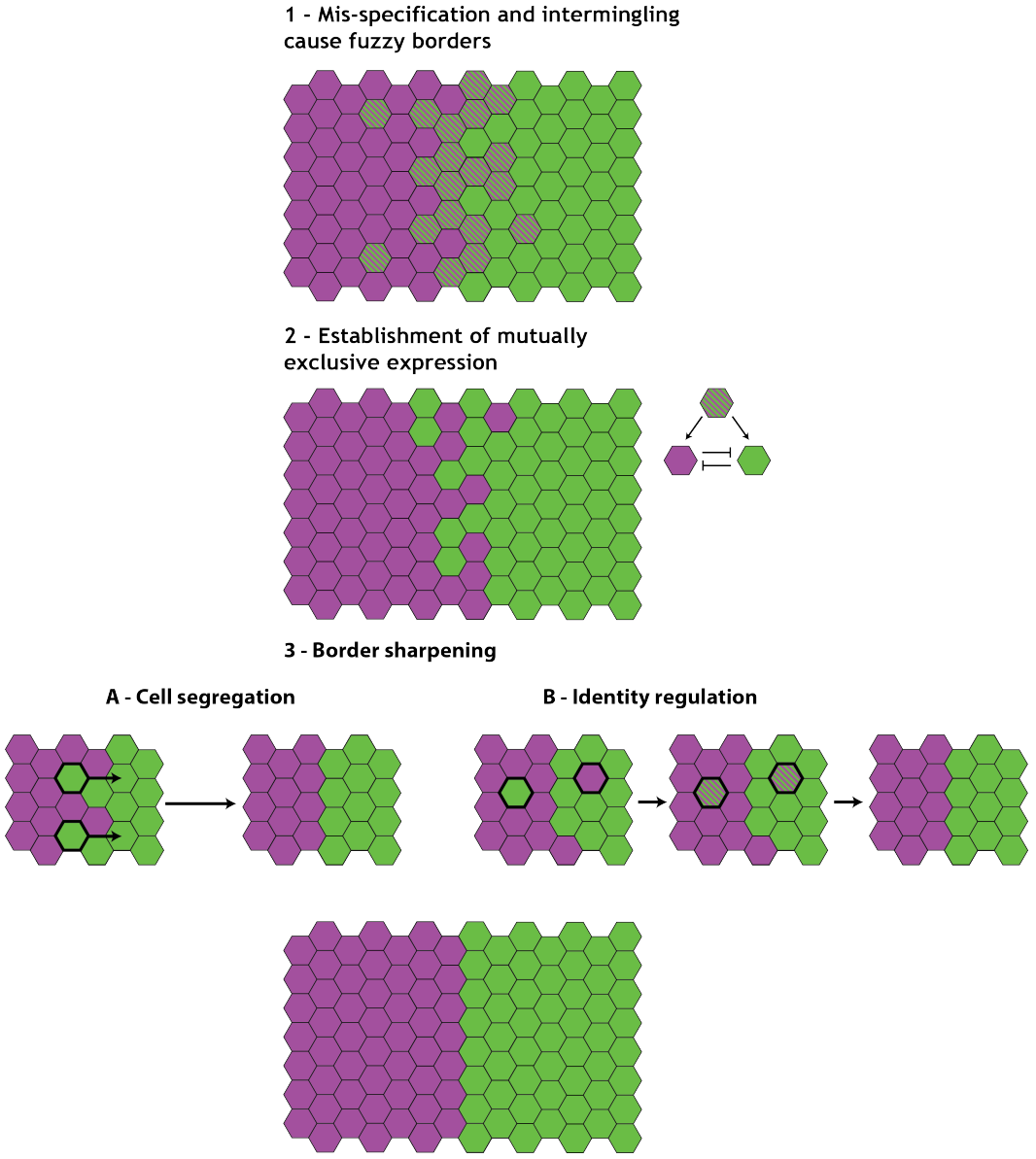

Figure 1-6 Proposed mechanisms that may contribute to border sharpening

Fuzzy and overlapping regions of cell identity are initially specified at segment borders due to noise in signals that induce segmental gene expression and cell intermingling across borders (1). Cells are capable of resolving this overlapping identity via mutual inhibition and autoregulation (2); while this resolution of dual identity may contribute to border sharpening, additional sharpening mechanisms are required: cell segregation may drive ectopic cells to become sorted into the correct territory (A); in addition, cell identity may be regulated such that ectopic cells adopt the same identity as their neighbours (B).

1.9 Aims and achievements

There is good evidence that during rhombomere border sharpening, cells resolve an ambiguous, dual identity, which may be initially mis-specified at segment interfaces due to noisy morphogen gradients. However, it is less clear to what extent cells intermingled between segments switch identity. Both these cases involve regulation of cell identity, which may contribute to hindbrain border sharpening. The primary aims of the research presented in this thesis are: firstly, to study the contribution of cell identity regulation to sharpening of gene expression borders in the hindbrain, using zebrafish as a model organism, and, secondly, to investigate potential mechanisms by which cell identity is regulated during border sharpening.

The first aspect of my work focuses on understanding the extent to which regulation of cell identity occurs during border sharpening. To address this, I have generated a novel zebrafish reporter line to improve our ability to study cell identity in live embryos during border sharpening. I find that this reporter line indicates a contribution of identity regulation to border sharpening. An additional approach I took to investigate the contribution of cell identity regulation to border sharpening was to increase cell intermingling between rhombomeres and compromise alternative sharpening mechanisms. I demonstrate that this perturbation increases the requirement for cell identity switching to sharpen gene expression borders, as detected using the novel reporter line.

The second aim of this project was to increase our understanding of the mechanisms by which cells may switch and resolve their identity during border sharpening. I focused my efforts on attempting to reveal the potential contribution of community effects and non cell-autonomous regulation of identity. Evidence that I present here is consistent with segmental regulation of RA signalling contributing to border sharpening.

Chapter 2. Materials & Methods

2.1 Zebrafish strains and maintenance

Wild type and transgenic zebrafish embryos were obtained by natural spawning and raised at 23 °C to 28.5 °C as described (Westerfield, 1993). Embryos were staged by hours post-fertilisation (hpf) at 28.5 °C and/or morphological features (such as somite stage (ss)) as described (Kimmel *et al*, 1995).

Wild types:

Lon/AB

ZIRC/AB

Transgenics:

pGFP5.3^{e1Tg} (Pax2GFP) (Picker *et al*, 2002)

EphA4a crispr1 mutant (mut_EphA4a_e3) EphA4a^{fci503} (unpublished) was created by Jordi Cayuso in the Wilkinson laboratory.

Mutant/Transgenic lines (generated during the project):

Tg[hsp70/UAS:Cyp26b1;α-crystallin:RFP]^{fci501Tg}

Tg[egr2b:H2B-Citrine]^{fci500Tg}

EphrinB3b TALEN mutant (mut_efnB3b_e1(2bpdel)) EphrinB3b^{fci502}

EphrinB3b;EphA4a double homozygous mutant

Fin-clipping protocol

Fish were anaesthetised in 0.02% 3-aminobenzoic acid ethyl ester (MS-222). A small portion (< 50%) of the caudal fin was removed using surgical scissors and genomic DNA extracted for analysis and genotyping.

2.2 Zebrafish embryo techniques

2.2.1 Morpholino injection

Morpholino oligonucleotides (MOs) were obtained from GeneTools (Oregon, USA) and were dissolved, aliquoted and frozen at 1mM concentration as described (Gerety & Wilkinson, 2011) (Egr2b TB MO1 and Egr2a TB MO1). All other MOs were aliquoted and stored at room temperature in glass vials. MOs were injected with a p53 translation-blocking MO to avoid MO-mediated toxicity (Robu *et al*, 2007; Gerety & Wilkinson, 2011). MOs shown in Table 2-1 were injected into the yolk of blastomeres at the 1-4 cell stage. Due to the known issue of batch-to-batch variation in MO efficiency, MOs were titrated for optimum knock down to cause published phenotypes, using published concentrations as a starting point. For the EphA4 MO, knock down efficiency has previously been optimised in the Wilkinson lab to cause loss of EphA4 protein by immunohistochemistry. For the Egr2b MO (unpublished), knock down efficiency was optimised to give phenotypes reported for the Egr2b$^{fh227/fh227}$ mutant (Bouchoucha *et al*, 2013).

Table 2-1 Sequences of morpholinos and quantities injected.

For translation-blocking MOs, where applicable, the region binding to the ATG of the target gene is highlighted. TB, Translation-blocking; SB, splice-blocking.

Name	Sequence	Quantity injected	Reference
Egr2b TB MO1	AGTTTTAGCTGT**CAT**CGTGAAGTCC	4 ng	-
Egr2a TB MO1	CATGTGCTC**CAT**GTTGGGAAGATTT	4 ng – 8 ng	-
Hoxb1a TB MO1	GGAACTGTC**CAT**ACGCAATTAA	4 ng	(McClintock *et al*, 2002)
Hoxb1b TB MO1	AATT**CAT**TGTTGACTGACCAAGCAA	4 ng	(McClintock *et al*, 2002)
Hoxa2 TB MO1	AATTCGTAATT**CAT**CTCCTCCAAG	4 ng – 8 ng	(Hunter & Prince, 2002)
Hoxb2 TB MO1	CAAAATT**CAT**CGCTTCGCCTGG	4 ng – 8 ng	(Hunter & Prince, 2002)
Cyp26a1 TB MO1	CGCGCAACTGATCGCCAAAACGAAA	No phenotype observed	(Emoto *et al*, 2005)
Cyp26a1 SB MO1	CCCTCAAACCCTGCCGATCAAAAAT	2.6 – 5.2 ng	(D'Aniello *et al*, 2013)
Cyp26a1 SB MO2	TCTTATCATCCTTACCTTTTTCTTG	1.3 – 2.6 ng	(D'Aniello *et al*, 2013)
Cyp26b1 TB MO1	CTCGAAGAG**CAT**GGCTGTGAACGTC	1.4 – 3.2 ng	(Hernandez *et al*, 2007)
Cyp26c1 SB MO1	AAACTCGGTTATCCTCACCTTGCGC	1.4 – 3.2 ng	(Hernandez *et al*, 2007)
EphA4a TB MO1	AACACAAGCGCAGC**CAT**TGGTGTC	4 – 5 ng	(Cooke *et al*, 2005)
p53 TB MO1	GCGC**CAT**TGCTTTGCAAGAATTG	4 ng	(Langheinrich *et al*, 2002)
Control MO	CCTCTTACCTCAGTTACAATTTATA	-	GeneTools

2.2.2 RNA injection

Capped RNA for microinjections was synthesised using the mMessage mMachine® kits (Life Technologies) from linearised plasmid DNA following the manufacturer's protocol. After *in vitro* transcription, the DNA template was removed by TURBO DNase treatment as described in the mMessage mMachine® protocol. Synthesised RNA was purified using the RNeasy ® Mini Kit (Qiagen). Table 2-2 describes the constructs used to generate capped RNA, with the exception of RNA encoding TALENs. 50-200 pg RNA was injected into the cell of 1-cell embryos as described in the text, unless otherwise stated.

Table 2-2 Constructs used to generate capped RNA

Construct	Restriction enzyme to linearise	Polymerase to synthesise RNA	Source
pT3Ts/Tol2	XbaI	T3	(Balciunas *et al*, 2006)
pCS2-H2B-eGFP	NotI	SP6	(Megason, 2009)
pCS2-H2B-mRFP1	NotI	SP6	(Megason, 2009)
Cas9	PmeI	T7	Joung lab (Addgene #42251)

2.2.3 Heat shock

Heat shock of embryos was performed 37 °C for 30 minutes in 0.65x Danieau's solution at the stages indicated.

2.2.4 Cell transplantation

Donor embryos were injected with 100 pg H2B-GFP RNA at the one cell stage. In preparation for transplantation, donor and host embryos were dechorionated by treatment with 20 ml of 1 mg/ml Pronase (Sigma) in 0.65x Danieau's solution for 2 – 5 minutes. Embryos were then rinsed three times with 50 ml washes of 0.65x

Danieau's solution. If required, additional removal of chorions was achieved manually. Labelled donor cells were removed from donor embryos at the 30%-50% epiboly stage (approximately 4 hpf) and transferred into the unlabelled host embryos using an air-controlled glass needle (BM100T-15, ends fire-polished ES-blastocyst injection needle; size 65 (ID~30µm), with spike, straight (BioMedical Instruments)). Donor cells were targeted to the future hindbrain, based on known fate maps (Kimelman & Martin, 2012), as illustrated in Figure 2-1. After transplantation, chimeric embryos were kept in 0.65x Danieau's solution with 2.5% Penicillin-Streptomycin (Sigma) until the desired stage.

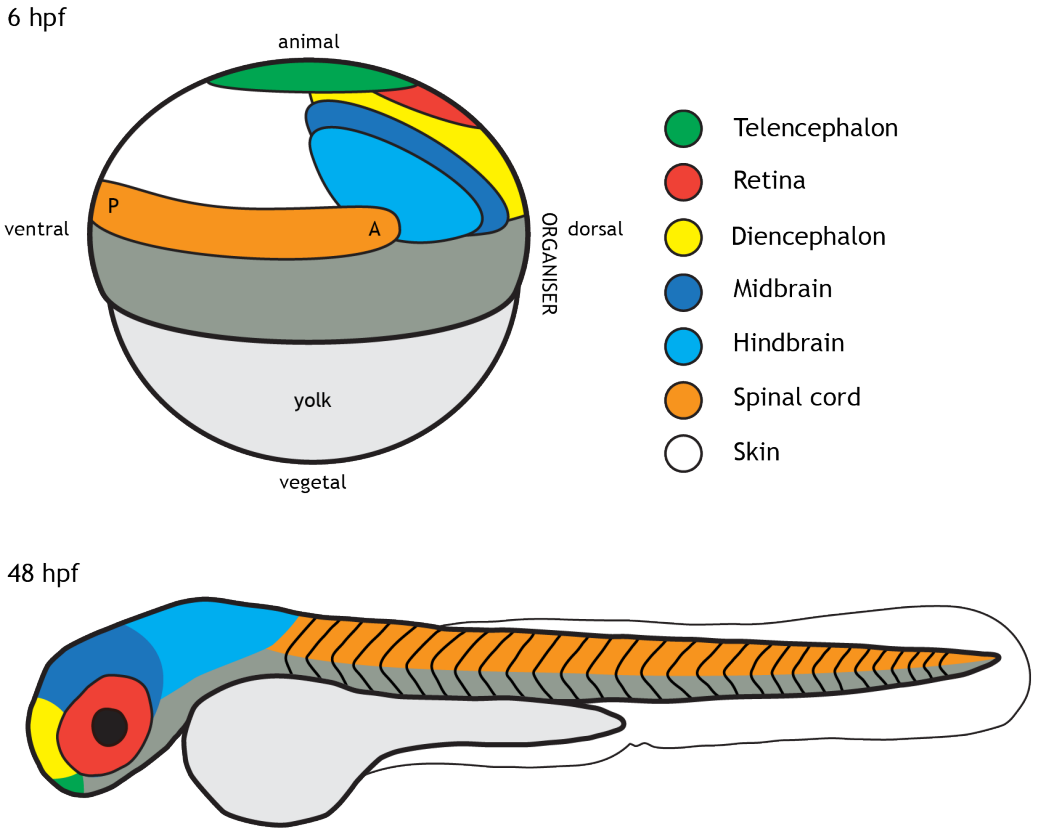

Figure 2-1 Fate map of zebrafish embryo

The top image is a fate map of the zebrafish embryo at the onset of gastrulation (6 hpf). The bottom image shows a lateral view of a 48 hpf embryo. The prospective hindbrain and hindbrain is shown in blue. A, P: anterior, posterior. Based on (Kimelman & Martin, 2012)

2.2.5 Live imaging of zebrafish embryos

Dechorionated live embryos were embedded in 0.6% low melting agarose (Sigma) /0.5x Danieau's solution within a 1% agarose (Bio-Rad Laboratories Inc.)/0.5x Danieau's solution-coated petri dish created with a mould with individual wells to help orientate embryos with the hindbrain towards the objective. The petri dish was then filled with 0.5x Danieau's solution. Embryos were imaged using a Zeiss LSM 700 confocal microscope with a water dipping 40x lens, NA 1.0, with 0.8x digital zoom. ZEN 2010 software was used, together with the Multi-Time Series (MTS) macro (Carl Zeiss MicroImaging) for sequential acquisition of images of multiple samples at multiple locations. For individual samples, a 2 x 1 (horizontal) tilescan, with 5% overlap, was used. Images were acquired every 5 or 6 minutes, with 2x line averaging and a z-slice depth of 1 µm.

Live embryos (F_0 Tg[egr2b:H2B-Citrine]) were also imaged, unmounted using a Leica M205 FA fluorescence stereo microscope with DFC 360 FX camera.

Movie Processing and cell tracking

ImageJ (NIH)
3D drift was corrected for using the Correct 3D Drift ImageJ plug-in (Parslow *et al*, 2014).
FluoRender (v. 2.19.4 and 2.20.0) University of Utah was used to create 3D projections of time-lapse movies.
Cell were manually tracked using the MTrackJ ImageJ plug-in.

2.3 Solutions

Danieau's Solution (30x stock; 0.65x and 0.5x working solutions)
30x Danieau's solution:
58 mM NaCl
0.7 mM KCl
0.4 mM $MgSO_4$
0.6 mM $Ca(NO_3)_2$

5.0 mM HEPES pH 7.6

Tricaine (3-amino benzoic acid ethyl ester) (Sigma-Aldrich)

Tricaine stock solution:

400 mg tricaine

97.9 ml H_2O

2.1 ml 1 M Tris (pH 9)

pH adjusted to 7.0

Working solution for anaesthesia:

4.2 ml tricaine stock solution

100 ml fish water

Embryo/fin Lysis Buffer

10 mM Tris-HCl pH 8.0

10 mM EDTA

0.2% Triton X-100

200 µg/ml Proteinase K

2.4 Zebrafish *in situ* hybridisation and immunohistochemistry

Embryos of the desired stages were fixed in 4% paraformaldehyde/PBS at 4 °C overnight or at room temperature for 3 hours, washed in PBS/Tw, manually dechorionated and stored in 100% methanol at -20 °C for a minimum of 2 hours. For ISH of embryos older than 24 hpf, embryos were raised in 0.2mM 1-phenyl 2-thiourea (Sigma) in fish water from 24 hpf onwards to inhibit melanin synthesis.

2.4.1 Probe synthesis for ISH

Antisense riboprobes used for ISH were synthesised from linearised cDNA clones using T3, T7 or SP6 polymerase (Promega), as listed in Table 2-3, and labelled with either digoxigenin-UTP or fluorescein-UTP (Roche).

Table 2-3 Probes used for ISH.

* (963 bp sub-cloned from full-length cDNA as described in reference

Target	Restriction enzyme / polymerase	Reference
Frb35 (Egr2a) *	EcoRI/Sp6	(Sun *et al*, 2002)
Egr2b (full-length)	PstI/T3	(Oxtoby & Jowett, 1993)
Egr2b 3'UTR	SphI/T3	(Oxtoby & Jowett, 1993)
EphA4a	BamHI/T7	(Xu *et al*, 1994)
EphrinB3b	EcoRI/T7	(Chan *et al*, 2001)
Hoxb1a	KpnI/T3	(McClintock *et al*, 2001)
Hoxa2	KpnI/T3	(Prince *et al*, 1998)
Hoxb2	XbaI/T7	(Prince *et al*, 1998)
Hoxb3	PstI/T7	(Prince *et al*, 1998)
Cyp26a1	SalI/T7	(Kudoh *et al*, 2002)
Cyp26b1	BglII/Sp6	(Zhao *et al*, 2005)
Cyp26c1 (formerly known as Cyp26d1)	SmaI/T7	(Gu *et al*, 2005)
Rfng	EcoRI/T7	(Cheng *et al*, 2004)
Wnt8b	EcoRI/T7	(Kelly *et al*, 1995)
Gsc	NotI/T7	(Schulte-Merker *et al*, 1994)
Citrine	XmaI/T3	(Megason, 2009)

2.4.2 ISH reagents

Table 2-4 Reagents used for ISH

Reagent	Component
PBS/Tw	PBSA; 0.1 % Tween-20 (Sigma)
4% Paraformaldehyde	4% Paraformaldehyde (Sigma) in PBS/Tw
Proteinase K	(10 µg/ml mastermix, diluted 1/1000)
Hybridisation Solution	50% formamide (Ambion); 5x SSC; 50 µg/ml heparin (Sigma); 500 µg/ml tRNA (Sigma); 5% dextran sulphate (Sigma); 0.092 M citric acid (Sigma) 0.1% Tween-20 (prepared in DEPC-dH_2O)
Blocking Solution	2 mg/ml bovine serum albumin (BSA; Sigma); 2% sheep serum (Sigma) in PBS/Tw
Colouration Buffer (NBT/BCIP)	100 mM Tris-HCl pH 9.5; 50 mM $MgCl_2$ (Sigma); 100 mM NaCl; 0.1 % Tween-20
Colouration Buffer (Fast Blue)	100 mM Tris-HCl pH 8.2; 50 mM $MgCl_2$ (Sigma); 100 mM NaCl; 0.1 % Tween-20
Colouration Buffer (Fast Red)	100 mM Tris-HCl pH 8.2; 0.1% Tween-20
NBT/BCIP Colouration Solution	4.5 µl/ml NBT (nitro blue tetrazolium, 75 mg/ml in 70% dimethyl formamide (Roche)); 3.5 µl/ml BCIP (5-bromo-4-chloro-3-indolyl phosphate, 50 mg/ml in 70% dimethyl formamide (Roche)) in Colouration Buffer
Fast Blue Colouration Solution	2.5 µl/ml Fast Blue BB (100 mg/ml in dimethyl formamide (Sigma)); 2.5 µl/ml NAMP (naphtol-AS-MX-phosphate, 100 mg/ml in dimethyl sulphoxide (Sigma)) in Fast Blue Colouration Buffer
Fast Red Colouration Solution	1 Fast Red/NAMP tablet (Sigma) in 2 ml Fast Red Colouration Buffer
Glycine	0.1 M glycine pH 3.0 (Severn Biotech Ltd.)

2.4.3 ISH protocol

Embryos were rehydrated in a graded series of methanol / PBS + 0.1% Tween-20 (Sigma) treatments (75% methanol / 25% PBS/Tw and 37.5% methanol / 62.5 % PBS/Tw). Embryos older than 20 hpf were permeabilised with Proteinase K (10 µg/ml; Roche) for timings shown in Table 2-5. Embryos were washed 3 x 5 minutes in PBS/Tw after Proteinase K treatment, then refixed in 4% PFA for 30 minutes, and washed 5 x 5 minutes in PBS/Tw after refixation. Embryos were then incubated in Hybridisation Solution at 68 °C for a minimum of 2 hours. Labelled riboprobes in Hybridisation Solution were added to the embryos and incubated overnight at 68 °C.

On the second day, probes were removed from the embryos and a series of post-hybridisation washes were conducted as shown in Table 2-6. Embryos were then incubated in Blocking Solution at room temperature for a minimum of 2 hours. Anti-digoxigenin or anti-fluorescein antibody conjugated to alkaline phosphatase (1:2000; Roche) in Blocking Solution was then added and embryos were incubated overnight at 4 °C.

On the third day, the antibody was removed by washing 10 x 30 minutes in PBS/Tw. Embryos were then washed 3x 5 minutes in Colouration Buffer before incubation in Colouration Solution. The colour reaction was monitored and, once the colour had developed completely, the embryos were washed 3 x 5 minutes in PBS/Tw. Embryos were then fixed in 4% PFA for 20 minutes and washed an additional 3 x 5 minutes before being processed for deyolking and mounting as described below.

Table 2-5 Proteinase K treatment

Developmental stage (hpf)	Length of Proteinase K treatment (minutes)
20	2
24	4
30	7.5

Table 2-6 Post-hybridisation washes

Wash	Components	Length of wash (minutes)	Temperature of wash (°C)
1	66% formamide; 33% 2x saline-sodium citrate (SSC); 0.1% Tween-20	5	68
2	33% formamide; 66% 2xSSC; 0.1% Tween-20	5	68
3	2x SSC; 0.1% Tween-20	5	68
4	0.2x SSC; 0.1% Tween-20	20	68
5	0.1x SSC; 0.1% Tween-20	2x 20	68
6	66% 0.2x SSC; 33% PBS/Tw	5	25

2.4.4 Two colour fluorescent ISH protocol

Two colour fluorescent *in situ* hybridisation was carried out using Fast Blue (Sigma) and Fast Red (Roche; now discontinued) substrates as described (Lauter *et al*, 2011). Two different riboprobes – one digoxigenin labelled, the other fluorescein labelled – were simultaneously added to the embryos in Hybridisation Solution and incubated overnight. The Fast Blue colour reaction was conducted on day three as for single ISH, using Fast Blue Colouration Buffer and Fast Blue Colouration Solution. Care was taken to avoid overdeveloping the Fast Blue colour, as the Fast Blue colour reaction involves the production of a precipitate that can impede the development and detection of the second Fast Red colour reaction. After the Fast Blue colour reaction was complete, the embryos were washed 3 x 5 minutes in PBS/Tw and then incubated 3 x 20 minutes in 0.1 M glycine pH 3.0 (Severn Biotech Ltd.) to inactivate the anti-digoxigenin-conjugated alkaline phosphatase. Embryos were washed an additional 3 x 5 minutes in PBS/Tw, then fixed for 15 minutes in 4% PFA and then washed again for 3 x 5 minutes. Anti-fluorescein-AP antibody (1:2000) was then added in Blocking Solution and the embryos incubated overnight at 4 °C. The Fast Red colour reaction was conducted using Fast Red Colouration Buffer and Fast Red Colouration Solution. Embryos were then washed 3 x 5 minutes in PBS/Tw, fixed for 20 minutes in 4% PFA and washed an additional

3 x 5 minutes in PBS/Tw. In order to stain nuclei, embryos were incubated in 4'-6-diamidino-2-phenylindole (DAPI) for 60 minutes at room temperature and washed 4 x 15 minutes in PBS/Tw before being processed for deyolking and mounting.

2.4.5 Immunohistochemistry antibodies

The primary antibodies used for immunohistochemistry are listed in Table 2-7.

Table 2-7 Primary antibodies

Target/epitope	Dilution	Species	Source (Cat. #)
EphA4a	1:500 (1:400)	Rabbit	Wilkinson lab (Irving *et al*, 1996) (N/A)
GFP (also Citrine)	1:500 (1:400)	Rabbit	Torrey Pines (TP401)
Myc	1:500 (1:400)	Mouse	Santa Cruz (sc-40)

The following secondary antibodies were used:
Goat Anti-Rabbit Alexa Fluor® 488 (IgG H + L) (1:500 dilution) (Molecular Probes)
Goat Anti-Rabbit Alexa Fluor® 594 (IgG H + L) (1:500 dilution) (Molecular Probes)
Goat Anti-Rabbit Alexa Fluor® 647 (IgG H + L) (1:500 dilution) (Molecular Probes)
Goat Anti-Mouse Alexa Fluor® 488 (IgG H + L) (1:500 dilution) (Molecular Probes)

2.4.6 Immunohistochemistry protocol

Samples were washed 3 x 5 minutes in PBS/Tw, then incubated for a minimum of 2 hours in 5% goat serum / PBS/Tw at room temperature. Primary antibodies were added in 5% goat serum / PBS/Tw and incubated overnight at 4 °C. Embryos were then washed 10 x 30 minutes in PBS/Tw at room temperature. Secondary antibodies were added in 2.5% goat serum / PBS/Tw and embryos incubated overnight at 4 °C. For visualisation of F-actin, Cy3-conjugated phalloidin (1:200) was added with the secondary antibodies and incubated overnight at 4 °C. Embryos were then washed 2 x 30 minutes in PBS/Tw and then incubated in 4'-6-diamidino-2-phenylindole (DAPI) for 60 minutes at room temperature to stain

nuclei. Embryos were then washed 6 x 30 minutes in PBS/Tw, then processed for deyolking and mounting.

2.4.7 Alcian blue cartilage staining protocol

Embryos were transferred to 20 μM PTU (1-phenyl 2-thiourea) (Sigma) in fish water at 24 hpf to inhibit pigment formation. 4.5 day old embryos were fixed overnight in 4% PFA at 4 °C, then washed 3 x 5 minutes in PBS/Tw. Embryos were then incubated for 2 x 20 minutes in acid alcohol (70% ethanol + 1% concentrated hydrochloric acid). Embryos were stained with Alcian blue (1% solution in acid alcohol; Sigma) for a minimum of 4 hours. Once cartilage staining was complete, Alcian blue was removed by washing in acid alcohol 3 x 5 minutes, then 3 x 5 minutes in 70% ethanol, once in 50% ethanol, then 3 x 5 minutes in PBS/Tw. Embryos were stored in 70% glycerol/PBS prior to mounting and imaging.

2.4.8 Mounting and imaging samples

Embryos were manually deyolked and flat-mounted (ventral side in contact with slide) or side-mounted (lateral side in contact slide) in 75% glycerol (Fisher Bioreagents®)/PBS under a glass coverslip. Samples were photographed using a Zeiss Axioplan2 with Axiocam HRc camera. Fluorescent images for fixed samples were obtained using either a Leica TCS SP2 confocal microscope or a Zeiss LSM700 confocal microscope. The fluorescent Fast Blue signal was detected by excitation with a 633 nm laser and detection at wavelengths greater than 650 nm; the fluorescent Fast Red signal was detected by excitation with a 561 nm laser and detection of wavelengths greater than 570 nm.

2.5 Pharmacological treatments

R115866 (HY-14531; MedChem Express) 10mM stock in dimethyl sulphoxide: Embryos were treated in their chorions from the stages specified with 10 μM R115866 in Danieau's solution.

2.6 *Tol2* Transposon-mediated transgenesis

DNA (5 – 20 pg) was injected into the cell of one-cell stage embryos along with 36 pg *Tol2* transposase RNA. *Tol2* RNA was synthesised *in vitro* from the linearised pT3Ts/Tol2 plasmid (Balciunas *et al*, 2006).

2.6.1 *Tol2* transposon transgenesis constructs

Pax3CNE1:Egr2b-Myc

pMiniTol2-Pax3CNE1-TKprom-Gal4-UAS:Egr2b-Myc was created by replacing the H2B-citrine coding sequence from pMiniTol2-Pax3CNE1-TKprom-Gal4-UAS:H2B-citrine (Moore *et al*, 2013; a gift from James Briscoe) with the *egr2b* coding sequence and C-terminal Myc tag, amplified from hsp70:Egr2b-Myc (plasmid details below) using the following primers:
Forward primer: GATCGTCGACGCTGGACTTCACGATGACA
Reverse primer: GGATCATCATCGATGGTAC

pMiniTol2-Hsp70/UAS:Cyp26b1-ACR

pMiniTol2-Hsp70/UAS:Cyp26b1-ACR was created by R. Gonzalez-Quevedo in the Wilkinson lab. This construct contains zebrafish *cyp26b1* coding sequence under the control of both a heat-shock inducible hsp70 promoter and UAS promoter. The construct also contains the α-crystallin promoter driving RFP expression in the lens.

Hsp70:Egr2b-Myc

Hsp70:Egr2b-Myc expression vectors were generated using the MultiSite Gateway® cloning kit (Life Technologies) along with plasmids from the Tol2Kit (Kwan *et al*, 2007), according to manufacturers' protocols.

The *egr2b* middle entry vector (pME-*egr2b*) was created by BP recombination between the pDONR-221 vector and the *egr2b* coding sequence (Oxtoby & Jowett, 1993) flanked by attB sites. The *egr2b* coding sequence was amplified by PCR (using the Expand High Fidelity^{PLUS} PCR System (Roche)) using primers incorporating attB sites:

GGGGACAAGTTTGTACAAAAAAGCAGGCTGGACTTCACGATGACAGCTAAAACTTTG
and
GGGGACCACTTTGTACAAGAAAGCTGGGTGGTTTGAACTGGACGAGCAGATGC.

LR recombination of pDestTol2pA, p5E-hsp70, pME-Egr2b and p3E-Myc-pA was used to create the final Hsp70:Egr2b-Myc expression vector.

LR recombination of pDestTol2pACryGFP, p5E-hsp70, pME-Egr2b and p3E-Myc-pA was used to create the final Hsp70:Egr2b-Myc-ACG expression vector.

Table 2-8 Tol2Kit plasmids used to create *Tol2* transgenesis constructs

Plasmid	Source (Addgene #)
pDONR-221	Gateway (Invitrogen)
p5E hsp70	Nathan Lawson lab
p3E mTpA	Nathan Lawson lab
pDestTol2pA	Nathan Lawson lab
pDestTol2pACryGFP	Joachim Berger & Peter Currie (64022)

2.7 Design and synthesis of Transcription Activator-Like Effector Nucleases (TALENs)

TALENs were designed and constructed as previously outlined (Cermak *et al*, 2011). The Cornell University TAL Effector Nucleotide Targeter 2.0 (https://tale-nt.cac.cornell.edu/) was used to obtain a list of potential TALENs binding sites within the target gene locus, close to the translation start site and preferably within the first exon. Parameters for TALEN design were used as described (Dahlem *et al*, 2012): each DNA binding domain consists of 16-20 repeat variable di-residues (RVDs) and the spacer between the two target sequences in the genome is 14-17 nucleotides in length and ideally contains a restriction enzyme site. Recommendations from (Streubel *et al*, 2012) were used to manually select TALENs of optimal binding strength based on their repeat variable di-residue (RVD) content: use of the NN RVD was minimised; use of total (NN + HD) was

maximised; stretches of more than 5 weak RVDs were avoided and ideally TALENs consisted of 3-4 properly spaced strong RVDs. Candidate TALEN target sequences were also BLASTed to further confirm lack of off-target binding within the zebrafish genome.

DNA encoding TALENs was synthesised using the 5-day protocol for the Golden Gate cloning technique (Engler *et al*, 2009; Cermak *et al*, 2011). Plasmids used in the construction process (Golden Gate TALEN and TAL Effector Kit 1.0) were obtained from Addgene (Cat #1000000016); destination vectors pCS2TAL3-DD and pCS2TAL3-RR (Dahlem *et al*, 2012) were also obtained from Addgene (plasmids #37275 and #37276). TAL effector domains and FokI nuclease were cloned into these destination vectors to form the final pCS2-TAL vector for each TALEN, from which mRNA was synthesised from the from SP6 promoter using the mMessage mMachine® kit (Life Technologies). Embryos were injected with equal amounts (100 – 300 pg) of RNA encoding each of the left and right TALEN arms, together with RNA encoding Citrine or RFP at the one cell stage (for selection of efficiently injected embryos at 24 hpf).

RVD Sequences of TALENs:

EphrinB3b (left) TALEN:
NG HD NN NN NN NN NI NG NG NG HD NI NI NI NG NN NN HD

EphrinB3b (right) TALEN:
HD NI NN NN NI NN NI NI NG NG HD HD HD NI NI NG HD HD NI NG

Egr2b (left) TALEN:
HD HD NI NN HD NI NN HD NG NG HD NN HD NN HD NI NI HD HD NI

Egr2b (right) TALEN:
NG HD HD HD NI NG NN NG NI NN NN NG NI NI NI NI NN NG NG NG

2.7.1 HRM analysis of TALEN-induced mutations

Genomic DNA (gDNA) was obtained from whole individual 3 days post-fertilisation (dpf) embryos and fin clips from adult fish by proteinase K-mediated lysis in DNA extraction buffer (10 mM Tris-HCl pH 8.0; 10 mM EDTA; 0.2% Triton X-100; 0.2 mg/ml Proteinase K). TALEN-induced indel mutations were detected using high resolution melt curve (HRM) analysis as described in (Dahlem *et al*, 2012). Primers were manually designed to amplify approximately 100 bases of DNA around the TALEN target site in a real-time PCR in the presence of MeltDoctor™ HRM Dye (Applied Biosystems) using an ABI 7900 qPCR machine according to the manufacturers' instructions. Following gDNA amplification, the reaction was slowly heated and the change in fluorescence with temperature was recorded with high precision to generate a melting curve for each sample. Analysis of melt curves was conducted using the High Resolution Melting (HRM) Software V2.0.2 from Life Technologies. Primers used in HRM analysis are shown in Table 2-9.

Table 2-9 Primers used for HRM analysis of TALEN-induced mutations.

Target	Forward HRM primer	Reverse HRM primer
ephrinB3b	GAGAGAGTATCCCGCACACACG	TAGATGGGCTCCATGTTGGT
egr2b	GGATATGAGCACGGAGAAGC	ATCACGCCCTCTGGGTTC

2.7.2 TALEN-mediated genomic insertion

The donor construct for inserting H2B-Citrine within the coding region of *egr2b* was modified from a donor plasmid created by Sean Constable to insert eGFP at the *plzfa* locus (Constable, 2015). This plasmid has a pBluescript II KS backbone and contains the left and right TALEN bindings sites at the *plzfa* locus, inverted and flanking the TALEN spacer region remains in the same orientation as in the zebrafish genome. The coding region for eGFP is preceded by the sequence encoding the P2A self-cleaving peptide and is followed by the SV40 polyadenylation signal from the pCS2^{+} vector. The *egr2b* H2B Citrine TALEN donor plasmid was created by replacing the *plzfa* TALEN region with the *egr2b* left and right TALEN binding sequences and spacer region using the following annealed oligonucleotides:

Oligonucleotide 1:
CTTCCCAGTTAGGTAAAATGGGTCGTTCCCTCGCAACCTGGTTGCGCGAAGC
TGCTGGACAT
Oligonucleotide 2:
CGATGTCCAGCAGCTTCGCGCAACCAGGTTGCGAGGGCCAGCAAACTTTTAC
CTACATGGGAAGAGCT

The eGFP coding region was replaced with the H2B-Citrine coding region from pCS2-H2B-Citrine (a gift from the Sean Megason lab (Megason, 2009)). The α-crystallin promoter driving RFP was taken from previously described constructs (Gerety & Wilkinson, 2011) and inserted 3' to the expression cassette.

Embryos were injected at the 1 cell stage with 200 pg mRNA encoding left and right *egr2b* TALENs and 30 pg donor plasmid. H2B-Citrine expression was detected in injected embryos by IHC. At 3 dpf, injected embryos were screened for presence of RFP expression in the lens and raised to adulthood.

2.8 CRISPR/Cas9-mediated homology-independent knock-in

The general strategy used by Kimura *et al*, 2014 was followed, with differences as described in Chapter 3.

2.8.1 Genomic DNA sequencing and target selection

The region upstream of the zebrafish *egr2b* gene was amplified from genomic DNA isolated from individual wildtype embryos at 3 dpf using the following primers:

Forward primer: GCAGTTTCTAAACCCACGGG
Reverse primer: CACAAAGCCACCGAGACTCA

This sequence of the gDNA region was verified by Sanger sequencing (GATC Biotech). No polymorphisms were detected within the amplified region.

Potential gRNA target sites were selected both manually and using CHOPCHOP (Montague *et al*, 2014); predicted off-targets were predicted using CHOPCHOP and ZiFit Targeter software (http://zifit.partners.org/ZiFiT/ChoiceMenus.aspx) (Sander *et al*, 2007, 2010). ZiFit was also used to design the oligonucleotides to be cloned to create gRNAs (for sites with only one GG, an additional GG was manually added to the sequence prior to submission to ZiFit for oligonucleotide selection).

2.8.2 gRNA synthesis and injection

gRNA synthesis broadly followed the Joung lab protocol for constructing guide RNA expression vectors (Hwang *et al*, 2013). To create a gRNA expression vector, two oligonucleotides (shown in Table 2-10) were annealed: the oligonucleotides (at a final concentration of 2 µM each) were combined with annealing buffer (40 mM Tris-HCl pH 8.0; 2 mM $MgCl_2$; 50 mM NaCl; 1 mM EDTA pH 8.0) in a 10 µl reaction. A thermocycler was used to heat the sample to 95 °C, then cool the sample to 4 °C at a rate of 1 °C per 30 seconds. 3 µl of annealed oligonucleotides were then directly used in a 10 µl ligation reaction. The annealed oligonucleotides were cloned into a BsaI-HF-digested pDR274 vector (Addgene #42250). The mBait gRNA expression vector was cloned by Qiling Xu in the Wilkinson lab.

gRNAs were synthesised *in vitro* from the T7 promoter in these plasmids using the T7 RiboMAX™ Large Scale RNA Production System (Promega) and purified using the RNeasy ® Mini Kit (Qiagen). Cas9 RNA was synthesised from Addgene plasmid #42251. Embryos were injected at the one cell stage with 50 – 200 pg gRNA and 200 pg cas9 RNA.

Table 2-10 gRNA targets and corresponding oligonucleotide sequences

All sequences are given 5' to 3'. Where the 5' "GG" is absent from the genomic sequence, this is indicated in brackets

Name	Target Sequence	Oligonucleotide 1 Sequence	Oligonucleotide 2 Sequence
Egr2b gRNA1	(GG)ATTCTGAGCTATCCAGTACGG	TAGGATTCTGAGCTATCCAGTA	AAACTACTGGATAGCTCAGAAT
Egr2b gRNA2	(GG)TTTCCGATGCTCAATTTCCGG	TAGGTTTCCGATGCTCAATTTC	AAACGAAATTGAGCATCGGAAA
Egr2b gRNA3	(GG)AGGGGTGTAGATGTTTACCGG	TAGGAGGGGTGTAGATGTTTAC	AAACGTAAACATCTACACCCCT
Egr2b gRNA4	(GG)ACGAGCGCCCGTACAGAAAGG	TAGGACGAGCGCCCGTACAGAA	AAACTTCTGTACGGGCGCTCGT
Egr2b gRNA5	(GG)ACGTGTCACCGCATTGATAGG	TAGGACGTGTCACCGCATTGAT	AAACATCAATGCGGTGACACGT
Egr2b gRNA6	(C)CAACACAGAGCCGTCAGATGG	TAGGCAACACAGAGCCGTCAGA	AAACTCTGACGGCTCTGTGTTG
Hoxb1a gRNA1.1	GGAGGCTTTTCTCGATTTCTCAGG	TAGGAGGCTTTTCTCGATTTCTCAGG	AAACCCTGAGAAATCGAGAAAAGCCT
Hoxb1a gRNA5.1	GGTGCGCTGACAAACTTCTGGAGG	TAGGTGCGCTGACAAACTTCTGGAGG	AAACCCTCCAGAAGTTTGTCAGCGCA
Hoxb1a gRNA6	GGTCACGGCGCCAATGGTGAGGGG	TAGGTCACGGCGCCAATGGTGAGGGG	AAACCCCCTCACCATTGGCGCCGTGA
Hoxb1a gRNA4	GGCACGAGCAAATACTCCAGAGG	TAGGCACGAGCAAATACTCCAGAGG	AAACCCTCTGGAGTATTTGCTCGTG
mBait gRNA	GGCTGCTGCGGTTCCAGAGGTGG	TAGGCTGCTGCGGTTCCAGAGG	AAACCCTCTGGAACCGCAGCAG

2.8.3 Donor plasmid construction and modification

H2B-Citrine Donor Plasmid (v1) was created by modifying an existing donor plasmid with a pBluescript II KS backbone (*egr2b* Citrine Donor Plasmid), modified from a previous version of the *egr2b* H2B-Citrine Donor Plasmid for TALEN-mediated gene knock-in, lacking the α-Crystallin promoter driving RFP. A 207 bp region was excised from this plasmid using SacI and AatII, removing the *egr2b* TALEN target site, attP site and p2a sequence. Phosphorylated oligonucleotides containing the mBait gRNA target site and additional restriction enzyme sites for future cloning options were annealed and ligated to the donor plasmid backbone.

Oligonucleotides to incorporate the mBait gRNA target site and restriction enzyme sites to create mBait-H2B-Citrine Donor Plasmid (v1):

Oligonucleotide 1:
AGCGCGGCTGCTGCGGTTCCAGAGGTGGATCGATCTCGAGAAGCTTGACGT
Oligonucleotide 2:
CAAGCTTCTCGAGATCGATCCACCTCTGGAACCGCAGCAGCCGCGCT

H2B-Citrine Donor Plasmid (v2) was created by addition of a Kozak sequence to the 5' end of the H2B-Citrine coding sequence (Kozak, 1987). To achieve this, the entire H2B-citrine coding sequence and polyA (1371 bp) was excised from H2B-Citrine Donor Plasmid (v1) using HindIII and NotI and replaced with a canonical Kozak sequence GCCACC, H2B-Citrine coding sequence and polyA (1384 bp) amplified from pCS2-H2B-Citrine (a gift from the Sean Megason lab) using the following primers:

Forward primer: GATCAAGCTTCTGCAGTCGACGGTACCGCCACC
Reverse primer: CGCCGCGGCCGCGAATTAAAAAACCTCCCACAC

H2B-Citrine Donor Plasmid (v3) (also referred to as mBait-cFos-H2B-Citrine Donor Plasmid) (see Appendix 8.2) was created by the addition of the cFos minimal promoter sequence between the mBait gRNA target sequence and H2B-citrine

coding sequence of H2B-Citrine Donor Plasmid (v2), digested using ClaI and HindIII. Oligonucleotides containing the cFos minimal promoter sequence were annealed and ligated with the linearised H2B-Citrine Donor plasmid (v2).

Oligonucleotide 1:
CGATCCAGTGACGTAGGAAGTCCATCCATTCACAGCGCTTCTATAAAGGCGC
CAGCTGAGGCGCCTACTACTCCAACCGCGACTGCAGCGAGCAACTA
Oligonucleotide 2:
AGCTTAGTTGCTCGCTGCAGTCGCGGTTGGAGTAGTAGGCGCCTCAGCTGGC
GCCTTTATAGAAGCGCTGTGAATGGATGGACTTCCTACGTCACTGGAT

Embryos were injected with the following at the one cell stage:

10-20 pg Donor plasmid
100 pg gRNA (genomic gRNA)
50 pg mBait gRNA
350 pg Cas9 RNA

F_0 founders were screened by mosaic H2B-Citrine fluorescence and raised to adulthood.

2.9 Software

ZEN 2010 (Zeiss)
Leica Confocal Software (LCS) (Leica Microsystems)
ImageJ (NIH)
FluoRender (v. 2.19.4 and 2.20.0) (University of Utah)
Adobe Illustrator CS5.1 (Adobe)
High Resolution Melting (HRM) Software V2.0.2 (Life Technologies)

Chapter 3. Studying cell identity regulation in border sharpening

3.1 Introduction

During my project I aimed to investigate the contribution of cell identity regulation to hindbrain border sharpening. Possible mechanisms that may contribute to hindbrain border sharpening include Eph/ephrin-mediated cell sorting, plasticity of cell fate and selective elimination of misplaced cells. Current evidence does not suggest that selective cell death has a significant role in border sharpening, as there is no apparent increased cell death at segment interfaces during sharpening, which would be expected if misplaced cells were selectively removed at borders. Although there is evidence to indicate that cell mixing occurs between segments (Fraser *et al*, 1990), the extent to which cell identity switching occurs *in vivo* and contributes to border sharpening is not clear.

While cell transplantation experiments have demonstrated that cells are capable of changing their *hox* expression status when challenged by artificial situations where they are in the vicinity of cells of a different identity (Grapin-Botton *et al*, 1995; Trainor & Krumlauf, 2000b; Schilling *et al*, 2001), it is not clear whether this contributes to border sharpening. At 10 ss, the majority of cells transplanted between rhombomeres are capable of changing their *hox* expression, while at 15 ss, only 40% of cells changed their identity. These results indicate that cells are capable of changing their identity at the stages when cells are known to intermingle between rhombomeres. By the stage that cells lose this plasticity, mixing of cells between rhombomeres is restricted (Fraser *et al*, 1990).

In order to assess the contribution of identity regulation to border sharpening, it is necessary to monitor the identity and behaviour of cells during the process of border sharpening. To date, there are limited *in vivo* studies using reporter lines to study border sharpening in live embryos. A recent study monitored rhombomere border sharpening within a transgenic zebrafish line in which the chick *Egr2* autoregulatory element A drives GFP expression in r3 and r5 (Calzolari *et al*, 2014). The findings of this study support cell sorting, mediated by Eph/ephrin signalling, as

the major mechanism of border sharpening and no contribution of identity switching was observed; using self-maintained expression of a different reporter, which perdures beyond the timescale of border sharpening, did not indicate presence of any ectopic cells outside r3 or r5 once sharpening of gene expression domains is complete (Calzolari *et al*, 2014).

In order to study the contribution of cell identity regulation to hindbrain border sharpening, I created a novel zebrafish reporter line to label cells that express *egr2b* throughout the time at which border sharpening occurs, enabling visualisation of cell identity during border sharpening. Using this novel reporter line, I aimed to assess the relative contributions of cell identity regulation and cell sorting to hindbrain border refinement, through a combination of time lapse imaging during border sharpening and analysis of fixed samples after completion of border sharpening.

Results

3.2 Expression of *egr2b* and rhombomere border sharpening

A suitable target gene to create a reporter line to study rhombomere border sharpening is *egr2b*. Egr2b is expressed in and required for the segmentation of r3 and r5; a reporter of *egr2b* expression is therefore useful for monitoring border sharpening at the interfaces between r2/3, r3/4, r4/5 and r5/6. Because of its early, segmented expression in the hindbrain, e*gr2b* expression is frequently used to illustrate the fuzziness of rhombomere borders at early stages and the sharpening of these borders during hindbrain segmentation; for example in (Oxtoby & Jowett, 1993; Cooke *et al*, 2005).

In zebrafish, a protein with high sequence similarity to Egr2b – Egr2a (formerly known as Frb35) – has been shown to have a similar expression pattern to *egr2b* (Sun *et al*, 2002). Very little is known of the role of Egr2a in hindbrain segmentation, but due to the high sequence similarity with Egr2b, it is likely that there is functional redundancy between these two proteins. Because *egr2a* is first expressed slightly later than *egr2b*, and at lower levels (Sun *et al*, 2002), *egr2b* is a more suitable

target gene for the novel reporter line. To verify the suitability of *egr2b* as a marker of rhombomere identity during border sharpening, I have studied the localisation of *egr2b* mRNA during border sharpening. I carried out *in situ* hybridisation (ISH), examining *egr2b* expression at approximately 20 minute intervals, corresponding to the generation of successive somites from 1 somite stage (ss) (10.3 hpf), shortly after *egr2b* expression is first detected, to 9 ss (13 hpf) when *egr2b* expression has been reported to be sharp (Oxtoby & Jowett, 1993).

As shown in Figure 3-1, *egr2b* is expressed in presumptive r3 at 1 ss (10.3 hpf) and shortly after, expression in r5 is first detected between 1-2 ss. This difference in timing likely reflects the different factors contributing to initiation of *egr2b* expression in r3 and r5. The expression patterns shown in Figure 3-1 also illustrate the change in shape of early *egr2b* expression domains that occurs during early hindbrain patterning. *Egr2b* expression in each of pre-r3 and pre-r5 initially consist of two separate stripes (Figure 3-1 A), which merge to form curved, chevron-shaped domains by 3 ss (Figure 3-1 B). Convergent extension cell movements drive the narrowing of these domains along the neuroaxis; domains become straighter, shorter (laterally) and thicker (AP). At 8 ss, *egr2b*-expressing neural crest cells are observed migrating out of r5 into r6 and later into pharyngeal arches at 9 ss (Figure 3-1 G,H). Ectopic cells expressing *egr2b* can be detected outside of r3 /5 as late as 7 ss, although by this stage a considerable amount of sharpening has already occurred. Borders of *egr2b* expression become fully sharp and straight at 9 ss, which coincides with the morphological appearance of rhombomeres. The process of sharpening of the *egr2b* expression domain therefore occurs over approximately three hours from the initial onset of *egr2b* expression.

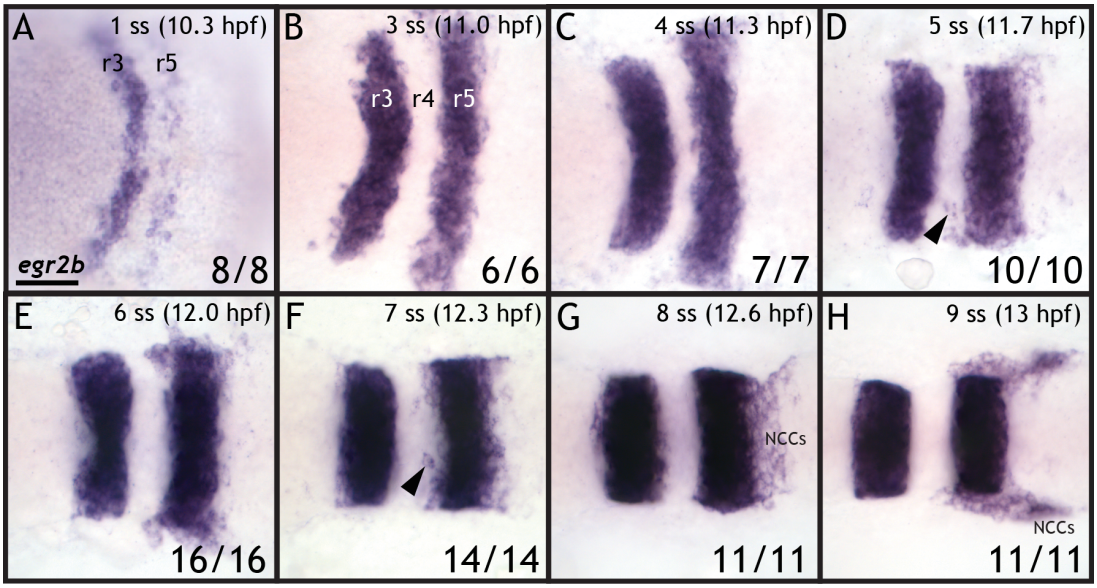

Figure 3-1 Time course of *egr2b* expression and hindbrain border sharpening

Expression of *egr2b* expression from 10.3 hpf (1 ss) to 9 ss (13 hpf) (A-H), showing sharpening of expression and change in shape of *egr2b* expression domains. Embryos are flat-mounted, with anterior to the left. Representative embryos for each stage are shown; numbers of embryos observed that are represented by the image, out of the total number of embryos studied, are shown in the bottom right. Arrowheads indicate ectopic cells expressing *egr2b* in r4. NCCs, neural crest cells. Scale bar: 50 μm.

An additional factor involved in hindbrain segmentation is Hoxb1a, which confers identity to cells of r4 (Bell *et al*, 1999; Rohrschneider *et al*, 2007). It has previously been reported that at early segmentation stages, cells that co-express *egr2b* and *hoxb1a* can be detected, which is consistent with these cells resolving or changing their identity (Zhang *et al*, 2012). In order to study the co-expression of *egr2b* and *hoxb1a*, I carried out two colour fluorescent ISH using probes against both *hoxb1a* and *egr2b*. As shown in Figure 3-2 (A-C), at 3 ss, when the expression domains of *egr2b* are not yet sharp, some *egr2b*-positive cells in presumptive r4 co-express *hoxb1a* (Figure 3-2 A'-C'). Similarly, cells at the interfaces of r3/4 and r4/r5 can also co-express *egr2b* and *hoxb1a* (Figure 3-2 A''-C''). As expression domains sharpen, the extent of this co-expression is reduced, and by 6 ss cells at rhombomere interfaces rarely appear to co-express *egr2b* and *hoxb1a* (Figure 3-2 D-F). These results are in agreement with previous studies of the co-expression of *egr2b* and *hoxb1a* (Zhang *et al*, 2012).

If cells between rhombomeres 3, 4 and 5 change identity, their expression profile may change from *hoxb1a*$^{+}$/*egr2b*$^{-}$ to *hoxb1a*$^{-}$/*egr2b*$^{+}$ and vice versa. The observed co-expressing cells may therefore arise due to cells changing identity via an intermediate dual identity. Alternatively, induction of both *egr2b* and *hoxb1a* expression may overlap within these cells, resulting from noisy RA signalling in early specification (Zhang *et al*, 2012; Sosnik *et al*, 2016) and are yet to be resolved by cross-repression between these factors. In addition, it is known that Hoxb1 contributes to initiation of *egr2b* expression in r3, which may also explain the presence of transcripts for these two conflicting factors in the same cells at early stages (Wassef *et al*, 2008; Labalette *et al*, 2015). It is more likely that most co-expressing cells at rhombomere borders occur due to initial overlapping identity, while cells more centrally-located within rhombomeres that co-express *hoxb1a* and *egr2b* are in the process of completely switching from one identity to the other.

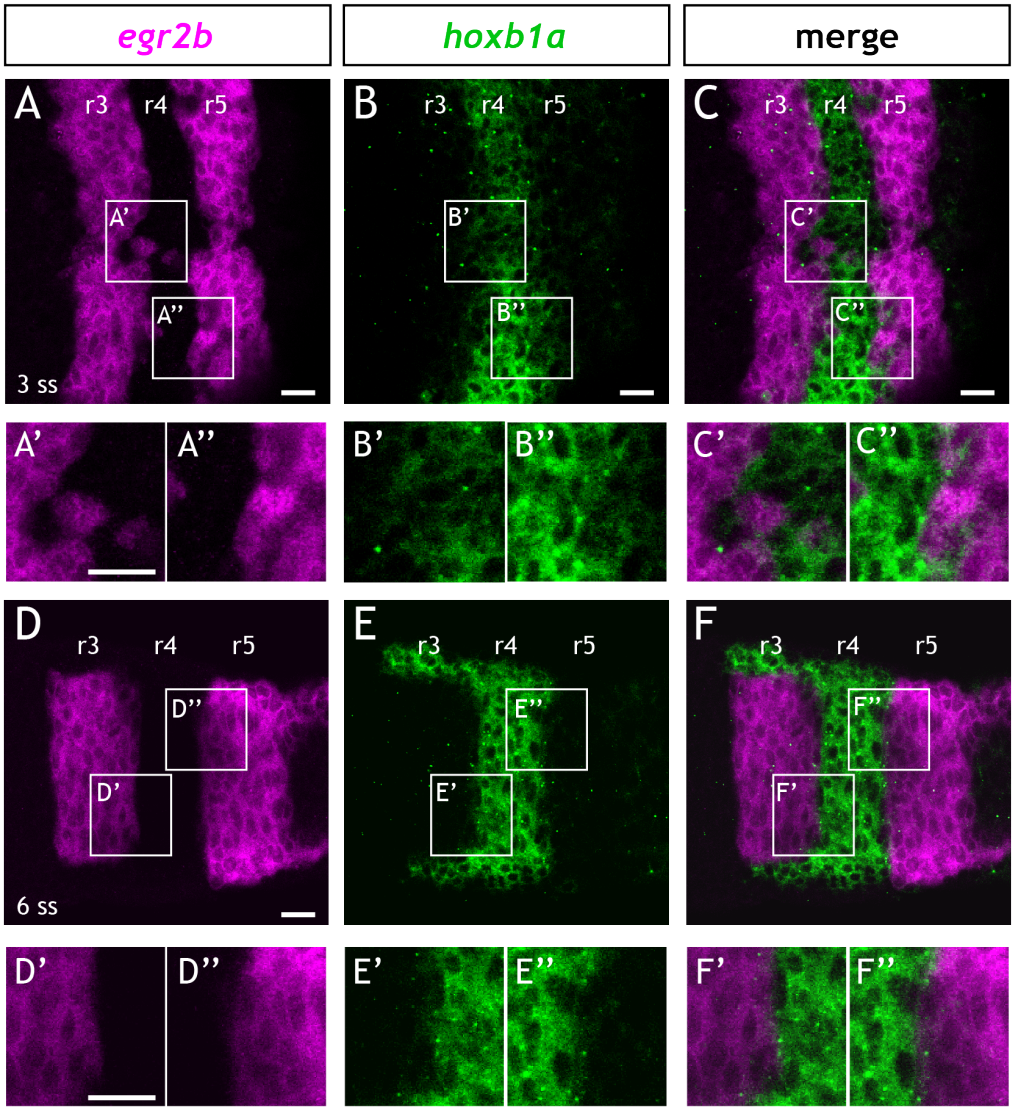

Figure 3-2 Expression of *egr2b* and *hoxb1a* during early hindbrain segmentation
Double *in situ* hybridisation showing expression of *egr2b* (magenta) and *hoxb1a* (green) during early segmentation, when expression domains are jagged in shape. Cells co-expressing *hoxb1a* and *egr2b* are detectable at the jagged interfaces r3, r4 and r5 at 3 ss (A-C; n = 5 embryos), but not at 6 ss (D-F; n = 6 embryos). Embryos are flat-mounted with anterior to the left. Scale bars: 20 μm.

An alternative approach to creating a new reporter line, which I considered taking, is to make use of the existing pGFP5.3 line, where the *pax2a* promoter and 5' untranslated region drives eGFP expression (Picker *et al*, 2002). In this line, eGFP is expressed not only within the Pax2a expression domain, but also in r3 and r5 (Picker *et al*, 2002). It has been suggested that expression in r3 and r5 arises from

a lack of additional repressive inputs to the transgene expression that repress endogenous *pax2a* expression here. It is unlikely that an enhancer trap event has occurred to explain transgene expression in r3 and r5 because the same ectopic expression is observed in two separate lines, with different reporter genes. A new *pax2a* reporter line, in which eGFP is inserted at the genomic locus of *pax2a*, does not show any reporter expression outside the *pax2a* expression domain (Ota *et al*, 2016). Because it is not clear what drives eGFP expression in the pGFP5.3 line, this line may not be suitable for studying hindbrain border sharpening – eGFP expression in r3 and r5 may not be driven by Egr2b itself. Moreover, I found that eGFP expression is also detectable at weak levels in r2 during border sharpening in pGFP5.3, while eGFP transcripts are not detectable in r5 until 6 ss, by which time a substantial amount of border sharpening has already occurred (Appendix Figure 8-1). This restricts the usefulness of the pGFP5.3 line to monitoring sharpening of the r3/4 border only, and therefore I did not pursue this approach further.

3.3 Creation of Tg[egr2b:H2B-Citrine] by CRISPR/Cas9-mediated targeted insertion

3.3.1 Overview of approaches for reporter line generation in zebrafish

In zebrafish, unlike mammalian model organisms, such as mouse, classic gene targeting and insertion by homologous recombination (Capecchi, 2005), is not a feasible approach for insertion of exogenous DNA. This is due to the low efficiency of homologous recombination, combined with a lack of an established embryonic stem cell line for zebrafish, requiring intensive screening for low frequency insertions to be conducted in the organisms themselves. There are currently several alternative approaches available for generation of reporter lines in zebrafish. During the course of my project, several additional approaches have also emerged. Here I will give an overview of the techniques available and explain my decisions for the approaches I selected.

BAC Transgenesis

A popular approach to creating zebrafish reporter lines uses bacterial artificial chromosome (BAC)-based DNA constructs, in which large chromosomal regions containing regulatory elements for a gene of interest are integrated into the zebrafish genome using Tol2 transposon-mediated transgenesis (Balciunas *et al*, 2006; Kawakami, 2007). BAC-based DNA constructs enable cloning and propagation of large DNA fragments, up to 300 kb in size (Shizuya *et al*, 1992; Suster *et al*, 2009). An advantage of BAC transgenesis is that it does not require that the regulatory regions for the target gene of interest are fully identified in order to achieve accurate recapitulation of its expression, and can therefore be used as an alternative to approaches using short constructs containing specific, identified regulatory regions. In addition, it is thought that a combination of the large size of the transgene and inclusion of additional *cis*-regulatory elements – such as enhancers, silencers and locus control regions (LCRs) – improves the ability of the inserted reporter to fully recapitulate the target gene's expression.

An additional advantage of BAC transgenesis is the ability to easily (albeit through random occurrence) insert multiple copies of a construct containing the gene for a fluorescent reporter within the genome, resulting from the nature of Tol2-mediated transgenesis (Kawakami, 2007), which can increase brightness and detection of the reporter. However, this can also be problematic during generation of a stable transgenic reporter line due complications of varied copy numbers of the transgene between siblings. An additional limitation of BAC-mediated transgenesis in zebrafish arises from the non-specific nature of Tol2-mediated transgene integration in the genome. Local position effects, such as chromatin architecture, may prevent the reporter from accurately recapitulating the target gene's expression pattern. In addition, fairly low germline transmission rates have been reported for BAC transgenesis in zebrafish of 1-5% or less (Yang *et al*, 2006; Higashijima, 2008) and the time taken to create constructs for injection, combined with screening for germline transmission, can be costly.

In zebrafish, enhancer elements B and C, which drive initiation of *egr2b* expression, have been identified, and are located within 100 kb upstream of *egr2b* (Chomette *et al*, 2006; Labalette *et al*, 2011, 2015). In zebrafish, a 1 kb fragment that can drive

specific expression of a reporter gene in r3 and r5 has been identified and is thought to contain the additional autoregulatory element A (Bouchoucha *et al*, 2013). However, it is known that the chick *egr2* enhancer element C not only drives reporter expression in r3 and r5, but also in rhombomere 4 in both mouse and zebrafish, where *egr2b* itself is not expressed (Chomette *et al*, 2006; Labalette *et al*, 2015). It is thought that this discrepancy in reporter expression is due to an inability of additional repressive elements (that do affect *egr2b* expression) to repress reporter expression here. It is unclear whether these additional, unknown elements will be included in a BAC to recapitulate *egr2b* expression. For these reasons, and due to recent developments in targeted genomic insertion of reporters (reviewed in Beil *et al*, 2012 and discussed below), I decided to use alternative methods to BAC transgenesis to create an *egr2b* reporter line.

Targeted genome insertion using custom nucleases

In recent years, there have been significant developments of technologies for targeted insertions within the zebrafish genome. Zinc-finger nucleases (ZFNs) (Durai *et al*, 2005), transcription activator-like effector (TALE) nucleases (hereafter referred to as TALENs) (Cermak *et al*, 2011) and the type II clustered regularly interspaced short palindromic repeats (CRISPR)/CRISPR-associated protein (Cas) system (Jinek *et al*, 2012) can be used to created site-specific double-stranded DNA breaks (DSBs) within the genome. As discussed in greater detail in Chapter 4, TALENs consist of a FokI nuclease fused to an array DNA-binding elements (Miller *et al*, 2011). When a pair of TALENs bind to their target sequences within the genome, the FokI nuclease is able to cut within the intervening DNA sequence, creating a DSB. The CRISPR/Cas9 system has been adapted from a bacterial adaptive immune mechanism. As shown in Figure 3-3, this system includes the Cas9 nuclease, CRISPR RNA (crRNA) – which contains approximately 20 bases of complementary sequence to the target sequence followed by the protospacer-adjacent motif (PAM) sequence “NGG” and mediates the RNA-DNA interaction at the target site – and a *trans*-activating crRNA (tracrRNA), which interacts with crRNA and Cas9 nuclease. The crRNA and tracrRNA have since been incorporated into a single guide RNA (gRNA) (Jinek *et al*, 2012). The Cas9/gRNA complex is capable of causing targeted DSBs in the genome as shown in Figure 3-3. The CRISPR/Cas9 system was first reported to create targeted mutations in

cultured human cells (Cong *et al*, 2013; Mali *et al*, 2013); and shortly after was also used to create targeted mutations in zebrafish (Hwang *et al*, 2013).

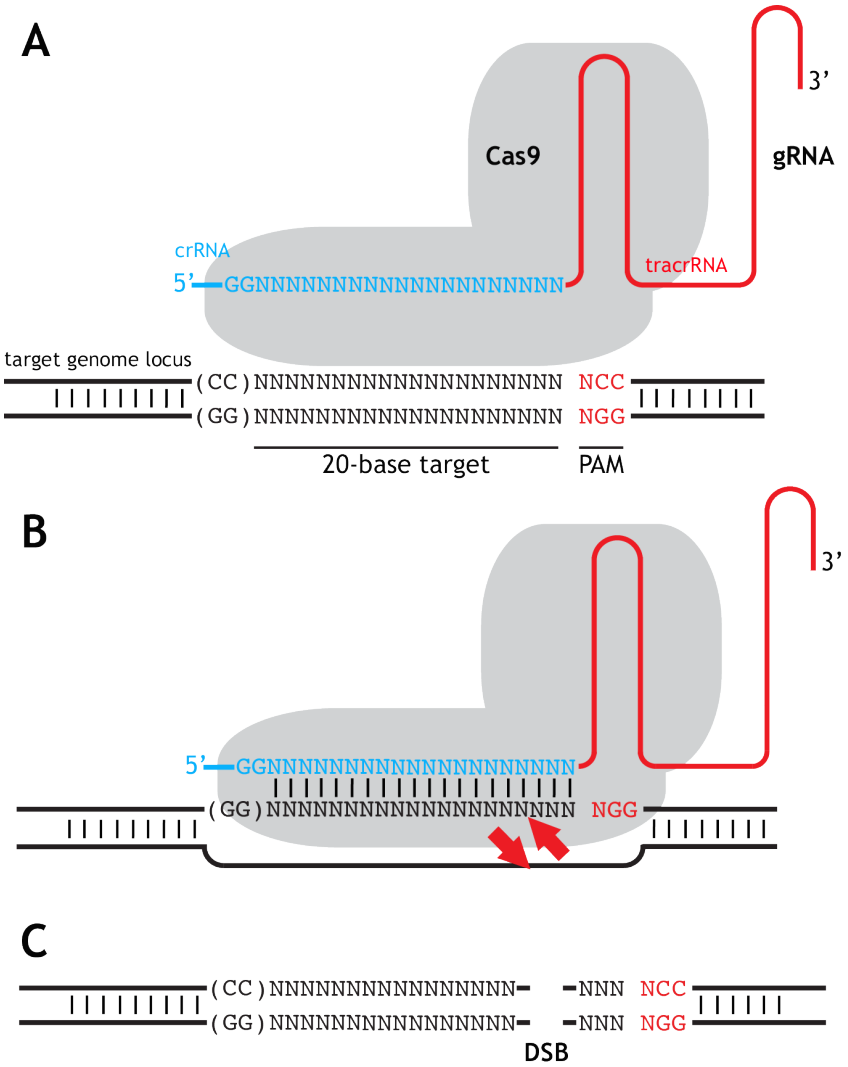

Figure 3-3 CRISPR/Cas9-mediated targeted DSB creation

A: A Cas9-nuclease (grey) forms a complex with a gRNA, consisting of crRNA (blue) and tracrRNA (red); The crRNA has approximately 20 bases of complementarity to the target site in the genome, which has a 3' protospacer adjacent motif (PAM) domain.

B: Binding of the Cas9-gRNA complex to the complementary target sequence in the genome causes the Cas9 nuclease to cut both strands of the genomic DNA between 3 and 7 bases upstream of the PAM; this causes creation of a double-stranded DNA break (DSB) (C).

Once targeted DSBs have been created within the genome by any of these approaches, appropriate donor DNA can become inserted at the target site via

various repair mechanisms, including homologous recombination (HR) and non-homologous end-joining (NHEJ). HR requires a homologous DNA sequence to the damaged strand to be repaired, in contrast to NHEJ, which does not require a homologous template to be present.

Homologous recombination

HR-mediated knock-in in zebrafish is limited largely by its low efficiency, despite the fact that the frequency of HR is enhanced by DSB formation (Rouet *et al*, 1994). Insertion of DNA at TALEN-induced DSBs using 1 kb homology arms causes knock-in and transmission with 1.5% frequency (Zu *et al*, 2013), which limits the suitability of this approach for systematic targeted insertions. An additional drawback of HR-mediated genome insertion is that the construction of the donor vector, incorporating long homology arms, is fairly complicated and time-consuming. Therefore, at the time at which I was selecting a knock-in strategy to take, HR did not appear to be a suitably efficient approach. More recently, however, it has been demonstrated that using homology arms of different lengths improves the efficiency of HR-mediated genome insertion at TALEN-induced DSBs to 10% germline transmission (Shin *et al*, 2014). HR-mediated knock-in using the CRISPR/Cas9 system, with CRISPR target sites flanking the insertion cassette, has comparable germline transmission efficiency (10%) (Irion *et al*, 2014).

Non-homologous end-joining

A different method of insertion of exogenous DNA at DSBs uses the alternative non-homologous end-joining (NHEJ) repair mechanism. This technique has five times greater transformation efficiency than HR in both cultured cells (Cristea *et al*, 2013; Maresca *et al*, 2013) and zebrafish (Auer *et al*, 2014a; Kimura *et al*, 2014). Because this approach does not require long regions of homology, construction of the donor plasmid is far simpler than for homology-mediated insertion. However, NHEJ is inherently more error-prone than HR, and may therefore give rise to indel mutations at the target site, reducing the precision of integration, with potential consequences for transgene expression.

3.3.2 Reporter selection for studying the extent of cell identity regulation

As illustrated in Figure 3-4, stable reporters that perdure beyond the time at which gene expression borders in the hindbrain become sharp can be used to study the extent of identity regulation during border sharpening. Cells that activate *egr2b* expression – and therefore also reporter expression – will contain the stable reporter protein after sharpening is complete. This means that any r3 or r5 cells that switch to an alternative identity should be detectable by presence of the reporter protein, even though *egr2b* will have been downregulated. As previously shown in Figure 3-2, co-expression of *egr2b* and *hoxb1a* at rhombomere borders in early segmentation occurs, strongly suggesting that some cells that have initially expressed *egr2b* may ultimately have an r4 identity.

I selected the YFP variant Citrine, fused to histone H2B, as the fluorescent reporter protein to monitor cell identity switching. Citrine is a fast-folding and bright yellow fluorescent protein, 75% brighter than eGFP and at least three-times as photostable as an alternative, fast-folding YFP variant, Venus (Heikal *et al*, 2000; Griesbeck *et al*, 2001; Nagai *et al*, 2002). Fusion of Citrine to the histone protein H2B will cause accumulation and concentration of the reporter within the nuclei of cells, which should improve detection of the reporter and aid tracking of reporter-expressing cells. In addition, fusion of H2B to proteins has also been found to significantly increase their stability, which means the reporter protein will still be present and detectable after sharpening has occurred (Brennand *et al*, 2007; Ninov *et al*, 2012).

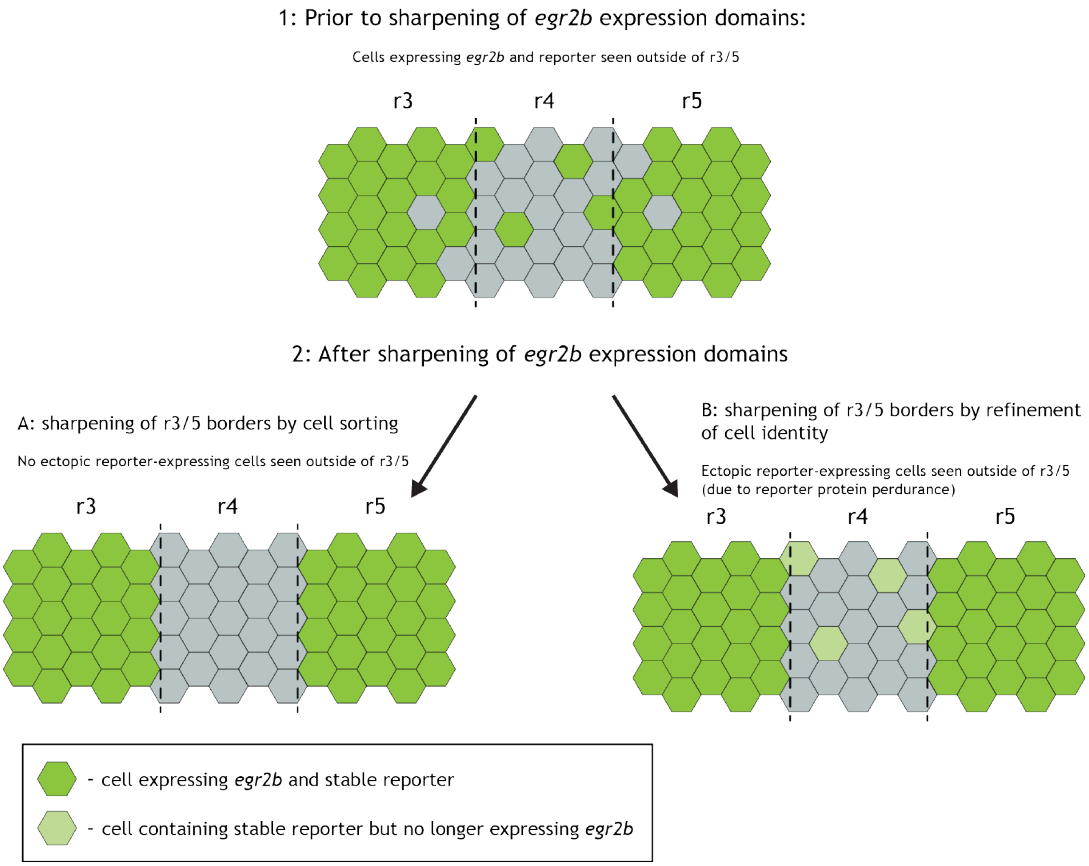

Figure 3-4 Using stable reporters of gene expression to study the contribution of identity regulation to border refinement

At early stages, reporter protein distribution should reflect the expression pattern of the target gene, *egr2b* (1). After sharpening of egr2b expression, no ectopic *egr2b*-expressing cells will be detectable outside r3 or r5 (2). If border sharpening is mediated purely by cell sorting, ectopic cells containing the stable reporter protein will be detectable outside r3 and r5 after sharpening of gene expression domains (A). In contrast, cells that switch identity will still contain stable reporter protein once border sharpening is complete (B).

3.3.3 TALEN-targeted NHEJ-mediated insertion within the coding region of *egr2b*

The initial approach that I took to insert H2B-Citrine at the *egr2b* locus utilised the ability of TALENs to induce targeted double-stranded DNA breaks within the genome, resulting in non-homologous integration of donor DNA, developed by Constable, 2015, as shown in Figure 3-5 (Constable, 2015). This uses 4-5 nucleotide overhangs at the DSB created by FokI to mediate seemingly precise

ligation via NHEJ of donor DNA, digested by the same TALENs at the target site (Miller *et al*, 2011; Maresca *et al*, 2013). As shown in Figure 3-5, this approach inserts the reporter within the coding sequence of the target gene, and a self-cleaving p2A peptide sequence is provided upstream of the reporter gene in the construct for multicistronic expression, preventing creation of an Egr2b-H2B-Citrine fusion protein (Szymczak *et al*, 2004). However, this means that for reporter synthesis to occur, integration must occur precisely so that insertion is in-frame, although good germline transmission rates of 26% – not taking insertion frame into account – have been observed (Constable, 2015). An additional potential limitation of this approach is that reporter insertion within the coding region of the target gene is likely to compromise the function of the targeted gene, although this may not have deleterious effects in embryos heterozygous for the insertion, as heterozygous Egr2b mutants appear to exhibit normal hindbrain patterning (Bouchoucha *et al*, 2013).

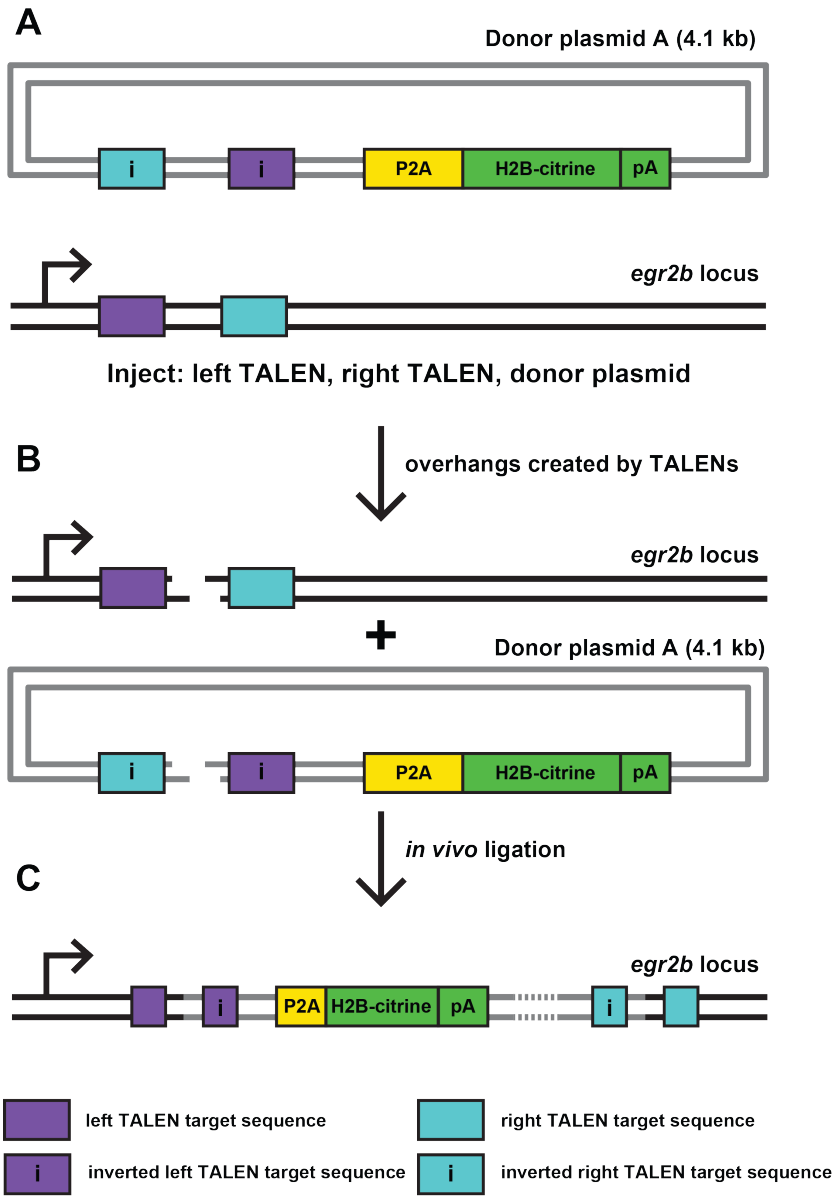

Figure 3-5 TALEN-mediated reporter knock-in scheme

A: The sites bound by left (purple) and right (blue) TALENs at the *egr2b* locus are shown; a donor plasmid contains the same TALEN targets sites, but inverted and flanking an uninverted spacer region.

B: When TALENs bind at their target sites, FokI is able to heterodimerise (from two monomers from the left and right TALENs) and creates double-stranded DNA breaks (DSBs) within both spacer regions in the genome and donor plasmid. The nature of this digest by FokI nuclease leads to creation of short single stranded overhangs at the cut site as shown. Because the spacer sequence within both the genome and donor plasmid are identical, the same overhangs are created within each region.

C: An *in vivo* ligation event repairs the DSBs, and can lead to integration of the entire donor plasmid at the TALENs target site in the genome; this ligation is mediated by the complementarity of the cut spacer regions in both the genome and donor plasmid.

Although TALEN synthesis is not as simple as the protocol for gRNA construction for the CRISPR/Cas9 system, the straightforward 5-day GoldenGate protocol for TALEN assembly was already well established in the Wilkinson lab (Engler *et al*, 2009; Cermak *et al*, 2011). I created a pair of TALENs targeting the *egr2b* locus and injected these with a donor plasmid containing the same TALEN target sites and H2B-Citrine reporter. Unfortunately, at the time that I began using this approach to insert H2B-Citrine at the *egr2b* locus, we did not appreciate how imprecise non-homologous insertion at the TALEN cut site was, which reduces the likelihood of in-frame transmission through the germline. This is likely due to the error-prone nature of NHEJ, but was not evident from previous reports of an equivalent technique *in vitro* (Maresca *et al*, 2013). I was never able to detect H2B-Citrine expression by eye in over 200 injected embryos, although some sparse expression could be detected by immunohistochemistry in 10% of injected embryos (2 out of 20). In order to improve selection of embryos with high likelihood of germline transmission of the insertion, we incorporated the α-crystallin promoter, driving RFP expression (ACR) in the donor plasmid. In embryos in which the donor construct is inserted, RFP will be expressed in the lens of embryos from 3 dpf; this can enable pre-selection of F_0 embryos that are likely to transmit the inserted transgene through the germline. With this approach, I observed germline transmission of transgene insertion in 3.5% of injected embryos; however, none of these were inserted in frame with *egr2b* due to indel mutations occurring at the target site.

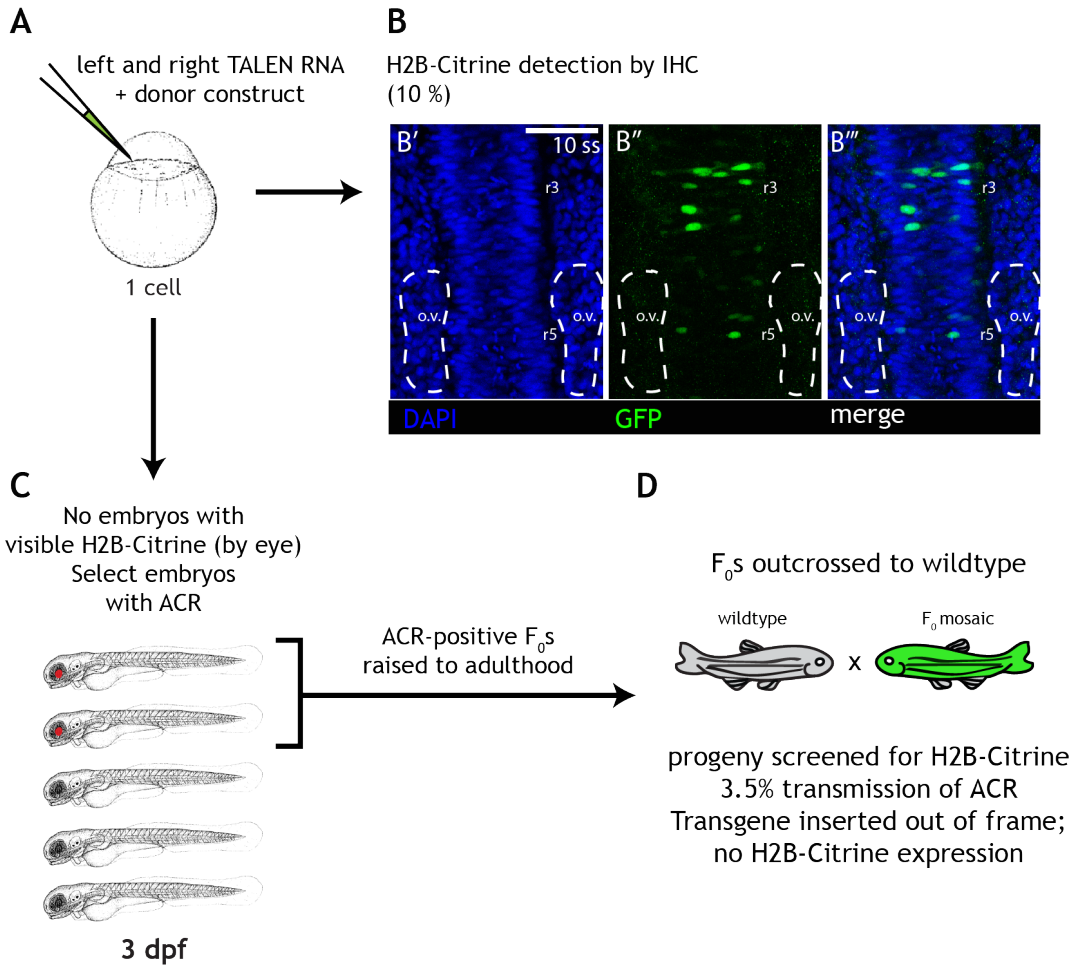

Figure 3-6 Methodology for TALEN-mediated reporter knock-in at *egr2b* locus

A: Embryos are injected at the one cell stage with RNA encoding left and right TALENs targeting egr2b, together with the H2B-Citrine donor plasmid.

B: Maximum intensity projection of an embryo (n = 2 out of 20 embryos) with sparse H2B-Citrine in r3 and r5. The embryo is flat-mounted, with anterior to the top. O.V., otic vesicle. Scale bar: 50 µm.

C: No H2B-Citrine was detectable by eye in injected embryos. Injected embryos with detectable α-Crystallin-RFP were raised to adulthood

D: F_0 adults were outcrossed to wildtypes and screened for ACR and H2B-Citrine; while 3.5% of F_0s transmitted the transgene through the genome, no H2B-Citrine was detected in these embryos, and sequencing confirmed that insertion had occurred out of frame with *egr2b*.

3.3.4 Targeted insertion of H2B-Citrine at the *egr2b* locus using the CRISPR/Cas9 system

Following my lack of success in creating a stable transgenic line by TALEN-mediated insertion of H2B-Citrine within the *egr2b* coding region, I adopted a different strategy to insert the reporter gene at the *egr2b* locus. Whilst my PhD was underway, developments in alternative targeted knock-in techniques were developed, and in recent years there have been several reports of efficient generation of targeted genome insertions in zebrafish using the CRISPR/Cas9 system in combination with homology-independent repair (Auer *et al*, 2014a; Kimura *et al*, 2014; Ota *et al*, 2016). Initially, Auer *et al* used the CRISPR/Cas9 system to insert long DNA fragments via homology-independent DSB repair within the eGFP coding region of existing transgenic lines with high efficiency (Auer *et al*, 2014a, 2014b). This involves an extremely efficient gBait gRNA, which cleaves within the eGFP gene, and provision of a donor vector, also containing the gBait target sequence. Both the gBait site in the transgene in the genome and the site in the donor vector are concurrently cleaved, causing integration of the donor plasmid at the target site. With this approach, 31% efficiency of forward integration (though not necessarily in frame) has been reported, which is further increased to 40% if combined with pre-selection of F_0s (Auer *et al*, 2014a). However, this approach is only suitable for insertion at pre-existing eGFP transgenes and is still limited by the necessity for in-frame and forwards integration of the donor plasmid. Subsequently, this method was modified and improved, demonstrating efficiency of insertion of reporter at any genomic site by providing two gRNAs: one targeting within the genome, and an unrelated but efficiently cleaved gRNA targeting a site within the donor vector (Kimura *et al*, 2014). The genome site and donor vector are both separately cleaved by CRISPR/Cas9 and these two unrelated DSBs are able to join, causing insertion of the reporter in the genome (Kimura *et al*, 2014). This method incorporated a *hsp70* promoter within the donor plasmid and targeted the region 200-600 bp upstream of the target gene for insertion, essentially creating an enhancer-trap. This means a significant advantage of this approach is that in-frame reporter insertion is no longer crucial for reporter expression, thus removing the need for precise integration, which should increase the efficiency of this technique. In addition, provision of a minimal promoter in donor plasmid means that both

forward and reverse integration in the genome should still permit reporter expression under endogenous *cis*-regulation elements. A further advantage of this approach is that a common donor vector can be used for integration at any target site in the genome.

A benefit of switching to the CRISPR/Cas9 system over TALENs for this approach is that potential target sites are far less constrained for CRISPR/Cas9: the only constraint in this case in a 3' GG (of the PAM domain of the gRNA), whilst TALEN target sites require two regions, with an intervening sequence of 14 – 17 bases, that will bind to TALENs optimally, maximising the number and distribution of strong TALEN-base interactions and minimising weak TALEN-base interactions as described (Streubel *et al*, 2012). This means that several different gRNAs targeting the region upstream of *egr2b* can be generated and tested to aid selection of an efficient gRNA.

For these various reasons, I proceeded to use the CRISPR/Cas9 system and NHEJ-mediated integration to insert the coding sequence for the fluorescent reporter H2B-Citrine with a minimal promoter at the *egr2b* locus, upstream of the transcriptional start site, thereby putting H2B-citrine expression under control of endogenous *cis*-regulatory elements of *egr2b*. As shown in Figure 3-7, the technique I adopted to create the Tg[egr2b:H2B-Citrine] reporter line was largely based on that previously used to insert *hs:Gal4* at the *evx2* locus, producing eGFP expression within the *evx2*-expression domain when crossed to a Tg[UAS:eGFP] line (Kimura *et al*, 2014). It is possible that there is some leakiness of the *hsp70* promoter, as Kimura *et al* reported some eGFP expression in cells without detectable expression of the target gene, Evx2. Therefore, rather than use the *hsp70* promoter, I used the mouse cFos minimal promoter, which is only active in zebrafish in the presence of additional enhancer elements and has previously been used in zebrafish enhancer trap techniques (Dorsky *et al*, 2002; Fisher *et al*, 2006; Scott & Baier, 2009). As an alternative to the gBait gRNA target site previously used by Auer *et al*, 2014a, the mBait gRNA target site, derived from the mouse *Mcr4* gene, is included in the donor vector, and will be efficiently cleaved by the corresponding mBait gRNA; this is because the gBait target sequence arises within the sequence of *citrine*.

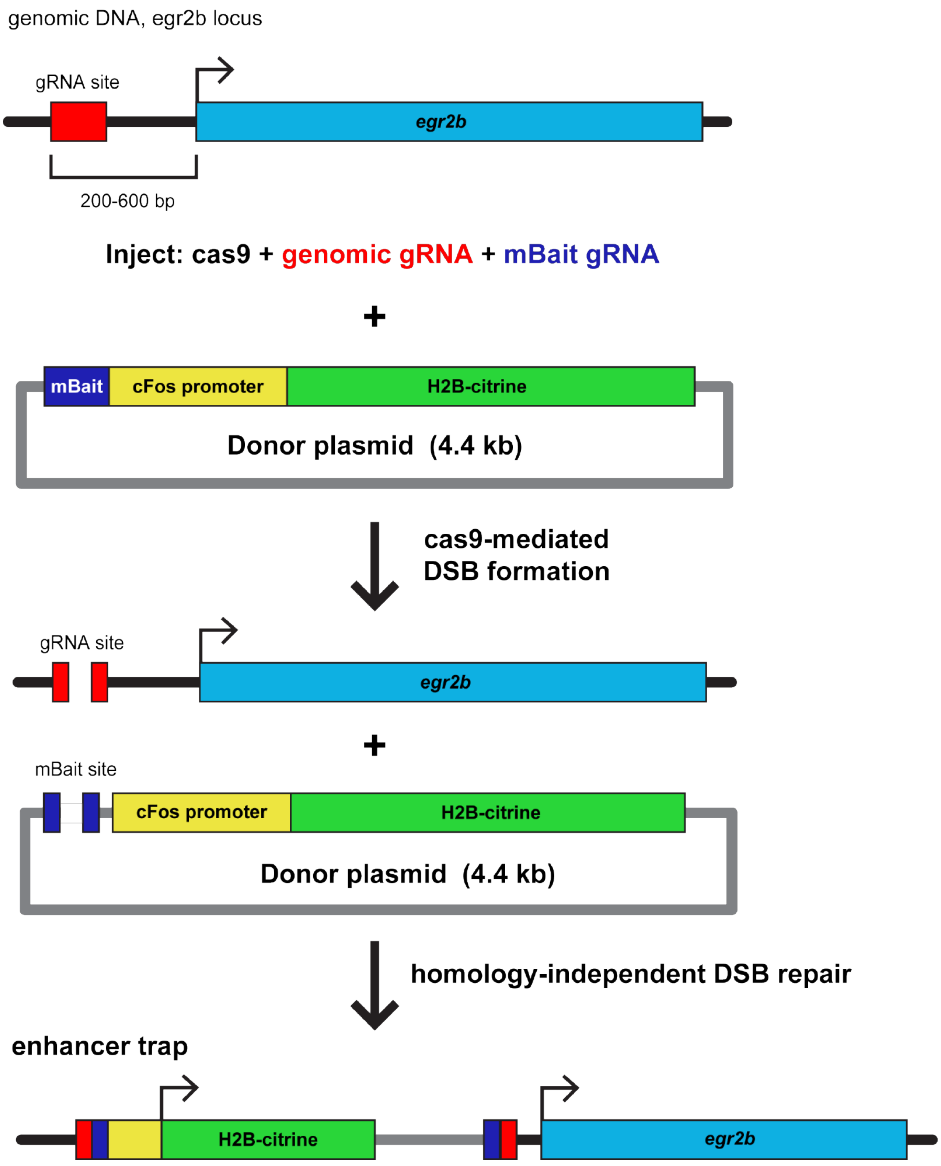

Figure 3-7 Scheme showing CRISPR/Cas9-mediated targeted integration of mBait-cFos:H2B-citrine at the *egr2b* locus

A gRNA site upstream of *egr2b* is selected and used to create a targeted DSB in the genome. A donor plasmid, containing the mBait gRNA target sequence (enabling *in vivo* linearisation by Cas9/mBait gRNA) provides the reporter gene and the cFos minimal promoter, which can subsequently integrate at the genome gRNA site, upstream of *egr2b*. Figure and approach based on Kimura *et al*, 2014.

Insertion of cFos:H2B-Citrine upstream of the transcriptional start site of *egr2b* should cause expression of H2B-citrine under control of endogenous *cis*-regulatory

elements of *egr2b*. As shown in Figure 3-8, I prepared 6 gRNAs targeting sequences between 740 and 50 bp upstream of the transcriptional start site of *egr2b*; 200 – 900 bp upstream of the translational start site (ATG) of *egr2b*. When injected together with the donor plasmid, I observed H2B-Citrine in approximately 5% of embryos injected with either gRNA1 or gRNA4, but not the other 4 gRNAs tested (data not shown). The donor plasmid ultimately used to create the Tg[egr2b:H2B-citrine] line (mBait-cFos-H2B-Citrine-pA Donor Plasmid) was created by several cumulative modifications to the donor construct previously used to insert H2B-Citrine at the *egr2b* locus. These modifications included removal of the TALEN target site, attP site and p2a sequence and addition of mBait gRNA sequence, cFos minimal promoter and Kozak sequence for H2B-Citrine. As shown in Figure 3-8, embryos were injected with RNA encoding Cas9, gRNA1 (targeting the *egr2b* locus), mBait gRNA and the donor plasmid. Approximately 5% of embryos injected were found to contain some mosaic citrine in r3 and r5 by IHC (Figure 3-8 C,D) and in live embryos (Figure 3-8 E). As shown in Figure 3-8 (C,D) some cells containing H2B-Citrine were also detected outside of r3 and r5, including in the otic vesicle; these cells are more likely to result from episomal expression of the transgene than from cells expressing *egr2b* initially and switching identity. 23 of these Citrine-expressing injected F_0 embryos (Figure 3-8 E) were raised to adulthood and screened for germline transmission of the H2B-Citrine transgene by outcrossing to wildtype fish and monitoring Citrine expression in the resulting embryos by both *in situ* hybridisation analysis of *citrine* transcripts and detecting Citrine protein (Figure 3-8 F). One fish out of the 23 F_0s screened was found to transmit the transgene through the germline, although transmission from this founder was only approximately 8%. These heterozygous F_1 fish were raised to establish a stable Tg[egr2b:H2B-Citrine] line.

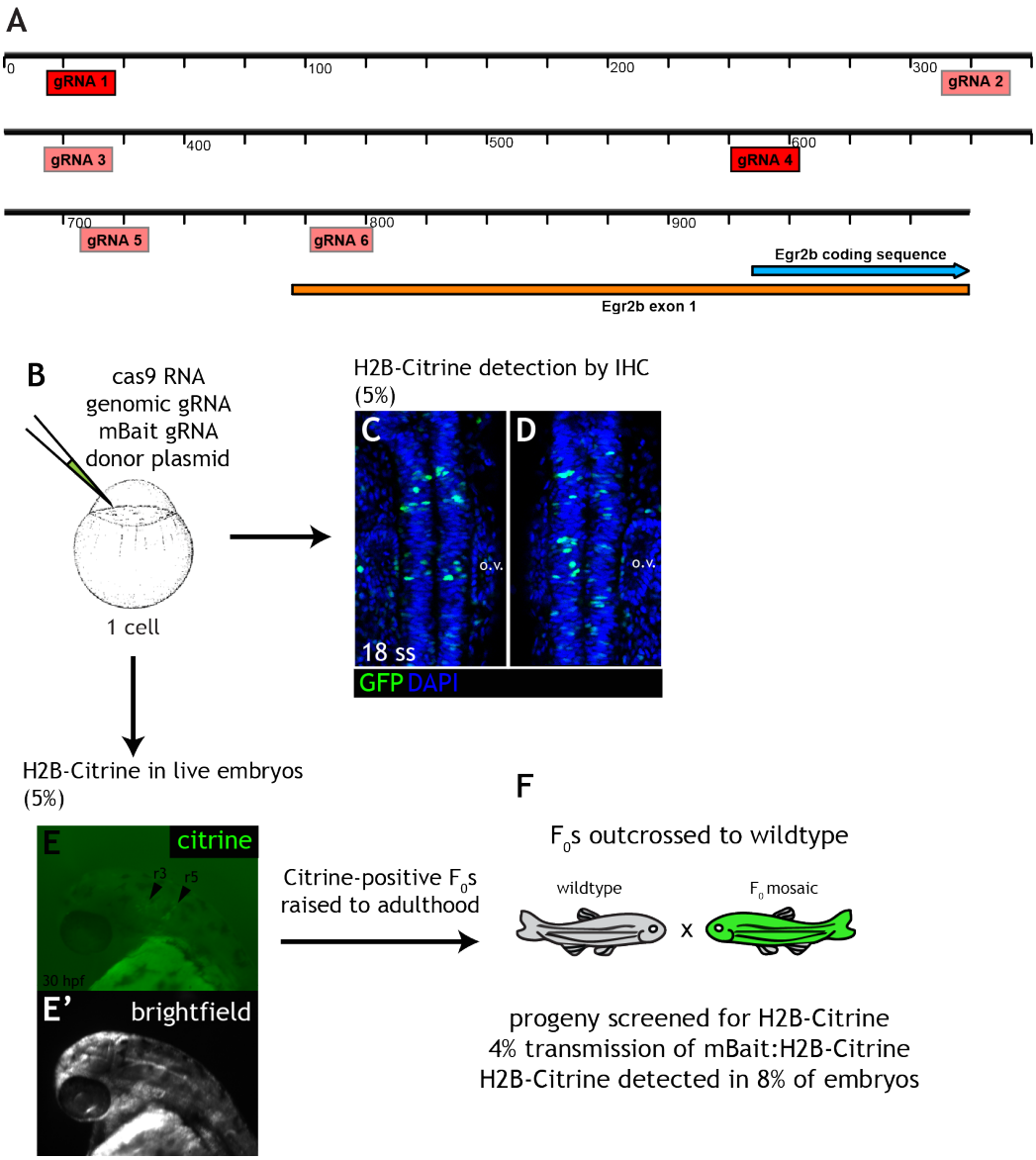

Figure 3-8 Creation of Tg[egr2b:H2B-Citrine]

A: Six gRNA target sites were selected that bind upstream of *egr2b*. Only two of these (gRNA 1 and gRNA 4; red) were found to cause insertion of the reporter construct.

B: Embryos were injected at the one cell stage with RNA encoding Cas9, gRNA1, mBait gRNA and the mBait-cFos:H2B-Citrine donor plasmid. Highly mosaic H2B-Citrine expression was detected in r3 and r5 of approximately 5% of injected embryos by IHC; in addition to other regions in the hindbrain and otic vesicle (C,D; single confocal sections) and in live embryos (E).

F: An F_0 founder was identified by outcrossing to wildtypes and detecting H2B-Citrine expression in the resulting progeny. The resulting H2B-Citrine-positive F_1s were raised to adulthood.

3.4 Characterisation of Tg[egr2b:H2B-Citrine] reporter line

To characterise the new Tg[egr2b:H2B-Citrine] line, I analysed expression of both *egr2b* and *citrine*. This can indicate whether *citrine* expression recapitulates *egr2b* expression, and whether insertion of the H2B-Citrine transgene at the *egr2b* locus in homozygous Tg[egr2b:H2B-Citrine] embryos compromises endogenous *egr2b* expression, which could have consequences for the suitability of this line to monitor border sharpening.

3.4.1 Insertion of H2B-Citrine at the *egr2b* locus does not compromise *egr2b* expression or function

It is possible that insertion of H2B-Citrine at the *egr2b* locus will compromise expression of endogenous *egr2b*. It was recently reported that CRISPR/Cas9-mediated insertion of mBait-hs-eGFP at the *pax2a* locus compromises Pax2a function and causes loss of the midbrain-hindbrain boundary (MHB) in embryos homozygous for transgene insertion, as expected for Pax2a loss-of-function (Ota *et al*, 2016). It is known that Egr2b function is necessary for maintenance of *egr2b* expression, and in a non-functional Egr2b mutant, *egr2b*^{fh227} (Monk *et al*, 2009), activation of *egr2b* expression occurs as normal in r3 and r5, but expression of *egr2b* is reduced from 6 ss and in r5 from 10 ss (Chomette *et al*, 2006; Bouchoucha *et al*, 2013).

To determine whether Egr2b function is compromised in homozygous Tg[egr2b:H2B-Citrine] embryos, I in-crossed identified homozygous Tg[egr2b:H2B-Citrine] adults and studied *egr2b* and *citrine* expression in the resulting homozygous embryos. As shown in Figure 3-9, *egr2b* and *citrine* expression do not appear to be compromised in Tg[egr2b:H2B-Citrine] – in all homozygous embryos examined no reduction of *egr2b* or *citrine* expression at later stages is observed.

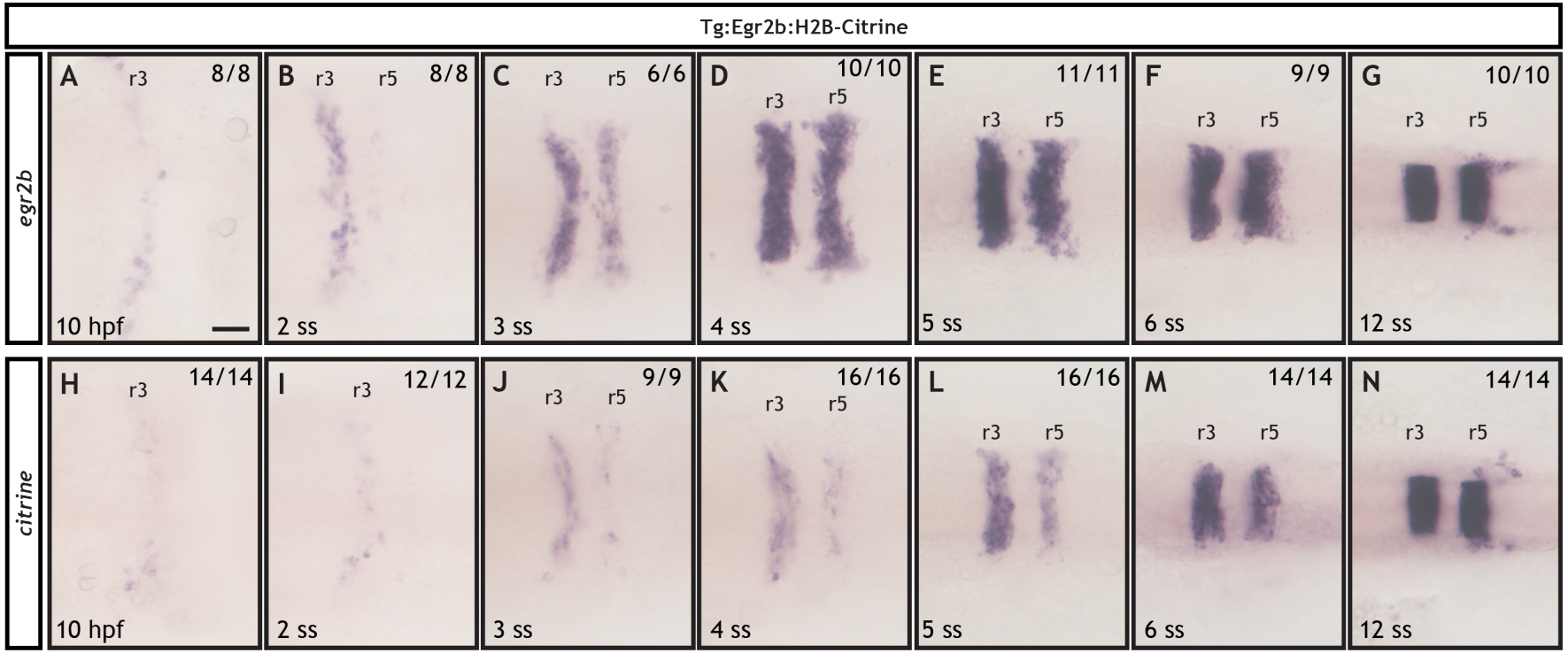

Figure 3-9 Time course of *egr2b* and *citrine* expression in Tg[egr2b:H2B-Citrine]

Whole mount *in situ* hybridisation comparing localisation of *egr2b* (A-G) and *citrine* (H-N) transcripts in *Tg[egr2b:H2B-Citrine]* (homozygous for H2B-Citrine). *egr2b* and *citrine* transcripts are both first detected in r3 at 10 hpf (A,H) *egr2b* transcripts are first detected in r5 at 2ss (B), while *citrine* transcripts are first detected in r5 slightly later, at 3 ss (J); citrine transcripts are detected in fewer cells of r3 and r5 until approximately 6 ss, when expression of *egr2b* and *citrine* are indistinguishable (F,M). Embryos are flat mounted, with anterior to the left. Frequencies of embryos observed represented by the image shown, out of the total number of embryos studied are shown in the bottom right. Scale bar: 50 μm.

One possible explanation for maintenance of *egr2b* expression in Tg[egr2b:H2B-Citrine] is functional redundancy between Egr2b and Egr2a. Egr2a has high sequence similarity to Egr2b and *egr2a* has a similar expression pattern to *egr2b* (Sun *et al*, 2002). Very little is known of the role of Egr2a in hindbrain segmentation, but due to the high sequence conservation with Egr2b, it is likely that there is functional redundancy between these two proteins. In order to investigate the potential functional redundancy between Egr2a and Egr2b, I designed and used morpholino oligonucleotide (MOs) to knock down their functions and assessed *egr2b* expression in these and control embryos. MOs were co-injected with a morpholino targeting p53 to prevent potential p53-activating morpholino toxicity (Robu *et al*, 2007; Gerety & Wilkinson, 2011). As shown in Figure 3-10, knock down of Egr2a alone has no effect on *egr2b* expression compared to control embryos (Figure 3-10 E,F). In contrast, knock down of Egr2b alone causes reduced *egr2b* expression in r3 by 10ss (Figure 3-10 G). Simultaneous knock down of both Egr2a and Egr2b does not increase the extent of reduced *egr2b* expression compared to knock down of Egr2b alone (Figure 3-10 H).

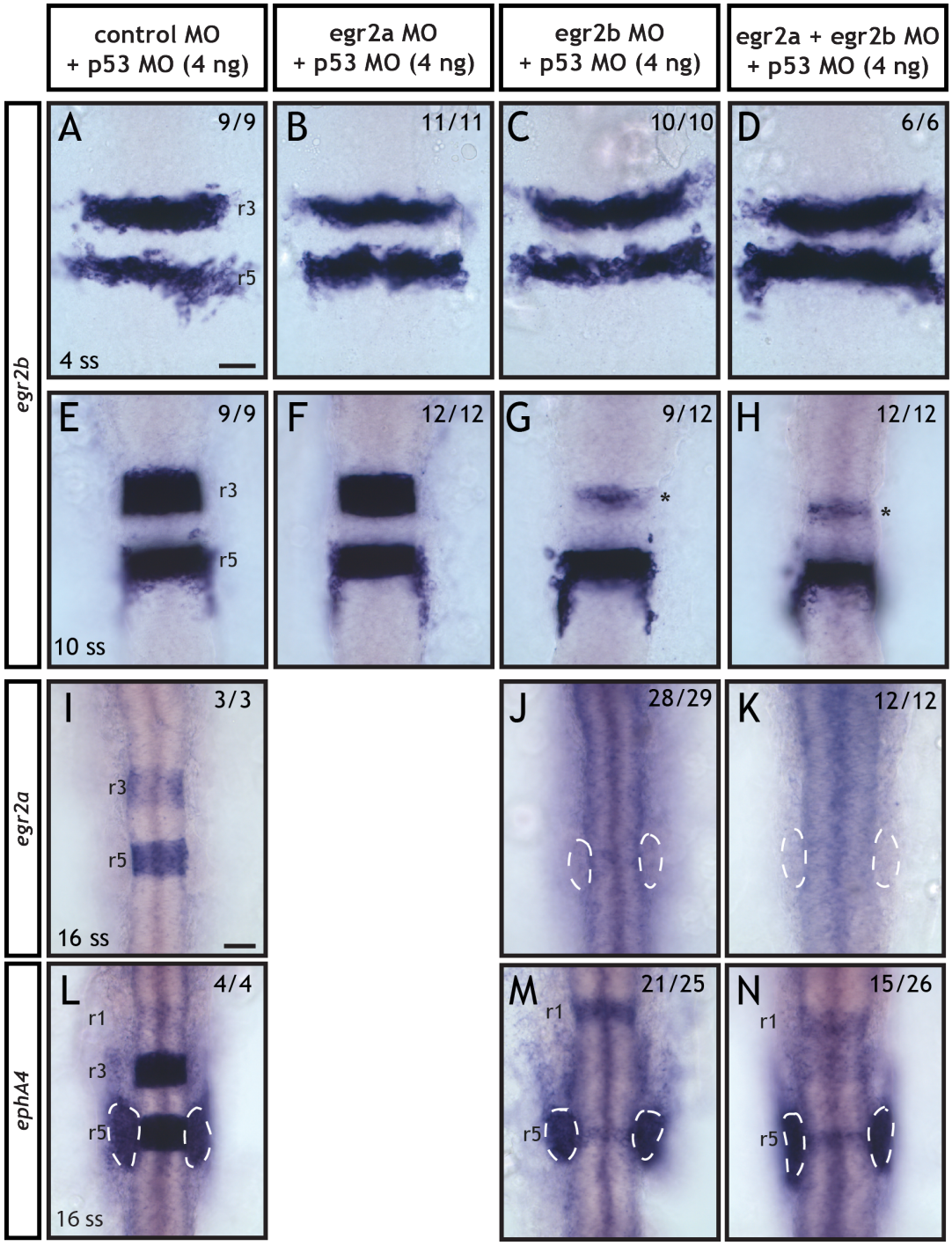

Figure 3-10 Egr2a and Egr2b do not appear to be functionally redundant

Expression of *egr2b* (A-H), *egr2a* (I-K) and *ephA4* (L-N) was analysed in wildtype control embryos, Egr2a morphant embryos, Egr2b morphant embryos and double Egr2a;Egr2b morphant embryos. At 4 ss, there is no clear difference in egr2b expression between control embryos (A), Egr2a morphants (B), Egr2b morphants (C) or Egr2a;Egr2b double morphants (D). At 10 ss, expression of *egr2b* is comparable between control (E) and Egr2a morphant embryos (F). At 10ss, expression of *egr2b* is reduced to a similar extent in r3 of Egr2b morphants (G;

asterisk) and Egr2a;Egr2b morphants (H; asterisk). At 16 ss, expression of *egr2a* is completely lost from r3 and r5 in both Egr2b morphants (J) and Egr2a;Egr2b double morphants (K) compared to control embryos (I). Expression of EphA4 is absent from r3 and reduced in r5 of both Egr2b morphants (M) and Egr2a;Egr2b double morphants (N) at 16ss, compared to control embryos (L). Embryos are flat-mounted with anterior to the top. Frequencies of embryos observed represented by the image shown, out of the total number of embryos studied are shown in the top right. Scale bars: 50 μm.

It has been demonstrated in chick that distinct regions of Egr2 are necessary for regulating transcription of different target genes in chick (Desmazières *et al*, 2009). Therefore, while Egr2a and Egr2b may not be functionally redundant for maintenance of *egr2b* expression, other transcriptional activities could be redundant. To investigate this, I also studied the expression of *ephA4* in single and double morphant embryos. As shown in Figure 3-10, knock down of Egr2b alone or in combination with Egr2a causes a significant reduction of *ephA4* expression in both r3 and r5. This demonstrates that multiple transcriptional activities of Egr2b are not redundant with Egr2a. Knock down of either Egr2b alone or with Egr2a also appears to cause a complete loss of *egr2a* expression by 16 ss (Figure 3-10 J-L). However, the background *in situ* hybridisation staining was greatly increased in all morphant embryos studied, and therefore low levels of *egr2a* expression may be undetectable. The apparent loss of *egr2a* expression upon Egr2b knock down would explain the observed lack of functional redundancy between Egr2a and Egr2b, as Egr2b appears to be necessary for *egr2a* expression in both r3 and r5. It is tempting to consider that *egr2a* may be entirely regulated by Egr2b, as this would explain the delay in onset of *egr2a* expression compared to *egr2b* expression.

These findings indicate that insertion of H2B-Citrine at the *egr2b* locus in homozygous Tg[egr2b:H2B-citrine] embryos does not compromise expression or function of *egr2b*, supporting the use of Tg[egr2b:H2B-Citrine] as a suitable tool for studying border sharpening in the presence of functional Egr2b.

3.4.2 *Citrine* expression is more heterogeneous than *egr2b* expression at early stages in Tg[egr2b:H2B-Citrine]

It can also be seen from expression analysis of *egr2b* and *citrine* in homozygous Tg[egr2b:H2B-Citrine] embryos (Figure 3-9) that while induction of *egr2b* and *citrine* expression occurs at similar stages, at early stages, until 6 ss, *citrine* transcripts are only detectable in a subset of cells of r3 and r5 that express *egr2b*. However, by later stages (12 ss) *citrine* expression becomes far more homogeneous within r3 and r5 and its expression pattern is almost identical to that of *egr2b*. The reason for this early apparent heterogeneity of *citrine* expression in homozygous Tg[egr2b:H2B-Citrine] embryos is unclear, although it is likely that the *citrine* transgene may simply be expressed at lower levels than *egr2b*. The heterogeneity of *citrine* expression may therefore reflect heterogeneity in *egr2b* expression, which may not be evident from *egr2b* expression analysis due to higher expression levels and the sensitivity of the *in situ* hybridisation technique used. It is possible that the inserted cFos promoter interacts with enhancer elements less efficiently than the endogenous *egr2b* promoter does. Alternatively, the cFos promoter may only interact with some, but not all, *cis*-regulatory elements that regulate *egr2b* expression. Particularly, it could be that *citrine* expression is only driven by the autoregulatory element of *egr2b* expression.

3.4.3 Knock down of Egr2 prevents maintenance, but not initiation, of H2B-Citrine expression in Tg[egr2b:H2B-Citrine]

In order to investigate whether expression of *citrine* in Tg[egr2b:H2B-Citrine] is driven only by the *egr2b* autoregulatory element A, I studied expression of *citrine* and *egr2b* in embryos in which both Egr2a and Egr2b were knocked down (referred to as Egr2 morphants). As shown in Figure 3-11, initiation of *egr2b* expression still occurs in Egr2 morphants; *egr2b* transcripts are detected in r3 until approximately 11 ss, and in r5 until 16 ss. It can also be seen that initiation of *citrine* expression still occurs in Egr2 morphant Tg[egr2b:H2B-citrine] embryos, although from as early as 3 ss expression levels of *citrine* appear lower in Egr2 morphants than in control embryos. This likely reflects the fact that *citrine* appears to be expressed at lower than *egr2b* expression even in control embryos, as previously discussed. It is

clear from these results that expression of H2B-Citrine is driven by initiator regulatory elements as well as the *egr2b* autoregulatory element.

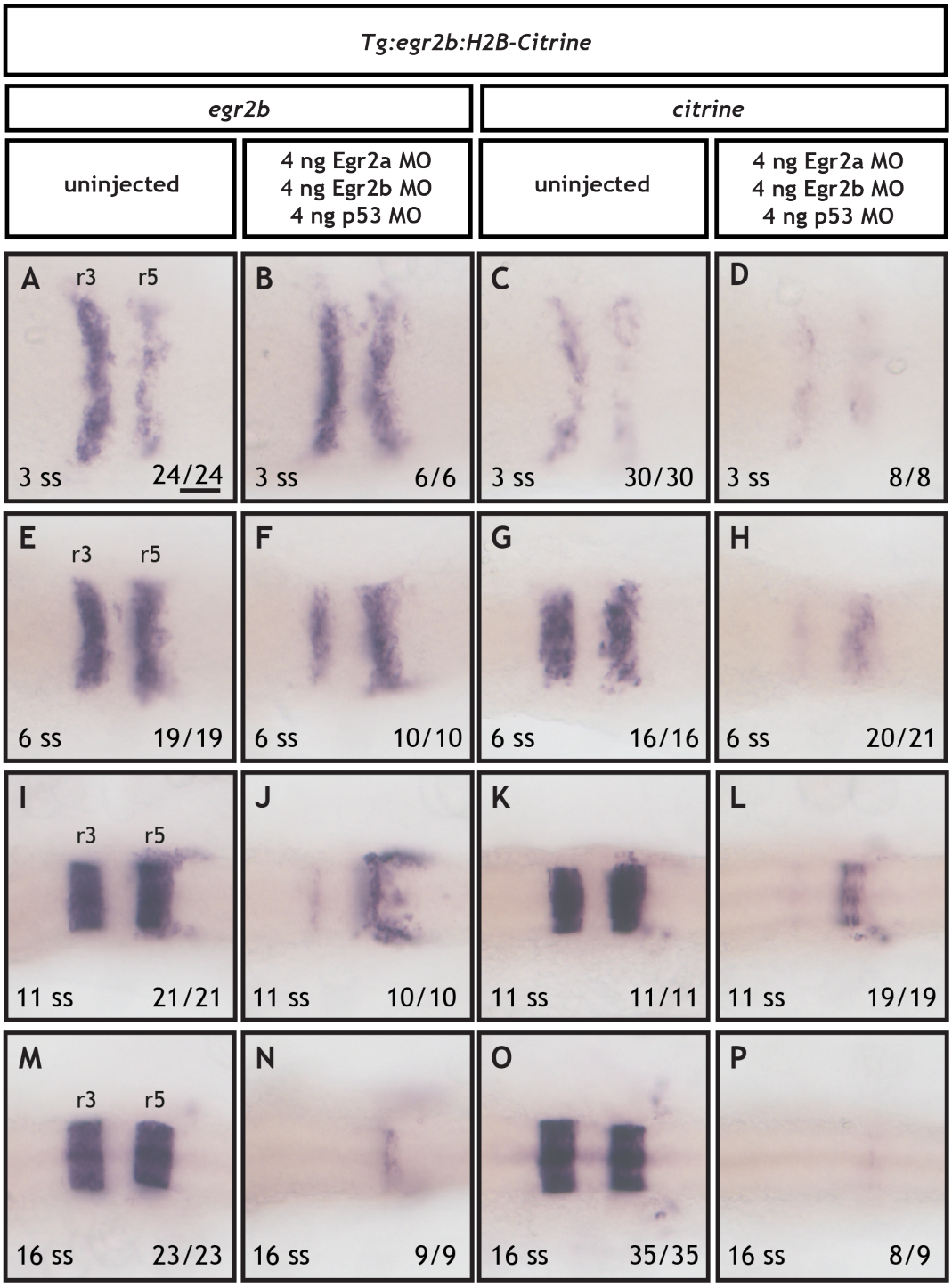

Figure 3-11 Expression of *egr2b* and *citrine* in Tg:egr2b:H2B-Citrine combined with knock down of Egr2a and Egr2b

Expression of *egr2b* (A,E,I,M) and *citrine* (C,G,K,O) in uninjected *Tg:egr2b:H2B-Citrine* at various developmental stages compared to embryos injected with Egr2a and Egr2b morpholinos (B,F,J,N,D,H,L,P). Knock down of Egr2a and Egr2b does not prevent initiation of *egr2b* (B) or *citrine* (D) expression, compared to uninjected control embryos (A,C). Knock down

of Egr2a and Egr2b reduces levels of *citrine* transcripts detected in r3 and r5 by 6 ss, compared to uninjected controls (G); at this stage, this effect is less pronounced for *egr2b* expression compared between morphant and control embryos (I,J). By 16ss, only very low levels of *egr2b* (N) and *citrine* (P) transcripts are observed in r5 compared to control embryos (M,O). Embryos are flat-mounted with anterior to the left. Frequencies of embryos observed represented by the image shown, out of the total number of embryos studied are shown in the bottom right. Scale bar: 50 μm.

3.5 Studying border sharpening in Tg[egr2b:H2B-Citrine]

3.5.1 Expression of H2B-Citrine in Tg[egr2b:H2B-Citrine] prior to border sharpening

While characterising the Tg[egr2b:H2B-citrine] line, I also studied the localisation of H2B-Citrine protein at stages during border sharpening. As shown in Figure 3-12, not all cells that contain *citrine* transcripts contain detectable levels of Citrine protein at the stages studied; although it should be noted that detection of Citrine by immunohistochemistry may be slightly compromised by conducting IHC after ISH. Interestingly, at these stages when rhombomere borders are not yet sharp, cells can be observed outside r3 and r5 that contain both *citrine* transcript and detectable H2B-Citrine protein (Figure 3-12; arrowheads).

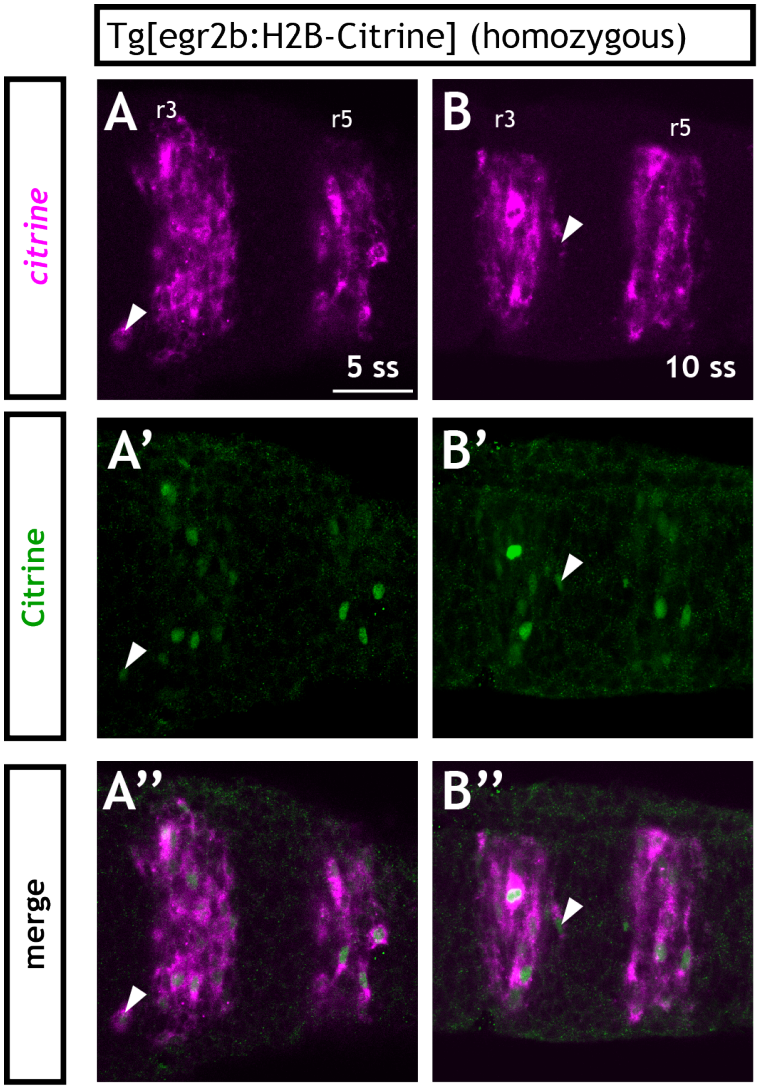

Figure 3-12 Comparison of citrine transcripts and Citrine protein in homozygous Tg[egr2b:H2B-Citrine] embryos

Expression of *citrine* transcripts and H2B-Citrine protein was studied in homozygous Tg[egr2b:H2B-Citrine] embryos at 5 ss (A) and 10 ss (B). H2B-Citrine protein is not detected in all cells that contain *citrine* transcript at either 5 ss or 10 ss. At both of these stages, ectopic cells outside r3 and r5 can be detected that contain both *citrine* transcripts and H2B-Citrine protein (arrowheads). Embryos are flat-mounted with anterior to the left. Scale bar: 50 μm.

3.5.2 Time-lapse imaging in heterozygous Tg[egr2b:H2B-Citrine] embryos

I have demonstrated that the Tg[egr2b:H2B-Citrine] reporter line recapitulates *egr2b* expression, and, at early stages, ectopic Citrine-expressing cells can be seen outside of r3 and r5, although at these early segmentation stages, H2B-Citrine cannot be detected in all cells that express *egr2b*. I proceeded to use the Tg[egr2b:H2B-Citrine] reporter line to visualise and monitor cells during border sharpening. Time lapse imaging in live embryos provides more information than static snap-shots of gene expression at single time points as provided by *in situ* hybridisation of fixed samples, and it is possible to track Citrine-expressing cells from early stages when gene expression borders are fuzzy through to later stages, when borders are sharp.

The majority of these movies were conducted in heterozygous embryos, prior to having homozygous adults available to in-cross. Where possible, the entire depth of the hindbrain (dorsal-to-ventral) was imaged at 6 minute intervals from roughly 4 ss to 14 ss. Select cells detected at the edges of r3 and r5, or more clearly outside of r3 and r5, were tracked from early stages, when gene expression domains are known to be fuzzy, through to later stages when gene expression domains are sharp. As shown in Figure 3-13, the vast majority of cells that are observed (and assumed to be) outside of r3 and r5 at early stages become sorted into r3 and r5; very rarely are any ectopic cells containing Citrine observed outside r3 and r5 by the end of imaging (14 ss). From these data acquired in heterozygous Tg[egr2b:H2B-Citrine] embryos, cell identity regulation does not appear to significantly contribute to hindbrain border sharpening.

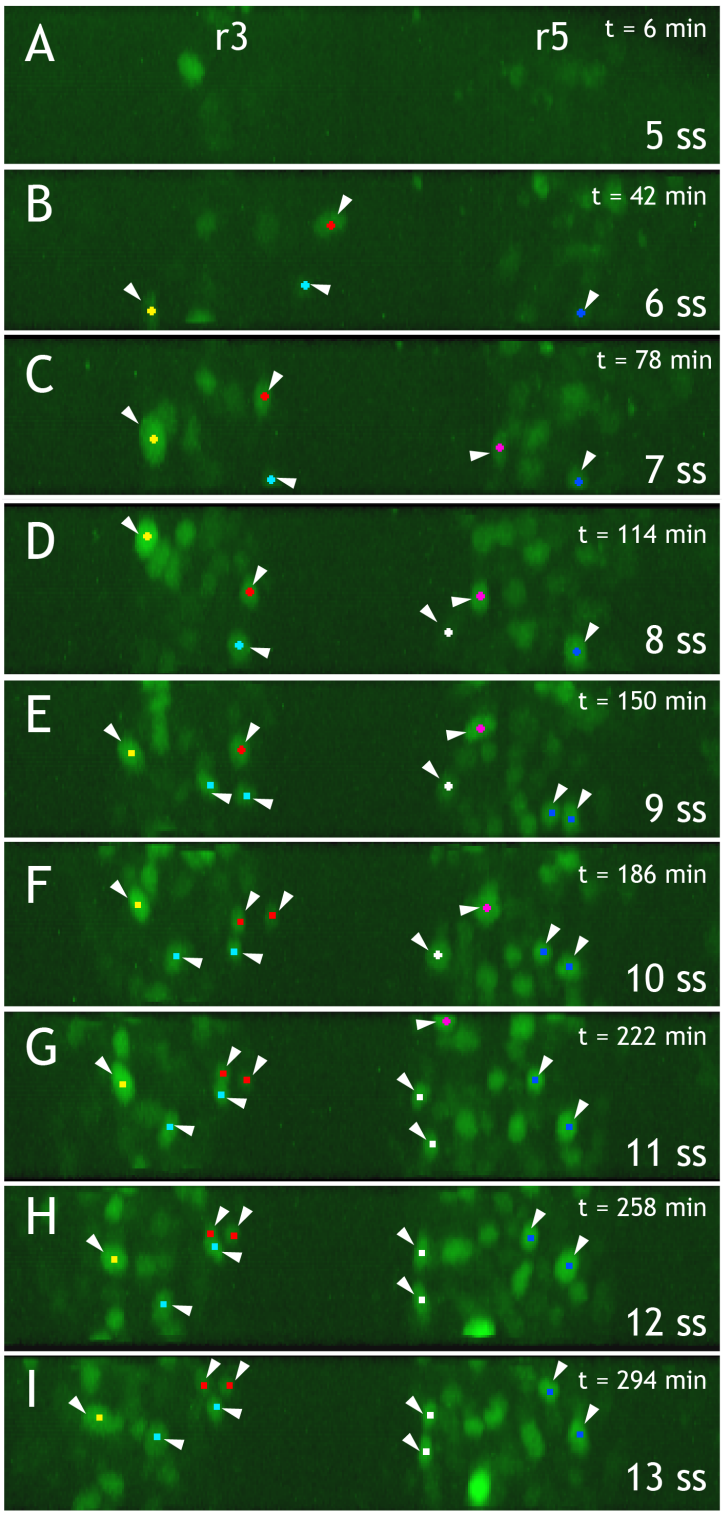

Figure 3-13 Time lapse imaging heterozygous Tg[egr2b:H2B-Citrine]

Select time points from a movie in Tg[egr2b:H2B-Citrine]. A maximum intensity lateral projection is shown, with anterior to the left. Selected tracked cells are labelled with coloured dots; mother and daughter cells are labelled with the same colour. Note that neural crest cells containing

H2B-Citrine emerge from r5 from approximately 9 ss (unlabelled). Approximate stages at different time points were calculated from the initial and final stages of embryos. Ectopic cells with H2B-Citrine are rarely observed outside r3 and r5 by 13 ss (n = 12 embryos imaged in this way; one ectopic cell observed).

3.5.3 Detection of ectopic H2B-Citrine in Tg[egr2b:H2B-Citrine] homozygous embryos after completion of border sharpening

Once I had generated homozygous adults, I studied expression of H2B-Citrine in homozygous Tg[egr2b:H2B-Citrine] embryos. As shown in Figure 3-14, I detected H2B-Citrine expression in fixed homozygous Tg[egr2b:H2B-Citrine] embryos using IHC to amplify detection of the protein. At early stages, prior to border sharpening, there are several ectopic H2B-Citrine-containing cells that appear to be outside r3 and r5 (Figure 3-14A, arrowheads). Interestingly, by 16 ss (after completion of border sharpening, several H2B-Citrine-containing cells are still detected outside r3 and r5 (Figure 3-14B; arrowheads). As previously discussed, detection of ectopic H2B-Citrine-containing cells at these stages indicates that switching of cell identity has occurred (Figure 3-4).

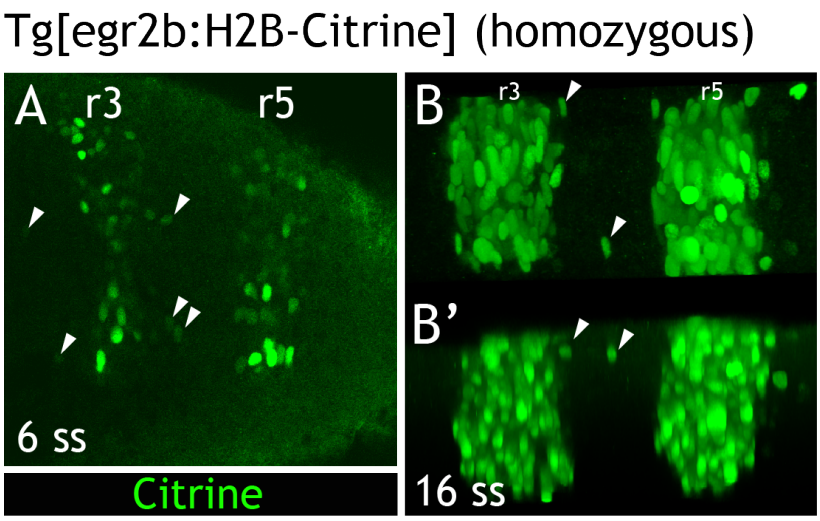

Figure 3-14 Detection of H2B-citrine in homozygous Tg[egr2b:H2B-Citrine] by immunohistochemistry

At 6 ss, some H2B-Citrine cells are detected outside of r3 and r5 (A; arrowheads, n = 6 embryos). By 16 ss, H2B-Citrine-expressing cells are still detectable in r2 (mean = 1.2 cells), r4 (mean = 2.4 cells) and r6 (mean = 2.4 cells) (B; arrowheads, n = 14 embryos). Embryo A is flat-mounted with anterior to the left; B and B' show dorsal and lateral maximum projections, respectively.

3.5.4 Autoregulation by Egr2b is necessary for accumulation of sufficient levels of Citrine for detection

I have shown that while several ectopic H2B-Citrine expressing cells are detected after completion of sharpening in homozygous Tg[egr2b:H2B-Citrine] embryos, there are seldom any ectopic cells observed at these stages in heterozygous Tg[egr2b:H2B-Citrine] embryos. This is likely due to insufficient expression of H2B-Citrine in heterozygotes, which only have a single copy of the transgene at the *egr2b* locus. As previously shown in Figure 3-11, when Egr2a and Egr2b are knocked down in Tg[egr2b:H2B-Citrine], induction of *citrine* expression still occurs, but lower levels of transcripts are detected than in control embryos. As well as being essential for maintenance of *egr2b* expression, the autoregulatory activity of Egr2b is known to be necessary for a substantial increase in *egr2b* expression at early stages: comparison of normalised *egr2b* mRNA levels between wildtype embryos and *egr2b*$^{fh227/fh227}$ embryos, which lack functional Egr2b, indicates that the autoregulatory loop causes a two-fold increase in maximal mRNA level

(Bouchoucha *et al*, 2013). I therefore investigated what levels of Citrine protein can accumulate in Tg[egr2b:H2B-Citrine] in the absence of Egr2b-mediated autoregulation. As shown in Figure 3-15, knock down of Egr2a and Egr2b greatly reduces the number of Citrine-containing cells observed in r3 and r5 of homozygous Tg[egr2b:H2B-citrine] embryos. This indicates that Egr2b-mediated autoregulation is required for sufficient expression of the *citrine* transgene for accumulation of sufficient H2B-Citrine protein to be detected. This may have consequences for the extent of identity switching that can potentially be detected in Tg[egr2b:H2B-Citrine], as cells that change their identity from r3/r5 identity to a non-r3/r5 identity may not activate the Egr2b autoregulatory loop (for example, due to overlapping induction of *hoxb1a*, which will repress *egr2b* expression). Thus some cells that change their identity may never contain sufficient H2B-Citrine to be detected, leading to an underestimate of the extent of identity switching.

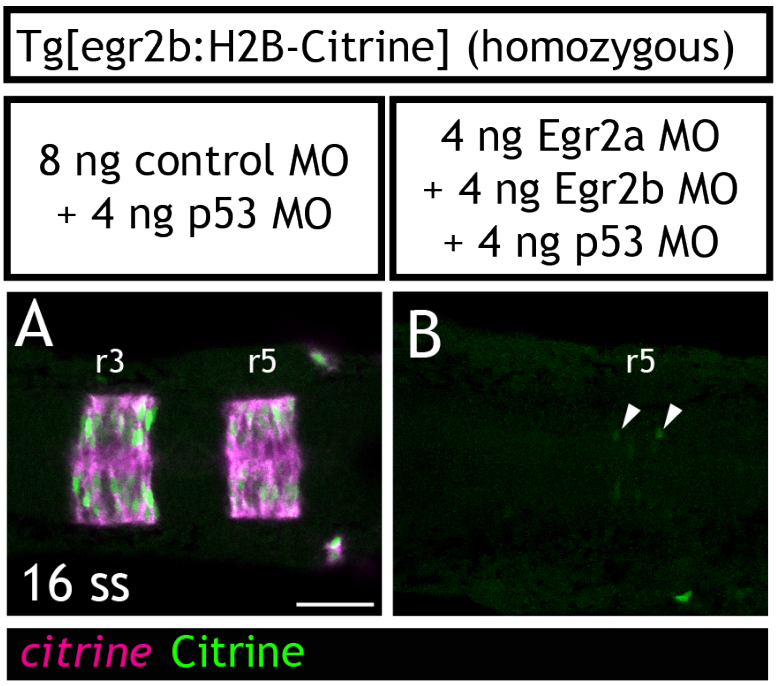

Figure 3-15 Expression of citrine is severely reduced by knock down of Egr2

H2B-Citrine protein and citrine transcripts were visualised in Tg[egr2B:H2B-Citrine] homozygous embryos injected with Egr2a and Egr2b morpholinos. Knock down of Egr2 severely reduces the number of H2B-Citrine-containing cells within r3 and r5 by 16 ss (B; arrowheads; n = 5 embryos) in contrast to control embryos (A; n = 5 embryos). Embryos are flat-mounted with anterior to the left. Scale bar: 50 μm.

3.6 Knock down of Hoxb1 causes increased numbers of *egr2b*-expressing cells within r4

During experiments investigating the impact of Hoxb1 knock down on hindbrain patterning, I observed that simultaneous knock down of Hoxb1a and Hoxb1b not only causes an expected expansion of r3 at the expense of r4 (McClintock *et al*, 2002; Labalette *et al*, 2015), but also causes ectopic *egr2b*-expressing cells to be detected within r4 at 16 ss, as shown in Figure 3-16(D). If *egr2b*-expressing cells can switch identity by downregulating *egr2b* and assume an r4 identity, knock down of Hoxb1, which confers identity to r4 and is known to repress *egr2b* expression, may compromise this switching and explain the observed phenotypes. In addition, cells within pre-r4 that co-express *egr2b* and *hoxb1a* at early stages may be incapable of downregulating *egr2b* if they lack Hoxb1. One way to investigate the cause of these ectopic cells in r4, and determine whether compromised identity resolution contributes, is to knock down Hoxb1a and Hoxb1b in Tg[egr2b:H2B-citrine], and conduct time lapse imaging to determine how these ectopic cells arise and whether there is any evidence that cells are still capable of resolving their identity. As shown in Figure 3-17, knock down of Hoxb1a and Hoxb1b in Tg[egr2b:H2B-citrine] causes additional *citrine*-expressing cells to be observed in r4 at 16 ss and contain H2B-Citrine. In future experiments, it will be interesting to see if these cells arise due to increased intermingling between r3, r4 and r5.

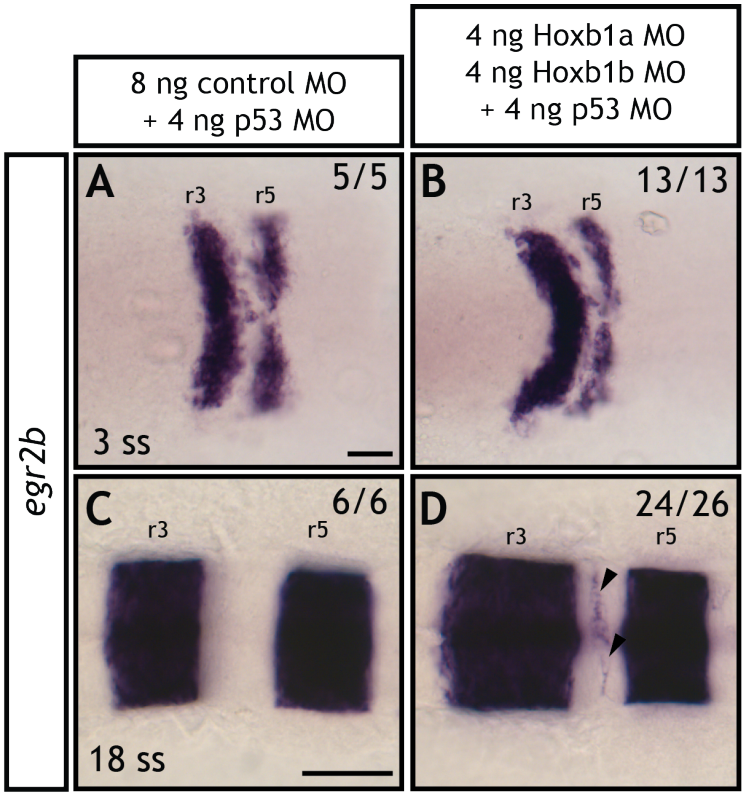

Figure 3-16 Expression of *egr2b* in Hoxb1 morphants

Expression of *egr2b* was analysed in embryos in which Hoxb1a and Hoxb1b were knocked down (B, D). At 3 ss, there is no clear difference in *egr2b* expression between control embryos (A) and Hoxb1a;Hoxb1b morphants (B). However, at 18 ss, knock down of Hoxb1a and Hoxb1b causes increased numbers of *egr2b*-expressing cells to be detected within r4 (D; arrowheads; average of 5.7 cells; n = 26 embryos) in comparison to control embryos (C; average of 0; n = 6 embryos). Knock down of Hoxb1a and Hoxb1a also causes an expansion of r3 at the expense of r4 (D). Embryos are flat-mounted with anterior to the left. Frequencies of embryos observed represented by the image shown, out of the total number of embryos studied are shown in the bottom right. Scale bars: 50 μm.

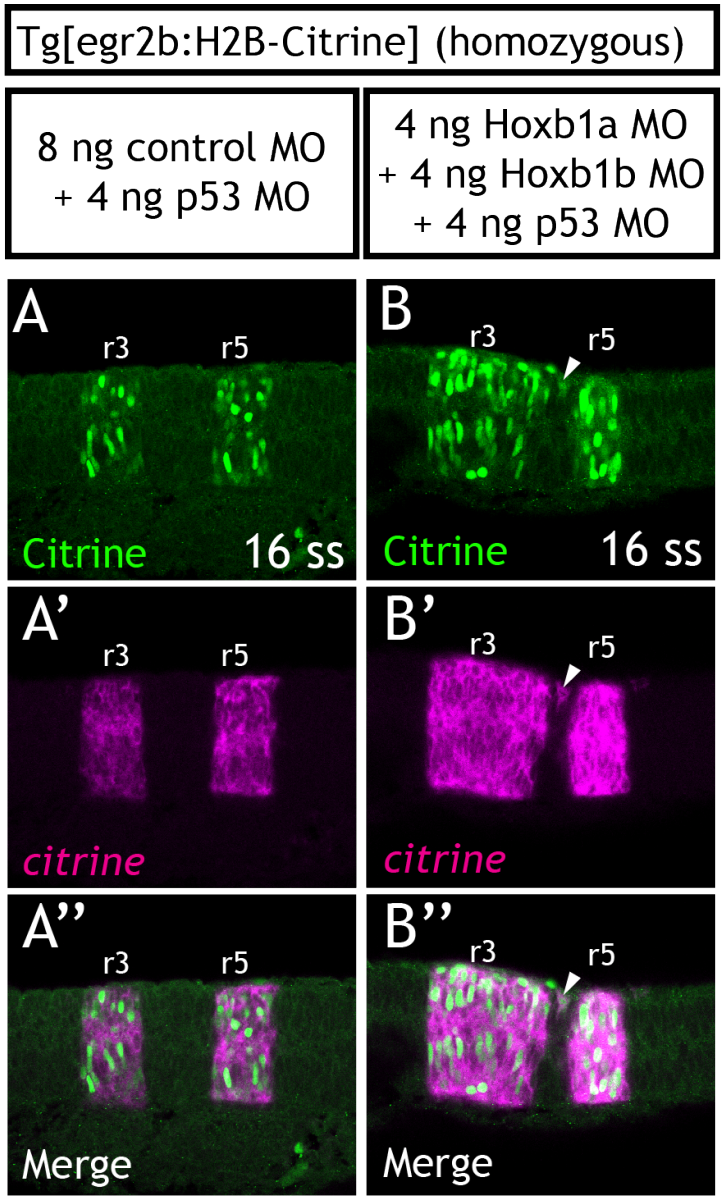

Figure 3-17 Knock down of Hoxb1 in Tg[egr2b:H2B-Citrine] gives rise to ectopic Citrine-expressing cells in r4

Hoxb1a and Hoxb1b were knocked down in Tg[egr2b:H2B-Citrine] and expression of *citrine* and H2B-Citrine protein were visualised. Knock down of Hoxb1 causes ectopic *citrine*-expressing cells, which also contain H2B-Citrine to be detected in r4 (B; arrowheads, n = 8 embryos), in contrast to control embryos (A; n = 4 embryos). Embryos are flat-mounted, with anterior to the left.

3.7 Discussion

In this chapter I have described the creation of a novel zebrafish reporter line, Tg[egr2b:H2B-Citrine], using the CRISPR/Cas9 system. So far, this line has provided some additional, albeit limited, evidence for identity regulation contributing to hindbrain border sharpening. However, as I will discuss, there are several technical reasons why this line may underestimate the frequency of identity switching during border sharpening.

3.7.1 Creation of Tg[egr2b:H2B-Citrine] by targeted genomic insertion

In addition to its importance for studying cell identity switching during hindbrain border sharpening, the creation of Tg[egr2b:H2B-Citrine] described here contributes to our currently limited knowledge of the efficiency of targeted genomic insertion in zebrafish.

The frequency with which transgene insertion was detected in injected embryos here (approximately 5%) is comparable to that previously reported (5-10%) (Kimura *et al*, 2014). However, I achieved far lower rates of germline transmission of the transgene (4%) than have been previously described (20-60%) (Kimura *et al*, 2014). There are several possible explanations for this. Firstly, it is likely that targeted insertion at different loci will be transmitted with varied frequencies. In support of this, a recent case of using the same technique to create a new *pax2a* transgenic line reported comparable germline transmission frequencies to those achieved here (5%) (Ota *et al*, 2016). This suggests that, for at least some genes, this particular knock-in approach is not as efficient as initially reported. A second reason for lower germline transmission efficiency than expected may be that, unlike Kimura *et al*, I was unable to identify injected F_0 embryos with widespread Citrine expression throughout r3 and r5 to raise to adulthood. Kimura *et al* report that when fish with poor or no reporter expression were raised, none were found to transmit the insertion through the germline; it has been suggested that selection of embryos with widespread reporter fluorescence is crucial to acquire positive founders (Kimura *et al*, 2014). A lack of widespread Citrine expression in my case could be partly due to varied efficiency of the gRNA targeting the genomic loci, but also

appears to be due to expression levels of the transgene at the *egr2b* locus: even in heterozygous Tg[egr2b:H2B-Citrine] embryos, Citrine expression is highly varied and undetectable in some cells of r3 and r5. Despite this knock-in approach now appearing less efficient than initially reported, it nonetheless remains a valuable and useful method to generate novel transgenic zebrafish, as supported by my success in adopting this technique. In addition, a potential limitation of this knock-in approach – depending on the desired application – is that the timing and level of target gene expression, which determines the extent to which the reporter can be detected, will be limited by the expression level of the target gene. For certain applications, additional modifications and improvements may be required in cases where the target gene is expressed at low levels for short durations (discussed below).

It is interesting that, unlike reported for another gene (Ota *et al*, 2016), I do not observe any functional consequence of transgene insertion at the *egr2b* locus – even in embryos homozygous for the insertion. It was recently found that insertion of mBait-hs-eGFP at both alleles at the *pax2a* locus causes loss of the midbrain-hindbrain boundary, comparable with the *no isthmu*s (*noi*) mutant, as expected for loss of Pax2a function (Ota *et al*, 2016). Ota *et al* suggest that this knock-in approach can be applied universally to study loss-of-function phenotypes. However, I have demonstrated here that – at least for some genes – homozygous transgene insertion is not sufficient to cause a loss-of-function phenotype. The functional consequences for targeted insertion therefore appear to be context-dependent.

I have also presented evidence here regarding the efficiency of an alternative approach, using TALENs, to generate an *egr2b* reporter line. This TALEN-mediated approach caused insertion and transmission of the transgene with comparable frequency to CRISPR-mediated insertion (3.5%). However, this approach was limited by the requirement for in-frame integration of the reporter construct for expression of the reporter protein, due to targeting the insertion within the coding region of *egr2b*. This resulted in very mosaic reporter expression in injected embryos, meaning that pre-screening F_0s for fluorescence by eye was not possible, unlike for the CRISPR-mediated approach. Incorporation of the α-

Crystallin:RFP cassette did enable F_0s to be selected by integration of the donor plasmid, but not by the frame of integration, so raising sufficient numbers of injected embryos positive for α-Crystallin:RFP should enable founders with in-frame insertion to be detected, as previously reported (Constable, 2015). This approach is also limited by the requirement for modification of the donor construct to incorporate different TALEN sites for different targets, so does not allow easy testing of multiple target sites quickly and easily, in contrast to the CRISPR-mediated approach.

3.7.2 Early heterogeneity of citrine expression in Tg[egr2b:H2B-Citrine] may reflect heterogeneity in early *egr2b* expression

It is interesting that early *citrine* expression in Tg[egr2b:H2B-Citrine] appears more heterogeneous than early *egr2b* expression. Although c*itrine* is expressed at lower levels than *egr2b* in Tg[egr2b:H2B-Citrine], it should be expressed at proportional levels to *egr2b*; *citrine* expression is therefore likely to reflect heterogeneity in *egr2b* expression that is otherwise not detectable using *in situ* hybridisation to detect *egr2b* transcripts at these stages. A potential contribution to apparent differences in *egr2b* and *citrine* transcript levels is differential sensitivity of detection of these two different transcripts; it may not be possible to detect low levels of *citrine* as effectively as equivalent low levels of *egr2b* by ISH. It would be interesting to see whether more sensitive gene expression analysis techniques, such as ISH with tyramide signal amplification (Clay & Ramakrishnan, 2005) and hybridisation chain reaction ISH (Choi *et al*, 2010, 2014) are capable of detecting more widespread *citrine* expression at early stages. The heterogeneity of *citrine* expression is more pronounced at early stages, and is gradually lost at a timescale that corresponds to the sharpening of rhombomere borders, raising the possibility that whatever mechanisms establish homogeneous *egr2b* expression may also contribute to border sharpening. In mouse, a *Egr2*$^{Cre/+}$ *lox* reporter displays similar heterogeneity of reporter expression within r3 and r5 at early stages; but reporter expression also becomes homogeneous eventually (Voiculescu *et al*, 2001). It was suggested that the early heterogeneity in this case arises from a delay in activation of the reporter, due to the time taken for accumulation of the Cre recombinase

(Voiculescu *et al*, 2001). In addition, quantification of *egr2b* expression, as measured using the hybridisation chain reaction (HCR) *in situ* hybridisation approach, has revealed variation and noise in levels of expression within r3 and r5 at 3 ss (Sosnik *et al*, 2016). HCR is a more quantitative technique than ISH alone, due to incorporation of additional amplification steps (Choi *et al*, 2010, 2014). It has been suggested that this early noise in *egr2b* expression within and between embryos arises due to noise in the RA gradient that regulates AP identity (Sosnik *et al*, 2016; Schilling *et al*, 2016).

3.7.3 Assessing the contribution of cell identity regulation to border sharpening in Tg[egr2b:H2B-Citrine]

In this chapter I have presented additional evidence suggesting that regulation of identity does contribute to the establishment of sharp borders of *egr2b* expression during hindbrain segmentation. In homozygous Tg[egr2b:H2B-Citrine] embryos, H2B-Citrine-expressing cells can be detected outside of r3 and r5 at stages at which the expression of *egr2b* is known to be sharp. It appears that two copies of the transgene, one on each allele, are necessary for sufficient reporter expression to detect ectopic cells that switch identity, as the majority of ectopic H2B-Citrine-expressing cells in heterozygous Tg[egr2b:H2B-Citrine] embryos are seen to sort to the correct territory, rather than persist in an ectopic location. Due to time constraints, at the time of writing, I have only a few examples of time-lapse experiments in identified homozygous Tg[egr2b:H2B-Citrine] embryos to demonstrate where these ectopic cells originate from: whether they are originally specified in r3 or r5 then leave later, or if they are initially specified within r2 or r4 or r6. To build on this finding and demonstrate that cells can switch identity from one identity to another during border sharpening, the Tg[egr2b:H2B-Citrine] reporter line could be combined with an additional reporter, where a different-coloured stable fluorescent reporter could be driven by endogenous *cis*-regulatory elements driving *hoxb1a* expression, and to combine this with the Tg[egr2b:H2B-Citrine] line described here. In this case, cells that have co-expressed *egr2b* and *hoxb1a* should contain both reporters at late stages. This could additionally be combined with time lapse imaging to track these cells throughout the sharpening process. I

have attempted to create an additional reporter for *hoxb1a*, but as yet, have been unsuccessful in finding any gRNAs (out of four tested) that efficiently cut at the *hoxb1a* locus, as tested by both HRM and co-injection with the mBait-cFos-H2B-Citrine-pA donor construct.

I have suggested a possible reason why using Tg[egr2b:H2B-Citrine] to study identity switching is likely to underestimate the extent of cell identity switching. Cells that do not activate the Egr2b autoregulatory loop are unlikely to accumulate sufficient H2B-Citrine reporter to be detected; in particular, cells that switch identity from an r3 or r5 identity to a non-r3/r5 identity may downregulate *egr2b* expression before sufficient Citrine accumulates for their detection. There are several ways this problem could potentially be avoided by modifying the existing transgenic line. Insertion of additional reporter genes in frame, resulting in multimerised reporter proteins, could increase the strength of the reporter signal as described (Genové *et al*, 2005); however, this is more likely to disrupt *egr2b* expression. Alternatively, incorporation of a Gal4-UAS-mediated self-activating loop, driving self-maintenance of Citrine expression, may enable sufficient accumulation of Citrine for detection, at least by later stages. However, this approach still relies on sufficient accumulation of Gal4 to activate self-maintenance of Citrine expression. Similarly, replacing H2B-Citrine with Cre recombinase, in combination with an appropriate Cre-responder line, could be used to permanently label all cells to previously express *egr2b*. Again this requires sufficient accumulation of Cre recombinase to drive recombination and label cells, which may not occur in cells that switch identity.

My findings here conflict with previously published data studying border sharpening in live zebrafish embryos. Live imaging of cells at the r5/6 border has previously found no evidence of cell identity switching at this border, and all ectopic cells expressing the *egr2b* reporter were sorted into r5 (Calzolari *et al*, 2014). These time lapse experiments made use of the transgenic line Tg[elA:GFP], in which the chick *Egr2* autoregulatory element A drives expression of GFP as previously reported (Chomette *et al*, 2006; Labalette *et al*, 2011; Bouchoucha *et al*, 2013). However, in the Tg[elA:GFP] line, only one of three known regulatory elements of *egr2b* drive reporter expression, and so this line will not fully recapitulate endogenous *egr2b* expression. Crucially, only maintenance, and not initiation of

egr2b expression will be reflected in the reporter expression. Because there is a narrow time window between activation of *egr2b* and upregulation of Ephs and ephrins that restrict cell intermingling, if the reporter is not expressed early, it will be too late to detect this early mixing.

An additional approach taken by Calzolari *et al* to study identity switching used the Mü4127 transgenic line, created by insertion of an enhancer trap cassette – containing KalTA4 and mCherry – 1.5 kb downstream of *egr2b* (Distel *et al*, 2009; Calzolari *et al*, 2014). In this line, mCherry is expressed in r3 and r5, and mCherry protein is detectable from approximately 16 ss, although KalTA4 expression, as detected by *in situ* hybridisation, is not expressed until 90 minutes after onset of *egr2b* expression (Distel *et al*, 2009). In addition, KalTA4 expression turns off between four and six hours earlier than *egr2b* expression. These differences in KalTA4 expression compared to *egr2b* expression have been suggested to be due to the inserted cassette being at an increased distance from *cis*-regulatory elements of *egr2b* than *egr2b* itself (Distel *et al*, 2009). In Calzolari *et al*, 2014, the Mü4127 line was additionally crossed the 4xKaloop effector strain (containing a bicistronic 4xUAS effector construct driving GFP expression, followed by a self-cleaving T2A peptide and KalTA4) in order to drive self-maintained GFP expression in r3 and r5 via the KalTA4;UAS effector loop. Even with this self-maintained reporter expression, no ectopic cells containing GFP were detected outside of r3 or r5 after completion of sharpening (Calzolari *et al*, 2014). However, in embryos derived from crossing Mü4127 with the 4xKaloop line, it has been reported that there is an even greater delay in onset of GFP expression compared to *egr2b* expression; *gfp* transcripts are not detected until 2.5 hours after onset of *egr2b* expression (Distel *et al*, 2009). The delay in reporter expression here again means that the narrow window before intermingling is restricted is missed and cells that induce *egr2b* expression but intermingle are unlikely to be detected.

3.7.4 Assessing the contribution of cell death to hindbrain border sharpening

Another potential mechanism – in addition to Eph/ephrin-mediated cell sorting and regulation of cell identity – that may also contribute to border sharpening is the selective cell death of ectopic cells. It has recently been reported that mis-specified epithelial cells can be eliminated from *Drosophila* imaginal discs by increased actomyosin contractility and tension at the interface between mis-specified cells and surrounding cells (Bielmeier *et al*, 2016). Intriguingly, this mechanism of elimination depends on the size of the mis-specified cell cluster, whereby individual cells are eliminated via apoptosis, while small clusters of mis-specified cells are not eliminated and instead continue to proliferate and form cysts. It has been demonstrated that this elimination-based mechanism can mediate elimination of cells mis-expressing many different transcription factors, and this mechanism may therefore be shared between many different epithelial cell types. It has been suggested that cell surface cues, expressed downstream of mis-expressed transcription factors, possibly including Ephs and ephrins (Fagotto *et al*, 2014) may be involved in cell elimination and actomyosin contractility at the interface. However, a selective cell death-based mechanism is not thought to significantly contribute to border sharpening, as there is no evidence for increased levels of cell death at rhombomere borders, although this may not be detected if only small numbers of mis-placed cells are refined by selective cell death. Whilst in the time-lapse movies I have acquired I do occasionally see death of ectopic cells, it does not appear that this level of death is greater than background levels within rhombomeres during development, particularly as the process of imaging may increase levels of death by photo-toxicity.

3.7.5 The impact of Hoxb1 knock down on border sharpening and cell identity regulation

I have also demonstrated here that knock down of Hoxb1a and Hoxb1b causes increased numbers of ectopic *egr2b*-expressing cells to be observed in r4. Perhaps the most likely explanation for this is an inability of ectopic *egr2b*-expressing Hoxb1 morphant cells to switch their identity to that of r4. It is known that *hoxb1a*

represses *egr2b* expression via upregulation of Nlz1 proteins: in the absence of Nlz, expression of *egr2b* in r3 expands posteriorly into r4 (Labalette *et al*, 2015). Knock down of Hoxb1a and Hoxb1b severely reduces *nlz1* expression in r3/r4, while knock down of Nlz1 prevents the repressive effect of Hoxb1a overexpression on *egr2b* expression (Runko & Sagerström, 2003; Labalette *et al*, 2015). Dominant negative Nlz causes expansion of r3 and r5 into r4 and results in overlapping expression of *egr2b* and *hoxb1a* at the borders of these rhombomeres, suggesting that cell fate specification and resolution of overlapping identity is altered (Runko & Sagerström, 2003). Interestingly, it has been demonstrated that the chick *egr2b* regulatory element C drives expression of a GFP reporter within r4 (in addition to r3 and r5) in both zebrafish and mouse, despite the fact that extensive *egr2b* expression is never normally observed here (Chomette *et al*, 2006; Labalette *et al*, 2015). This indicates that element C does have activity within r4 and that additional, repressive inputs to element C are required to prevent *egr2b* expression here, but are unable to repress reporter expression. Therefore, it is possible that ectopic *egr2b*-expressing cells in r4 of Hoxb1 morphants arise due to normal amounts of cell intermingling and/or noise in gene induction and only persist due to a lack of Hoxb1-induced downregulation of *egr2b*. It is also possible that Hoxb1 knock down affects cell intermingling, potentially through regulation of Eph/ephrin expression and signalling. However, this appears unlikely, as rhombomere borders remain fairly straight and sharp in Hoxb1 morphants, while perturbation of Eph/ephrin signalling is known to compromise border sharpness (Xu *et al*, 1995; Cooke *et al*, 2005). To date, no Ephs or ephrins have been shown to be subject to regulation by Hoxb1 in r4.

An additional possible explanation for ectopic *egr2b*-expressing cells in Hoxb1a;Hoxb1b double morphants is that loss of Hoxb1b perturbs the orientation of cell division in the neuroepithelium (Zigman *et al*, 2014). Hoxb1b mutant embryos display randomly oriented cell divisions relative to the axis of the neuroepithelium within r3 and r4 at 6-12 ss, compared to wildtype cells, which divide in a stereotyped orientation, perpendicular to the AP axis (Zigman *et al*, 2014; Kimmel *et al*, 1994; Geldmacher-Voss *et al*, 2003). The requirement for Hoxb1b for oriented cell divisions in r3 is surprising, as *hoxb1b* was not previously thought to be expressed anterior to the r3/4 border (McClintock *et al*, 2001).

However, it has been shown in mouse that *Hoxa1* expression extends into r3 (Makki & Capecchi, 2011). This aberrant orientation of division in r3 and r4 is likely to increase the dispersal of cells' progeny between r3 and r4, causing ectopic *egr2b*-expressing cells to arise in r4. When Hoxb1a activity is additionally lacking, it is possible that any *egr2b*-expressing cells that arise in r4 are unable to switch their identity and thus retain ectopic *egr2b* expression, as I observe. In order to determine how ectopic *egr2b*-expressing cells arise in Hoxb1 morphants and to establish whether compromised identity regulation contributes to their persistence, time lapse imaging of Hoxb1 morphant Tg[egr2b:H2B-Citrine] embryos can be conducted. It should then be possible to ascertain whether ectopic cells arise due to either mis-oriented cell division or increased cell intermingling, or whether the ectopic cells observed reflect normal occurrence of ectopic cells due to normal mis-specification and intermingling and identity regulation, by comparing their frequency with that of control cells.

3.7.6 Conclusions

In this chapter I have provided evidence that some regulation of cell identity contributes to hindbrain border sharpening, although the approaches I have used may provide an underestimate of the extent to which cell identity regulation occurs. As discussed, improvements to the techniques used here to observe cell identity switching should help provide a clearer indication of the extent to which cells switch identity. Additional tools could also be developed to more clearly demonstrate whether cells completely switch identity from one type to another, or whether they resolve an initially overlapping identity at segment borders.

Chapter 4. Consequences of perturbed Eph/ephrin signalling on border sharpening and cell identity regulation

4.1 Introduction

As discussed in Chapter 3, I have presented some evidence that regulation of cell identity contributes to rhombomere border sharpening. An alternative approach to reveal the contribution of identity regulation to border sharpening is to increase the requirement for cell identity switching in border sharpening. I therefore investigated whether increasing the amount of cell intermingling between rhombomeres increases the amount of cell identity switching that occurs at the time when borders are usually becoming sharp. If cell identity switching contributes to refinement of ectopic cells, it is expected that increasing the number of misplaced cells will increase the amount of identity switching that occurs; for cells expressing *egr2b* in r2, 4 or 6, identity switching may be detectable using Tg[egr2b:H2B-Citrine] as previously described in Chapter 3. Eph/ephrin-mediated cell sorting and segregation restricts cell intermingling between rhombomeres (Xu *et al*, 1995, 1999). Therefore, a suitable approach to increase cell mixing between rhombomeres is to disrupt Eph/ephrin signalling. Knock down of EphA4, which is expressed in r3 and r5, increases the jaggedness of certain rhombomere borders, which is enhanced by simultaneous knock down of EphrinB2a (Cooke *et al*, 2005; Kemp *et al*, 2009). Perturbation of Eph/ephrin signalling should therefore increase intermingling and the possibility of cell identity switching.

In this chapter, I present evidence that perturbation of Eph/ephrin signalling increases the extent of identity switching that occurs in Tg[egr2b:H2B-Citrine], as determined by analysis of Citrine-containing cells and their gene expression status. I also describe a novel EphrinB3b mutant that I have generated using targeted nuclease technology. As expected from knock down studies, this mutant has a

border sharpness phenotype and will be a valuable tool for future studies of border sharpening and identity regulation upon perturbation of Eph/ephrin signalling.

Results

4.2 Knock down of EphA4 increases the amount of cell identity switching

In order to study whether perturbed Eph/ephrin signalling increases the amount of identity switching during border sharpening, I used previously published morpholinos to knock down EphA4, which has been shown to increase the fuzziness of *egr2b* expression at stages when borders are usually sharp (Cooke *et al*, 2005). As shown in Figure 4-1(A-D), knock down of EphA4 perturbs the sharpness of *citrine* expression in Tg[egr2b:H2B-Citrine] at the r2/r3, r3/r4 and r5/r6 borders by 16 ss (asterisks). The r4/5 border remains sharp when EphA4 is knocked down (black arrowheads). Although borders of *citrine* RNA expression are fuzzy, at these late stages, ectopic *citrine*-expressing cells are rarely observed in r2, r4 or r6. This is in agreement with previous observations (Cooke *et al*, 2005; Kemp *et al*, 2009), and is consistent with the hypothesis that identity regulation contributes to refinement of identity upon perturbation of Eph/ephrin signalling. As previously discussed, H2B-Citrine protein in Tg[egr2b:H2B-Citrine] can be used to identify cells that have previously expressed *egr2b* due to the perdurance of H2B-Citrine beyond the timescale of border sharpening.

I studied expression of *egr2b* and *hoxb1a*, in combination with visualising H2B-Citrine by immunohistochemistry (IHC) in Tg[egr2b:H2B-Citrine] homozygous embryos. However, I observed that conducting IHC for Citrine after ISH reduces the sensitivity of IHC – signal strength is reduced and background levels are increased. Because of this, fewer ectopic Citrine-expressing cells were detected in control embryos than previously detected in Tg[egr2b:H2B-Citrine] without IHC (Figure 3-14). Although this may cause an underestimation of the number of ectopic Citrine-expressing cells, comparisons between control and morphant embryos processed for both ISH and IHC will reveal any change in the amount of cell identity switching.

As shown in Figure 4-1 (E-G), EphA4 knock down increases the number of ectopic Citrine-containing cells (from an average of 2.5 cells in r2, r4 and r6 (n = 4 embryos) to 9.3 cells (n = 7 embryos)). These cells do not express *egr2b*, indicating that they have switched identity. Citrine-containing cells within r4 tend to express *hoxb1a* but do not express *egr2b*, indicating that while these cells have expressed *egr2b* previously, they have since downregulated *egr2b* and upregulated – or maintained expression of – *hoxb1a*. Overall, the presence of increased numbers of cells that contain H2B-Citrine but no longer express *egr2b* in Tg[egr2b:H2B-Citrine] with EphA4 knocked down indicates that cells are capable of switching identity, and that loss of EphA4 increases the extent of cell identity switching. Interestingly, knock down of EphA4 also increases the number of cells at the interface between r3 and r4 that contain H2B-Citrine but express both *egr2b* and *hoxb1a*, compared to control embryos. This suggests that EphA4 may contribute to both refinement and maintenance of rhombomere identity. It is not clear whether this is due to increased cell intermingling which continues at later stages than normal when EphA4 is knocked down, which may require refinement of cell identity at later stages than usual. Alternatively, it is possible that EphA4 may have a more direct impact on identity regulation, although the mechanism by which EphA4 could function in this way is not clear.

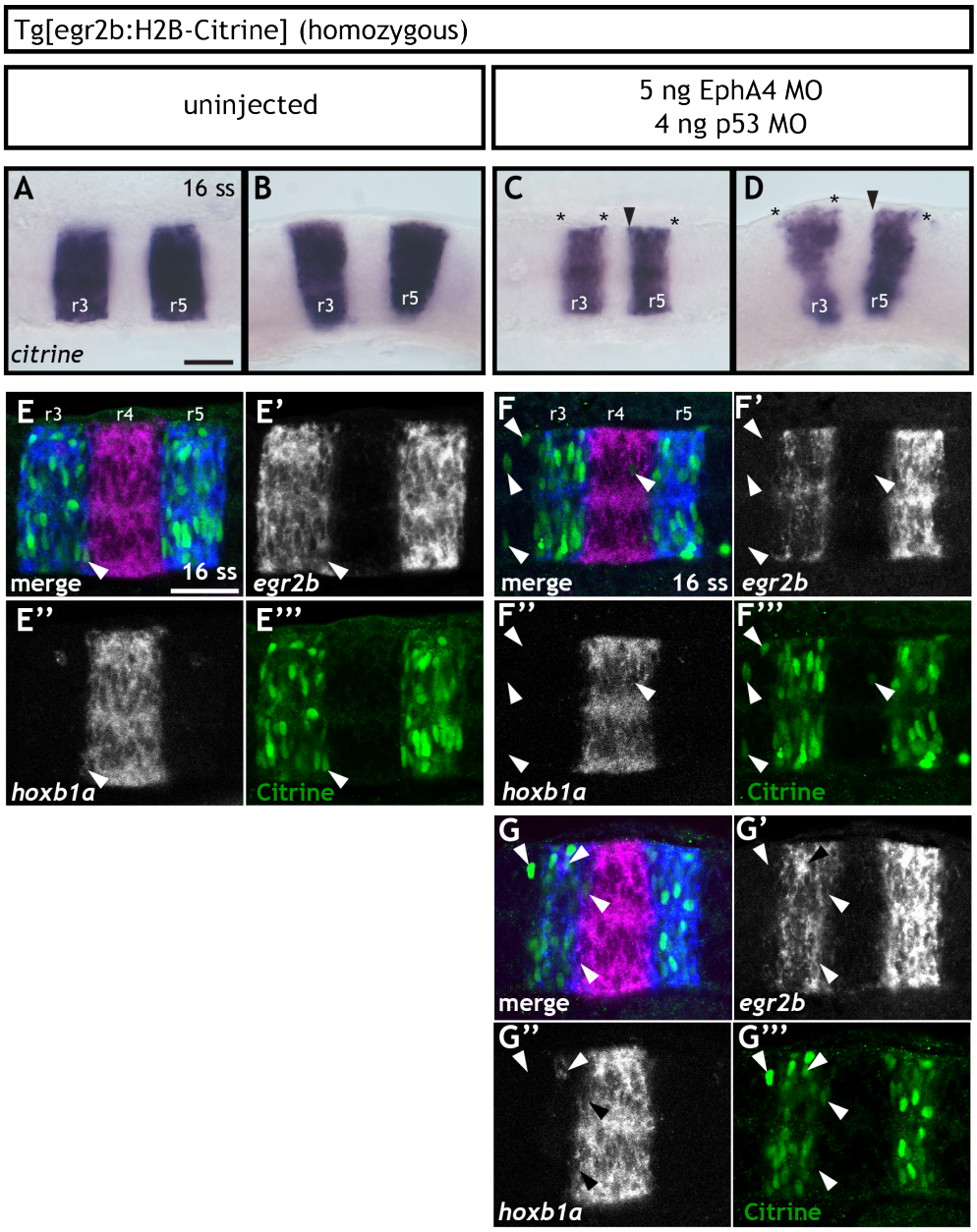

Figure 4-1 Knock down of EphA4 and rhombomere border sharpness in Tg[egr2b:H2B-Citrine]

Tg[egr2b:H2B-Citrine] embryos were injected with EphA4 morpholino and expression of various segmental markers studied. Knock down of EphA4 increases the fuzziness of *citrine* expression at rhombomere borders at 16 ss (C,D) compared to uninjected control embryos (A,B). When H2B-Citrine protein is visualised, the majority of Citrine-containing cells at 16 ss are located within r3 and r5 and express *egr2b* in control embryos (E). In control embryos, there are an average of 0.75 Citrine-positive, *egr2b*-negative cells detected in r2, 0.5 cells in r4 and 1.25 cells in r6 (n = 4 embryos). In comparison, EphA4 knock down increases the number of Citrine-

positive, *egr2b*-negative cells to an average of 5.4 cells in r2, 1.6 cells in r4 and 2.3 cells in r6 (F,G; n = 7 embryos; arrowheads). In addition, knock down of EphA4 increases the number of Citrine-containing cells at rhombomere borders that co-express *egr2b* and *hoxb1a*. At the r3/4 border, an average of 0.75 Citrine-positive cells co-express *egr2b* and *hoxb1a*, compared to 4.6 cells in EphA4 morphants (n = 7 embryos). At the r4/5 border, there are no Citrine-expressing cells that co-express *egr2b* and *hoxb1a* in control embryos (n = 4 embryos), compared to an average of 1.3 cells in EphA4 morphants (n = 7 embryos). Embryos in A and C are flat-mounted with anterior to the left; embryos in B and D are side-mounted with anterior to the left. Scale bars: 50 μm.

4.3 Generation and characterisation of an EphrinB3b mutant

An approach to further enhance perturbation of Eph/ephrin signalling is to simultaneously compromise both Eph and ephrin activity, as there is redundancy between multiple pairs of Eph receptors and ephrins in the hindbrain. It has previously been shown that simultaneous knock down of EphA4 and EphrinB2 enhances the fuzziness of rhombomere borders compared to single knock down of either protein alone, presumably because these are both capable of interacting with additional binding partners (Cooke *et al*, 2005). As shown in Figure 4-2, expression of multiple Ephs and ephrins in complementary rhombomeres enables interactions between multiple potential binding partners at interfaces between adjacent rhombomeres. These interactions may redundantly contribute to border sharpening, via Eph/ephrin mediated cell sorting and restriction of intermingling. Jordi Cayuso in the Wilkinson lab has also identified segmentally-restricted expression of EphB3 and EphrinB1 in the hindbrain as shown in Figure 4-2 (unpublished). A suitable ephrin to disrupt – in combination with loss of EphA4 activity – is EphrinB3b, which is a known ligand of EphA4 and is expressed in rhombomeres 2, 4 and 6, complementary to EphA4 expression in r3 and r5 (Gale *et al*, 1996b; Chan *et al*, 2001). As shown in Figure 4-3, at earlier stages, the *ephrinB3b* expression domain is initially more widespread, and *ephrinB3b* is expressed in r3 until approximately 4 ss and in r5 until approximately 7 ss. It is not known what regulates early induction and regulation of segmental *ephrinB3b* expression.

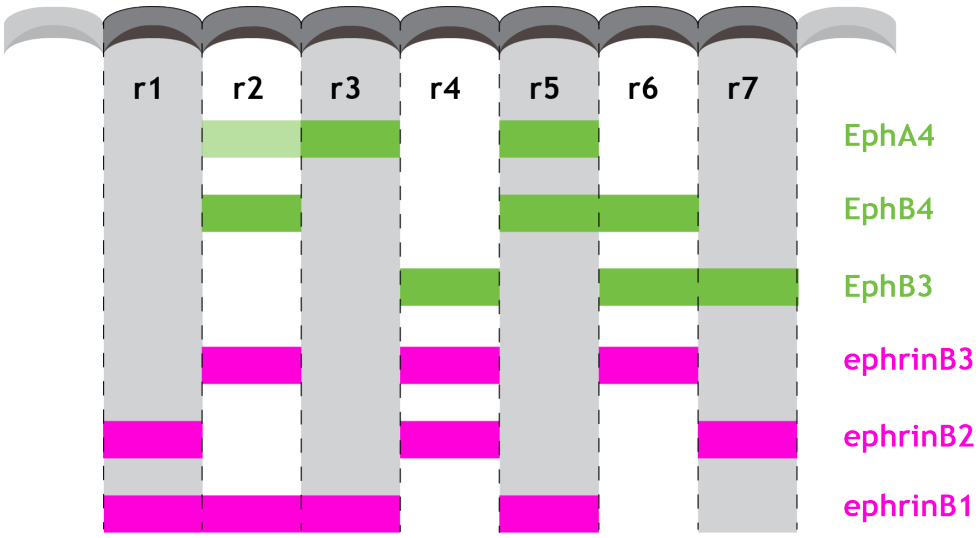

Figure 4-2 Expression of Ephs and ephrins within the zebrafish hindbrain

Schematic showing segmental, rhombomere-restricted expression of Ephs (green) and ephrins (magenta) in the zebrafish hindbrain. Ephs and ephrins are generally expressed in complementary domains, enabling interactions at rhombomere interfaces (dotted lines). Anterior is to the left; r1 – r7 = rhombomere 1 – 7.

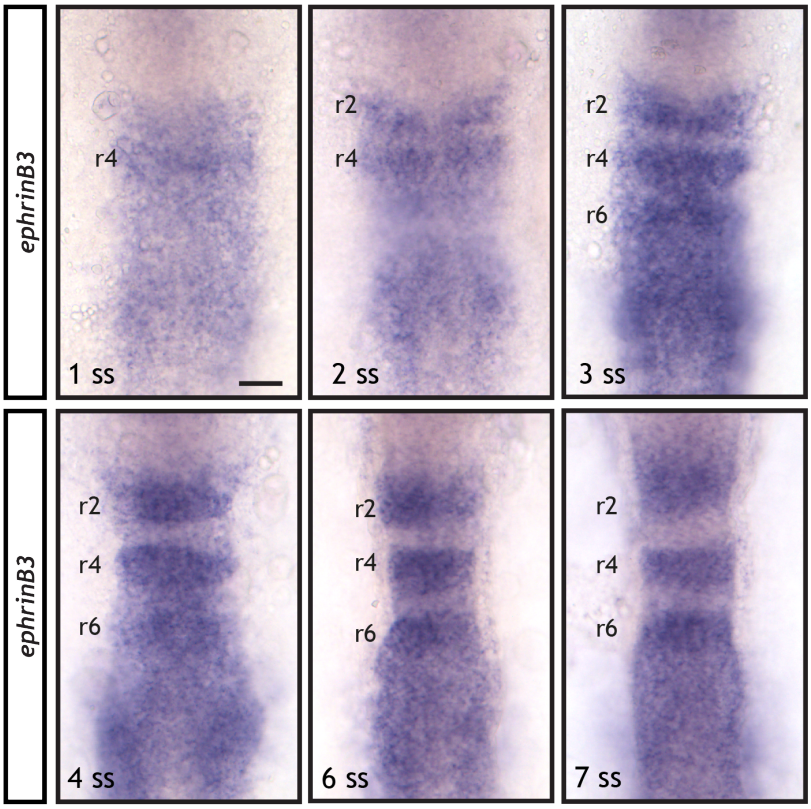

Figure 4-3 Time course of *ephrinB3b* expression during border sharpening
Expression of *ephrinB3b* was analysed in embryos from 1 ss to 7 ss. In addition to segmental expression in r2, r4 and r6, *ephrinB3b* is also expressed in r3 until approximately 4 ss and in r5 until approximately 7 ss. Embryos are flat-mounted with anterior to the top. Scale bar: 50 μm

Traditionally, loss-of-function experiments in zebrafish have relied heavily on morpholino antisense oligomers (MOs) to knock down gene products. Morpholinos are short oligomers, approximately 25 bases in length, which bind to their target RNA via complementary base pairing and interfere with either translation (in the case of translation-blocking morpholinos) or RNA transcript processing (in the case of splice-blocking morpholinos) by steric hindrance. This results in knock down of the target gene product. Knock down of EphrinB3b by morpholino injection has indicated that loss of EphrinB3b causes disruption of the r2/3, r3/4 and r5/6 borders (Terriente *et al*, 2012). However, other members of the Wilkinson lab have found that the EphrinB3b morpholino causes p53-activating toxicity, which is only partly rescued by co-injection with p53 morpholino (Robu *et al*, 2007; Gerety & Wilkinson, 2011). This toxicity could affect the phenotypes observed and conclusions drawn with knock down of *EphrinB3b*, as specific phenotypes caused by morpholinos can

sometimes be difficult to distinguish from non-specific effects (Eisen & Smith, 2008). A particular issue for using morpholinos when studying hindbrain border sharpening is that some morpholinos can cause a significant developmental delay; as previously illustrated in Figure 3-1, even small differences in stage can influence the sharpness of rhombomere borders. Care must therefore be taken when staging embryos in these experiments to not rely solely on time of development, but also morphological features, such as somite number (Kimmel *et al*, 1995). In addition, morpholinos may be unable to knock down certain gene products with complete efficiency, which can limit their effectiveness for studying certain processes and mechanisms.

Given these drawbacks to morpholinos, it would be beneficial to generate an EphrinB3b mutant. Many zebrafish mutants have been generated using TILLING (targeting induced local lesions in genomes) (McCallum *et al*, 2000; Wienholds *et al*, 2003; Sood *et al*, 2006). This involves large-scale, high-throughput sequencing of zebrafish with random N-ethyl-N-nitrosourea (ENU)-induced mutations. However, the nature of TILLING makes it an unfeasible technique to routinely use in the lab to generate novel mutants, and at the time of this project, no TILLING mutants for EphrinB3b had been reported. As previously described in Chapter 3, several new technologies have been developed in recent years that use targetable nucleases to create mutations at specific sites in the zebrafish genome, providing an alternative to morpholino knock down, as reviewed in (Schulte-Merker & Stainier, 2014). I therefore made use of targeted nucleases to generate a novel EphrinB3b mutant line. This mutant will not only be useful to address the contribution of cell identity switching to border refinement, but also to study other aspects of border sharpening and Eph/ephrin signalling in hindbrain development.

At the time I started this work, a suitable targeted knock out approach was available, which uses transcription activator like effector nucleases (TALENs). TALENs bind to DNA in a context-independent modular fashion (Bogdanove & Voytas, 2011). The DNA binding specificity of TALENs arises from the TALE components, which are derived from the plant pathogenic bacteria, *Xanthomonas* (Römer *et al*, 2007). As shown in Figure 4-4 (A), TALENs consist of a mutated FokI nuclease monomer – which will form an obligate heterodimer to cleave DNA –

fused to an array of re-engineered TALEs as modular DNA-binding elements (Miller *et al*, 2011). Within each DNA-binding module, a key pair of residues – the repeat variable di-residue (RVD) – confers nucleotide-binding specificity (Moscou & Bogdanove, 2009; Boch *et al*, 2009). As shown in Figure 4-4 (A), a pair of TALENs, each containing a single FokI monomer, target sequences of approximately 20-nucleotides in length flanking a spacer region, in which the heterodimerised FokI nuclease will cut DNA to create a double-stranded break within the spacer region. These DSBs may be erroneously repaired by endogenous cellular repair mechanisms, including intrinsically error-prone NHEJ, leading to insertion and/or deletion of bases at the cut site. Indel mutations might cause a frameshift and thus lead to premature termination of translation and/or non-sense mediated decay of mRNA transcripts. TALENs have emerged as a useful tool for the creation of heritable, targeted mutations within the zebrafish genome with high efficiency (Bedell *et al*, 2012; Cade *et al*, 2012). I made use of this approach to create an EphrinB3b mutant.

4.3.1 Creation of TALENs targeting *ephrinB3b*

I designed a pair of TALENs targeting the first exon of *ephrinB3b*, close to the translational start site to increase the likelihood that any frameshift mutations will cause complete loss of EphrinB3b function (and likely nonsense-mediated decay of the mutant transcript), as shown in Figure 4-4 (B). In order to confirm that these TALENs efficiently cause DSBs at the *ephrinB3b* target site, high resolution melt curve analysis (HRM) was used to compare the sequence composition at the cut site between wildtype and injected embryos as shown in Figure 4-5, which can be used to study efficiency of TALEN-induced mutations (Reed *et al*, 2007; Parant *et al*, 2009; Dahlem *et al*, 2012). HRM involves amplification of a short region around the TALEN target site in the presence of a double-stranded DNA-binding intercalating dye. This amplicon is then slowly heated to denature the DNA, and the resulting reduction in fluorescence with temperature is recorded. The shape of the melting curve obtained depends on the nucleotide composition and sequence of the amplicon. Comparison of melting curve shape between wildtype, uninjected embryos and embryos injected with TALENs therefore provides an indication as to

the frequency of indel mutations caused by the TALENs. A shown in Figure 4-5 (B) 100% of embryos injected with *ephrinB3b* TALENs had acquired mutations causing a shift to the melt curve.

An alternative screening method is restriction fragment length polymorphism (RFLP), which requires a recognition site for a restriction enzyme within the spacer region of the TALEN target site, which is likely to be altered and compromise restriction digest if indel mutations arise. An advantage of screening by HRM over RFLP is that HRM can detect many different mutant alleles, while RFLP may give rise to false negative results as it is possible that the restriction enzyme recognition site will remain intact despite mutations occurring. In addition, it is not always possible to select a suitable TALEN target site that contains a suitable restriction site, as was the case for TALENs targeting *ephrinB3b*.

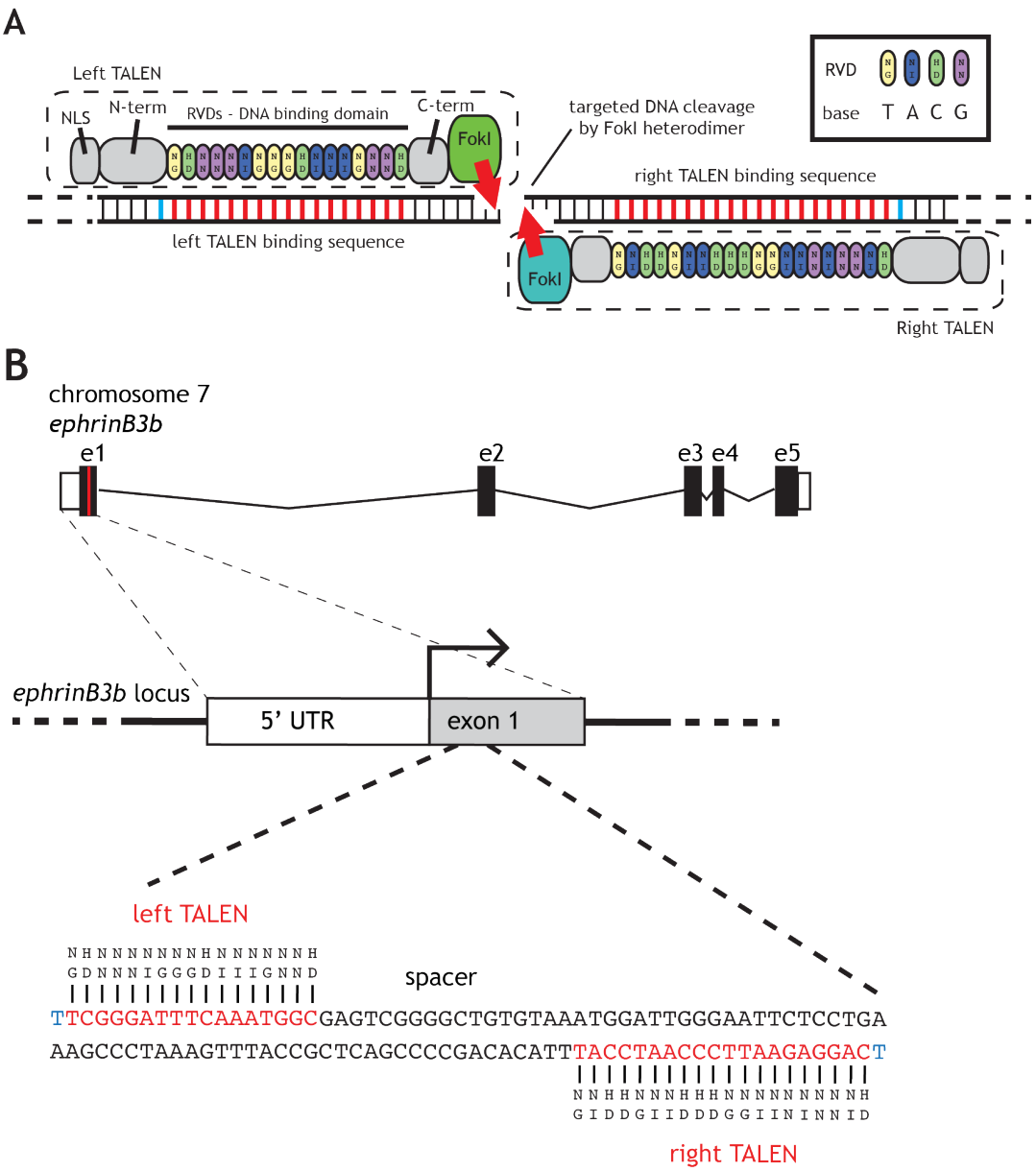

Figure 4-4 Using TALENs to target the *ephrinB3b* locus

A: Schematic illustrating TALEN structure and binding of a pair of TALENs to the target DNA sequence; binding specificity is mediated by repeat-variable di-residues (RVDs). Binding of both the left and right monomeric TALENs causes heterodimerisation of the FokI nuclease, which cleaves the DNA within the spacer region (red arrows). Common RVDs and their corresponding DNA bases are shown. NLS, nuclear localisation signal.

B: A pair of TALENs targeting exon 1 of *ephrinB3b*. DNA sequences bound by left and right TALENs are shown in red. e1 – 5, exons 1 – 5.

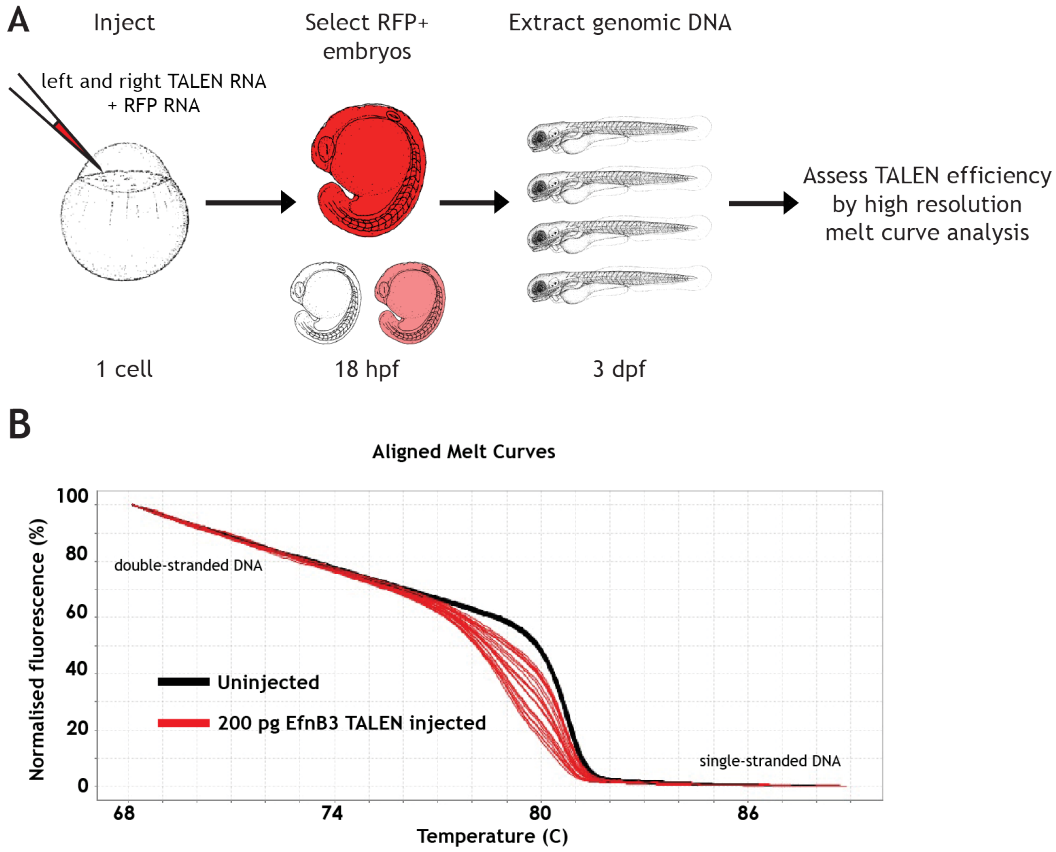

Figure 4-5 Creation and assessment of indel mutations at the EphrinB3b locus using TALENs

A: Generation of mutant embryos by injection of TALENs. Embryos are injected at the one cell stage with RNA encoding left and right TALENS. Co-injection with RNA encoding RFP allows selection of well-injected embryos. At 3 dpf, genomic DNA is extracted for analysis by high resolution melt curve analysis.

B: Assessing TALEN efficiency using high resolution melt curve analysis (HRM). Mutant DNA curves are shown in red; wildtype control curves are shown in black.

4.3.2 TALEN-induced mutations with *ephrinB3b* are heritable

Due to the error-prone nature of NHEJ-mediated repair of TALEN-induced DSBs, injected embryos will acquire multiple different mutations, in addition to wildtype alleles, in different cells. Because embryos injected with *ephrinB3b* TALENs will therefore be mosaic for loss-of-function mutations, they will not necessarily display any phenotypic consequences. In order to fully remove EphrinB3b function it is

necessary to create a stable mutant zebrafish line, homozygous for a deleterious *ephrinB3b* mutation. As shown in Figure 4-6 (A), mosaic F_0 founders were screened by outcrossing to wildtype fish and assessing their progeny by HRM (B) to identify which F_0 adults transmit TALEN-induced mutations at the *ephrinB3b* locus. Of 12 F_0 fish tested, 8 were found to transmit mutations to the next generation (67%). F_1 fish from identified F_0 carriers were raised to adulthood, and genotyped by fin-clipping and HRM analysis. The genomic region around the TALEN target site was sequenced to identify F_1 fish with frameshift mutations (Figure 4-6(C)). A single founder was found to transmit both a 9 bp (denoted mutant “A”) and a 2 bp deletion, with a 2 bp substitution (denoted mutant “B”, but hereafter referred to as EphrinB3b mutant) within the TALEN spacer region. These two mutants can be distinguished by the shape of their HRM curves. The 9 bp deletion in mutant A is unlikely to compromise function of EphrinB3b, due to deletion of only three amino acids from the N-terminus. The heterozygous F_1 fish with the 2 bp deletion were in-crossed to raise homozygous mutants, which were found to be viable.

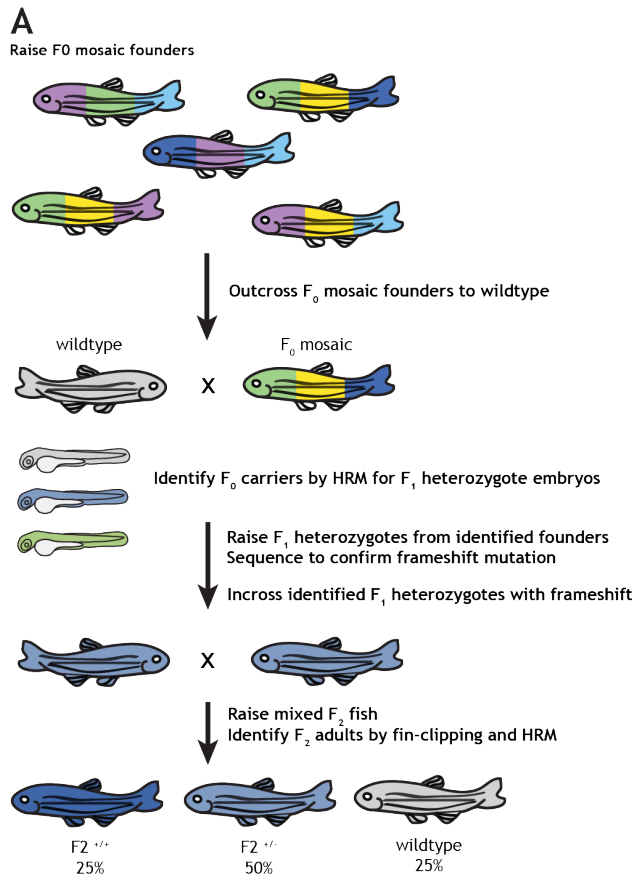

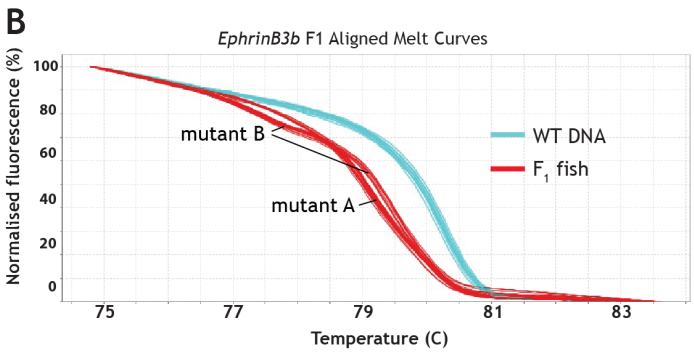

C

```
wildtype                    TTCGGGATTTCAAATGGCGAGTCGGGGCTGTGTAAATGGATTGGGAATTCTCCTGA
mutant "A" 9 bp deletion    TTCGGGATTTCAAATGGCGAGT---------GTAAATGGATTGGGAATTCTCCTGA
mutant "B" 2 bp deletion    TTCGGGATTTCAAATGGCGAGTCGGGAT--TGTAAATGGATTGGGAATTCTCCTGA
```

Figure 4-6 Generation of homozygous EphrinB3b mutant fish from mosaic F_0 founders

A: generation of homozygous EphrinB3b mutant fish from mosaic F_0 founders

B: Using HRM to identify F_0 carriers by analysing heterozygous F_1 embryos. The sensitivity of HRM allows different indel mutations to be distinguished by the shape of their melt curves. Two different mutant curves are shown in red; wildtype control curves are shown in blue.
C: Sequencing the *ephrinB3b* TALEN target site (black, bold) to identify frameshift mutations. The ATG start codon of *ephrinB3b* is shown in red. Inserted/substituted bases are shown in blue. As shown, two different mutant alleles were transmitted by a single founder; one of which was a 9 bp deletion “mutant A”; the other a 2 bp deletion and 2 bp substitution “mutant B”.

4.4 Boundary cell marker expression is absent or reduced at specific boundaries of EphrinB3b$^{-/-}$

Due to lack of a suitable EphrinB3b antibody, it was not possible to verify loss of the EphrinB3b protein in the EphrinB3b mutant by immunohistochemistry. However, it is known that Eph/ephrin signalling is required for specification of specialised boundary cells that arise at rhombomere interfaces after completion of border sharpening; dominant negative EphA4 causes reduced expression of *pax6* at certain rhombomere boundaries (Xu *et al*, 1995). In addition, EphA4 knock down causes loss of *sema3Gb, foxb1.2* and *rfng* expression at specific boundaries (Cooke *et al*, 2005), while EphrinB3b knock down reduces *rfng* expression at the same boundaries (Terriente *et al*, 2012). Therefore, in order to verify that the new EphrinB3b mutation causes loss of functional EphrinB3b, I studied the expression of boundary cell markers in the EphrinB3b mutant. When expression of the boundary marker *rfng* was studied in embryos from in-crossed F_1s heterozygous for the 9 bp deletion, no difference in expression was observed compared to wildtype embryos in 100% of mixed wildtype, heterozygous and homozygous embryos (data not shown), confirming that this mutation does not appear to compromise EphrinB3b function. As shown in Figure 4-7, in homozygous embryos containing the 2 bp deletion, expression of the boundary marker *rfng* is lost at the r2/3 boundary, and reduced at the r3/4 and r5/6 boundaries compared to wildtype expression (Figure 4-7 A-B). Expression of *wnt8b*, which is expressed in boundaries in addition to r3 and r5, at lower levels, is also lost at the r2/3 boundary in homozygous mutants (Figure 4-7 D-E). This indicates that the EphrinB3b mutant with 2 bp deletion does indeed lack functional EphrinB3b. In heterozygous EphrinB3b mutants, I observed a slight reduction in *rfng* expression at the r2/3

boundary, but otherwise embryos appear like wildtypes. This suggests that, at certain boundaries, EphrinB3b contributes to upregulation of boundary markers in a dosage-dependent manner. Morpholino knock down of EphrinB3b causes the loss of *rfng* expression at the boundary between rhombomeres 2 and 3 and a reduction of *rfng* expression at r3/4 and r5/6 boundaries (Terriente *et al*, 2012). It was not previously clear whether the incomplete loss of *rfng* at certain boundaries results from incomplete EphrinB3b knock down and residual activity or from partial redundancy with signalling between other ephrins and Ephs at these boundaries. Based on my observations in the EphrinB3b mutant, residual *rfng* expression seen at certain boundaries in the EphrinB3b morphant is likely due to redundancy between EphrinB3b with other ephrins at these borders, rather than incomplete MO knock down. For example, EphrinB2 in r4 and r6 may be capable of interacting with EphA4 (expressed in r3 and r5) at the r3/4, r4/5 and r5/6 borders, as shown in Figure 4-2. However, EphrinB2 knock down alone does not appear to have a significant impact on rhombomere boundary marker expression (Cooke *et al*, 2005). It is likely that the same redundancy of Eph/ephrin interactions mediated by EphrinB3b for expression of boundary markers will have consequences for the severity of sharpening defects at certain rhombomere borders.

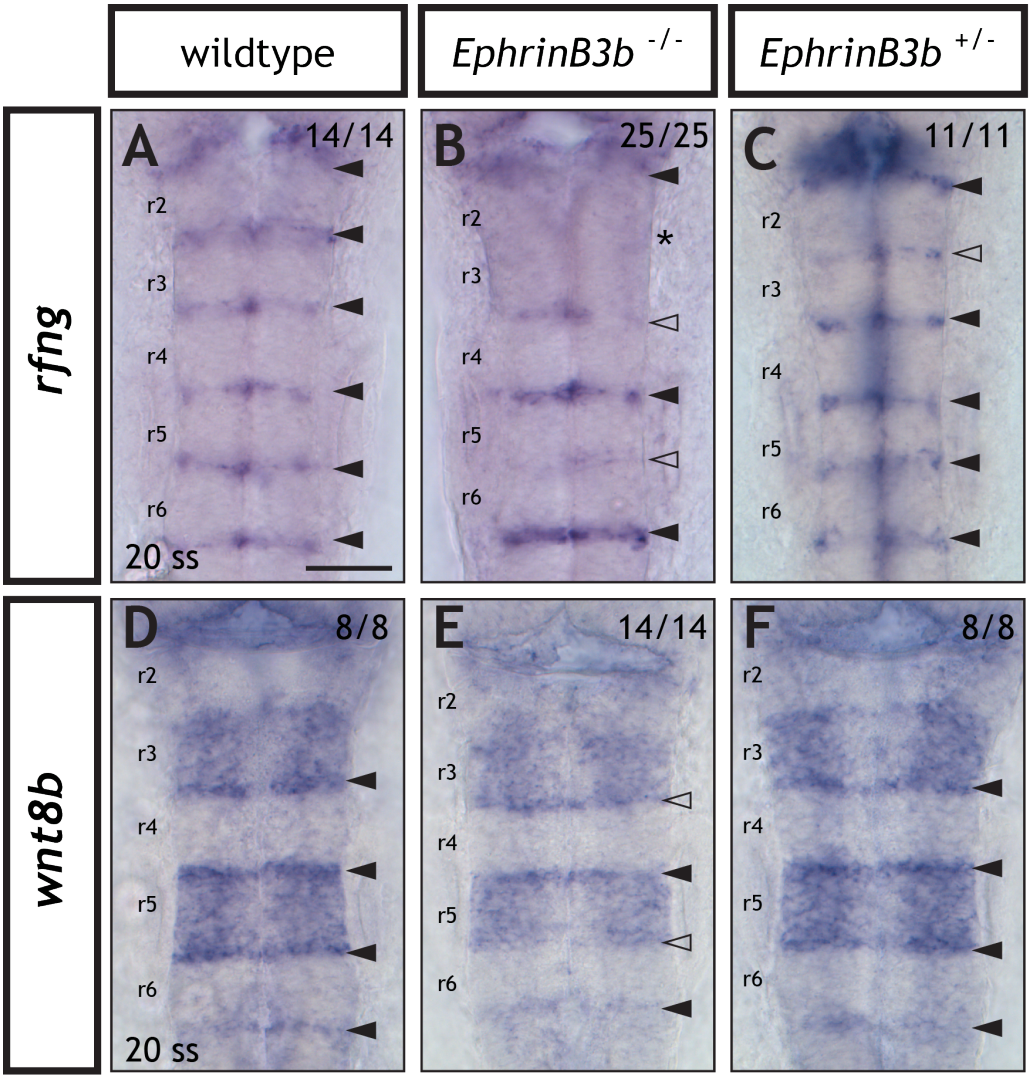

Figure 4-7 Expression of rhombomere boundary markers in EphrinB3b mutants

Expression of boundary markers *rfng* and *wnt8b* were analysed in wildtype embryos and EphrinB3 mutant embryos at 20 ss. In homozygous mutants, *rfng* expression is lost from the r2/3 boundary (asterisk) and reduced at the r3/4 and r4/5 boundaries (empty arrowheads) (B). Expression of rfng at the r4/5 and r6/7 boundaries is comparable in the homozygous mutant and control embryos (A,B; black arrowheads). In heterozygous mutants, *rfng* expression is slightly reduced at the r2/3 boundary (empty arrowhead), but expression at all other boundaries is comparable to wildtype embryos (A,C; black arrowheads). In wildtype embryos, expression of *wnt8b* can only be clearly detected at the r3/4, r4/5, r5/6 and r6/7 boundaries (D; black arrowheads). Expression of *wnt8b* is reduced at the r3/4 and r5/6 boundaries in EphrinB3b homozygous mutants compared to wildtypes (D,E; empty arrowheads). In heterozygous EphrinB3b mutants, there is no clear difference in level of expression of *wnt8b* at any boundaries compared to wildtypes (D,F; black arrowheads). Embryos are flat-mounted, with

anterior to the top. Frequencies of embryos observed represented by the image shown, out of the total number of embryos studied are shown in the top right. Scale bar: 50 μm.

4.5 Border sharpening in EphrinB3b mutants

In order to study the impact of loss of EphrinB3b on rhombomere border sharpness, I studied expression of *egr2b* at several time points during and after completion of border sharpening, in combination with knock down of EphA4. The morpholino used to knock down EphA4 does not appear to cause significant toxicity or p53 activation when co-injected with p53 morpholino. In EphrinB3b mutants injected with EphA4 morpholino at 8 ss, the borders of *egr2b* expression are fuzzier compared to wildtypes (Figure 4-8 A,B) and ectopic *egr2b*-expressing cells are more frequently observed in r2 and r4. At this stage, there are also neural crest cells at the r5/6 border, which obscures any border fuzziness and ectopic cells from r5 here (Figure 4-8(A,B)). At even later stages (16 ss), *egr2b* expression remains fuzzy at the r2/3, r3/4 and r5/6 boundaries in both EphrinB3b mutants and EphA4 morphants (Figure 4-8(C-E)). Knock down of EphA4 in the EphrinB3b mutant increases the extent of this fuzziness (Figure 4-8 (F)). This suggests that both EphrinB3b and EphA4 are capable of interacting with additional Ephs and ephrins at certain rhombomere interfaces to contribute to border sharpening and that there is some redundancy between both EphA4 and EphrinB3b. As shown in Figure 4-2, EphB4 is expressed in r5 and may interact with EphrinB3b at the r4/5 border to contribute to sharpening here, even in the absence of EphA4, although EphB4 is thought to be highly selective for EphrinB2. For other borders, to date, there are no known Ephs that might interact with EphrinB3b to contribute to sharpening that have been identified. Alternatively, it is possible there are sharpening mechanisms that are not dependent on complementary Eph/ephrin expression, such as increased cell adhesion within segments (Cooke *et al*, 2005).

Interestingly, at 16 ss, there are fewer ectopic *egr2b*-expressing cells observed in r4 of EphrinB3b mutants with EphA4 knocked down compared to 8 ss (Figure 4-8 B,F). This is consistent with additional mechanisms to Eph/ephrin-mediated sorting contributing to border sharpening between 8 ss and 16 ss, such as cell identity regulation. Alternatively, it is possible that residual Eph/ephrin signalling (involving

other Ephs and ephrins) may contribute to some segregation between 8 ss and 16 ss. More recently, an EphA4 mutant has been created by Jordi Cayuso in the Wilkinson lab (unpublished). Because I have shown that additional loss of EphA4 in the EphrinB3 mutant enhances border sharpening defects, I have crossed the EphrinB3b mutant to this EphA4 mutant. As shown in Figure 4-8 (G,H), embryos obtained from identified EphA4;EphrinB3 double homozygotes have comparable sorting defects to EphrinB3b mutants with EphA4 knocked down by morpholino at 16 ss. This double mutant will be a valuable tool for studying cell identity regulation and border sharpening. Unfortunately, at the time of writing, it has not yet been possible to study *egr2b* expression at earlier stages in double mutant embryos due to poor fertility and small clutch sizes.

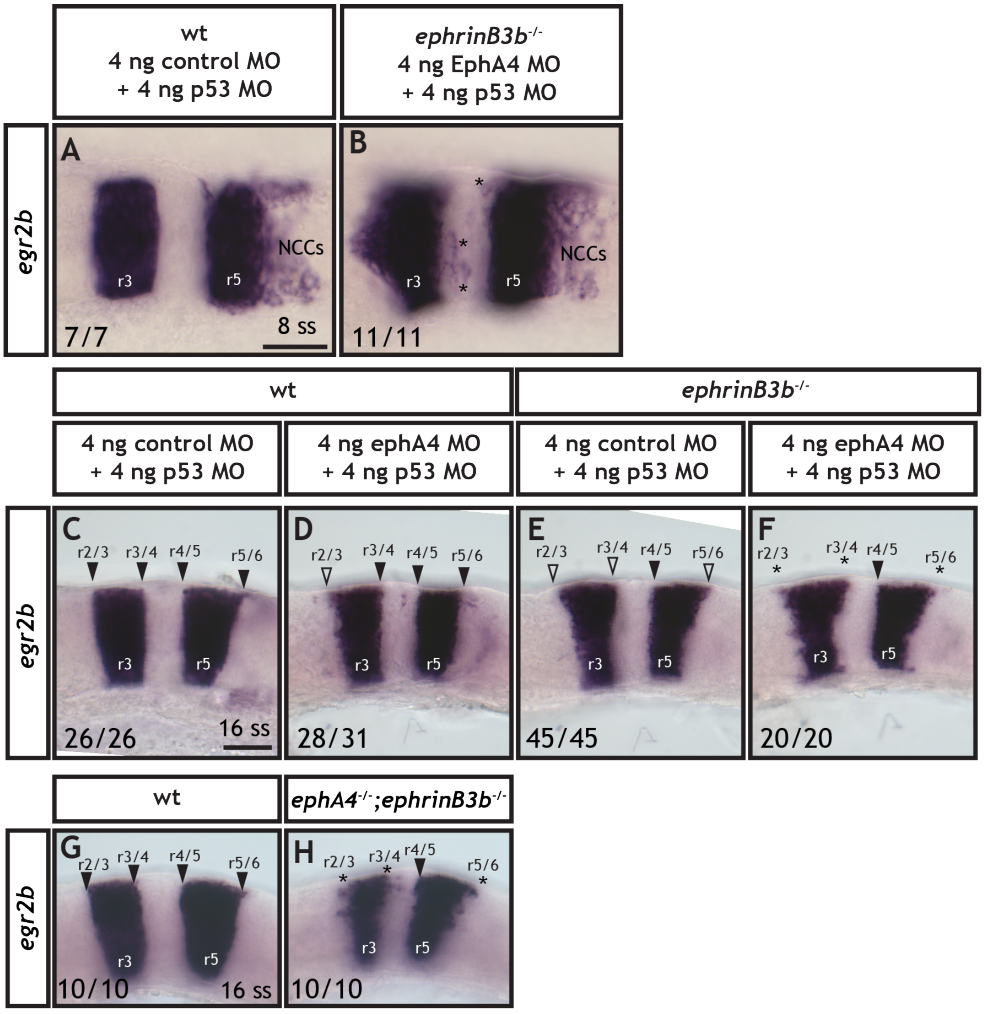

Figure 4-8 Expression of *egr2b* in EphrinB3b mutants, in combination with EphA4 knock down and EphA4;EphrinB3b double homozygous mutants

Expression of *egr2b* was analysed in wildtype embryos and EphrinB3b mutant embryos, injected with either control morpholino or EphA4 morpholino. In comparison to wildtype embryos at 8 ss (A), EphrinB3b mutant embryos injected with EphA4 morpholino have increased numbers of ectopic *egr2b*-expressing cells within r4 (B; asterisks). At 16 ss, certain rhombomere borders are fuzzier in EphA4 morphants (D; arrowheads) or EphrinB3b mutants (E; arrowheads) compared to wildtype embryos (C; arrowheads). In EphrinB3b mutants injected with EphA4 morpholino, the sharpness of r2/3, r3/4 and r5/6 boundaries is severely compromised (F; asterisks), although the r4/5 border remains sharp (black arrowhead). In double EphA4;EphrinB3b homozygous embryos, border sharpness is compromised to a comparable degree to EphrinB3b mutants with EphA4 knocked down (H,F; asterisks). Embryos A and B are flat-mounted, while embryos C – H are side mounted, with anterior to the left. Frequencies of embryos observed represented by the image shown, out of the total number of embryos studied are shown in the bottom right. NCCs, neural crest cells. Scale bars: 50 μm.

4.6 EphrinB3b does not appear to affect cell adhesion within r2, r4 or r6

In addition to studying the impact of perturbed Eph/ephrin signalling on hindbrain border sharpening, I also studied the distribution of EphrinB3b mutant cells within mosaic embryos, which may provide some insight into the mechanisms of Eph/ephrin-mediated establishment and maintenance of sharp borders. It has been suggested that EphrinB2 promotes cell adhesion within r4, independently of EphA4: EphrinB2 morphant cells are excluded from r4 and r7 within wildtype hosts, while wildtype cells form tight clusters within r1, r4 and r7 of EphrinB2 morphant hosts (Kemp *et al*, 2009). In addition, EphA4 morphant cells are excluded from r3 and r5 of wildtype hosts and accumulate at rhombomere boundaries (Cooke *et al*, 2005). Although these cell sorting patterns were interpreted as evidence for regulation of cell adhesion (Cooke *et al*, 2005; Kemp *et al*, 2009), recent work suggests that a more likely mechanism is the regulation of cortical tension (Calzolari *et al*, 2014; Cayuso *et al*, 2015). Similar analysis in embryos mosaic for EphrinB3b have not yet been reported, but based on its expression pattern and role in border sharpening it might be expected that EphrinB3b can has a similar function in promoting cell affinity in rhombomeres where it is expressed.

As shown in Figure 4-9, when cells from EphrinB3b mutant donors are transplanted into wildtype hosts at early gastrula stages, donor cells are not restricted or sorted from r2, (Figure 4-9 B) r4 (Figure 4-9 A,B) or r6 (Figure 4-9 A) – where EphrinB3b is expressed. Morphant donor cells are instead distributed throughout these rhombomeres, similar to within r3 and r5, where EphrinB3b is not expressed. This result is surprising, given the previous observations made in mosaic EphrinB2 embryos (Kemp *et al*, 2009) and suggests that EphrinB3b may not have the same role within r2, r4 or r6 as EphrinB2 has in r1, r4 and r7.

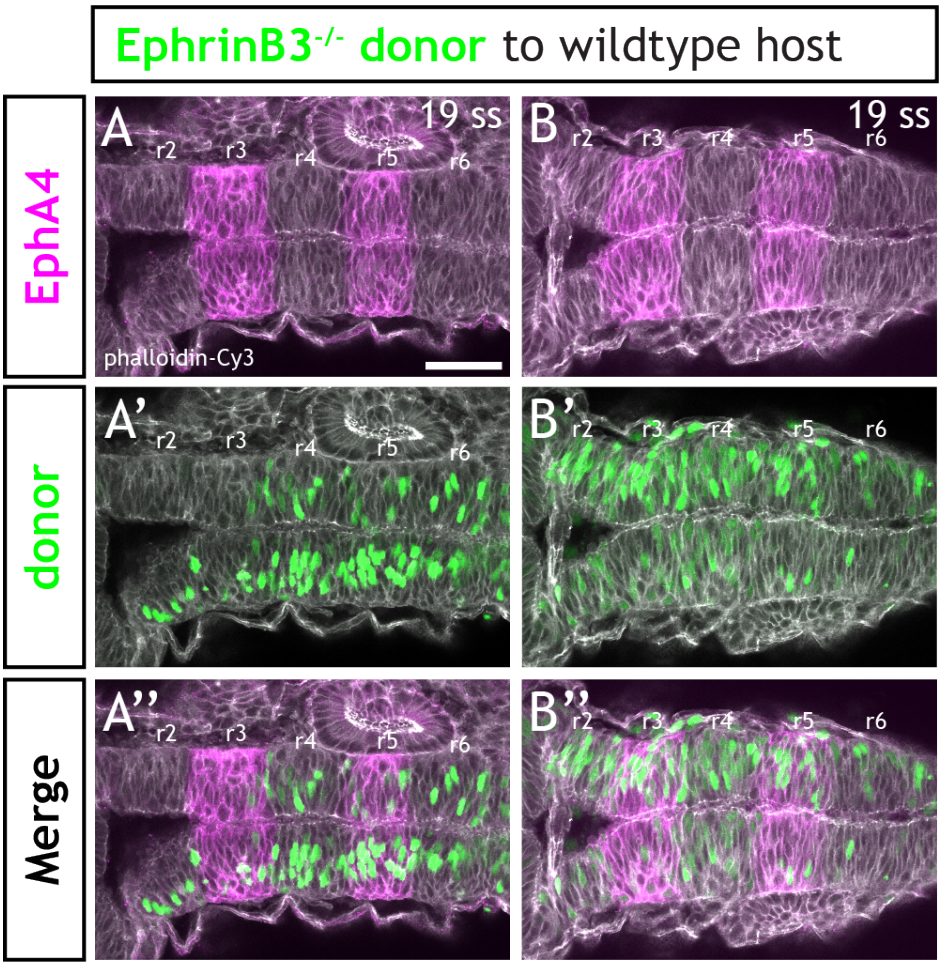

Figure 4-9 Distribution of EphrinB3$^{-/-}$ donor cells in wildtype hosts after completion of border sharpening

Cells from homozygous EphrinB3 mutant hosts, injected with H2B-GFP as a tracer, were transplanted into wildtype hosts at early gastrula stages. Two different embryos are shown (A,B). At 19 ss, the distribution of donor cells was assessed in combination with EphA4 immunohistochemistry. Cy3-conjugated phalloidin was used to visualise actin at cell membranes. EphrinB3 mutant cells are distributed throughout rhombomeres and are not excluded from r2, r4 or r6 (n = 8 embryos. Embryos are flat-mounted with anterior to the left. Scale bar: 50 µm.

4.7 Discussion

In this chapter I have studied the impact of compromised Eph/ephrin signalling on hindbrain border sharpness. Not only does this provide insight into the role of Eph/ephrin signalling in establishment and/or maintenance of sharp rhombomere borders, but this also reveals contributions of cell identity switching to hindbrain border sharpening, building on results previous discussed in Chapter 3.

4.7.1 Additional evidence for a contribution of identity switching in hindbrain border sharpening

I have shown here that knocking down EphA4 increases the extent of cell identity switching at rhombomere borders, using the Tg[egr2b:H2B-Citrine] line to infer identity switching based on presence of H2B-Citrine-containing cells that no longer express *egr2b* and – in r4 – express *hoxb1a*. It appears that identity switching is more dramatically increased at the r2/3 interface, and least affected at the r4/5 interface, which is due to increased mixing of cells across the r2/3 border when EphA4 is knocked down.

Combining my findings here with published data, it appears that loss of either EphA4 (Cooke *et al*, 2005; Terriente *et al*, 2012) or EphrinB3b alone is sufficient for complete loss of boundary markers from the r2/3 border, but not the r4/5 border. In the EphrinB3b mutant described here, boundary marker expression is reduced but not completely lost at the r3/4 and r5/6 borders. Alternative Eph/ephrin interactions at these interfaces may be mediated by EphB3 (expressed in r4 and r6) and EphrinB1 (expressed in r3 and r5), or by additional, as yet unidentified, Ephs and Ephrins. The r4/5 border appears to have the greatest potential redundancy of Eph/ephrin interactions, as three known pairs of Ephs and ephrins are differentially expressed across this interface. In embryos with individual or simultaneous loss of EphA4 and EphrinB3b, the severity of border sharpness phenotypes appears to correlate with the severity of boundary marker phenotypes; it therefore seems reasonable to assume that redundancy in Eph/ephrin-mediated boundary specification is shared with Eph/ephrin-mediated border sharpening. It is not clear

whether Eph/ephrin signalling between different binding partners has different contributions to border refinement in normal development.

It is expected that increased identity switching with perturbed Eph/ephrin signalling is due to increased cell mixing across borders, rather than increased mis-specification of cells at borders. It is interesting that EphA4 knock down increases the number of H2B-Citrine-containing cells that co-express *hoxb1a* and *egr2b* at the r3/4 border. Detection of H2B-Citrine in these cells suggests that they have initiated *egr2b* expression and maintenance at early stages (as discussed in Chapter 3). It therefore appears that EphA4 is involved in regulation of cell identity at rhombomere borders, but it is not clear whether this is an indirect effect of increased intermingling and dispersal of cells at later stages than normal or a more direct effect.

The increased extent of identity switching with EphA4 knock down reported here is in contrast to published findings using an alternative reporter line as previously discussed in detail in Chapter 3 (Calzolari *et al*, 2014). Knock down of EphA4 in the Mü4127 transgenic line, crossed to 4xKaloop fish to drive self-sustained GFP expression in r3 and r5, slightly increased the number of ectopic cells expressing GFP, but all of these maintained expression of *egr2b* (Calzolari *et al*, 2014). However, as discussed previously, a potential explanation for this difference is that GFP is not expressed at detectable levels in cells that switch identity.

The observations made in this chapter also suggest that further perturbing Eph/ephrin signalling – for example, simultaneous loss of both EphA4 and EphrinB3b – will increase the amount of cell identity switching observed at the r3/4 and r5/6 borders in Tg[egr2b:H2B-Citrine]. When *egr2b* expression is analysed in EphrinB3b mutants with EphA4 knocked down, at early stages there are increased numbers of ectopic cells observed outside r3 and r5; however, by later stages, there are far fewer ectopic *egr2b*-expressing cells, but borders of *egr2b* expression remain fuzzy. This is consistent with previous studies in double EphA4; EphrinB2 morphant embryos, (Kemp *et al*, 2009). It is not clear whether this (later) refinement is due to residual Eph/ephrin activity or alternative sharpening mechanisms – such as identity switching. Transplantation of cells between rhombomeres at these

stages has demonstrated that cells retain plasticity of *hox* expression status (Trainor & Krumlauf, 2000b; Schilling *et al*, 2001). Likewise, Kemp *et al* show that 80% of cells transplanted from r3 to r4 between 10 and 12 ss lose *egr2b* expression. It will be insightful to combine the EphrinB3b mutant with loss of EphA4 in Tg[egr2b:H2B-Citrine] and perform time lapse imaging to study whether these ectopic cells – which will presumably express detectable Citrine – become sorted to r3 or r5 or persist in adjacent rhombomeres and whether they maintain expression of *egr2b*. An alternative approach to completely block Eph/ephrin signalling in the hindbrain is to express dominant negative Ephs or Ephrins. For example, truncated EphA4, lacking the kinase domain but still capable of binding to ephrins, severely perturbs border sharpening (Xu *et al*, 1995). Alternatively, soluble ephrinBs may be used to block Eph/ephrin signalling. These are capable of binding to Eph receptors but are unable to cluster and therefore unable to induce signalling in receptor-expressing cell; in addition, overexpression of soluble ephrinBs can block signalling from endogenous ephrins by competing with endogenous ephrins for binding to Ephs (Davis *et al*, 1994; Chan *et al*, 2001).

4.7.2 New insights into the mechanisms of Eph/ephrin-mediated border sharpening

Results presented here also provide insights into which particular Ephs and ephrins may interact within the hindbrain to mediate border sharpening. I have demonstrated that simultaneous loss of EphA4 and EphrinB3b causes more dramatic sharpening defects than loss of either protein alone. It is likely that this is partially due to both EphA4 and EphrinB3b interacting with additional Ephs and ephrins; for example, EphA4 can interact with EphrinB2 at the r3/4 and r4/5 borders, while EphrinB3b may be able to interact with EphB4 at the r4/5 border.

Experiments described here with embryos mosaic for EphrinB3b may contribute to our understanding of the mechanisms of Eph/ephrin-mediated border sharpening. EphA4 and EphrinB2 both affect either cell adhesion or cortical tension throughout the segments that they are expressed in (Cooke & Moens, 2002; Kemp *et al*, 2009). This activity could be due to either ligand-independent signalling or

overlapping expression of other ligands/receptors in these segments. While it has been suggested that these activities contribute to border sharpening, the observation that segregation of cells in these mosaics occurs on the same timescale as border sharpening may just be an inevitable consequence of the effect of EphA4 and EphrinB2 on cell adhesion or cortical tension, which is just a “side-effect” of overlapping expression with a low affinity ligand/receptor. I have shown that EphrinB3b does not appear to share an equivalent role to EphA4 or EphrinB2 within segments. This could be because EphrinB3 has a different or lack of a potential ligand-independent activity. Alternatively, EphrinB3 expression may not overlap with a suitable receptor to affect adhesion/tension within these segments.

Chapter 5. Investigating the role of community effects in cell identity respecification and border refinement

5.1 Introduction

In addition to studying the contribution of identity regulation to border refinement, I have also investigated potential mechanisms of cell identity respecification. These experiments addressed the contribution of community effects to regulation of cell identity during border sharpening, which is a potential mechanism by which cells switch identity.

5.1.1 Community effects in development

The “Community Effect” describes signalling within groups of cells, whereby the ability of a precursor cell to respond to signals promoting a particular identity is increased if a sufficient number of surrounding cells are simultaneously responding in the same way to inductive signals – as illustrated in Figure 5-1(A-B). The first description of a community effect in animal development came from studying the ability of animal cap cells derived from *Xenopus laevis* blastula to differentiate as muscle when sandwiched between layers of vegetal cells; animal cells arranged in a monolayer are unable to activate muscle gene expression, while the majority of animal cells arranged as a solid group are capable of differentiating to muscle (Gurdon, 1988). Similar community effects have been described in *Drosophila*, where cells from the dorsal epidermal anlage transplanted to the ventral neurogenic region tend to retain an epidermal fate if transplanted as groups, but more often adopt a neural fate if transplanted singly (Stüttem & Campos-Ortega, 1991).

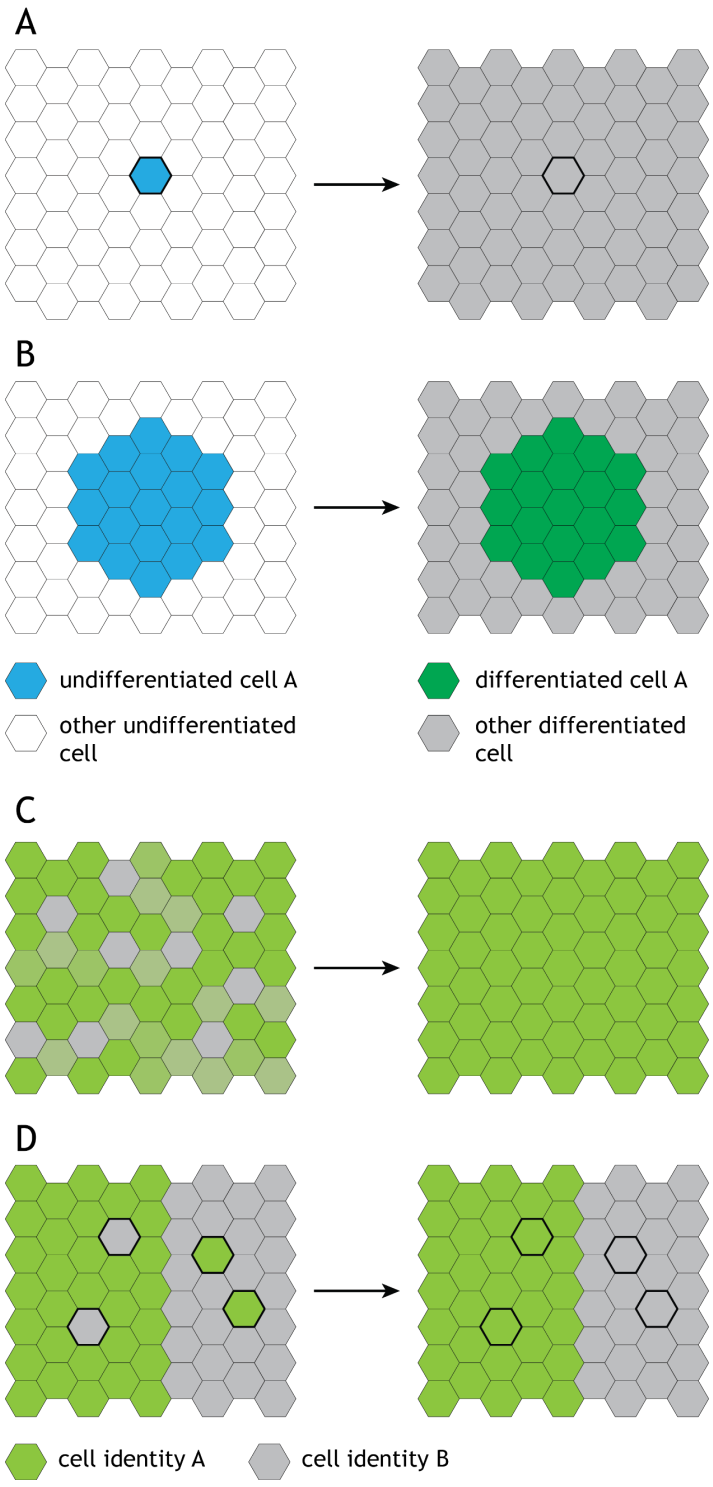

Figure 5-1 Community effects and regulation of cell identity in development

Isolated undifferentiated cells of a particular identity are unable to differentiate when surrounded by other undifferentiated cells of a different identity (A); in contrast, when sufficient numbers of cells of a particular identity are in close proximity, these are able to differentiate via the community effect (B). Community effects may help establish homogeneous levels of gene

expression within a territory of initially heterogeneous gene expression through spatial averaging (C). Hypothesised contribution of the community effect in mediating refinement of ectopic cells at compartment boundaries (D). Diagrams A and B are based on (Saka *et al*, 2011).

Conceptually, community effects can help establish and maintain homogeneous gene expression levels within territories through spatial averaging of gene induction (as illustrated in Figure 5-1C). Modelling of the community effect of Nodal signalling in sea urchin ectoderm has suggested that the *nodal cis*-regulatory system – via positive feedback through Smad activation – and diffusion of Nodal protein is capable of smoothing out variation in *nodal* transcription rates within a field of cells of initially heterogeneous *nodal* expression (Bolouri & Davidson, 2010). It has also been suggested that community effects may encourage cells at compartment borders to adopt the same identity as neighbouring cells, as shown in Figure 5-1D (Gurdon, 1988; Gurdon *et al*, 1993). In the *Drosophila* imaginal disc, community effects have been suggested to account for the ability of cells from adjacent compartments to contribute to the regeneration of damaged posterior or dorsal compartments via inductive signals from neighbouring cells in the damaged compartment (Herrera & Morata, 2014). These signalling events, including non cell-autonomous induction of *engrailed* expression by neighbouring cells expressing *engrailed*, in combination with an upregulation of JNK signalling and transient loss of epigenetic regulation, mediate a genetic reprogramming event that appears to involve community effects (Herrera & Morata, 2014); reviewed in (Morata & Herrera, 2016).

5.1.2 Evidence that community effects can regulate cell identity in the hindbrain

Some evidence that community effects regulate cell identity in the hindbrain at the time when border sharpening occurs has come from cell transplantation studies. Large coherent groups of 10-30 cells are able to maintain their original *hox* expression status after transplantation to a different AP position of the hindbrain during stages at which borders are not yet sharp. In contrast, individual cells and smaller groups of cells have been found to be capable of changing their *hox*

expression after transplantation, to match their new AP position (Trainor & Krumlauf, 2000b; Schilling *et al*, 2001). Cells less than two cell diameters from the periphery of larger groups of transplanted cells still exhibited some plasticity of *hox* expression status, unlike cells within the centre of the cluster. This suggests that mutually-inductive community effects regulate *hox* expression within groups of cells, possibly up to a distance of three cell diameters. Such community effects that maintain an ectopic *hox* expression status appear capable of overcoming any additional inputs to identity imposed by global cues that establish anteroposterior identity, such as the concentration of RA and Fgfs. It is possible that community effects that maintain identity within groups of transplanted cells are also involved in regulation of cell identity at rhombomere borders in normal development, and may contribute to refinement of the identity of individual cells.

Additional evidence that community effects may be involved in regulation of cell identity during hindbrain border sharpening comes from the observation that perturbation of Eph/ephrin signalling by expression of truncated EphA4 gives rise to large groups of misplaced *egr2b*-expressing cells, rather than individual ectopic cells (Xu *et al*, 1995). These groups of misplaced cells may maintain their identity via community effects, while individual cells are unable to maintain an ectopic identity and are respecified due to community effects imposed by the surrounding cells. Community effects require sufficient numbers of cells of a particular identity in close proximity in order for maintenance of identity; Eph/ephrin-mediated clustering of cells may therefore contribute to maintenance of cell identity. During border sharpening, Eph/ephrin-mediated restriction of cell intermingling may ensure that only small groups and individual cells cross between adjacent prospective rhombomeres at early stages; the identity of these cells may then be refined by switching of identity. If Eph/ephrin signalling is blocked, causing dispersal of cells of a particular identity amongst cells of a different identity, community effects may cause a change in identity of isolated cells.

5.1.3 Proposed mechanism by which localised regulation of retinoic acid signalling regulates cell identity via a community effect

One mechanism by which cell identity – and cell identity switching – in the hindbrain may be regulated by community effects is via maintenance of segment-specific concentrations of RA during border sharpening. Potential candidates that could regulate segmental RA concentrations are members of the Cyp26 family of RA-degrading cytochrome p450 enzymes. Because RA is membrane-permeable, localised degradation of RA by Cyp26 enzymes can non cell-autonomously affect RA levels in nearby cells (Hernandez *et al*, 2007; White *et al*, 2007; Rydeen *et al*, 2015). Evidence that Cyp26 enzymes can regulate identity in the hindbrain via community effects has been demonstrated by the ability of sufficiently large groups of cells (but not individual cells) overexpressing Cyp26c1 to induce ectopic expression of *hoxb1a* within the centre of the group in the posterior hindbrain (Lee & Skromne, 2014).

Figure 5-2 shows a hypothesised model by which segment-specific concentrations of RA may be established and maintained during border sharpening, such that local concentrations of RA mediate cell identity switching via community effects. In this model, an initial posterior-to-anterior gradient of RA is established by Cyp26a1, which results in noisy induction of segmentally-expressed transcription factors. During early hindbrain patterning, *cyp26a1* is expressed in a smooth anterior-to-posterior gradient across the hindbrain, under feedback and feedforward regulation by RA and FGF signalling, respectively (Kudoh *et al*, 2002; White *et al*, 2007). Cyp26a1-mediated self-enhanced degradation of RA allows RA-induced patterning to be robust despite fluctuations and noise in RA levels and Cyp26a1 plays an important role in modulating noise in *egr2b* expression and contributes to sharpening of rhombomere borders at early segmentation stages (Sosnik *et al*, 2016). However, Cyp26a1 does not have a significant impact on sharpness of *egr2b* expression by later stages (between 10 ss and 18 ss) (Sosnik *et al*, 2016; Emoto *et al*, 2005; Hernandez *et al*, 2007); this is likely due to presence of additional border sharpening mechanisms, including Eph/ephrin-mediated cell sorting. The negative feedback loop between RA and *cyp26a1* expression means that Cyp26a1 is a less likely candidate for regulating identity by altering RA levels,

as misplaced cells along the AP axis of the hindbrain (either due to intermingling between rhombomeres or in the case of cell transplantation between rhombomeres) would be expected to change their *cyp26a1* expression to match local RA levels.

As proposed in Figure 5-2, subsequent to the initial induction of segmental identity genes by RA, segmentally-expressed transcription factors regulate expression of Cyp26b1 and Cyp26c1, which maintain segment-specific concentrations of RA to reinforce and refine segmental identity. In contrast to *cyp26a1*, the expression of *cyp26b1* and *cyp26c1* is not directly regulated by RA, as initiation of *cyp26b1* and *cyp26c1* expression still occurs in embryos treated with the retinaldehyde dehydrogenase inhibitor 4-(diethylamino)benzaldehyde (DEAB), although by later stages loss of RA does indirectly affect expression of c*yp26b1* and c*yp26c1* (Hernandez *et al*, 2007). This means that cells that become misplaced along the AP axis of the hindbrain will retain their original *cyp26b1* and *cyp26c1* expression status. The segmental expression patterns of *cyp26b1* and *cyp26c1* (formerly known as *cyp26d1*) during border sharpening are consistent with these enzymes having a role in cell identity regulation through modulation of RA signalling (Zhao *et al*, 2005; Gu *et al*, 2005; Hernandez *et al*, 2007). However, there is currently little known about the factors that regulate segmental expression of *cyp26b1* and *cyp26c1* in the hindbrain.

This model of RA regulation shown in Figure 5-2 is consistent with observations that isolated ectopic cells change their identity, while groups of ectopic cells do not. Because expression of Cyp26b1 and Cyp26c1– which is not directly regulated by RA – is retained by ectopic cells, large groups of cells with different Cyp26 levels to their surroundings will locally modify RA concentrations and thus will not perceive the correct concentration of RA for their AP position, and maintain their original identity. However, isolated ectopic cells will not sufficiently modulate the local concentration of RA and so perceive the correct concentration of RA for their AP position and therefore switch identity.

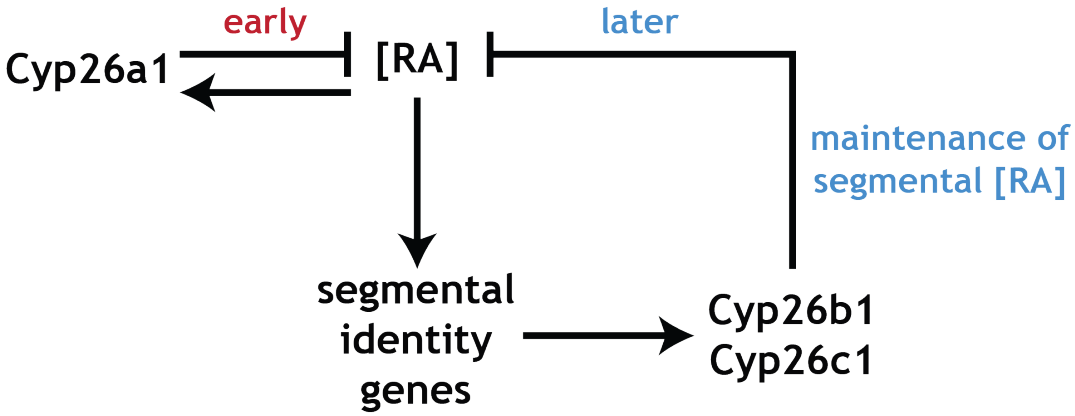

Figure 5-2 Proposed model for establishment and maintenance of segment specific concentrations of RA

An initial posterior-to-anterior gradient of RA is established by Cyp26a1, which results in fuzzy induction of segmentally-expressed transcription factors. Subsequently, these segmentally-expressed transcription factors regulate the segmental expression of Cyp26b1 and Cyp26c1, which maintain segment-specific concentrations of RA and permit maintenance and refinement of segmental identity. *Cyp26a1* expression is directly regulated by RA while *cyp26b1* and *cyp26c1* are not directly regulated by RA.

In this chapter I first investigate whether community effects do regulate cell identity in the hindbrain, which I have proposed as a mechanism by which cells may switch identity at rhombomere borders. Subsequently, I investigate whether these community effects could be mediated by modulation of RA signalling via Cyp26 enzymes as proposed in Figure 5-2 by addressing whether Cyp26b1 and Cyp26c1 are subject to regulation by segmental identity genes and whether Cyp26 enzymes can regulate cell identity via community effects.

Results

5.2 Do community effects influence the identity of cells in the hindbrain?

5.2.1 Can ectopic cells maintain a different identity to their surroundings?

To study whether community effects can contribute to regulation of cell identity in the hindbrain, I investigated whether individual cells and groups of cells can

maintain a different identity to their surroundings, despite potential community effects from neighbouring cells that may challenge their identity. I studied the ability of cells to maintain their identity in embryos mosaic for Egr2 by transplanting cells from wildtype donor embryos into the prospective hindbrains of early gastrula-stage host embryos in which Egr2a and Egr2b had been knocked down (referred to as Egr2 morphant embryos). For simplicity, I refer to territories that would have become r3 or r5 in the presence of Egr2 as r3* and r5*. Based on findings in *Egr2*-null mouse embryos, cells of r3* will acquire either r2 or r4 identity, while cells of r5* will acquire r6 identity (Voiculescu *et al*, 2001). In the morphant hosts, maintenance of *egr2b* expression does not occur, and *egr2b* expression is lost from r3* by 16 ss, but some *egr2b* transcripts are still detectable in r5* of host embryos at this stage (Figure 5-3 F). For this reason, I have focused on maintenance of *egr2b* expression in r3*. As shown in Figure 5-3 A (white arrowheads), when wildtype cells are located within r3* and r5*, they tend to form tight clusters and are capable of maintaining *egr2b* (A) and EphA4 (B) expression. This is in agreement with observations made in mosaic mouse embryos mutant for *Egr2* (Voiculescu *et al*, 2001). Similarly, it has also been shown in zebrafish that wildtype cells transplanted into *valentino* (*val*) mutant hosts cluster, maintain *ephB4a* expression and form sharp, actin-enriched interfaces with host cells when located within r6 or r7 (denoted rX in *val*¯ embryos) (Cooke *et al*, 2001).

Wildtype donor cells located in r3* express EphA4 (Figure 5-3 B; white arrowheads), while Egr2 morphant host cells no longer express EphA4 in r3 or r5 (Figure 5-3 H). EphA4 is known to drive the clustering of wildtype cells in the centre of r3 and r5 (Cooke *et al*, 2005). In the case of wildtype cells clustering within r3* of the Egr2 morphant host, the situation is slightly different. Based on findings in mouse, host cells in r3* are expected to have cell surface and intermingling properties like those of r2/4, which may provide additional repulsive cues to contribute to the clustering of wildtype r3 cells here (Voiculescu *et al*, 2001). However, as shown in Figure 5-3 (C; white arrowheads), loss of EphA4 from donor cells is sufficient to greatly reduce the extent of their clustering in r3* of morphant hosts; donor cells lacking EphA4 tend to either be isolated or loosely grouped within these rhombomeres. This indicates that EphA4 drives the clustering of wildtype cells from Egr2 morphant cells in r3*; any additional differences in surface

properties between Egr2 morphant and wildtype cells do not cause significant clustering of the wildtype cells. Interestingly, as shown in Figure 5-3 C, isolated EphA4 morphant cells in r3* are still capable of maintaining *egr2b* expression at 16 ss, even when completely surrounded by cells that lack Egr2 activity. This suggests that global positional information conferred to cells through the RA gradient is dominant over community effects, which is consistent with my hypothesis that community effects in the hindbrain may involve RA itself.

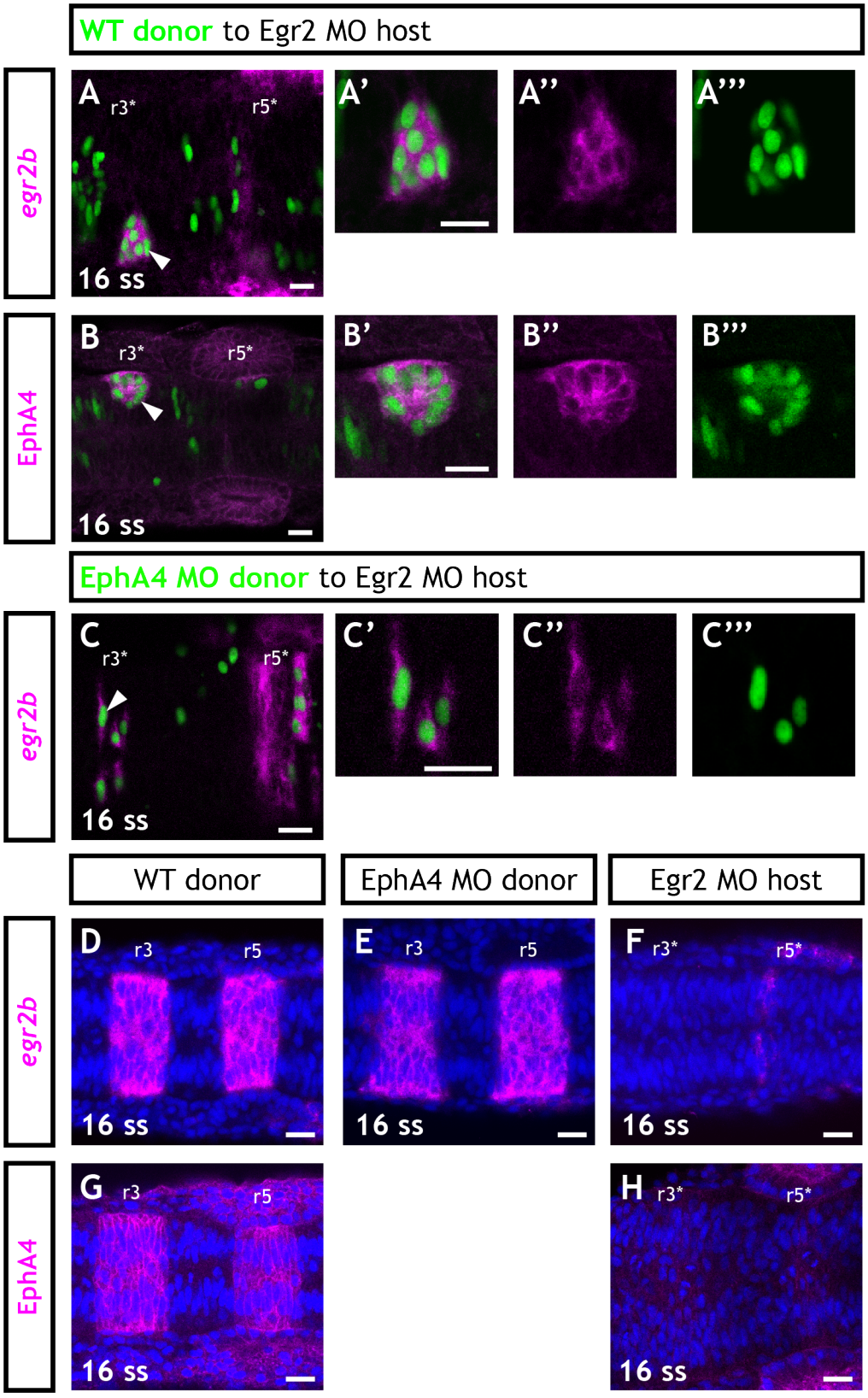
WT donor to Egr2 MO host
egr2b
EphA4
A
A'
A''
A'''
B
B'
B''
B'''
r3*
r5*
16 ss
EphA4 MO donor to Egr2 MO host
C
C'
C''
C'''
WT donor
EphA4 MO donor
Egr2 MO host
D
E
F
G
H
r3
r5

Figure 5-3 Maintenance of *egr2b* expression in mosaic embryos

Cells from wildtype donor embryos were transplanted into Egr2 morphant hosts at the early gastrula stage. *egr2b* transcripts can still be detected in r5* of Egr2 morphants (F; n = 4 embryos). Wildtype donor cells form tight clusters within r3* of Egr2 morphant hosts and maintain *egr2b* (A; n = 11 embryos) and EphA4 (B; n = 5 embryos) expression, in contrast to Egr2 morphant hosts (F, H). When cells from EphA4 morphant donor embryos were transplanted into Egr2 morphant hosts, donor cells no longer cluster in r3*, but maintain *egr2b* expression (C; white arrowheads; n = 5 embryos). Embryos are flat-mounted with anterior to the left. r3* and r5* refer to territories that would have become r3 or r5 in the presence of Egr2. Scale bars: 20 μm.

To investigate whether cells are capable of maintaining *egr2b* expression when surrounded by cells of an r4 identity, I also studied the expression of *hoxb1a* in embryos mosaic for Egr2 activity. As expected, in Egr2 morphants, the anterior border of *hoxb1a* expression is shifted more anteriorly, at the expense of r3 (Figure 5-4; A-D). Clustered wildtype donor cells maintain *egr2b* expression and do not express *hoxb1a* (Figure 5-4; A-B). However, EphA4 morphant donor cells express both *egr2b* and *hoxb1a* when located in r3* and surrounded by *hoxb1a*-expressing cells (Figure 5-4; C-F; white arrowheads) and some EphA4 morphant donor cells at the anterior border of *hoxb1a* expression also appear to co-express *egr2b* and *hoxb1a* (Figure 5-4; E-F; white arrowheads). This indicates that while community effects from r3* cells are insufficient to prevent maintenance of *egr2b* expression in wildtype cells at the correct AP position of r3 at this stage, they are sufficient to either induce or prevent downregulation of *hoxb1a* in these cells.

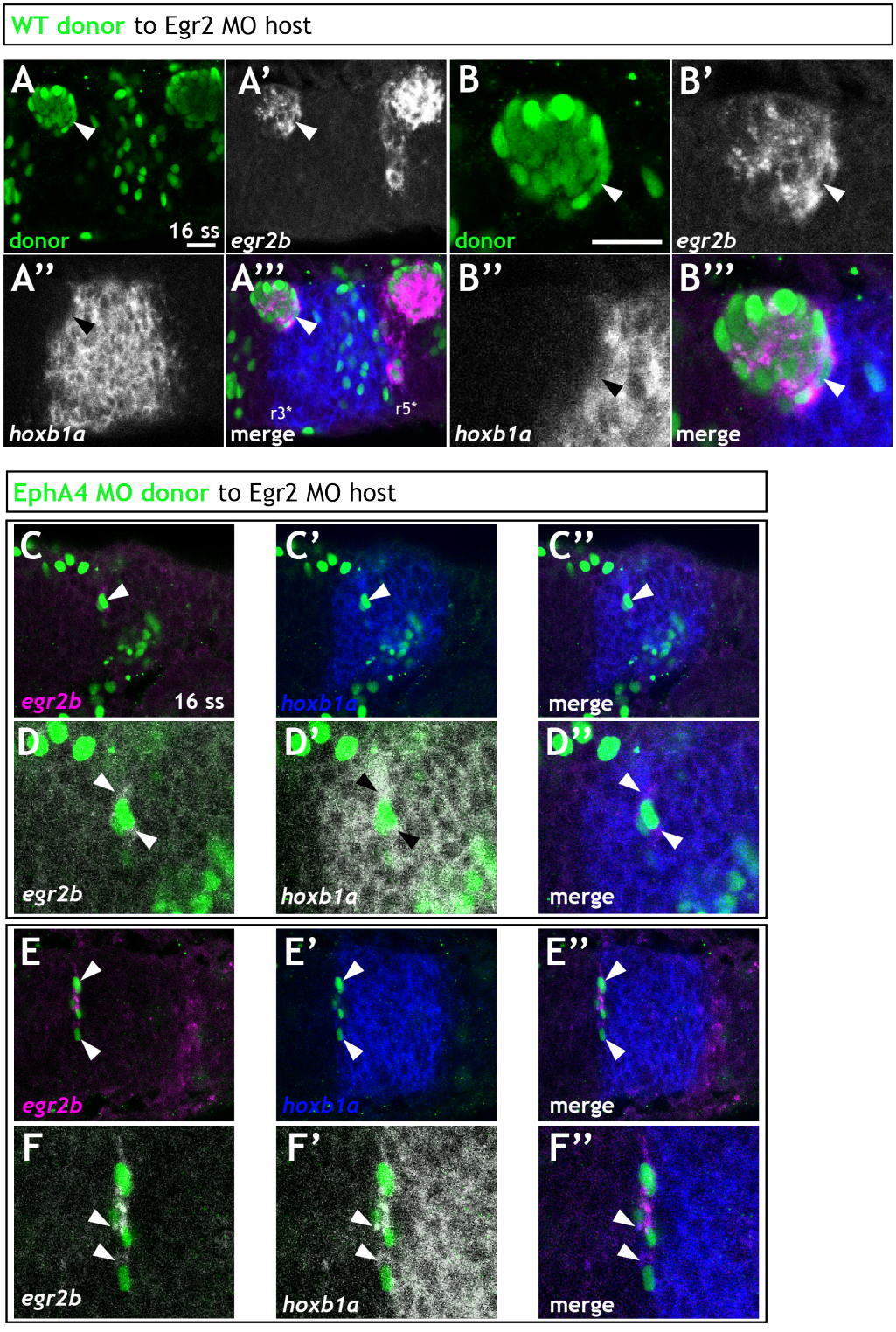

Figure 5-4 *hoxb1a* and *egr2b* expression analysis in embryos mosaic for Egr2 activity

Cells from wildtype (A,B) and EphA4 morphant (C-F) donors were transplanted into Egr2 morphant embryos at the early gastrula stage. Tight clusters of wildtype donor cells within r3* of Egr2 morphant hosts maintain a lack of *hoxb1a* expression (A,B; arrowheads n = 3). In contrast, isolated EphA4 morphant cells within r3* co-express *egr2b* and *hoxb1a* when located within the *hoxb1a*-expressing domain and at the periphery of the *hoxb1a*-expressing domain (C-F; arrowheads n = 3 embryos). Embryos are flat-mounted with anterior to the left. Scale bars: 20 μm.

5.2.2 Egr2b can regulate cell identity non cell-autonomously

Another approach I took to study whether community effects regulate cell identity in the hindbrain was to see whether transcription factors that confer cell identity are capable of affecting cell identity non cell-autonomously. This non cell-autonomous activity may involve regulation of Cyp26b1 and Cyp26c1 and local modulation of RA levels, as I have previously suggested. One transcription factor that may regulate cell identity non cell-autonomously via community effects in r3 and r5 is Egr2b. In chick, Egr2 has been reported to induce its own expression, and the expression of its target gene *EphA4*, non cell-autonomously (Giudicelli *et al*, 2001; Prin *et al*, 2014). However, the techniques used to investigate the non cell-autonomous activity of Egr2 in these previous studies – electroporation to induce gene expression, and double *in situ* hybridisation to detect and distinguish between ectopic and endogenous *Egr2* expression – are somewhat limited for studying non cell-autonomous activity and could lead to false positive results. Low but undetected levels of exogenous Egr2 may have also been introduced by electroporation in cells in which endogenous *Egr2* induction was observed. Egr2 is known to directly activate its own expression cell autonomously and it has been demonstrated that even very low amounts of Egr2 can trigger feedback autoregulation of *egr2* (Bouchoucha *et al*, 2013).

In order to verify that Egr2b has a non cell-autonomous activity in the hindbrain during border sharpening, I made use of transient transgenesis to achieve mosaic overexpression of Egr2b with a carboxy-terminal Myc tag for detection of the exogenous protein by immunohistochemistry. The C-terminal Myc tag is not expected to compromise the function of Egr2b, as the C-terminal region of Egr2b is

poorly evolutionarily conserved and is therefore unlikely to have a key functional role. In addition, no difference in activity has been observed between wildtype or C-terminal Myc-tagged mouse Egr2 in chick (Giudicelli *et al*, 2001). Initially, I created a construct where expression of Egr2b-Myc is under the control of the heat shock-inducible *hsp70* promoter: hsp70:Egr2b-Myc. Injection of this construct, combined with heat shock at 4 ss causes mosaic overexpression of Egr2b-Myc, detectable in the nuclei of cells by 7 ss as shown in Figure 5-5. To investigate the transcriptional activity of exogenous Egr2b-Myc and observe any non cell-autonomous activity, I studied induction of endogenous *egr2b*, which is a known transcriptional target of Egr2b. The probe used to selectively detect endogenous *egr2b* transcripts only hybridises to the 3' UTR of *egr2b* transcripts, which is absent from the exogenous transcripts. As shown in Figure 5-5 (white circles), it appears that Egr2b-Myc drives detectable expression of endogenous *egr2b*. However, because of varied – and sometimes incredibly low – levels of Egr2b-Myc expression induced by heat shock, it is difficult to be certain whether this expression is truly non cell-autonomous, or whether low, undetected levels of Egr2b-Myc drive *egr2b* expression cell autonomously here.

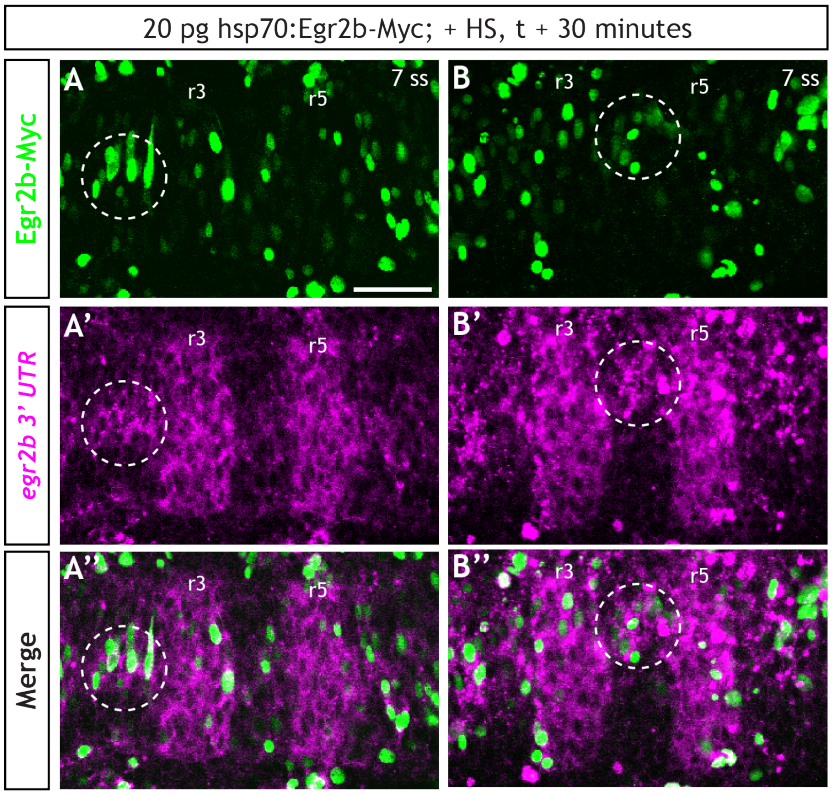

Figure 5-5 Detection of endogenous *egr2b* in embryos overexpressing Egr2b-Myc

Embryos were injected with 20 pg hsp70:Egr2b-Myc and heat shocked at 4 ss for 30 minutes at 37 °C. Embryos were fixed 30 minutes after heat shock (7 ss). Mosaic Egr2b-Myc can be detected, and induces endogenous egr2b both cell-autonomously and non cell-autonomously (A,B; circles). Embryos are flat-mounted, with anterior to the left. Scale bar: 50 μm.

Because of the difficulty in interpreting the results of mosaic overexpression of Egr2b-Myc, I subsequently used a different approach to overexpress Egr2b-Myc throughout a discrete region of the embryo. I made use of the Pax3 CNE1 *cis*-regulatory module to drive expression of Egr2b-Myc. CNE1 is a CNS-specific Pax3 enhancer that is transcriptionally active in a dorsally-restricted domain of the neural tube and hindbrain from bud stage (10 hpf) (Moore *et al*, 2013). I modified an existing construct with the Pax3 CNE1, in combination with a minimal thymidine kinase promoter and Gal4-5xUAS, which drives detectable Citrine expression in presumptive dorsal progenitors from 10 hpf (Moore *et al*, 2013), by replacing the *Citrine* in this construct with *egr2b-Myc*. As shown in Figure 5-6, at intermediate stages of segmentation (7 ss), Egr2b-Myc induces expression of endogenous

egr2b non cell-autonomously (Figure 5-6 A-C; circles). This is also evident in orthogonal views of z-stacks through embryos (Figure 5-6 D', E', F'), showing endogenous *egr2b* expression (anterior to r3) extends more ventrally than the domain in which Egr2b-Myc is expressed (white arrowheads).

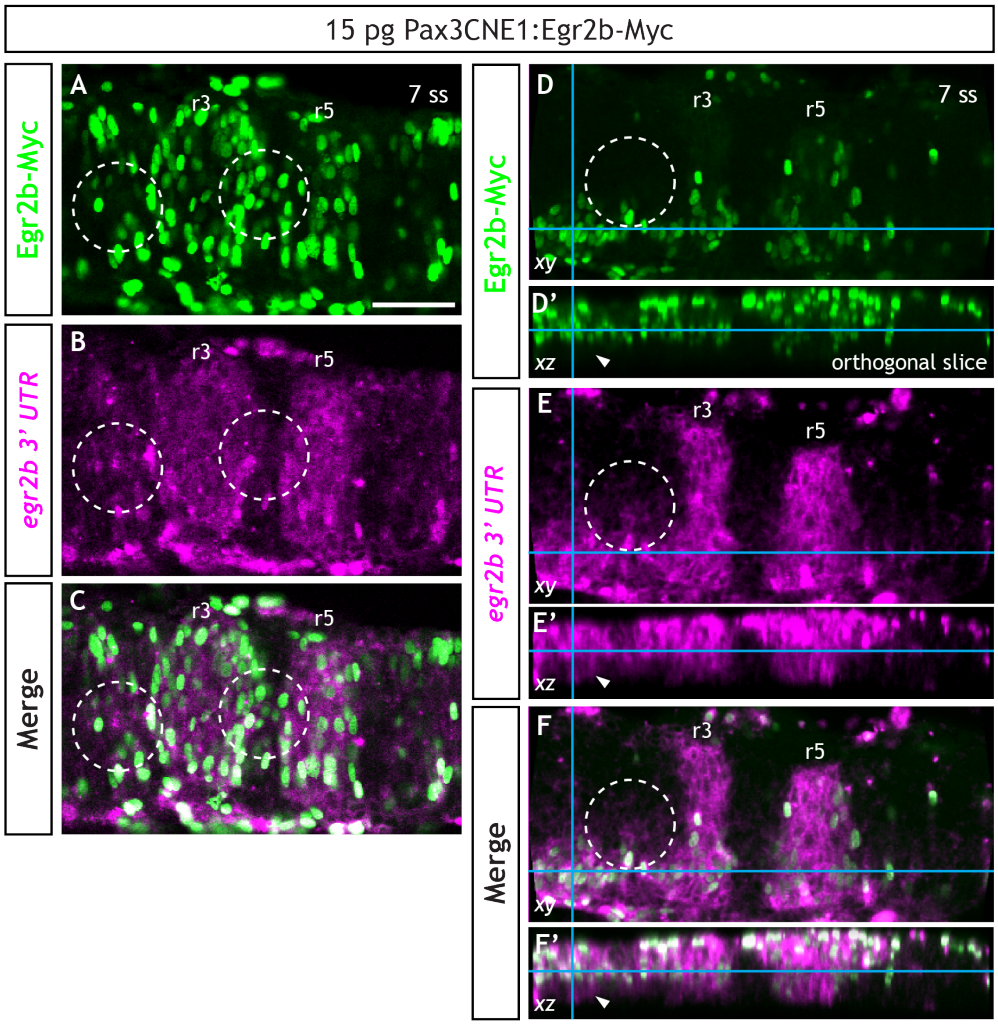

Figure 5-6 Overexpression of Egr2b-Myc induces *egr2b* expression non cell-autonomously at specific stages

Embryos were injected with 15 pg Pax3CNE1-Egr2b-Myc. At 7 ss, Egr2b-Myc-expressing cells induce endogenous *egr2b* expression both cell autonomously and non-cell autonomously (A-F; circles; n = 6 embryos). Dorsally-restricted Egr2b-Myc-expressing cells can induce endogenous *egr2b* expression non cell-autonomously in more ventral regions (D', E', F'; white arrowheads; n = 6 embryos). Embryos are flat-mounted, with anterior to the left; D', E' and F' show orthogonal views of the embryo in D, E and F. Scale bars: 20 μm.

However, as shown in Figure 5-7, by 16 ss, cells expressing Egr2b-Myc are found scattered throughout r3 and r5, but are excluded from r4, and are largely localised at rhombomere borders (Figure 5-7 A-C; white arrowheads). Egr2 directly regulates EphA4 expression (Theil *et al*, 1998) and as shown in Figure 5-7 (A-C), Egr2b-Myc can induce expression of EphA4, although by 16ss, ectopic EphA4 protein is only clearly detectable in clusters of Egr2b-Myc-expressing cells. Cells ectopically expressing EphA4 have previously been shown to sort to the borders of odd-numbered rhombomeres (Xu *et al*, 1999), which is likely to cause similar segregation of Egr2b-Myc cells. It is also possible that cells overexpressing Egr2b-Myc share additional aspects of Eph/ephrin expression with cells of r3 and r5, due to direct or indirect transcriptional regulation by Egr2b (such as a lack of *ephrinB2* and/or *ephrinB3* expression), which may also explain their localisation to rhombomere borders.

At these later stages, once segregation of Egr2b-Myc expressing cells has occurred, there is no detectable non cell-autonomous induction of *egr2b* by Egr2b-Myc in r4 (Figure 5-7 D; asterisks), in contrast to earlier stages. It is possible that factors within r4 may suppress the non cell-autonomous activity of Egr2b-Myc at these stages, possibly via opposing cell community effects. To investigate this further, I studied the impact of knocking down Hoxb1a and Hoxb1b on the induction of endogenous *egr2b* in r4 by Egr2b-Myc. Hoxb1a and Hoxb1b have partially redundant functions and are required for specification of r4 (McClintock *et al*, 2001, 2002); Hoxb1a is also known to indirectly repress *egr2b* expression through activation of Nlz factors (Labalette *et al*, 2015).

As shown in Figure 5-7 (F), when there are sufficient Egr2b-Myc-expressing cells in Hoxb1 morphants, a fusion of r3 and r5 can occur (arrowheads). When fewer Egr2b-Myc-expressing cells are present, these appear to remain restricted from r4 (Figure 5-7 E). In both of these cases, however, Egr2b-Myc still no longer induces *egr2b* expression non cell-autonomously at later stages. While Hoxb1a and Hoxb1b are important for the specification of r4, they are not necessarily dispensable for all features of r4 identity, and in their absence, additional factors may remain that are sufficient to suppress the non cell-autonomous activity of Egr2b. Evidence from this comes from the fact that in the absence of Hoxb1 in

mouse and of Hoxb1a and Hoxb1b in zebrafish, *egr2b* expression does not extend across the entire r4 region and the remaining r4 region retains some r2-like properties (Studer *et al*, 1996, 1998; McClintock *et al*, 2002). I also studied expression of *hoxb1a* in embryos overexpressing Egr2b-Myc. As shown in Figure 5-8, as expected, overexpression of Egr2b-Myc causes a reduction of *hoxb1a* expression in r4 (white arrowheads), but this does not appear to be non cell-autonomous. Intriguingly, overexpression of Egr2b-Myc appears to also upregulate expression of *hoxb1a* elsewhere in the hindbrain (Figure 5-8; blue arrowheads) and throughout the embryo (not shown). It is known that Egr2b upregulates *hoxa2* and *hoxb2* expression in r3 and r5 (Sham *et al*, 1993; Nonchev *et al*, 1996a, 1996b; Vesque *et al*, 1996). Hoxa2 and Hoxb2, in turn, are known to upregulate *hoxb1a* expression (Davenne *et al*, 1999; Gavalas *et al*, 2003). Egr2b therefore appears capable of both repressing and indirectly activating *hoxb1a* expression.

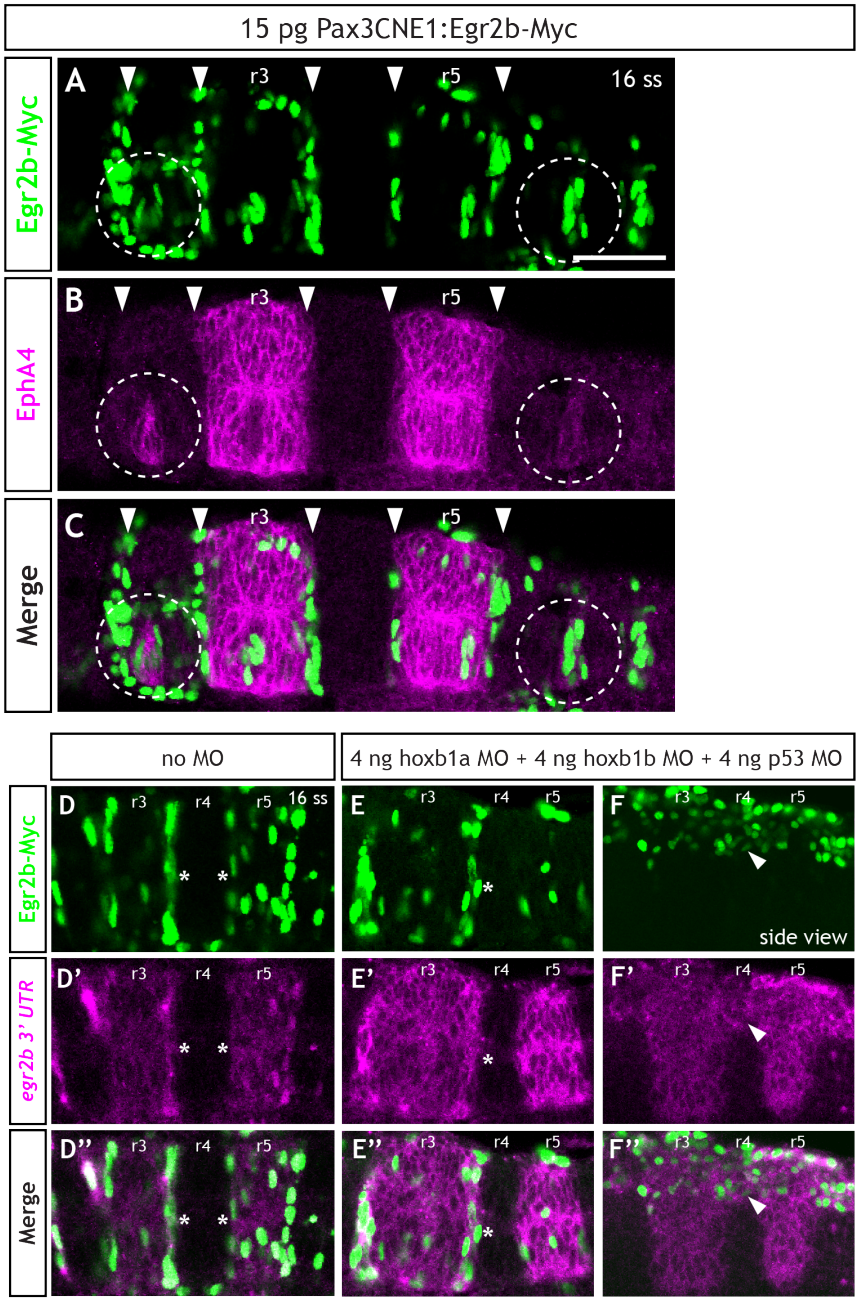

Figure 5-7 Egr2-Myc-expressing cells become segregated and no longer induce *egr2b* expression non cell-autonomously

Expression of EphA4 (A-C) and endogenous *egr2b* (D-J) in embryos overexpressing Egr2b-Myc, driven by Pax3 CNE1. Egr2b-Myc-expressing cells can induce ectopic EphA4 expression outside r3 and r5 (circles; n = 4 embryos) and tend to be located at the edges of r2, r3 and r5 (white arrowheads) (A,B,C). At 16 ss, Egr2b-Myc-expressing cells no longer induce endogenous *egr2b* expression non cell-autonomously (D; asterisks; n = 5 embryos). Knock down of Hoxb1a and Hoxb1b does not enable Egr2b-Myc to induce *egr2b* expression non cell-

autonomously in r4 at 16 ss (M-O; asterisks; n = 6). When sufficient Egr2b-Myc-expressing cells are present, a fusion of r3 and r5 can occur, but there is still no detectable non cell-autonomous induction of *egr2b* (P-Q; arrowheads; n = 2). Embryos shown in A – E are flat-mounted, with anterior to the left. Embryo F is side-mounted, with anterior to the left. Scale bar: 50 µm.

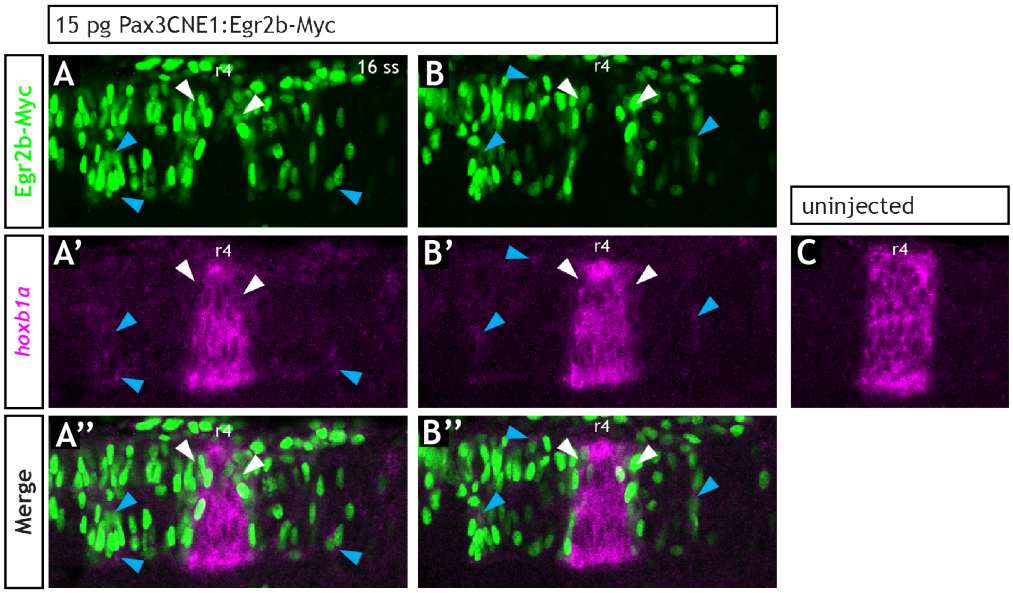

Figure 5-8 Egr2b-Myc both represses and activates *hoxb1a* expression

Overexpression of Egr2b-Myc reduces *hoxb1a* expression in r4 (A,B; white arrowheads; n = 11 embryos) compared to uninjected controls (C; n = 3 embryos) but also weakly induces *hoxb1a* expression elsewhere in the hindbrain (A,B; blue arrowheads; n = 11 embryos).

5.3 Do segmental identity genes regulate Cyp26 expression?

5.3.1 Egr2b regulates segmental expression of *cyp26b1* and *cyp26c1*

To investigate whether Egr2b may induce its own expression non-cell autonomously via local modulation of RA levels, I investigated whether Egr2b regulates segmental expression of *cyp26b1* and *cyp26c1*. As shown in Figure 5-9, knock down of Egr2 increases the levels of expression of *cyp26b1* and *cyp26c1* in r3 to those in r4. In addition, levels of *cyp26c1* expression in r5 are increased to those in r6 following Egr2 knock down. It therefore appears that Egr2 represses *cyp26b1* and *cyp26c1* expression in r3, and thus maintains differential Cyp26 activity between r3 and adjacent rhombomeres, r2 and r4. Egr2 also appears to

maintain different levels of *cyp26c1* expression between r5 and adjacent rhombomeres r4 and r6. To further demonstrate that Egr2b can repress *cyp26b1* and *cyp26c1* expression, I studied the expression of *cyp26b1* and *cyp26c1* in cells overexpressing Egr2b-Myc driven by the Pax3 CNE1 element, as previously described in 5.2.2. As shown in Figure 5-10, overexpression of Egr2b-Myc causes significant reduction of *cyp26c1* expression in r2, r4 and r5 compared to levels in control embryos (A,B,D,E, white arrowheads). In addition to supporting the idea that Egr2b maintains reduced *cyp26c1* expression, this suggests that endogenous levels of Egr2b are not sufficient for complete reduction of *cyp26c1* expression in r5; additional factors are likely involved in maintenance of *cyp26c1* expression here but are overcome when Egr2b-Myc is overexpressed. Overexpression of Egr2b-Myc also reduces *cyp26b1* expression in r2, r3 and r4, but not to as great an extent as it does *cyp26c1* (Figure 5-10 C,F, white arrowheads). This also suggests that endogenous levels of Egr2b in r3 are not sufficient to completely repress *cyp26b1* here and that additional factors appear to contribute to maintenance of *cyp26b1* expression in r3.

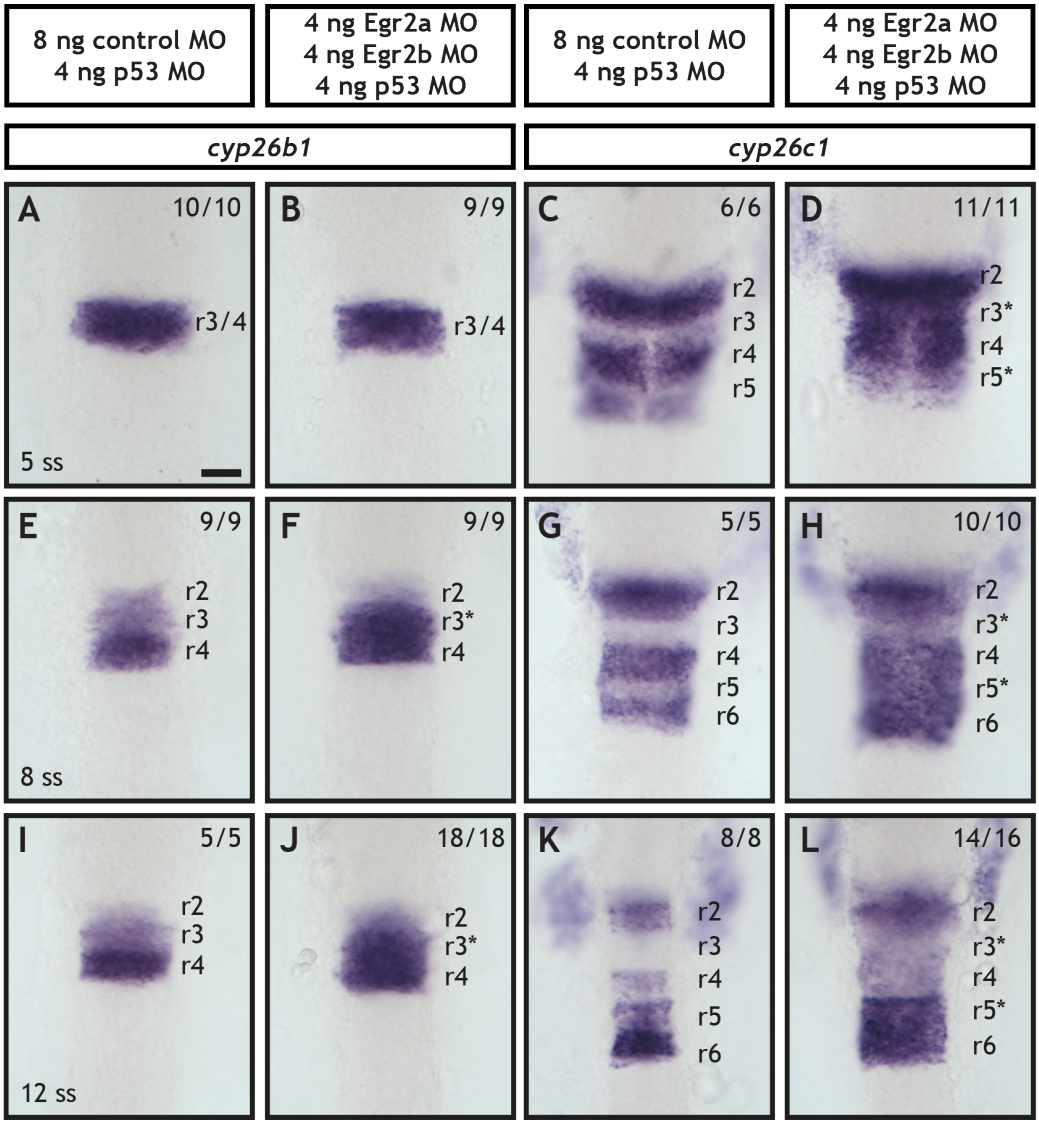

Figure 5-9 Expression of cyp26b1 and cyp26c1 in Egr2 morphants

Embryos were injected with either Egr2a and Egr2b morpholino (B,D,F,H,J,L) or control morpholino (A,C,E,G,I,K). Levels of *cyp26b1* expression are increased in r3* of Egr2 morphants from 8 ss (F,J) compared to control embryos (E,I). Levels of *cyp26c1* expression are increased in r3 of Egr2 morphants from 5 ss (D,H,L) compared to control embryos (C,G,K), and in r5* of Egr2 morphants from 8 ss (H,L) compared to control embryos (G,K). Embryos are flat-mounted with anterior to the top. r3* and r5* refer to territories that would have become r3 or r5 in the presence of Egr2. Frequencies of embryos observed represented by the image shown, out of the total number of embryos studied are shown in the top right. Scale bar: 50 μm.

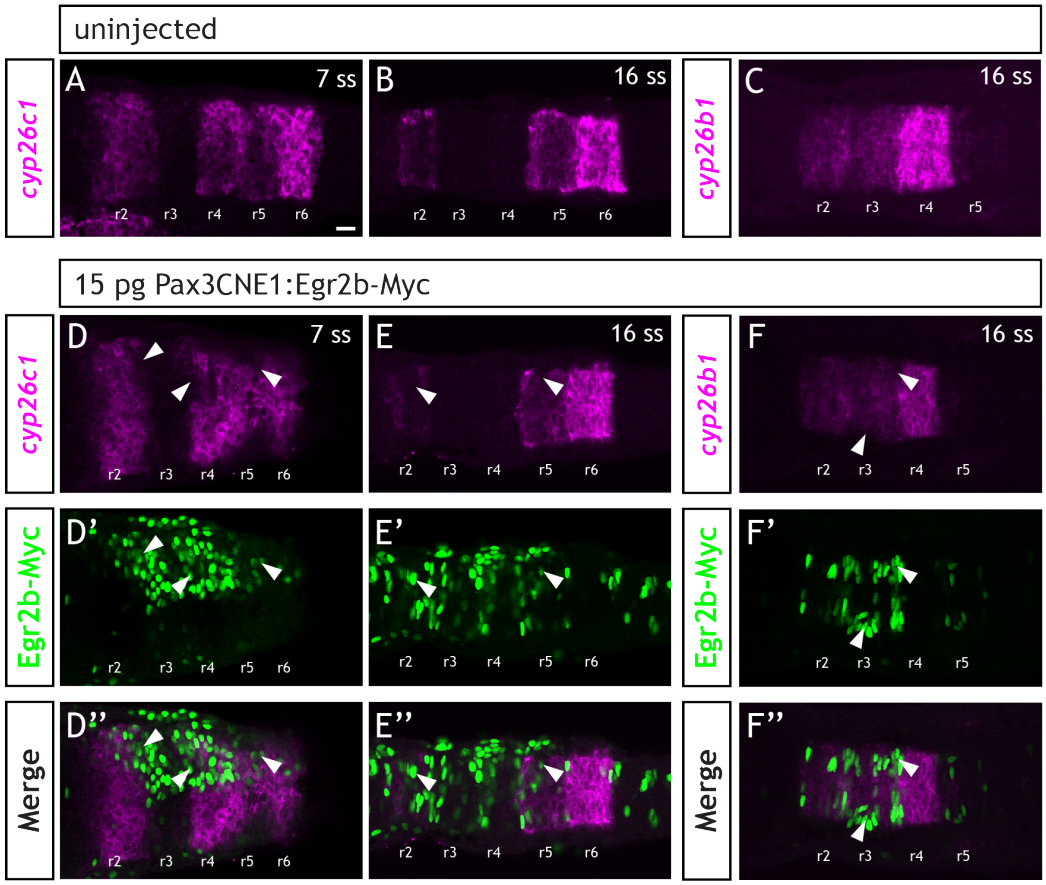

Figure 5-10 Overexpression of Egr2b-Myc reduces *cyp26b1* and *cyp26c1* expression

Embryos were injected with 15 pg Pax3CNE1:Egr2b-Myc and analysed for *cyp26b1* (F) and *cyp26c1* (D,E) expression compared with uninjected control embryos (A-C). Egr2b-Myc overexpressing cells express reduced levels of *cyp26c1* in r2, r4 and r5 at 7 ss (D; n = 8 embryos; white arrowheads) and 16 ss (E; n =5 embryos; white arrowheads) compared to control embryos (A; n = 4 embryos (7 ss controls); B; n = 4 embryos (16 ss controls)). Egr2b-Myc-expressing cells also express slightly reduced levels of *cyp26b1* in r2, r3 and r4 (F; n = 6 embryos; white arrowheads) compared to control embryos at 16 ss (n = 2 embryos). Embryos are flat-mounted with anterior to the left. Scale bars: 20 μm.

5.3.2 Hoxb1a and Hoxb1b do not directly regulate *cyp26b1* or *cyp26c1* expression

Additional segmentally-expressed transcription factors that may regulate segmental expression of *cyp26b1* and *cyp26c1* include Hoxb1a and Hoxb1b, which are

expressed in and required for the specification of r4 (McClintock *et al*, 2002). However, as shown in Figure 5-11, while expression patterns of *cyp26b1* and *cyp26c1* are altered upon knock down of Hoxb1a and Hoxb1b, these changes reflect the altered specification of rhombomere identity that have been described to occur in the absence of Hoxb1 activity, namely expansion of r3 at the expense of r4 (Studer *et al*, 1998; McClintock *et al*, 2002). Levels of expression of *cyp26b1* and *cyp26c1* within r4* are unchanged following knock down, suggesting that these genes are not directly regulated by Hoxb1a or Hoxb1b.

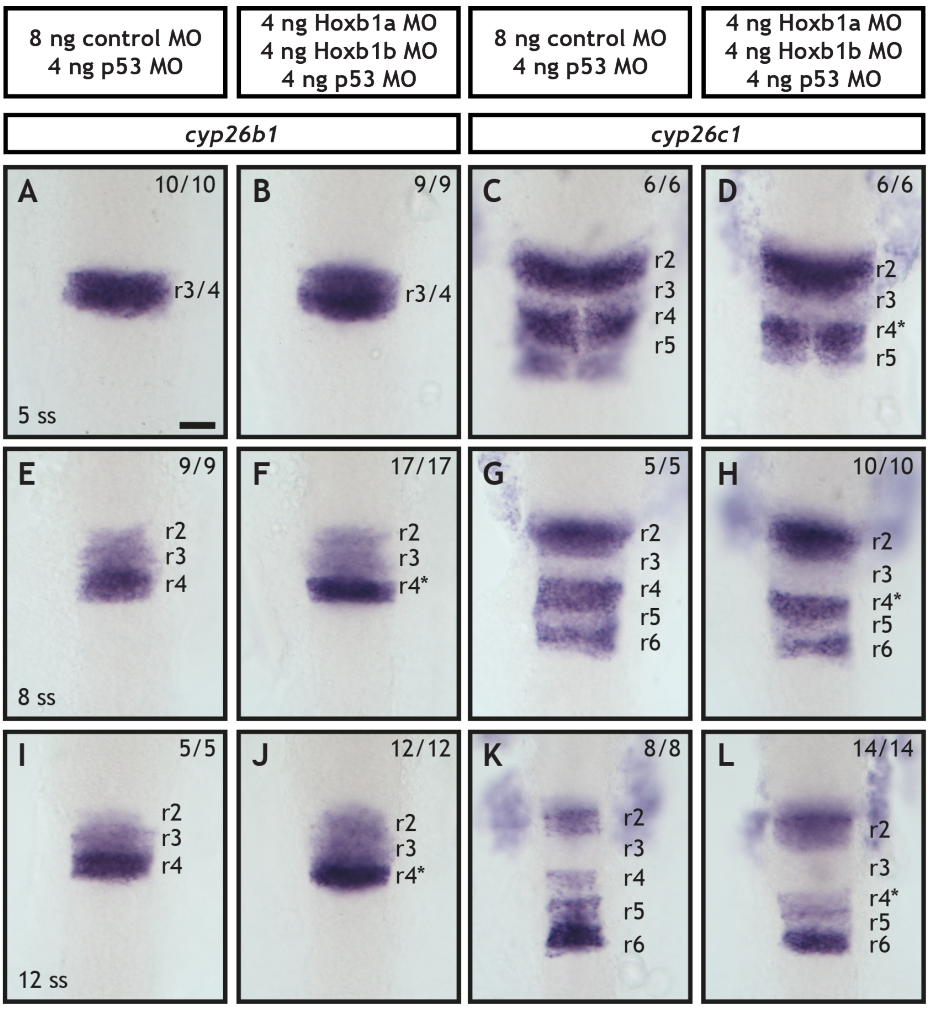

Figure 5-11 Expression of cyp26b1 and cyp26c1 in Hoxb1 morphants

Levels of *cyp26b1* (A-J) and *cyp26c1* (C-L) expression are unchanged in r4 following Hoxb1 knock down. From 8 ss, r3 is expanded in size, at the expense of r4; this is reflected in the expression of *cyp26b1* (F,J) and *cyp26c1* (H,L) in r3 of Hoxb1a morphants, compared to control embryos (E,I – *cyp26b1*; G,K – *cyp26c1*). Embryos are flat-mounted with anterior to the top.

Frequencies of embryos observed represented by the image shown, out of the total number of embryos studied are shown in the top right. Scale bar: 50 μm.

5.4 Can Cyp26 enzymes regulate cell identity via community effects?

I have hypothesised that Cyp26a1 shapes the initial gradient of RA along the AP axis and subsequently, segmentally-expressed Cyp26b1 and Cyp26c1, which are not directly regulated by RA, modify this gradient to reinforce segmental identity. It is known that Cyp26 activity is involved in the specification of r3, r4 and r5 through regulation of RA signalling, although the roles of individual Cyp26 enzymes in specification and maintenance of cell identity remain less clear (Hernandez *et al*, 2007). In order to study which Cyp26 enzymes may contribute to regulation of cell identity, I have investigated the consequences of perturbing the activities different combinations of Cyp26 enzymes. Subsequently, I attempted to study the impact of mosaic alteration of Cyp26 activity on hindbrain specification to study whether Cyp26 enzymes can regulate cell identity via community effects.

5.4.1 Cyp26 activity is involved in specification and maintenance of rhombomere identity

As a first step, I confirmed that Cyp26 activity regulates expression of *egr2b* and *hoxb1a* (Hernandez *et al*, 2007). Treatment of embryos with the compound R115866, also known as talarazole or rambazole, which is a potent and selective antagonist of Cyp26-mediated RA metabolism (Stoppie *et al*, 2000), will inhibit all Cyp26 activity. In zebrafish, R115866 treatment alters rhombomere specification, causing the entire hindbrain to adopt an r6/7 identity (Hernandez *et al*, 2007). It has also been demonstrated that phenotypes observed upon R115866 treatment are reversed by inhibition of RA synthesis, indicating that they result from a lack of RA degradation, rather than a lack of potentially bioactive Cyp26-derived RA metabolites (Hernandez *et al*, 2007).

As shown in Figure 5-12, treatment with R115866 from 50% or 75% epiboly to 20 ss causes a complete loss of *egr2b* expression in r3 and r5 (Figure 5-12 B,F), coinciding with an anterior expansion of *hoxb1a* expression (Figure 5-12 D,H); these findings are in accord with previously published data (Hernandez *et al*, 2007). I also investigated the impact of Cyp26 inhibition from later stages on hindbrain patterning. R115866 treatment from 95% epiboly to 20ss clearly causes reduced *egr2b* expression within r5, but has a subtler impact on expression of *egr2b* in r3 (Figure 5-12 I,J). This coincides with a corresponding anterior expansion of *hoxb1a* expression, but a clear void in *hoxb1a* expression is observed at a position that likely corresponds to r3, where *egr2b* is still expressed and – presumably – capable of repressing *hoxb1a* expression here (Figure 5-12 K,L). As shown in Figure 5-12, R115866 treatment from 2 ss to 20 ss does not affect hindbrain patterning compared to control DMSO-treated embryos, and the borders of *egr2b* expression appear to sharpen as normal. It therefore appears that global loss of Cyp26 activity does not compromise border sharpening, which occurs between 3 ss and 10 ss. However, the pharmacokinetics of R115866 in zebrafish have not been well described, and it is unclear of the time taken for R115866 to exert its effects on Cyp26 activity and, in turn, RA metabolism following treatment. It is possible that R115866 does not inhibit Cyp26 activity until some time after addition, by which stage any Cyp26-dependent sharpening may have already occurred.

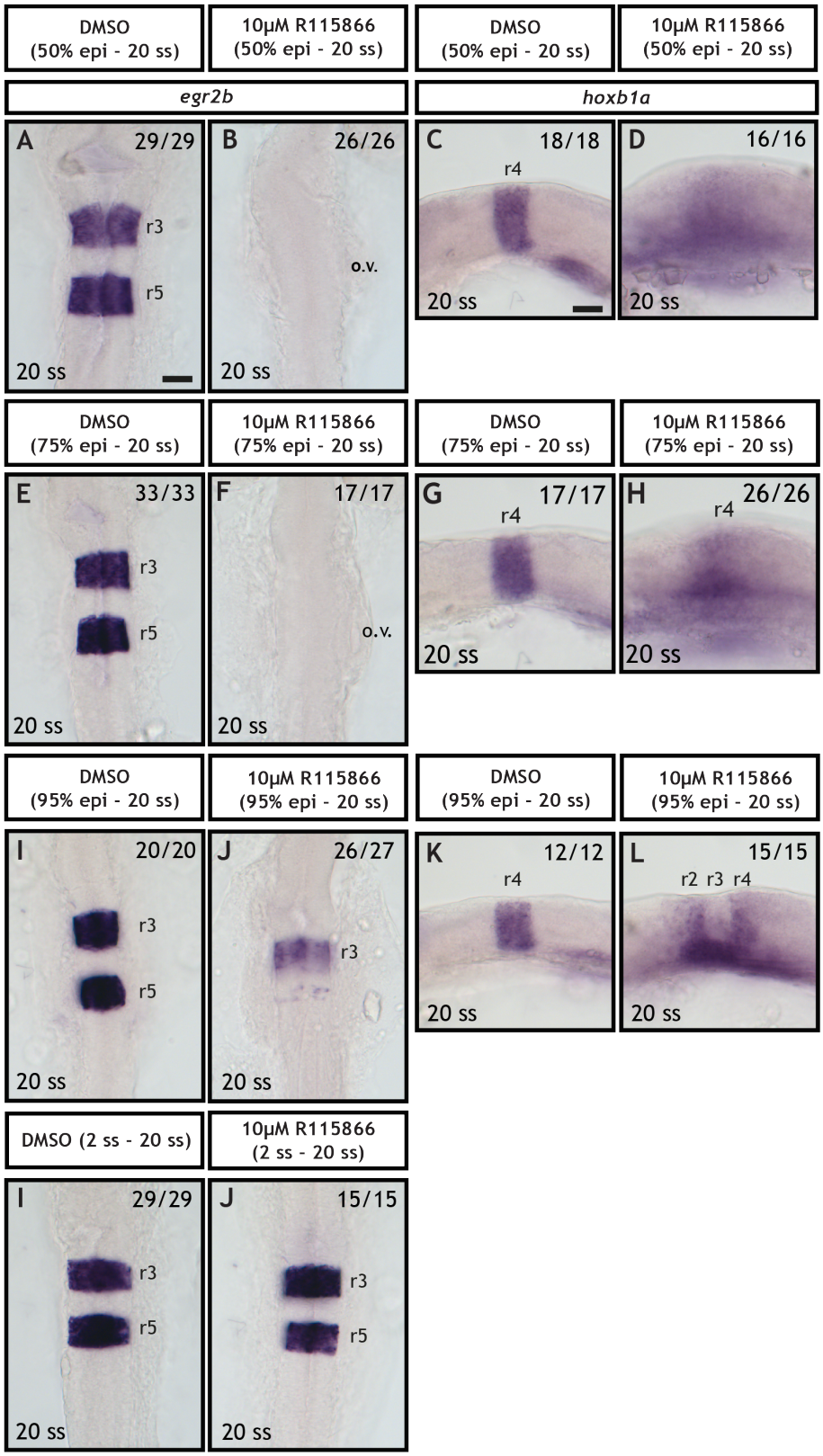

Figure 5-12 Loss of Cyp26 activity alters hindbrain specification

Embryos were treated with the Cyp26 inhibitor, R115866 from various starting stages and *egr2b* and *hoxb1a* expression analysed at 20 ss. R115866 treatment from 50% epiboly (5.3 hpf) or 75% epiboly (8 hpf) to 20 ss causes complete loss of *egr2b* expression from r3 and r5 (B,F) and expansion of *hoxb1a* expression (D,H) in contrast to DMSO-treated control embryos (A,E and C,G). R115866 treatment from 95% epiboly (9 hpf) to 20 ss causes severe reduction of *egr2b* expression in r5, but only slight reduction of *egr2b* expression in r3 (J) compared with DMSO-treated embryos (I). R115866 treatment from 95% epiboly to 20 ss also causes an anterior expansion of *hoxb1a* into r2, but not r3 (L) in contrast to DMSO-treated embryos (K). R115866 treatment from 2 ss to 20 ss does not affect *egr2b* expression (J) compared to DMSO-treated embryos (I). Embryos (A,B,E,F,I and J) are flat-mounted with anterior to the top; embryos (C,D,G,H,K and L) are side-mounted with anterior to the left. Frequencies of embryos observed represented by the image shown, out of the total number of embryos studied are shown in the top right. Epi: epiboly; o.v.: otic vesicle. Scale bars: 50 μm.

While studying the impact of Cyp26 inhibition on hindbrain patterning, I observed that early R115866 treatment, which causes a complete loss of *egr2b* expression by 20 ss, only causes a moderate reduction of *egr2b* expression by earlier stages. As shown in Figure 5-13, treatment with R115866 treatment from the dome stage (4.3 hpf) until 6 ss does not cause a complete loss of *egr2b* expression at 6 ss (C); even as late as 16 ss, *egr2b*-expressing cells are still detectable as a single but highly diffuse stripe (K). In these cases, *hoxb1a* expression is still expanded anteriorly, which is likely to contribute to the observed complete loss of *egr2b* expression by later stages. These new findings suggest that Cyp26 activity is partially involved in induction of cells to an *egr2b*-identity, but also contributes to maintenance of *egr2b* expression by later stages. It is likely that Cyp26b1 and Cyp26c1, rather than Cyp26a1, contribute to this later maintenance of *egr2b* expression. However, it is not clear from these experiments whether this requirement is also the case when induction of *egr2b* occurs normally, in the presence of Cyp26a1. It might be interesting to see whether recovery of Cyp26b1 and Cyp26c1 activity is sufficient to restore normal segmental gene expression by later stages after an initial loss of Cyp26 activity.

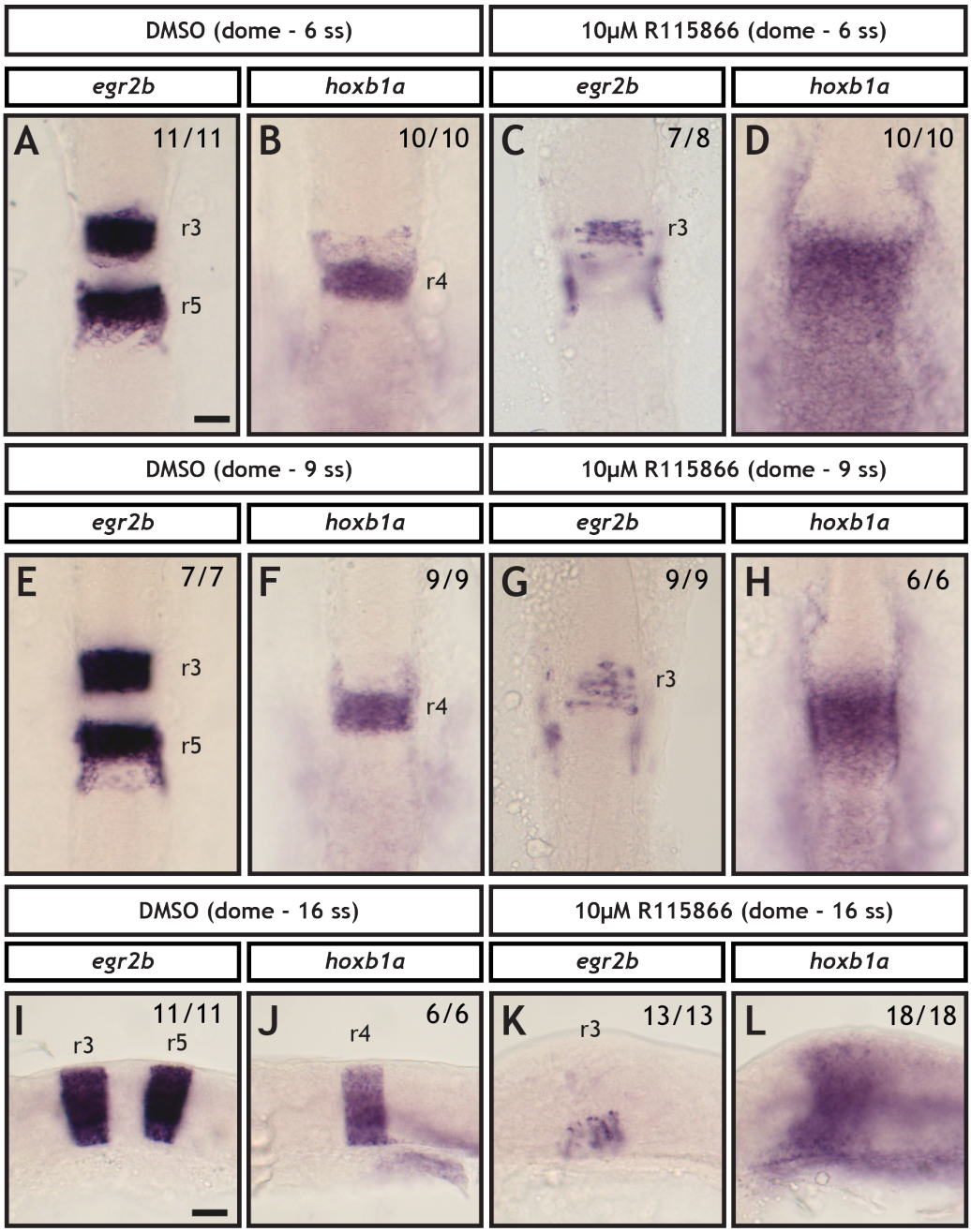

Figure 5-13 Persistence of *egr2b* expression in r3 upon Cyp26 inhibition at early stages

Treatment with R115866 to block Cyp26 activity from dome (4.3 hpf) to 6 ss (C), 9 ss (G) and 16 ss (K) causes a loss of *egr2b* expression from r5, but only partial loss of *egr2b* expression in r3 compared to DMSO-treated embryos (A,E,I). R115866 treatment from dome to 6 ss (D), 9 ss (H) and 16 ss (L) causes a slight anterior expansion, and posterior expansion, of *hoxb1a* expression, compared with DMSO-treated embryos (B,F,J). Embryos (A-H) are flat-mounted with anterior to the top; embryos (I-L) are side-mounted with anterior to the left. Frequencies of

embryos observed represented by the image shown, out of the total number of embryos studied are shown in the top right. Scale bar: 50 μm.

A limitation of chemical inhibition of Cyp26 proteins by R115866 is that it is not suitable for studying the loss of individual Cyp26 enzyme activity. Previous work has described hindbrain specification phenotypes in the Cyp26a1 mutant, *giraffe* (*gir*), in combination with Cyp26b1 and Cyp26c1 knock down by morpholino (Hernandez *et al*, 2007). As an alternative to the Cyp26a1 mutant, I knocked down Cyp26a1 using a cocktail of two splice-blocking morpholinos, which have been previously found to give comparable phenotypes to *gir* mutants (D'Aniello *et al*, 2013). In order to optimise the quantities of Cyp26a1 morpholinos to use, I assessed known phenotypes associated with loss of Cyp26a1, including reduced blood circulation at 28 hpf, reduced tail length and reduced size of pectoral fins at 80 hpf (Emoto *et al*, 2005). As shown in Figure 5-14, knock down of Cyp26a1, Cyp26b1 and Cyp26c1 causes loss of *egr2b* expression by 18 ss, although the penetrance of this phenotype is less than that for R115866 treatment, most likely due to incomplete knock down in some cases. It is also particularly challenging to accurately stage triple Cyp26 morphant embryos due to significant delays in their development compared to control embryos, in addition to perturbation of somitogenesis (Duester, 2007), which makes it difficult to accurately count somites. It is therefore possible that some Cyp26 morphant embryos studied may have been slightly younger and retained some *egr2b* transcripts even in the absence of Cyp26 activity, as shown in Figure 5-13.

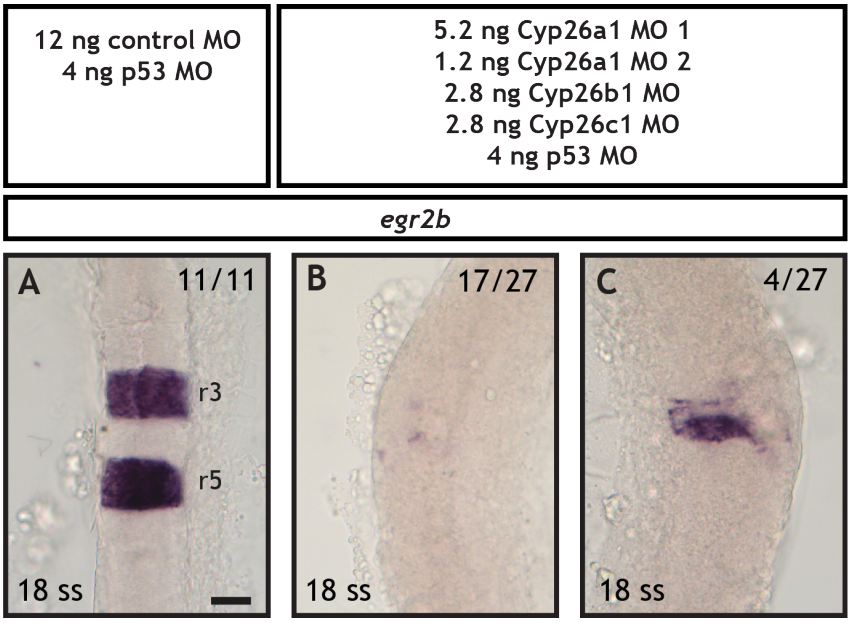

Figure 5-14 Knock down of Cyp26a1, Cyp26b1 and Cyp26c1 causes loss of *egr2b* expression

Egr2b expression was analysed in embryos in which Cyp26a1, Cyp26b1 and Cyp26c1 were knocked down by morpholino injection. Simultaneous knock down of Cyp26a1, Cyp26b1 and Cyp26c1 causes an almost complete loss of *egr2b* expression in both r3 and r5 by 18 ss in the majority of embryos studied (B,C) compared to control embryos (A). The remaining Cyp26 morphant embryos studied had comparable *egr2b* expression to control embryos (not shown; n = 6 of 27 embryos). Embryos are flat-mounted with anterior to the top. Frequencies of embryos observed represented by the image shown, out of the total number of embryos studied are shown in the top right. Scale bar: 50 μm.

5.4.2 Partial loss of Cyp26 activity reduces rhombomere border sharpness

If Cyp26 enzymes regulate cell identity via community effects to contribute to border refinement, it might be expected that loss of Cyp26 activity will affect rhombomere border sharpness. I have previously shown that complete Cyp26 inhibition from 2 ss to 20 ss does not affect the sharpness of rhombomere borders (Figure 5-12 I,J). It is likely that this is partly due to redundancy with alternative sharpening mechanisms, such as Eph/ephrin-mediated cell sorting. During optimisation of Cyp26 morpholino quantities, I observed that partial knock down of Cyp26a1, Cyp26b1 and Cyp26c1 severely reduces the sharpness of borders of *egr2b* expression in approximately half of embryos studied (Figure 5-15). Any

remaining sharpening mechanisms, such as Eph/ephrin-mediated cell sorting, appear insufficient to establish and/or maintain sharp rhombomere borders by the stages shown. This phenotype may result from increased initial mis-specification of cells along the AP axis due to reduction of Cyp26a1 activity; this will increase the extent of co-expression of conflicting factors at segment borders, widening regions of ambiguous identity between adjacent rhombomeres (Sosnik *et al*, 2016). By late stages, loss of Cyp26a1 alone only has a subtle effect on hindbrain patterning: r4 is slightly expanded in length, while the r1-3 region is reduced in length, but there is no impact on border sharpness (Emoto *et al*, 2005; Hernandez *et al*, 2007). It therefore appears that additional reduction of Cyp26b1 and Cyp26c1 activity compromises the identity switching of ectopic cells, such that cell sorting is insufficient to fully sharpen borders by 12 ss.

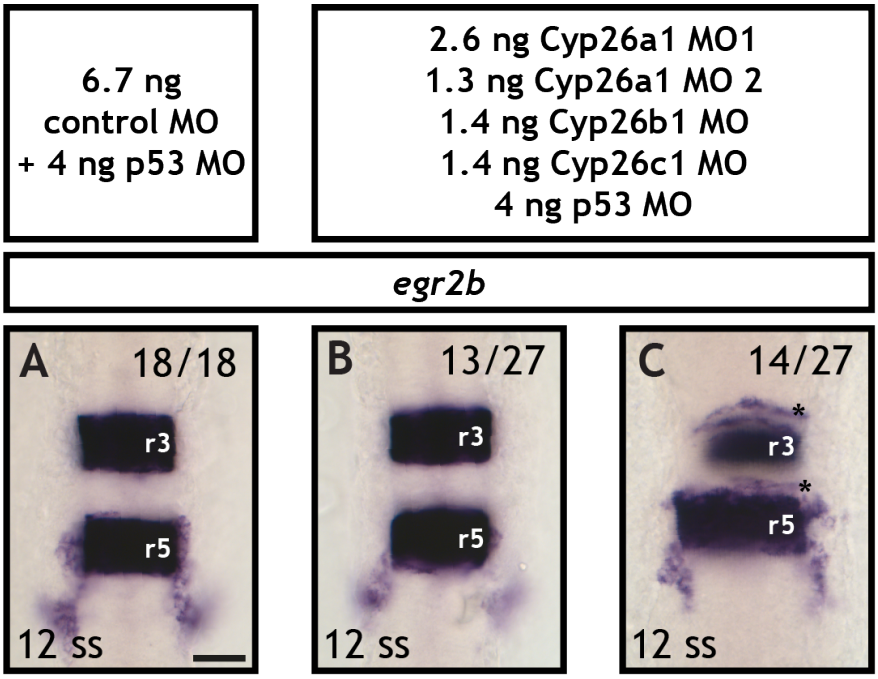

Figure 5-15 Partial knock down of Cyp26 enzymes perturbs rhombomere border sharpening

Egr2b expression was analysed in embryos injected with insufficient quantities of Cyp26a1, Cyp26b1 and Cyp26c1 morpholinos for complete knock down. In approximately half of morphant embryos, the borders of *egr2b* expression between r2 and r3 and between r4 and r5 are reduced in sharpness (C), in contrast to embryos injected with control morpholino (A). In the remaining Cyp26 morphant embryos studied (B), the sharpness of rhombomere borders is

comparable to control embryos (A). Embryos are flat-mounted with anterior to the top. Frequencies of embryos observed represented by the image shown, out of the total number of embryos studied are shown in the top right. Scale bar: 50 μm.

5.4.3 Loss of Cyp26b1 and Cyp26c1 perturbs border sharpness

Because I have hypothesised that Cyp26b1 and Cyp26c1 contribute to identity switching of ectopic cells, I also studied the impact of knocking down of Cyp26b1 and Cyp26c1 on border sharpness. As shown in Figure 5-16, knock down of Cyp26b1 and Cyp26c1 slightly reduces the sharpness of rhombomere borders at 12 ss. Previously, only a subtle shortening of the hindbrain and no patterning phenotypes have been reported for simultaneous knock down of Cyp26b1 and Cyp26c1 at 18 ss (Hernandez *et al*, 2007). However, this study focused on rhombomere identity rather than border sharpness and may therefore have overlooked this subtle phenotype. It is also possible that additional sharpening occurs in Cyp26b1/Cyp26c1 double morphants between 12 ss and 18 ss. It will be interesting to study whether in a case where cell intermingling is increased – increasing the requirement for identity switching for border refinement – the additional loss of Cyp26b1 and Cyp26c1 affects the extent of identity switching that can occur.

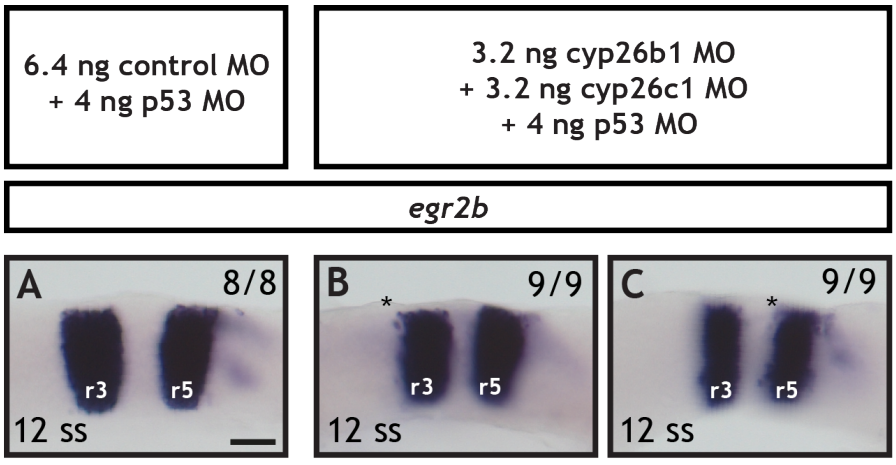

Figure 5-16 Knock down of Cyp26b1 and Cyp26c1 perturbs border sharpening
Egr2b expression was analysed in embryos in which Cyp26b1 and Cyp26c1 were knocked down. Cyp26b1/Cyp26c1 double morphant embryos have fuzzier borders of *egr2b* expression at 12 ss (B,C, asterisks) compared with those of embryos injected with control morpholino (A).

Embryos are side-mounted with anterior to the left. Frequencies of embryos observed represented by the image shown, out of the total number of embryos studied are shown in the top right. Scale bar: 50 μm.

5.4.4 Cyp26b1 appears sufficient to maintain some correct cell identity via community effects in embryos lacking Cyp26a1 and Cyp26c1

To further study the roles of different Cyp26 enzymes in hindbrain patterning, I studied hindbrain patterning in embryos lacking Cyp26a1 and Cyp26c1 activity. Here, it is expected that early loss of Cyp26a1 will increase mis-specification at segment borders, while a later loss of Cyp26c1 may compromise identity switching of ectopic cells. However, Cyp26b1 may still be able to mediate the refinement of ectopic cells by identity switching. As shown in Figure 5-17, in agreement with published results, simultaneous knock down of Cyp26a1 and Cyp26c1 does not dramatically affect *egr2b* expression in r5, although sometimes the borders of this rhombomere are slightly fuzzier and less refined than controls. As previously discussed, this fuzziness may result from increased mis-specification due to Cyp26a1 depletion (Sosnik *et al*, 2016), combined with a failure of cells to switch identity in the vicinity of r5 due to a lack of Cyp26c1. However, in Cyp26a1/Cyp26c1 double morphants, *egr2b*-expressing cells in r3 form a tight medium-sized cluster of cells on either the left or right side of the hindbrain (Figure 5-17 C, D) or two such clusters on each side of the hindbrain, sometimes loosely connected by one or two *egr2b*-expressing cells (Figure 5-17 B). It appears that Cyp26b1, which is expressed in r3, is capable of maintaining some *egr2b* expression in this region, as well as contributing to sharpening by identity switching of ectopic cells.

It is known that EphA4 can mediate the clustering of cells within r3 (Cooke *et al*, 2005). In order to study whether community effects – which are likely to be mediated by Cyp26b1 – maintain the identity of *egr2b*-expressing cells in r3 of Cyp26a1/Cyp26c1 double morphants, I repeated this knock down experiment in embryos lacking EphA4. Because morpholino knock down of EphA4, in combination with Cyp26a1 and Cyp26c1 knock down, caused high frequencies of lethality and deformities in injected embryos, likely due to non-specific toxic

morpholino effects, I instead knocked down Cyp26a1 and Cyp26c1 in embryos mutant for EphA4. The EphA4 mutant was generated and characterised by Jordi Cayuso in the Wilkinson lab (unpublished) and has been shown to have border sharpening defects and loss of boundary cell markers in agreement with studies of EphA4 morphant embryos (Cooke *et al*, 2005). Unfortunately, at the time of conducting these experiments, it was not possible to in-cross homozygous EphA4 mutants; I therefore crossed homozygous EphA4 mutants with heterozygous EphA4 mutants, which is expected to provide 50% homozygous EphA4 embryos ($EphA4^{-/-}$) and 50% embryos heterozygous for the EphA4 mutation ($EphA4^{+/-}$).

As shown in Figure 5-17 (G – I), in approximately 50% of embryos (likely corresponding to $EphA4^{-/-}$ embryos) the cluster of *egr2b*-expressing cells in r3 of embryos lacking Cyp26a1 and Cyp26c1 is no longer tightly aggregated and fewer cells appear to maintain *egr2b* expression here (Figure 5-17 I). In the remaining 50% of embryos (Figure 5-17 H), which are hypothesised to be $EphA4^{+/-}$, the r3 cluster of cells appears comparable to that in wildtype cells lacking Cyp26a1 and Cyp26c1 (Figure 5-17 G). Thus it appears that when *egr2b*-expressing cells are dispersed, maintenance of *egr2b* expression is compromised. These observations suggest that community effects, likely mediated by Cyp26b1, regulate *egr2b* expression in r3. I have previously shown that Egr2b is required for differential *cyp26b1* expression between r3 and r4 and that Egr2b represses *cyp26b1* expression in r3. It would be informative to confirm whether the *egr2b*-expressing cells in r3 of Cyp26a1 and Cyp26c1 morphants maintain a lower level of *cyp26b1* expression compared to the surrounding cells; this may maintain the optimum concentration of RA in the vicinity of these cells to maintain *egr2b* expression via a community effect.

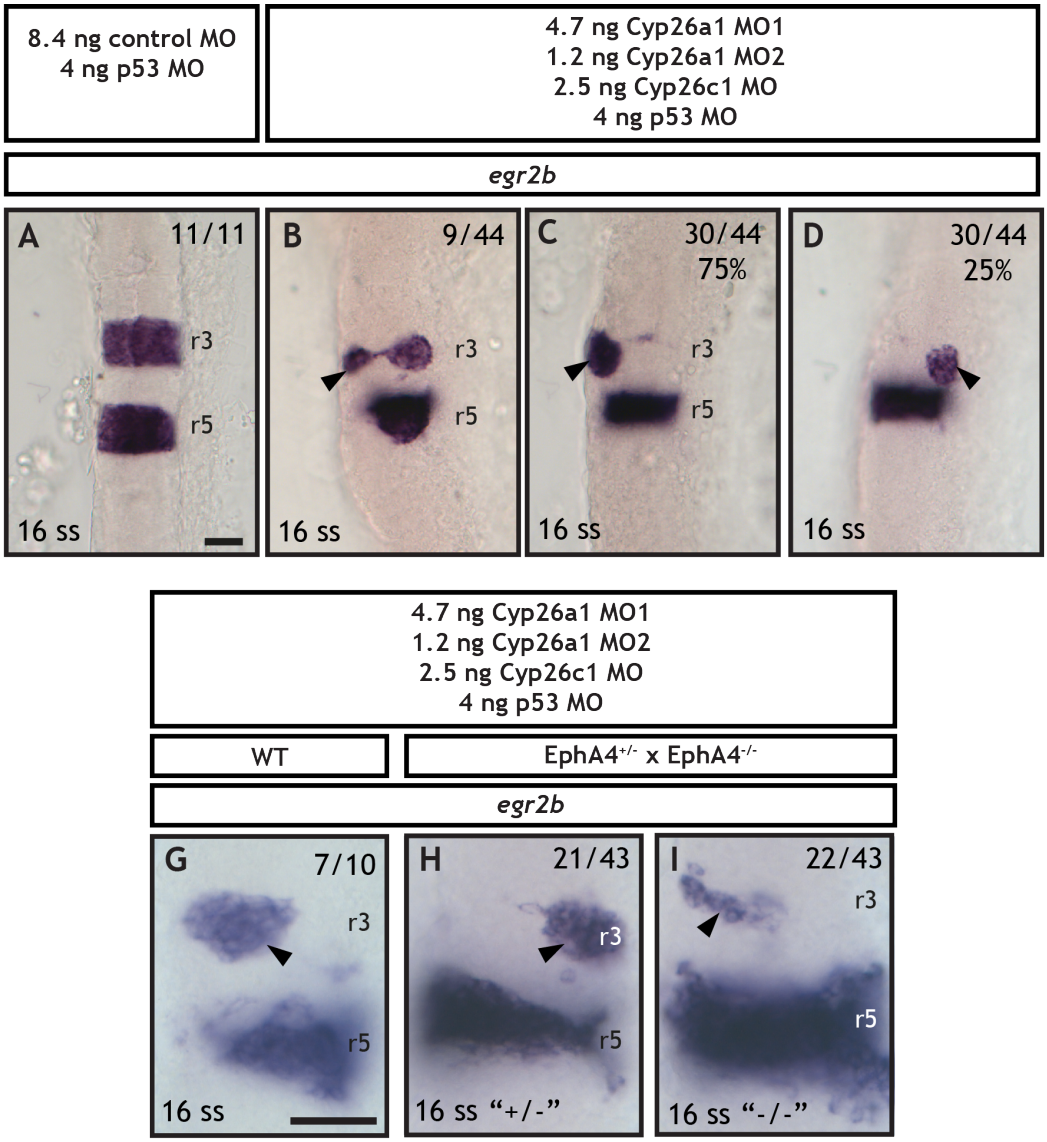

Figure 5-17 Maintenance of *egr2b* expression in embryos lacking Cyp26a1 and Cyp26c1 activity

Cyp26a1 and Cyp26c1 were knocked down in both wildtype embryos and embryos from an in-cross of EphA4$^{+/-}$ and EphA4$^{-/-}$ mutants; *egr2b* expression was analysed at 18 ss and 16 ss. Knock down of Cyp26a1 and Cyp26c1 in wildtype embryos does not significantly reduce *egr2b* expression in r5 compared with control embryos, but does cause a reduction in the size of *egr2b* expression in r3 at 18 ss (A-D) and 16 ss (G). In mixed EphA4 heterozygous and homozygous embryos lacking Cyp26a1 and Cyp26c1 activity, approximately 50% of embryos (thought to correspond to EphA4$^{+/-}$ embryos) maintain *egr2b* expression in r3 at 16 ss (H) comparably to wildtype Cyp26a1/Cyp26c1 morphant embryos (G). In the remaining embryos (thought to be EphA4$^{-/-}$ embryos) maintenance of egr2b expression in r3 is reduced (I) compared with wildtype Cyp26a1/Cyp26c1 morphant embryos (G). Embryos are flat-mounted

with anterior to the top. Frequencies of embryos observed represented by the image shown, out of the total number of embryos studied are shown in the top right. Scale bar: 50 μm.

5.4.5 What impact does mosaic loss of Cyp26 activity have on cell identity?

To further investigate whether Cyp26 enzymes can affect cell identity via community effects, one approach I took was to study the impact of mosaic loss of Cyp26 activity on cell identity. I hypothesise that individual cells with a different level of Cyp26 activity to their surroundings will not be capable of maintaining a different identity due to community effects on RA levels imposed by the surrounding cells. In contrast, I propose that a sufficiently-sized group of cells with different Cyp26 activity to its surroundings is able to maintain an ectopic identity by maintaining a different local level of RA.

As shown in Figure 5-18 (A-C), when cells from a Cyp26 morphant donor embryo, which lacks Cyp26a1, Cyp26b1 and Cyp26c1 activity, are transplanted into the future hindbrain of a wildtype host embryo, the majority of donor cells appear to die and have abnormally shaped nuclei, as seen with the H2B-GFP tracer. Unfortunately, it is difficult to accurately quantify the extent of death of these donor cells, as it is unclear whether punctate GFP staining corresponds to single or multiple cells. The cause of this excessive death of Cyp26 morphant donor cells is not clear. It is possible that mosaic morpholino-related toxicity and competition between wildtype host and morphant donor cells contributes to the elimination of morpholino-injected cells from the wildtype host, despite the fact that in Cyp26 morphant embryos there does not appear to be increased cell death compared with control embryos.

As shown in Figure 5-18 (B), surviving isolated Cyp26 morphant donor cells located in r3 or r5 are able to maintain *egr2b* expression. This is consistent with isolated cells with different Cyp26 expression being incapable of maintaining an ectopic identity due to community effects imposed by the surrounding cells. On one occasion, a cluster of Cyp26 morphant cells was observed in r3 or r5 (Figure 5-18 A), which appears to express lower levels of *egr2b* than host cells, suggesting that groups of cells of different Cyp26 activity may be capable of maintaining an ectopic

identity. The reduced *egr2b* expression corresponding to clustered donor cells is more uniform than reduced *egr2b* staining seen elsewhere in r3, which corresponds to the nuclei of cells. When *hoxb1a* expression was analysed in surviving donor cells, no ectopic *hoxb1a* expression outside r4 was observed for isolated donor cells (Figure 5-18 C). No clustered donor cells were observed during analysis of *hoxb1a* expression, so it remains unclear whether groups of Cyp26 morphant cells are capable of maintaining ectopic *hoxb1a* expression. The high frequency of death of donor cells makes it difficult to draw clear and meaningful conclusions from this experiment regarding identity regulation of donor cells. In addition, some *egr2b* expression was still frequently observed in Cyp26 morphants (Figure 5-18 E), indicating that Cyp26 knock down may not be complete in this experiment. It is expected that if groups of donor cells maintain a different identity – and therefore a different Eph/ephrin expression profile – to their surroundings, they will become sorted from the surrounding cells. However, only one cluster of donor cells within r3-r5 was observed during analysis of a total of 25 embryos.

As shown in Figure 5-18 (D), when wildtype donor cells are transplanted into Cyp26 morphant hosts, the majority of donor cells survive. It appears that some wildtype donor cells may be capable of retaining *egr2b* expression when grouped together, possibly due to an ability to retain a suitable concentration of RA for maintenance of *egr2b* expression. Unfortunately, in this experiment, some *egr2b* expression was still frequently observed in Cyp26 morphants (Figure 5-18 E), so the extent to which wildtype cells can rescue Cyp26 depletion is not clear. However, it does appear that isolated wildtype cells within the region corresponding to r3 or r5 of Cyp26 host embryos are not capable of retaining *egr2b* expression. A likely explanation for this is that Cyp26 activity in donor cells is insufficient to overcome the impact of reduced Cyp26 activity and increased RA signalling among the host cells.

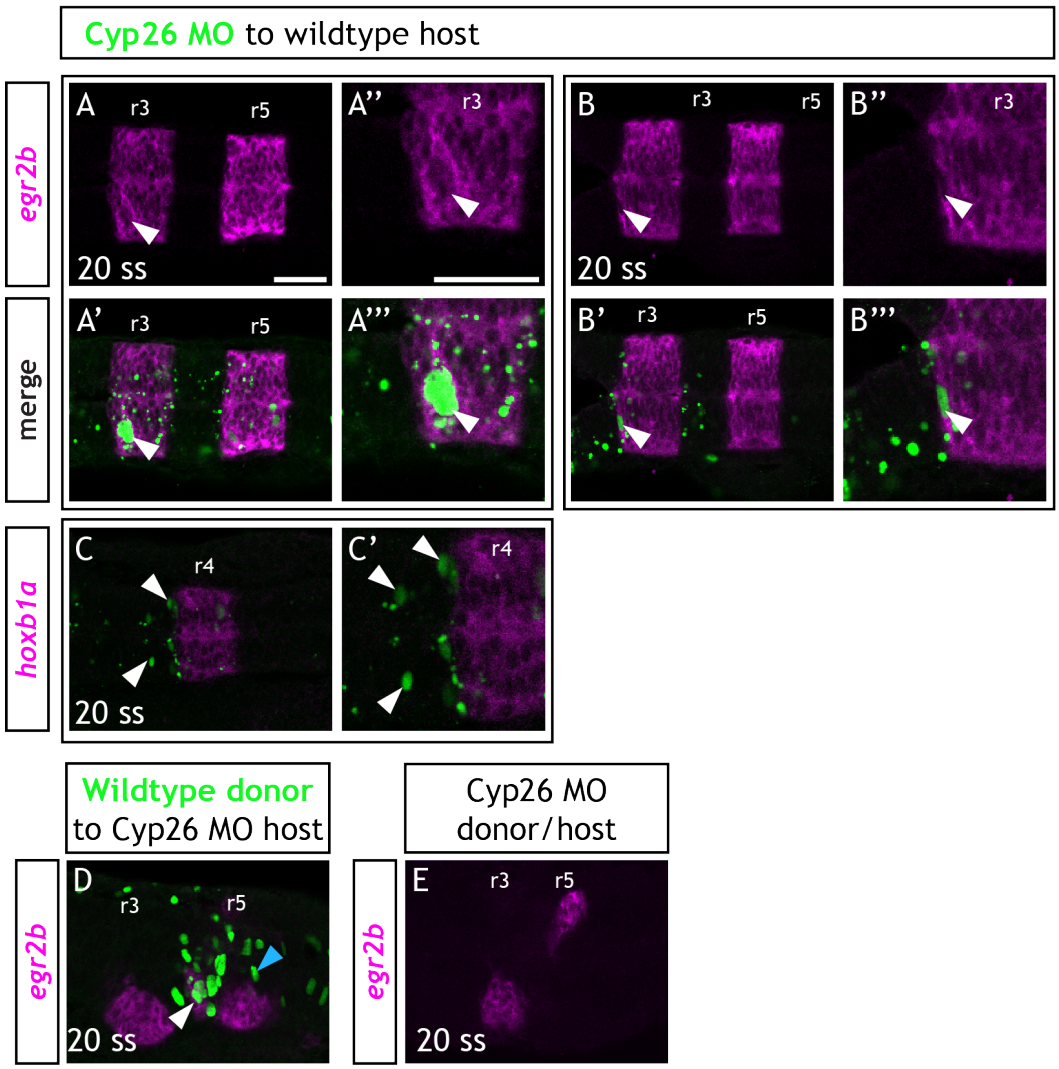

Figure 5-18 *egr2b* and *hoxb1a* expression analysis in embryos mosaic for Cyp26 activity

Cells from donor embryos (injected with Cyp26a1, Cyp26b1 and Cyp26c1 morpholino) were transplanted into wildtype hosts at the early gastrula stage (A-C, E). In Cyp26 morphant embryos, *egr2b* expression was greatly reduced, but not completely lost from r3 and r5 by 20 ss (E; n = 5 embryos). The majority of Cyp26 morphant cells appear to die within wildtype hosts (A-C; n = 25 embryos). In one case, a group of Cyp26 morphant cells arose in r3, and here *egr2b* expression appears reduced compared with the host cells (A; n = 1 embryo; white arrowheads; enlarged in A'' and A'''). In contrast, isolated Cyp26 morphant cells in r3 maintain *egr2b* expression at a comparable level to host cells (B; n = 13 embryos; white arrowheads; enlarged in B'' and B'''). Isolated Cyp26 morphant cells in r3 do not ectopically express *hoxb1a* (C; n = 12 embryos); no clusters of Cyp26 morphant cells were observed in embryos analysed for *hoxb1a* expression. When cells from wildtype donors were transplanted into Cyp26 morphant hosts, some wildtype donor cells maintain expression of *egr2b* (D; n = 5 embryos;

white arrowheads), while other wildtype donor cells do not maintain *egr2b* expression, despite being at the AP position of r3 or r5 (D; n = 5 embryos; blue arrowheads). Embryos are flat-mounted with anterior to the left. Scale bars: 50 μm.

5.4.6 What impact does mosaic increased Cyp26 activity have on cell identity?

To investigate whether Cyp26 enzymes can regulate cell identity in the hindbrain via community effects, I also analysed the impact of increased Cyp26 expression on hindbrain specification. I aimed to subsequently study the impact of mosaic increased Cyp26 activity on cell identity. To increase Cyp26 activity, I utilised a construct previously generated by Rosa Gonzalez-Quevedo in the Wilkinson lab (unpublished) to create the transgenic line Tg[UAS/hs:cyp26b1-ACR]. In this line, *cyp26b1* is under the control of both a heat shock-inducible *hsp70* promoter and a UAS promoter. Overexpression of *cyp26b1* can be achieved in this line by heat shock at 37 °C. It is expected that gain of Cyp26 activity during hindbrain patterning will produce comparable phenotypes associated with loss or reduction of RA signalling. The effect of reduced RA signalling upon rhombomere specification has already been well-described and involves anteriorisation of the posterior hindbrain, with loss of r5-r7 markers (Gale *et al*, 1999; Dupé & Lumsden, 2001; Maves & Kimmel, 2005).

As shown in Figure 5-19, overexpression of *cyp26b1* in Tg[UAS/hs:cyp26b1-ACR] embryos increases the fuzziness of *egr2b* expression at 12 ss compared to non-heat shocked control embryos (Figure 5-19 A-F). This is likely to result – at least in part – from a reduction of RA levels, which will increase mis-specification of cell identity along the AP axis, and will affect specification of r5 to a greater extent than r3. The phenotypes observed with increased Cyp26b1 activity here are variable and not completely comparable with known phenotypes for complete loss of RA signalling: in 12 of 36 embryos studied, overexpression of *cyp26b1* also caused a substantial reduction of *egr2b* expression in r5 (Figure 5-19 E,F), while in the remaining embryos, expression of *egr2b* was only slightly reduced in r5 (Figure 5-19 C-D). As shown in Figure 5-20, overexpression of *cyp26b1* does reduce the expression of some, but not all, *hox* genes in posterior rhombomeres, again

indicating that a complete loss of RA signalling does not occur. This is likely due to insufficient levels of transgene expression in the transgenic line generated to achieve a complete loss of RA signalling. It is also possible that compensatory upregulation of RA signalling components upon Cyp26b1 overexpression reduces the severity of phenotypes observed. For this reason, I have been unsuccessful in analysing the impact of mosaic overexpression of Cyp26b1 on cell identity regulation in the hindbrain. The observation that overexpression of Cyp26b1 increases the fuzziness of rhombomere borders is consistent with Cyp26 activity and RA signalling contributing to border sharpening.

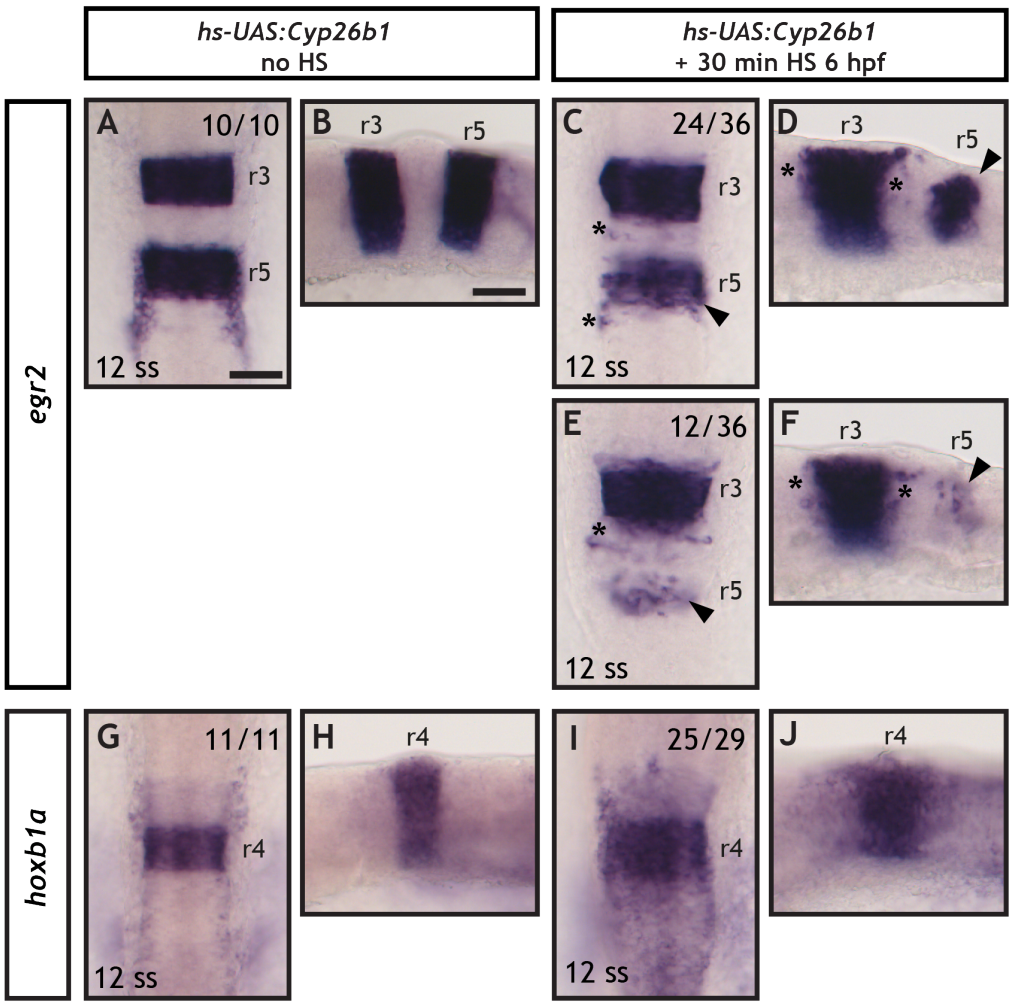

Figure 5-19 Overexpression of *cyp26b1* by heat shock alters *egr2b* and *hoxb1a* expression to varied degrees in Tg[UAS/hs:cyp26b1-ACR] embryos

Embryos from the transgenic line Tg[UAS/hs:cyp26b1-ACR] were heat shocked at 6 hpf to induce overexpression of Cyp26b1 and were compared with non-heat shocked control embryos.

Overexpression of *cyp26b1* reduces the sharpness of the r2/r3 and r3/4 borders (asterisks) and reduces *egr2b* expression in r5 to varied degrees by 12 ss (arrowheads) (C-F) compared to non heat shocked control embryos (A,B). Overexpression of *cyp26b1* causes an anterior and posterior expansion of *hoxb1a* expression in the majority of embryos studied (I,J) compared to non heat shocked controls (G,H). Embryos (A,C,E,G, and I) are flat-mounted with anterior to the top; embryos in B,D,F,H and J are side-mounted with anterior to the left. Frequencies of embryos observed represented by the image shown, out of the total number of embryos studied are shown in the top right. Scale bar: 50 μm.

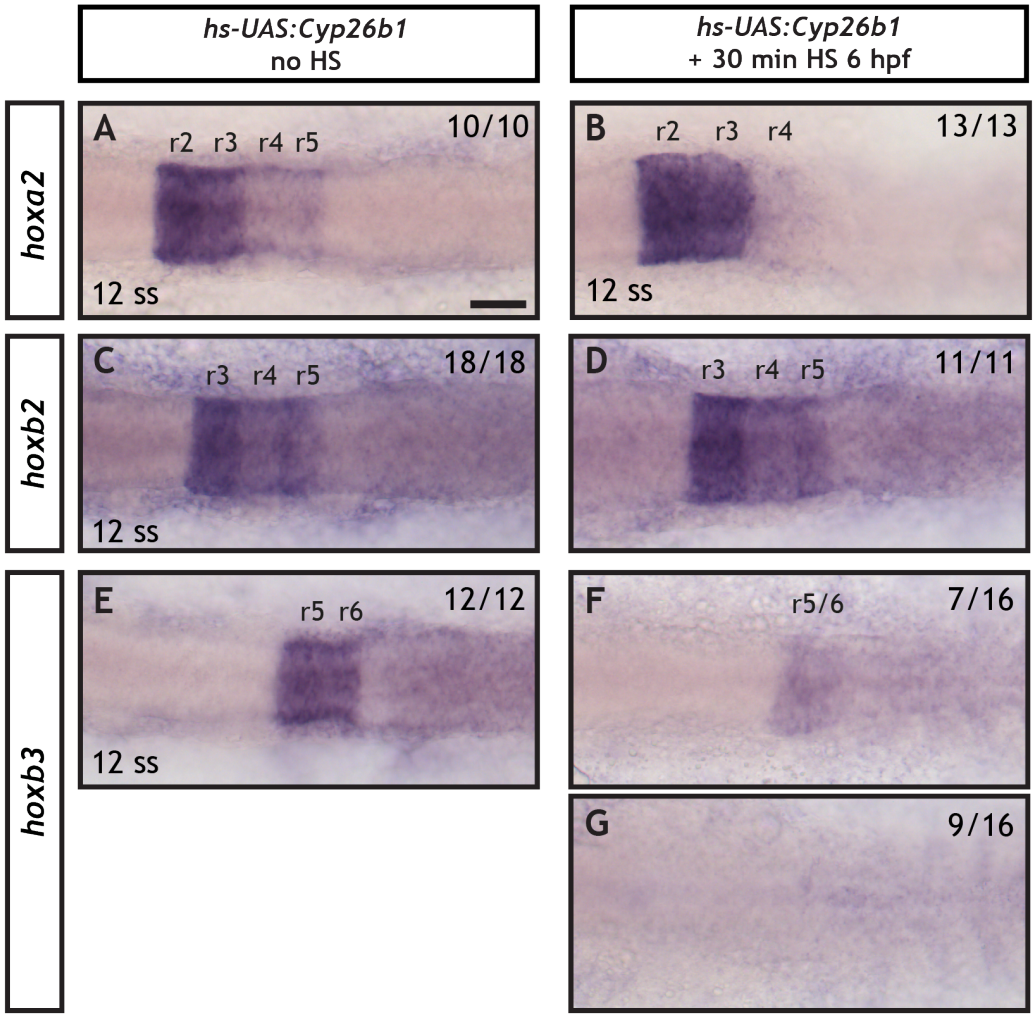

Figure 5-20 Overexpression of *cyp26b1* by heat shock alters *hox* expression in the posterior hindbrain of Tg[UAS/hs:cyp26b1-ACR] embryos

Embryos from the transgenic line Tg[UAS/hs:cyp26b1-ACR] were heat shocked at 6 hpf to induce overexpression of *cyp26b1* and were compared with non-heat shocked control embryos. Overexpression of *cyp26b1* reduces *hoxa2* expression in r4 and r5, but does not affect levels of expression in r2 or r3 (B) compared to non-heat shocked control embryos (A). Overexpression

of *cyp26b1* does not significantly change levels of *hoxb2* expression in any rhombomeres (D) compared to control embryos (C). Overexpression of *cyp26b1* reduces *hoxb3* expression in r5 and r6 to varied degrees (F,G) compared to control embryos (E). Embryos are flat-mounted with anterior to the left. Frequencies of embryos observed represented by the image shown, out of the total number of embryos studied are shown in the top right. Scale bar: 50 μm.

5.5 Discussion

In this chapter I have described experiments investigating whether community effects regulate cell identity and mediate cell identity switching during hindbrain border sharpening. I have also addressed whether, as hypothesised, transcription factors that confer identity to rhombomeres also regulate segmental expression of Cyp26b1 and Cyp26c1, which, in turn, may modulate RA levels within rhombomeres to maintain cell identity and mediate switching of identity of ectopic cells.

5.5.1 Cell identity in the hindbrain appears to be regulated by community effects

Egr2b regulates cell identity non cell-autonomously

I have presented evidence that in zebrafish, Egr2b can induce its own expression non cell-autonomously, indicating that Egr2b may regulate cell identity via a community effect. When Egr2b-Myc is overexpressed under control of the Pax3 CNE1, endogenous *egr2b* is expressed in more ventral domains than the dorsally-restricted domain of Egr2b-Myc expression. This strongly supports a non cell-autonomous activity of Egr2b-Myc. However, it remains possible that – at least shortly after onset of Pax3 CNE1 transcriptional activity – low, undetected levels of Egr2b-Myc could still be a problem and lead to an overestimate of the extent of the non cell-autonomous activity of Egr2b-Myc. To add an additional level of accuracy to studying the non cell-autonomous activity of Egr2b-Myc, I have also attempted to combine overexpression of Egr2b-Myc with cell transplantation into wildtype embryos, whereby only donor cells, and not the host cells, express Egr2b-Myc. In this case, any ectopic induction of endogenous *egr2b* expression in the host cells would indicate a non cell-autonomous activity of Egr2b-Myc. However, I found that

combining transient Egr2b-Myc transgenic expression with cell transplantation caused extremely low frequencies of Egr2b-Myc-containing cells to be observed in host embryos (<1% of donor cells expressed detectable Egr2b-Myc; although many of these cells were not within the Pax3 CNE1 domain). While creating a stable Pax3CNE1:egr2b-Myc transgenic line to use as donor embryos would alleviate this problem, I have not attempted to create this transgenic line, as it is unlikely to be viable. However, I have created an additional stable transgenic line to combine with cell transplantation to study the non cell-autonomous mechanism of Egr2b-Myc, in which *egr2b-Myc* expression can be induced by heat shock. At the time of writing, these Tg[hsp70:egr2b-Myc] fish are not yet available to use, due to low transmission frequency in F_0s. However, in the future this line will be useful for experiments studying the mechanism of the non cell-autonomous activity of Egr2b.

From my results presented here, it is not yet clear what the mechanism of non cell-autonomous induction by Egr2b is. It unlikely that the non cell-autonomous activity of Egr2b involves direct transcriptional activation of element A by Egr2b; for this to be the case, it would require that Egr2b protein is already present in cells receiving the non cell-autonomous signal, as element A activity is lost by mutation of its Egr2b binding sites (Chomette *et al*, 2006). As I have hypothesised, one possible mechanism by which Egr2b may induce its own expression non cell-autonomously is by regulation of Cyp26b1 and/or Cyp26c1, which in turn locally modify RA levels to drive *egr2b* expression. It will be informative to see whether altering Cyp26 activity and RA metabolism impacts upon the non cell-autonomous activity of Egr2b.

Alternatively, Egr2b may cell-autonomously induce the expression of an unknown cell-cell signalling factor/s that initiates expression of *egr2b* non cell-autonomously via initiating elements B and/or C. Subsequently, the autoregulatory loop involving element A will be activated in the receiving cells. An additional alternative mechanism of non cell-autonomous induction of *egr2b* could involve direct intercellular transfer of Egr2b protein between adjacent cells, as suggested by Chomette *et al*, 2006. There is evidence that some transcription factors can undergo intercellular transfer, reviewed by Prochiantz & Joliot, 2003 and Prochiantz & Di Nardo, 2015. For example, paracrine transfer of Engrailed protein has been shown to be involved in positioning of the diencephalic-mesencephalic boundary

(Joliot *et al*, 1997; Rampon *et al*, 2015). In *Xenopus*, intercellular translocation of Myc-Hoxd1 has been reported, and suggests that paracrine Hox protein transfer contributes to vertical signalling between mesoderm to neuroectoderm and AP patterning (Bardine *et al*, 2014). The sequences that appear to be necessary for intercellular transfer of homeodomain proteins involve conserved elements of the homeodomain itself, and thus may be conserved between all homeodomain-containing proteins, including Egr2b (Joliot & Prochiantz, 2004). However, the requirement for sequences within the DNA-binding homeodomain itself for internalisation and secretion also impedes investigations into the requirement of intercellular transfer because mutations introduced within these regions will also likely compromise transcriptional activity. Modelling that incorporates intercellular transfer of homeodomain proteins suggests that, in combination with autoactivation and mutual inhibition between pairs of homeodomain proteins, this phenomenon can explain boundary formation between adjacent domains (Holcman *et al*, 2007). My analysis of identity regulation in mosaic Egr2 embryos argues against the suggestion that Egr2b protein is subject to intercellular transfer, as any such transfer is insufficient to maintain detectable *egr2b* expression in neighbouring cells in which Egr2 is knocked down. However, it is possible that a lack of autoregulation mediated by endogenous Egr2b in the morphant host cells may limit the non cell-autonomous establishment of this autoregulatory loop, preventing detectable maintenance of *egr2b* expression.

The ability of community effects to regulate cell identity appears to depend on the extent of cell dispersal and the AP position of cells

I have observed that once Egr2b-Myc-expressing cells become sorted to the borders of r3 and r5, Egr2b-Myc is no longer able to exert a non cell-autonomous effect on cells within r4. A possible explanation for this is that, in order for Egr2b-Myc to induce non cell-autonomous expression of *egr2b*, it may be necessary for Egr2b-Myc-expressing cells to be intermingled with r4 cells, such that r4 cells are surrounded by Egr2b-Myc-expressing cells, and unable to maintain their identity via community effects. In previous experiments using electroporation to overexpress Egr2, overexpressing cells are distributed throughout the hindbrain and are intermingled with wildtype cells, unlike when Egr2b-Myc expression is driven by Pax3 CNE1. In future experiments using Tg[hsp70:egr2b-Myc] combined with cell

transplantation, it should be possible to achieve dispersed mosaic overexpression of Egr2b-Myc. An alternative explanation for the inability of Egr2b-Myc to function non cell-autonomously by later stages is that cells may only be competent to respond to non cell-autonomous induction by Egr2b-Myc during the window of time when they have plasticity of fate. It is possible that at these earlier stages there are certain permissive factors present that are required for the non cell-autonomous response to Egr2b. It is not clear what these factors are, and knock down of Hoxb1a and Hoxb1b is not sufficient to prevent repression of these factors in r4 at late segmentation stages.

From analysis of embryos mosaic for endogenous Egr2, I have also shown that community effects from Egr2 morphant cells are not able to prevent clustered or dispersed wildtype cells from maintaining *egr2b* expression. A possible explanation for this is that RA levels at the r3* position – which would have r3 identity in the presence of Egr2 - in Egr2 morphants are sufficient to maintain *egr2b* expression in wildtype cells and can overcome local non cell-autonomous effects (illustrated in Figure 5-21). An additional explanation is that wildtype donor cells in r3* may be juxtaposed between cells of r2 and r4 identity and may therefore receive a combination of non cell-autonomous signals promoting both r2 and r4 identity, with the net result of maintenance of an r3 identity. This situation is therefore different to that at rhombomere borders in normal development, where ectopic cells in the wrong rhombomere are surrounded by cells of a single different identity. Interestingly, I also found that induction of *hoxb1a* expression in wildtype cells by Egr2 morphant cells depends on whether the wildtype cells are clustered or isolated. This suggests that community effects are sufficient to upregulate *hoxb1a* expression non cell-autonomously, but these effects are weaker than the specification of r3 identity by graded signals. Opposing community effects from sufficient numbers of wildtype *egr2b*-expressing cells at the correct AP location are capable of preventing non cell-autonomous induction of *hoxb1a*, as illustrated in Figure 5-21. Co-expression of *egr2b* and *hoxb1a* is never observed at these stages in normal development, due to combined mutual inhibition and autoactivation between *egr2b* and *hoxb1a*. It will therefore be informative to see whether at even later stages of development the individual cells that co-express *egr2b* and *hoxb1a*

are still capable of maintaining *egr2b* expression, or whether they completely switch their identity and become r4-like.

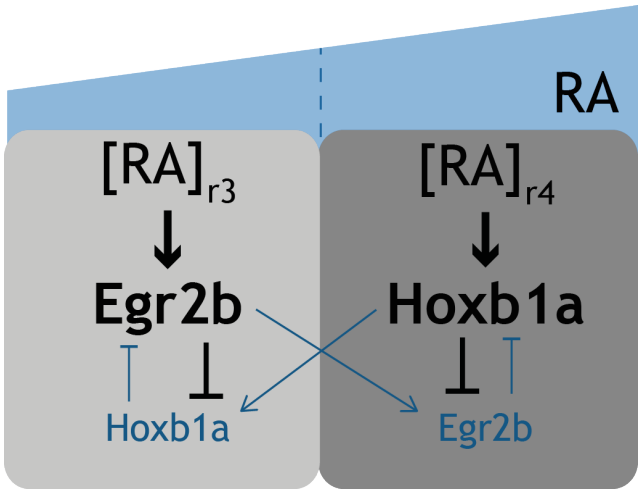

Figure 5-21 Model illustrating the relative strength of community effect signals
Graded RA along the AP axis, as regulated by Cyp26a1, leads to different concentrations of RA in r3 and r4. This causes Egr2b and Hoxb1a to be differentially expressed within these two rhombomeres. Egr2b and Hoxb1a may be able to induce their expression non cell-autonomously (blue arrows), but this effect is weaker than induction of expression by signalling depending on the AP position of cells (black arrows). The strength of non cell-autonomous community effect signals depend on the number of cells in contact, and if sufficient numbers of cells are present, they are able to overcome the graded AP signals.

5.5.2 Does local modulation of RA signalling by Cyp26 enzymes regulate cell identity and contribute to border sharpening?

Investigating the ability of Cyp26 enzymes to regulate identity in the hindbrain via community effects

It has previously been shown that Cyp26c1 can function via an apparent community effect to regulate ectopic expression of *hoxb1a* in the posterior hindbrain (Lee & Skromne, 2014). I attempted to investigate this further by studying the consequences of mosaic gain- and loss-of-function of Cyp26 factors on cell identity in the hindbrain. If, as hypothesised, Cyp26b1 and Cyp26c1 contribute to the refinement of identity of ectopic cells via a community effect, groups of cells with a different Cyp26 expression status to the neighbouring cells should be capable of maintaining a different identity to their surroundings. Isolated cells are

not expected to maintain a different identity to their surroundings, despite having a different Cyp26 expression status due to community effects imposed by RA signalling from the surrounding cells. However, due to technical difficulties, I have, as yet, been unsuccessful in demonstrating the ability of Cyp26 enzymes to regulate cell identity in the hindbrain via community effects, although my findings so far remain consistent with this hypothesis.

Mosaic loss of Cyp26 expression using morpholinos to knock down Cyp26a1, Cyp26b1 and Cyp26c1 does not appear to be a suitable approach to study mosaic loss of Cyp26 activity, due to high frequencies of death of morphant cells within wildtype hosts. It is likely that non-specific morpholino toxicity and p53 activation contributes to the extent of death of morphant cells (Robu *et al*, 2007). While I co-injected p53 morpholino into the Cyp26 morphant donor embryos, this may not have been sufficient to completely prevent p53 activation and its consequences. In addition, I did not knock down p53 in the host cells, which may also contribute to the apparent elimination of morphant donor cells. An alternative would be to use p53 mutant fish as donor and host embryos for this experiment. Unfortunately, I was unable to use p53 mutant fish in these experiments due to issues of infertility in our existing homozygous lines. A further limitation of mosaic loss of Cyp26 expression is the low extent of clustering of donor cells observed within host embryos. However, an additional approach to increase the extent of clustering of donor cells could be to knock down various Ephs and ephrins in host or donor cells. For example, wildtype cells are known to cluster within r3 and r5 or EphA4 morphant hosts (Cooke *et al*, 2005).

I have also attempted to study the consequences of mosaic overexpression of *cyp26b1* on cell identity specification. However, as previously discussed, a drawback of my approach to overexpress *cyp26b1* is that I am unable to achieve full loss of posterior markers as expected for complete loss of RA signalling. I have suggested that the varied severity of phenotypes I observe are due to varied transgene levels within the transgenic line Tg[UAS/hs:cyp26b1-ACR] and overall insufficient levels of *cyp26b1* overexpression to achieve complete loss of posterior rhombomeres.

Loss of Cyp26 activity affects border sharpening

If segmental regulation of RA signalling by Cyp26b1 and Cyp26c1 mediates identity switching at segment borders, it is expected that loss of these enzymes will compromise rhombomere border sharpness. Consistent with this, I have demonstrated here that knock down of Cyp26b1 and Cyp26c1 reduces the sharpness of the borders of r3 and r5. However, additional contributions from cell segregation appear to cause some border sharpening to still occur in the absence of Cyp26b1 and Cyp26c1. I have previously shown that, in embryos lacking EphA4 and EphrinB3 activity, there is increased cell intermingling between rhombomeres, and increased numbers of ectopic *egr2b*-expressing cells at early, but not late stages of segmentation. It would therefore be interesting to see whether loss of Cyp26b1 and Cyp26c1 activity in this situation with increased cell intermingling and compromised Eph/ephrin-mediated sorting increases the number of ectopic cells at later stages of segmentation.

The non cell-autonomous activity of Egr2b may involve localised modulation of RA signalling via Cyp26b1 and Cyp26c1

Consistent with my proposed mechanism by which Egr2b affects cell identity non cell-autonomously through local modulation of RA signalling, I have presented a novel finding that Egr2b regulates segmental expression of *cyp26b1* and *cyp26c1*. It is not known whether this involves direct transcriptional regulation by Egr2b. This finding builds on our limited understanding of how segmental expression of Cyp26 expression is regulated, as summarised in Figure 5-22. In zebrafish, knock down of Irx7 and Irx1b reduces *cyp26c1* expression, and *cyp26b1* expression to a lesser extent, indicating that induction of segmental *cyp26b1* and *cyp26c1* expression is regulated, either directly or indirectly, by Irx7 and Irx1b (Stedman *et al*, 2009). As shown in Figure 5-22, Irx1b and Irx7 induce segmental *cyp26b1* and *cyp26c1* expression, in parallel with their known roles in induction of *egr2b* in r3. From my findings, Egr2b is capable of subsequently modulating *cyp26b1* and *cyp26c1* expression by reducing their expression in r3 and r5. Other as yet unidentified transcription factors are likely to also contribute to segmental regulation of *cyp26b1* and *cyp26c1* expression. It is possible that the levels of Cyp26b1 and Cyp26c1 expression in r3, as regulated by Egr2b, maintain RA levels that are permissive for r3 identity, rather than r2 or r4 identities. As shown in Figure 5-21, Egr2b may

mediate non cell-autonomous effects on *hoxb1a* expression via cell-autonomous regulation of Cyp26 expression, causing non cell-autonomous modulation of RA signalling. This may in turn contribute to non cell-autonomous activation of *egr2b* expression, by removing repression of *egr2b* expression by *hoxb1a* in neighbouring cells. However, I have not demonstrated that Egr2b necessarily maintains the correct concentration in r3 for maintenance of *egr2b* expression. It might in fact be expected that lower levels of Cyp26 activity in r3, compared to r4, maintain higher concentrations of RA in r3 than r4.

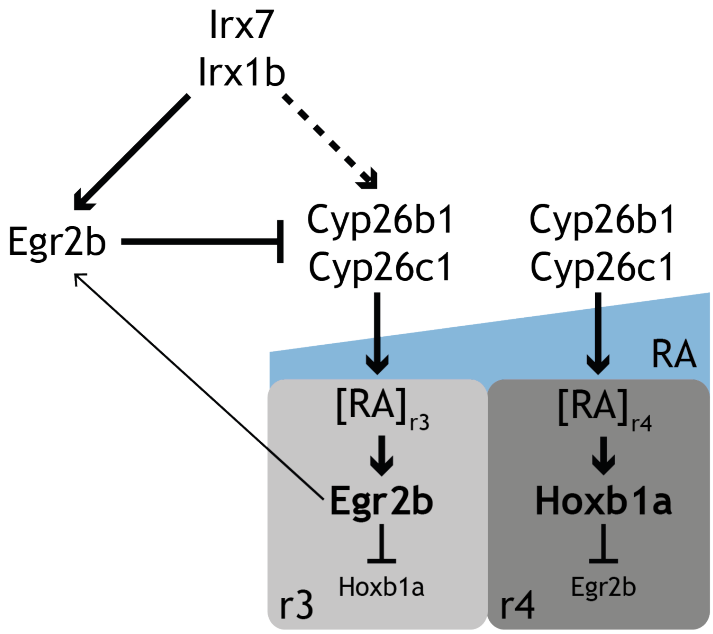

Figure 5-22 Regulation of *cyp26b1* and *cyp26c1* expression and potential consequences for regulation of r3 identity

Within prospective rhombomere 3, Irx7 and Irx1b contribute to initiation of *egr2b*, *cyp26b1* and *cyp26c1* expression. Subsequently, Egr2b represses *cyp26b1* and *cyp26c1* expression in r3. This may modulate RA signalling within r3 and refine RA levels to those permissive for *egr2b* – rather than *hoxb1a* – expression. Rhombomere identity is further enforced by mutual inhibition between Egr2b and Hoxb1a.

Regulation of RA signalling via Cyp26b1 and Cyp26c1 – a common mechanism of identity refinement by Hox factors?

Any sharpening mechanisms mediated via Egr2b will only contribute to sharpening of the borders of rhombomeres 3 and 5, where *egr2b* is expressed. I have also

suggested that segmentally expressed Hox factors contribute to regulating segmental expression of Cyp26 enzymes, enabling segment-specific modulation of RA levels in other rhombomeres. This may mediate identity switching and contribute to sharpening at other rhombomere borders. If this is the case, it would be expected that other Hox factors are capable of inducing their own expression non cell-autonomously, and that co-expression of conflicting Hox factors from different rhombomeres would therefore be expected to prevent non cell-autonomous induction by negating each other's effect on RA signalling. From results I have presented here, it does not appear that Hoxb1a or Hoxb1b regulate *cyp26b1* or *cyp26c1* expression during border sharpening. This may explain why knock down of Hoxb1a and Hoxb1b does not increase the non cell-autonomous activity of Egr2b-Myc in r4 at late segmentation stages. However, it has been shown in chick that co-electroporation of Hoxa3 or Hoxa4 with Egr2 is sufficient to reduce the non cell-autonomous range of EphA4 induction by Egr2 (Prin *et al*, 2014). It is possible that Hoxa3 and Hoxa4 could exert this effect by regulation of Cyp26b1 or Cyp26c1. Gain- and loss-of-function experiments investigating the ability of these and other Hox factors to modulate RA signalling by regulation of Cyp26 expression will be important to verify whether segmental regulation of RA signalling is a potential mechanism for border sharpening. Further to this, it may be interesting to investigate the consequences of combining co-expression of various *hox* genes with Egr2b-Myc overexpression on identity regulation in the hindbrain.

If segmental Hox factors regulate levels of RA within rhombomeres through regulation of Cyp26b1 and Cyp26c1, it might be expected than there is a stepwise, segmented gradient of RA throughout the hindbrain at these stages. However, at present, it is understood that a smooth gradient of RA is maintained during border sharpening. This comes from use of RA response elements (RAREs) driving LacZ and fluorescent reporters in mouse (Rossant *et al*, 1991; Sirbu *et al*, 2005) and zebrafish (Perz-Edwards *et al*, 2001; White *et al*, 2007), which show smooth graded reporter expression in the posterior hindbrain, though these reporters are not sufficiently sensitive to detect RA in rhombomeres anterior to the r6/r7 border. Genetically-encoded probes for RA (GEPRAs) have also been used to visualise smooth gradients of RA within more anterior regions of the hindbrain during border sharpening (Shimozono *et al*, 2013). More recently, phasor-FLIM has been

presented as an attractive method of measuring endogenous RA *in vivo* during hindbrain segmentation, using the unique autofluorescence lifetime of RA, in combination with phasor analysis to measure relative abundances (Stringari *et al*, 2011; Sosnik *et al*, 2016). This approach has also indicated the presence of a smooth RA gradient (Sosnik *et al*, 2016). Unfortunately, use of this approach has so far only been described prior to border sharpening and segmental expression of Cyp26b1 and Cyp26c1: at the onset of *egr2b* expression (80% epiboly) and several hours after border sharpening is complete, but only within rhombomeres 2, 4 and 6 (24 hpf). A significant drawback of this approach is that FLIM measurements are sensitive to fluorescence from additional transgenic markers – for example, mCherry fluorescence in the previously described Mü4127 transgenic line. For this reason, Phasor-FLIM has not yet been used to measure levels of RA within and between rhombomeres at the stages that border sharpening occurs (5 – 12 ss). It therefore remains possible that Cyp26b1 and Cyp26c1 cause the RA gradient to become more step-wise than smooth.

It is possible that Cyp26b1 and Cyp26c1 have subtle effects on RA within rhombomeres during border sharpening; smooth, graded transitions in RA levels may also arise between rhombomeres, which may not have been detected using GEPRAs to visualise RA, yet may still be capable of maintaining identity and contributing to border refinement. Hopefully, future developments in techniques to measure RA concentrations *in vivo* during segmentation, in combination with transgenic markers of rhombomeres, will be able to improve our understanding of segmental regulation of RA levels at the single-cell level. It is possible that new transgenic lines that label rhombomeres, such as the Tg[egr2b:H2B-Citrine] line described in Chapter 3, may be suitable for combining with Phasor-FLIM, as Phasor-FLIM has been used to distinguish between GFP and RA (amongst other fluorescent species) in *C. elegans* by virtue of their unique location in a 2D phasor plot (Stringari *et al*, 2011).

5.5.3 Conclusions

In conclusion, the observations made in this chapter are consistent with the hypothesis that community effects contribute to the regulation of cell identity in the hindbrain. Further work is needed to prove which Cyp26 enzymes are involved in community effects and identity switching during hindbrain patterning.

Chapter 6. Studying regulation of early EphA4 expression

6.1 Introduction

Whilst in previous chapters I have focused primarily on studying the role of identity regulation in hindbrain border sharpening, it is known that Eph/ephrin-mediated cell sorting makes a significant contribution to border sharpening. Cell identity refinement alone is clearly insufficient to completely sharpen borders, as loss of Eph/ephrin signalling disrupts border sharpening. Eph/ephrin signalling can contribute to establishment and maintenance of sharp rhombomere borders by mediating cell segregation (Xu *et al*, 1995, 1999; Cooke *et al*, 2005; Kemp *et al*, 2009). This function requires that Ephs and ephrins are expressed in complementary rhombomeres within the hindbrain and therefore a coupling between AP identity and Eph/ephrin expression status is important for border sharpening to occur correctly. However, it is still not fully understood how the expression of Ephs and ephrins is regulated in the hindbrain to achieve this. Expression of *ephA4* in r3 and r5 has been shown to be under direct transcriptional control of Egr2 in mouse (Theil *et al*, 1998). In zebrafish, Valentino upregulates *ephB4a* and represses *ephrinB2a* expression in r5 and r6 to contribute to border sharpening (Cooke *et al*, 2001; Hernandez *et al*, 2004). In mouse, Hoxa1 and Hoxb1 upregulate *EphA2* in r4, although it is not clear what contribution EphA2 makes to border sharpening (Chen & Ruley, 1998; Studer *et al*, 1998). Similarly, in mouse, Hoxa2 is required for EphA7 expression in r3, although it is not clear whether this involves direct transcriptional regulation (Taneja *et al*, 1996).

In this chapter, I describe a novel, Egr2-independent input to *ephA4* regulation, contributing to our understanding of segmental regulation of Eph/ephrin expression in r3 and r5. Subsequently, I investigate potential factors that may contribute to initiation of *ephA4* expression, independently of Egr2.

6.2 Some early *ephA4* induction is independent of Egr2

While looking at gene expression patterns in the early hindbrain, I studied how early *ephA4* expression relates to *egr2b* expression, as studies of the co-localisation of the transcripts for these genes in the early zebrafish hindbrain are limited. As shown in Figure 6-1 (A-F), during early segmentation, *egr2b* and *ephA4* transcripts are generally found in the same cells of prospective r3. As shown Figure 6-1 (D-F) there is a delay in induction of *ephA4* expression in r5 at 4 ss compared to *egr2b* induction. However, at 2 ss, there are cells detectable at the periphery of r3 that appear to contain *ephA4* transcripts, but not *egr2b* transcripts; these extend several cell diameters beyond the r3 expression of *egr2b* into r2, and occasionally into r4 (Figure 6-1 A-C; white arrowheads). At 4 ss, *ephA4* expression is also detected up to one cell diameter beyond the anterior edge of *egr2b* expression (Figure 6-1 D-F; white arrowheads). One possible explanation for these cells that contain *ephA4* but not *egr2b* transcripts is that *egr2b* may have previously been expressed and induced *ephA4* expression here. Subsequently, *egr2b* may be downregulated in these cells, while *ephA4* transcripts perdure. Alternatively, it is possible that *ephA4* is upregulated independently of Egr2.

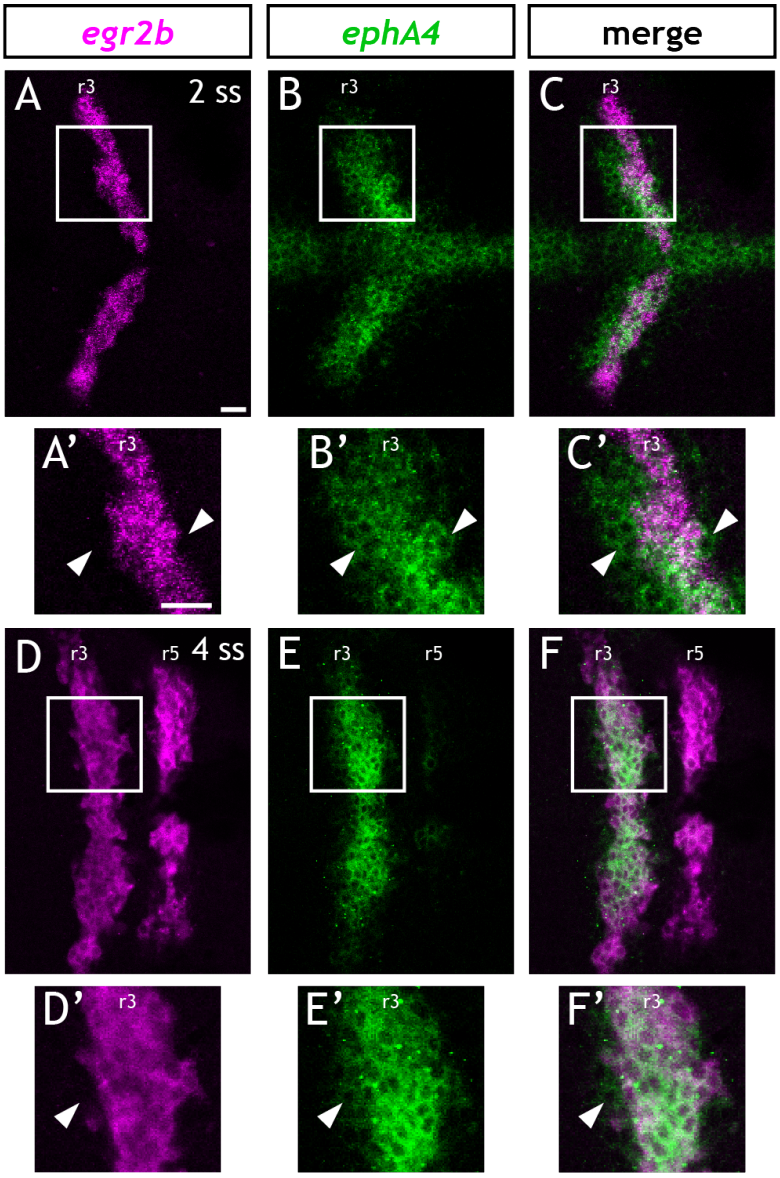

Figure 6-1 *egr2b* and *ephA4* expression analysis at early segmentation stages

egr2b and *ephA4* expression was analysed in 2 ss (A-C) and 4 ss (D-F) wildtype embryos. At 2 ss, the expression of *ephA4* extends several cell diameters beyond the expression of *egr2b* in r3 into r2 and occasionally into r4 (A-C; arrowheads; n = 5 embryos). *EphA4* expression is also observed in notochord at this stage. At 4 ss, the expression of *ephA4* still occasionally extends beyond egr2b expression into r2 (D-F; arrowheads; n = 5 embryos). Embryos are flat-mounted with anterior to the left. Scale bars: 20 µm.

In order to investigate the possibility of Egr2-independent inputs to *ephA4* induction, I knocked down Egr2a and Egr2b and studied expression of *ephA4* transcripts and EphA4 protein in these embryos. In these experiments I simultaneously knocked down Egr2a and Egr2b to ensure complete loss of Egr2 function, although, as previously discussed in 3.4, there does not appear to be functional redundancy between Egr2a and Egr2b at the level of *ephA4* expression or maintenance of *egr2b* expression. As shown in Figure 6-2, knock down of Egr2a and Egr2b does not significantly reduce *ephA4* expression at 3 ss (Figure 6-2 A,B), and *ephA4* transcripts are still detectable in r5 until 12 ss (Figure 6-2 D). By 18 ss, *ephA4* expression is completely lost in Egr2 morphants, but is still detectable in the otic vesicle, adjacent to r5 (Figure 6-2 F). Likewise, analysis by immunohistochemistry reveals that at 3 ss, EphA4 protein is still clearly present in r3 of Egr2 morphants (Figure 6-2 J), but EphA4 levels are greatly reduced in r3 and r5 of Egr2 morphants by 16 ss (Figure 6-2 L). A possible explanation for the residual *ephA4* expression in Egr2 morphants could be that knock down of Egr2a and Egr2b is incomplete, and that some functional Egr2a or Egr2b protein may be present and sufficient to maintain some *ephA4* expression. However, the observation that expression of *egr2b* and *ephA4* is completely lost by 18 ss in these morphants indicates that the morpholino knock down is efficient. This therefore demonstrates that some initiation of *ephA4* expression is independent of Egr2.

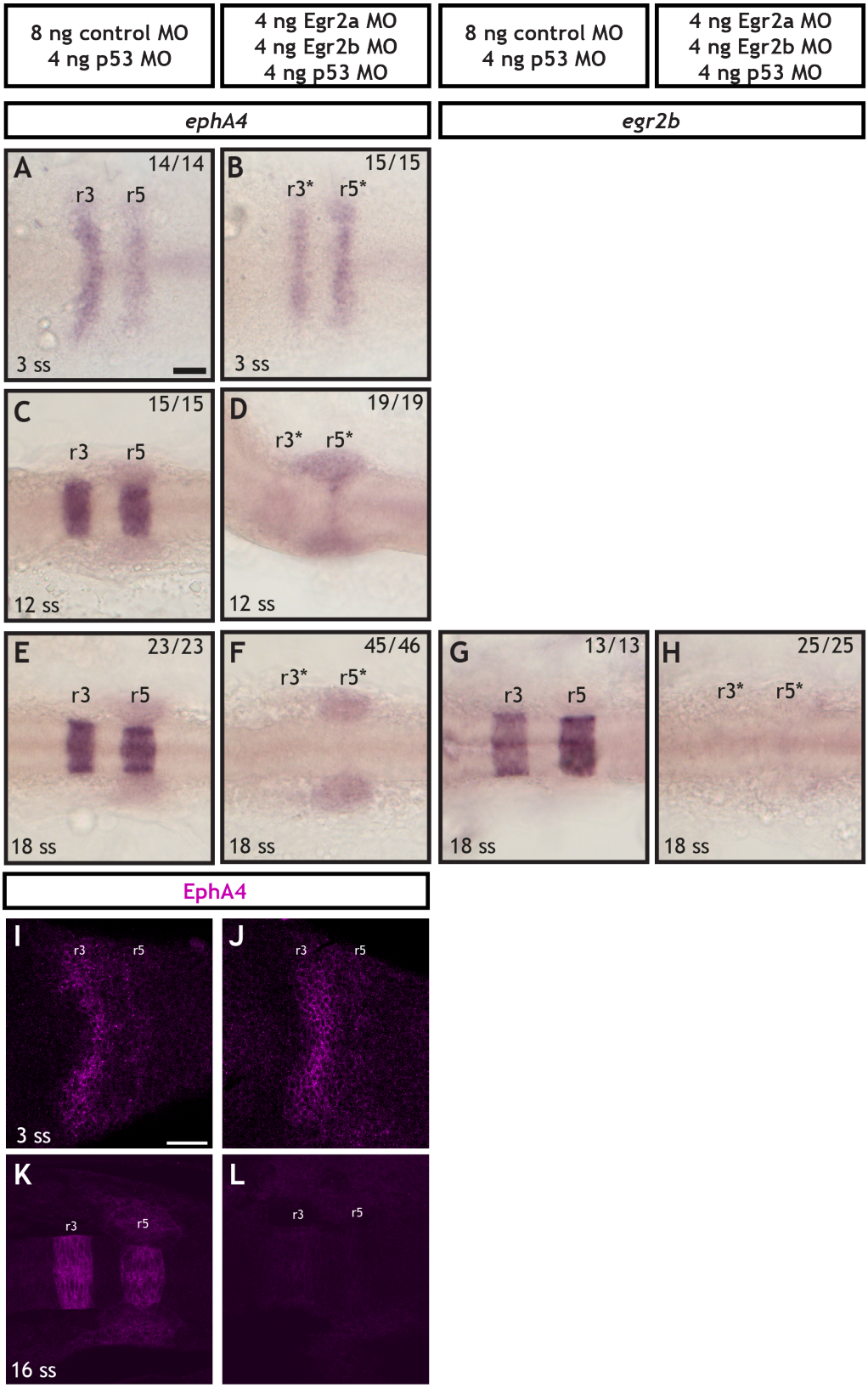
8 ng control MO
4 ng p53 MO
4 ng Egr2a MO
4 ng Egr2b MO
4 ng p53 MO
8 ng control MO
4 ng p53 MO
4 ng Egr2a MO
4 ng Egr2b MO
4 ng p53 MO
ephA4
egr2b
A
14/14
r3
r5
3 ss
B
15/15
r3*
r5*
3 ss
C
15/15
r3
r5
12 ss
D
19/19
r3*
r5*
12 ss
E
23/23
r3
r5
18 ss
F
45/46
r3*
r5*
18 ss
G
13/13
r3
r5
18 ss
H
25/25
r3*
r5*
18 ss
EphA4
I
r3
r5
3 ss
J
r3
r5
K
r3
r5
16 ss
L
r3
r5

Figure 6-2 *ephA4* expression analysis in Egr2 morphants

ephA4 expression in embryos injected with control morpholino (A,C,E) and Egr2 morpholinos (B,D,F). By 18 ss, *ephA4* expression is completely lost from r3 and r5 in Egr2 morphants (F) compared to control embryos (E). However, at 3 ss, *ephA4* expression is indistinguishable between control (A) and Egr2 morphant embryos (B). EphA4 protein can still be detected in Egr2 morphant embryos at 3 ss (J; n = 4 embryos), at comparable levels to control embryos (I; n = 3 embryos), but is completely lost from r3 and r5 by 16 ss (L; n = 8 embryos), in contrast to control embryos (K; n = 2 embryos). *egr2b* expression is completely lost from r3 and r5 by 18 ss in morphant embryos (H) in comparison to control embryos (G), confirming efficiency of Egr2 knock down. Embryos are flat-mounted with anterior to the left. Frequencies of embryos observed represented by the image shown, out of the total number of embryos studied are shown in the top right. Scale bars: 50 μm.

It is unclear what impact, if any, this Egr2-independent *ephA4* expression may have on border sharpening, and whether cells that express *ephA4*, but not *egr2b*, do ultimately contribute to r3 or r5. To investigate this further, I transplanted cells from donor embryos – in which either Egr2 or EphA4 were knocked down – into wildtype hosts and studied their localisation within the host embryos at 16 ss, using EphA4 protein localisation to identify r3 and r5. EphA4 morphant donor cells are largely excluded from r3 and r5 of wildtype hosts (Figure 6-3 A), which has been previously shown and is thought to result from differences in cell adhesion between EphA4 morphant cells and wildtype cells in r3 and r5 (Cooke *et al*, 2005). Egr2 morphant cells are similarly largely excluded from r3 and r5 (Figure 6-3 B). However, the later complete loss of EphA4 in Egr2 morphant embryos is likely to overcome any impact that early Egr2-independent *ephA4* expression may have on cell sorting – once morphant cells do lose EphA4 completely, they will become excluded from r3 and r5. It is therefore still not clear what impact, if any, the early difference between *ephA4* and *egr2b* expression may have on the final localisation of cells that induced *ephA4* expression independently of Egr2. In future experiments, it could be interesting to study the localisation of Egr2 morphant cells in wildtype hosts at earlier stages, before EphA4 is completely lost.

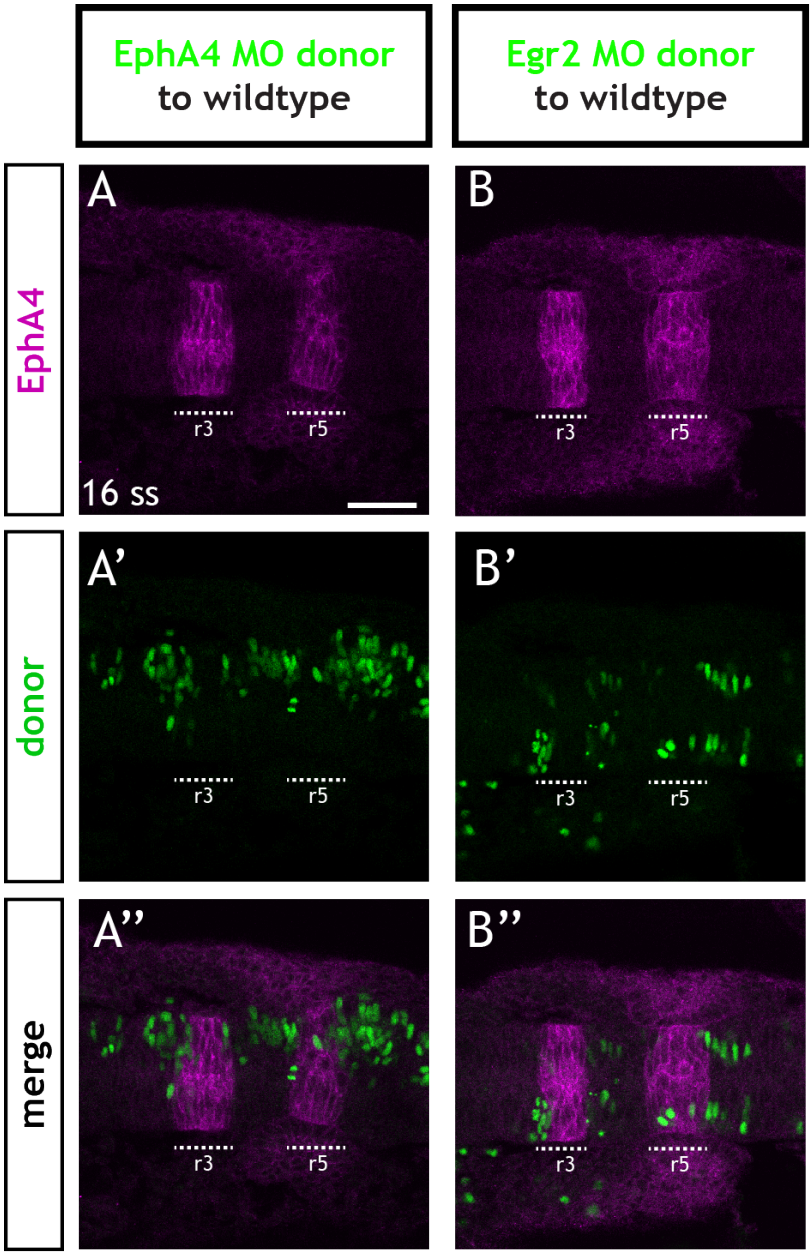

Figure 6-3 Distribution of EphA4 and Egr2 morphant cells within wildtype host embryos

Cells from EphA4 (A) and Egr2 (B) morphant embryos, injected with H2B-GFP RNA, were transplanted into wildtype host embryos at early gastrula stages. The majority of EphA4 morphant donor cells are sorted to the edges of r3 and r5 (as visualised by EphA4 immunohistochemistry) by 16 ss (A; n = 7 embryos). Egr2 morphant donor cells are sorted to the edges of r3 and r5 to a comparable extent (B; n = 9 embryos). Embryos are flat-mounted with anterior to the left. Frequencies of embryos observed represented by the image shown, out of the total number of embryos studied are shown in the top right. Scale bar: 50 μm.

6.3 Early *ephA4* induction is independent of Hoxb1a and Hoxb1b

It appears that induction of *egr2b* and *ephA4* expression occurs almost simultaneously in r3 (Figure 6-1 A-C), suggesting that *egr2b* and *ephA4* may be upregulated in parallel by common factors. Stochastic variation in gene induction, possibly in combination with different promoter binding affinities, could explain the observed spatial difference between *egr2b*- and *ephA4*-expressing cells. I have therefore investigated potential roles of factors that contribute to initiation of *egr2b* expression in the initiation of *ephA4* expression.

Possible candidates for upregulating *ephA4* in r3 (and r5) are Hoxb1a and Hoxb1b, which contribute to initiation of *egr2b* expression in r3 (Wassef *et al*, 2008; Labalette *et al*, 2015). In mouse, Hoxb1 and Hoxa1 are capable of regulating EphA2 expression (Chen & Ruley, 1998). It is therefore tempting to speculate that Hoxb1a and Hoxb1b may upregulate *egr2b* and *ephA4* in parallel, at least in r3. However, as shown in Figure 6-4, knock down of Hoxb1a and Hoxb1b, in combination with knock down of Egr2a and Egr2b, does not reduce early *ephA4* expression compared to knock down of Egr2a and Egr2b alone (Figure 6-4 A-C). This indicates that Hoxb1a and Hoxb1b do not regulate *ephA4* expression in r3 or r5 independently of Egr2.

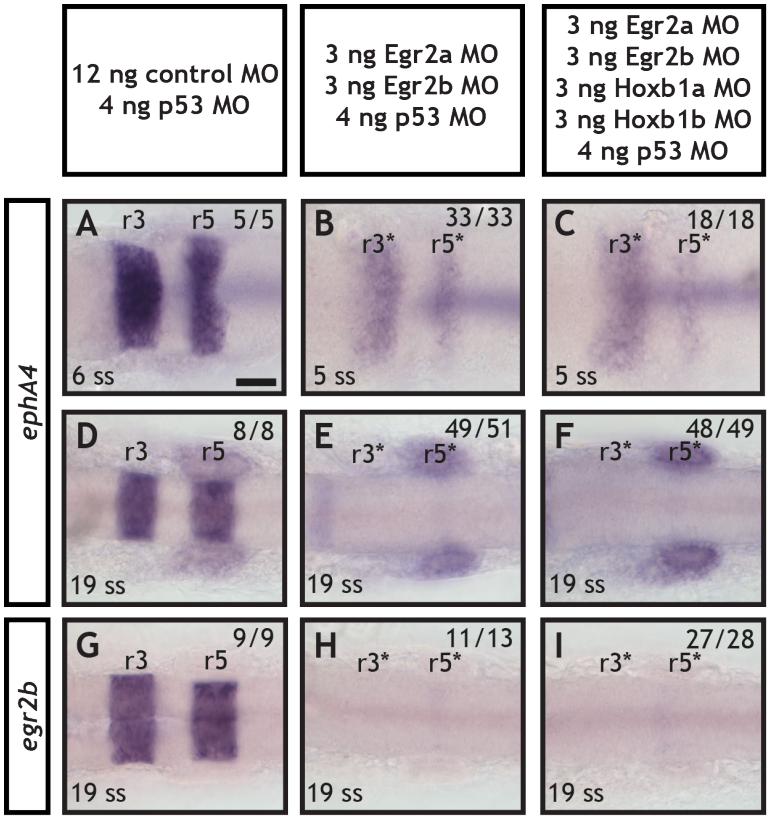

Figure 6-4 Expression of *ephA4* in Egr2 and Hoxb1 morphant embryos

Simultaneous knock down of Hoxb1a and Hoxb1b, in combination with knock down of Egr2 (C), does not further reduce *ephA4* expression compared to knock down of Egr2 alone (B). By 19 ss, simultaneous knock down of Hoxb1 and Egr2 still causes complete loss of *ephA4* (F) and *egr2b* (I) expression from r3 and r5, as for knock down of Egr2 alone (E,H), in contrast to control embryos (D,G). Embryos are flat-mounted with anterior to the left. Frequencies of embryos observed represented by the image shown, out of the total number of embryos studied are shown in the top right. Scale bar: 50 μm.

6.4 Investigating Hoxa2 and Hoxb2 as potential candidates for regulating early *ephA4* expression

Alternative candidates for regulating early *ephA4* expression independently of Egr2 are members of Hox paralogue group 2 (PG2): Hoxa2 and Hoxb2. At 90% epiboly, *hoxa2* is expressed in r2 and r3, while *hoxb2* is expressed in r3 and r5 (Prince *et al*, 1998). Since initiation of *ephA4* expression occurs in both r3 and r5 in the absence of Egr2 activity (Figure 6-2), Hoxa2 may upregulate *ephA4* in r3, while Hoxb2 may upregulate *ephA4* expression in r3 and r5. In mouse, Hoxa2 is necessary for the expression of *EphA7* (MDK1) (Taneja *et al*, 1996), in addition to positively regulating *EphA4* and *EphA7* expression in r3-derived PrV (Oury *et al*, 2006). In Hoxa2 mutant mice, *EphA4* is still expressed, but the AP extent of its expression in r3 is reduced, although it is unclear whether this is an indirect consequence of reduction in size of the r2-r5 region, rather than due to direct transcriptional regulation (Barrow *et al*, 2000).

6.4.1 *hoxa2* and *hoxb2* expression is reduced but maintained upon knock down of Egr2a and Egr2b

Egr2 is known to upregulate *hoxb2* in r3 and r5 and *hoxa2* in r3 (Sham *et al*, 1993; Vesque *et al*, 1996; Nonchev *et al*, 1996a, 1996b). Therefore, in order for Hoxa2 and/or Hoxb2 to regulate *ephA4* expression independently of Egr2, they themselves must also be expressed independently of Egr2. I studied the expression of *hoxa2* and *hoxb2* in Egr2 morphants at early stages, when Egr2-independent *ephA4* expression occurs. As shown in Figure 6-5, both *hoxa2* and *hoxb2* continue to be expressed at 5 ss and 4 ss, respectively, in the absence of Egr2a and Egr2b activity, albeit at slightly reduced levels. This is consistent with the possibility that Hoxa2 and Hoxb2 contribute to Egr2-independent *ephA4* expression.

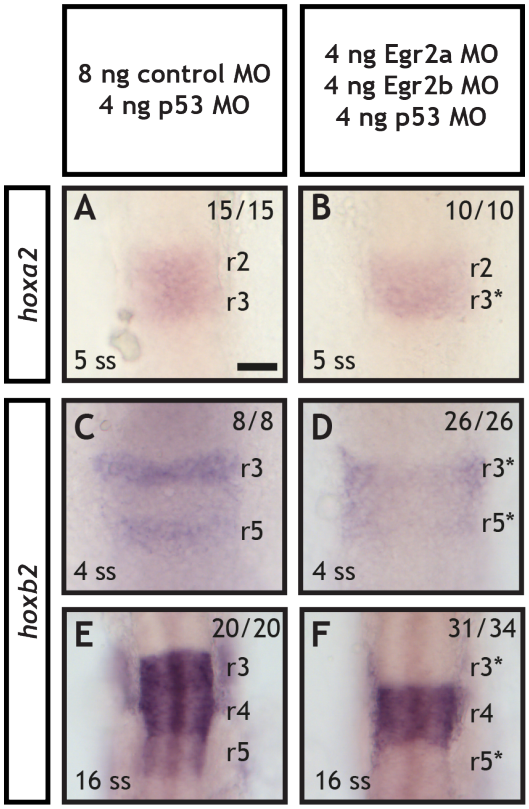

Figure 6-5 Expression analysis of *hoxa2* and *hoxb2* in Egr2 morphants

Knock down of Egr2 does not reduce *hoxa2* expression in r3 compared to control embryos at 5 ss (A,B). Similarly, knock down of Egr2 causes reduction, but not complete loss, of *hoxb2* expression in r3 and r5, compared to control embryos (C,D). However, by later stages, knock down of Egr2 causes complete loss of *hoxb2* expression from r3 and r5. Embryos are flat-mounted with anterior to the top. Frequencies of embryos observed represented by the image shown, out of the total number of embryos studied are shown in the top right. Scale bar: 50 μm.

6.4.2 Hoxa2 and Hoxb2 knock down reduces early *ephA4* expression

Morpholinos that knock down Hoxa2 and Hoxb2 have previously been described and have revealed that Hoxa2 and Hoxb2 function redundantly in zebrafish to pattern the second pharyngeal arch (Hunter & Prince, 2002). Knock down of either Hoxa2 or Hoxb2 alone does not have an observable phenotype, presumably due to functional redundancy between these factors. Simultaneous knock down of Hoxa2 and Hoxb2 causes a transformation of cartilage in the second pharyngeal arch to a mirror-image copy of cartilage of the first arch (Hunter & Prince, 2002). In addition, knock down of Hoxa2 and Hoxb2 reduces expression levels of *goosecoid* (*gsc*) in

the second pharyngeal arch (Hunter & Prince, 2002). In order to confirm efficiency of the two published morpholinos in my hands, I studied *gsc* expression at 30 hpf compared to control embryos and stained cartilage at 4.5 dpf using Alcian blue dye to observe any cartilage transformations as previously reported. As shown in Figure 6-6 (G-I), a full transformation of cartilage derived from the second arch was observed in 67% of embryos injected with 8 ng Hoxa2 and 8 ng Hoxb2 MO (I), while the remaining embryos studied appeared indistinguishable from control embryos. Expression of *gsc* was reduced in 100% of embryos injected with 8 ng Hoxa2 and Hoxb2 MO (Figure 6-6 F). The frequency of these phenotypes is comparable to those previously reported, where 84% of injected embryos had the severe cartilage phenotype, (Hunter & Prince, 2002). It is known that different batches of morpholinos can have different efficacies, which may explain the varied frequencies of phenotypes observed.

To address potential inputs from Hoxa2 and Hoxb2 to early *ephA4* expression, I studied expression of *ephA4* in embryos in which Hoxa2 and Hoxb2 are simultaneously knocked down. As shown in Figure 6-6 (B) knock down of Hoxa2 and Hoxb2 causes significant reduction of *ephA4* expression in r5, but only a slight reduction to *ephA4* expression in r3 at 4 ss compared to control embryos. This indicates that Hoxb2 (in r5 and possibly also r3) and possibly also Hoxa2 (in r3) contribute to initiation of *ephA4* expression. It is likely that remaining *ephA4* expression in these morphants is due to additional inputs from Egr2. However, my attempts to simultaneously knock down Egr2a, Egr2b, Hoxa2 and Hoxb2 in various combinations caused significant death and deformity (> 90%) of injected embryos, even with p53 MO present to reduce off-target effects.

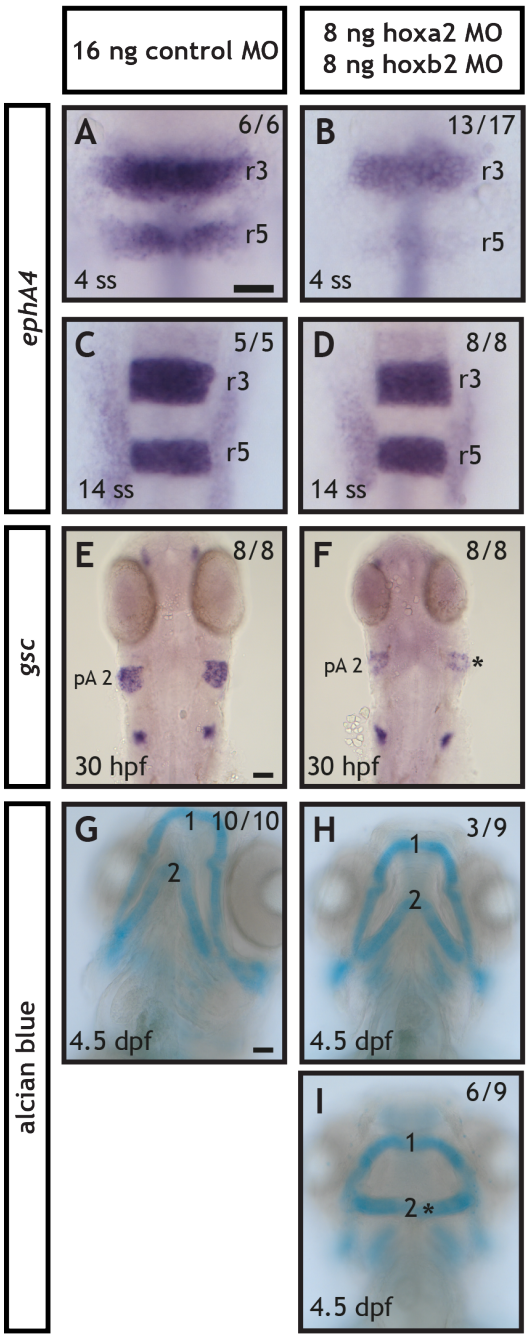

Figure 6-6 Expression of *ephA4* in Hoxa2;Hoxb2 double morphants

Embryos were injected with either 8 ng Hoxa2 morpholino and 8 ng Hoxb2 morpholino or 16 ng control morpholino. In the majority of Hoxa2;Hoxb2 double morphants, Alcian blue cartilage staining indicates a transformation of the cartilage derived from the second pharyngeal arch into a mirror-image of the first arch occurs (I; asterisk). The remaining morphant embryos had cartilage structures comparable to control embryos (G,H). Simultaneous knock down of Hoxa2 and Hoxb2 causes reduced expression of *gsc* in the second pharyngeal arch (pA2) in all embryos studied (F) compared to control embryos (E). At 4 ss, *ephA4* expression is almost

completely lost in r5 and reduced in r3 of Hoxa2;Hoxb2 double morphants (B) compared to control embryos (A). However, by 14 ss, *ephA4* is expressed at comparable levels in both r3 and r5 between Hoxa2;Hoxb2 double morphants (D) and control embryos (C).
Embryos are flat-mounted, with dorsal to the top. Frequencies of embryos observed represented by the image shown, out of the total number of embryos studied are shown in the top right. Scale bar: 50 μm.

6.5 Discussion

For Eph/ephrin signalling to mediate rhombomere border sharpening, it is necessary that Ephs and ephrins are expressed in complementary domains. Currently, there is limited understanding of how expression of Ephs and ephrins are segmentally regulated in the hindbrain, and the only clear case of a direct connection between AP identity and cell segregation in the hindbrain is the regulation of *ephA4* expression (in addition to regulation of *hox* genes *hoxa2* and *hoxb2*) by Egr2 in r3 and r5. It is known that Egr2 directly regulates expression of *ephA4* in r3 and r5; in mouse, ectopic expression of Egr2 induces *EphA4* expression, while mutation of Egr2-binding sites causes loss of expression of a reporter driven by an enhancer element of *EphA4* (Theil *et al*, 1998). However, this does not indicate whether Egr2 alone contributes to induction of *ephA4* expression. In mouse, it has previously been noted that, while *EphA4* up-regulation in r3 and r5 correlates with *Egr2* expression, at very early stages, *EphA4* is expressed in a broader domain, between the prospective r2/3 and r5 boundaries (Irving *et al*, 1996). *EphA4* expression is subsequently upregulated in r3 and r5 in wildtype, but not Egr2 mutant mice (Seitanidou *et al*, 1997). This indicates that Egr2 is required for upregulation of *EphA4* in r3 and r5. However, it was also reported that some low levels of *EphA4* expression in the r2 to r6 region persist in the absence of *Egr2*, suggesting that additional factors may also contribute to *EphA4* expression here (Seitanidou *et al*, 1997).

Through expression analysis and Egr2 loss-of-function experiments, I have shown that, similar to the situation in mouse, *ephA4* is expressed in a broader domain than *egr2b*, and that some induction of ephA4 expression in r3 and r5 is independent of Egr2. This Egr2-independent *ephA4* expression is restricted to early

segmentation stages – from approximately 1 ss to 5 ss – and by later stages, as previously reported, maintenance of *ephA4* expression in r3 and r5 is completely dependent on Egr2. Upregulation of *ephA4* and *egr2b* in parallel could help improve the robustness of very early border sharpening, through achieving segmental expression of *ephA4* earlier than if *ephA4* was only expressed downstream of Egr2. Subsequently, Egr2 is known to be necessary for maintenance of both its own expression and the expression of *ephA4*; therefore, at later stages the transcripts for these factors are co-localised and cells that do not express *egr2b* will be unable to maintain *ephA4* expression. As previously discussed, at early stages of hindbrain segmentation, there is noise in *egr2b* expression, which may cause corresponding downstream noise in *ephA4* expression with consequences for cell sorting. However, additional inputs to *ephA4* upregulation could help achieve more homogeneous *ephA4* expression – depending on how homogeneously these factors are expressed – therefore improving early border sharpening. However, from the data presented here, it remains unclear what impact early Egr2-independent *ephA4* expression has on cell sorting in early hindbrain segmentation. Once specific factors that drive early *ephA4* expression are identified, it will be informative to see if their loss compromises early sharpening of *egr2b* expression.

I have investigated possible contributions from Hox PG1 and PG2 factors in early induction of *ephA4*. I have demonstrated that Hox PG1 factors do not contribute to *ephA4* expression independently of Egr2, while it appears that Hoxa2 and Hoxb2 may contribute to induction of *ephA4* expression in r3 and r5. It will be interesting to study whether early *ephA4* expression is maintained in the absence of both Egr2 and Hox PG2 activity. While it does not appear that this can be achieved using combined morpholino knock down of these factors, alternative approaches, such as CRISPR/Cas9-mediated knock-out may be suitable.

Because Hox factors – in combination with their Pbx co-factors – bind to conserved Pbx-Hox binding site motifs within enhancer elements to regulate expression of their target genes (Parker *et al*, 2011), it may be insightful to study whether these sequences are present in the *cis*-regulatory regions of *ephA4* and if they can drive expression in the observed *ephA4* expression domain in the hindbrain and what

impact their loss has on *ephA4* expression. Gain-of-function experiments may then be used to determine whether Hoxa2 and/or Hoxb2 are sufficient to drive *ephA4* expression. Interestingly, mosaic expression experiments have shown that Hox factors regulate cell segregation in the hindbrain, although the relevant target genes that mediate this are unknown (Prin *et al*, 2014). Alternative factors that may contribute to induction of *ephA4* expression – at least in r3 – are Irx7 and Irx1b, which contribute to induction of *egr2b*, *hoxb1a* and *hoxa2* expression in r3 (Stedman *et al*, 2009). Morpholinos that effectively knock down Irx7 and Irx1b have already been described (Stedman *et al*, 2009).

In conclusion, I have demonstrated that Egr2-independent upregulation of *ephA4* – possibly mediated via Hox PG2 factors – contributes to early *ephA4* expression in r3 and r5, possibly in parallel with *egr2b* induction. This may improve the efficiency of early EphA4-mediated border sharpening.

Chapter 7. Discussion

During this project, I aimed to improve our understanding of how sharp borders form at rhombomere interfaces during hindbrain segmentation. Two separate but related avenues of my research aimed to assess the contribution of cell identity regulation to border sharpening, and to reveal the mechanistic basis for this identity regulation. I have obtained evidence that cell identity switching contributes to hindbrain border sharpening, which I will now discuss and present a model for how cell identity regulation may contribute to hindbrain border sharpening.

7.1 The contribution of identity switching to hindbrain border sharpening

The establishment of sharp borders between rhombomeres is important for subsequent rhombomere-derived patterning events to occur correctly. However, the processes that cause the necessary sharpening of rhombomere interfaces are not clear. A role for Eph/ephrin-mediated cell sorting in rhombomere border sharpening has been established previously, but the extent to which regulation of cell identity may also contribute is unclear. In this thesis, I have presented evidence that cell identity regulation contributes to sharpening the borders of *egr2b* expression. It should be noted that due to the small sample sizes acquired so far, I have not used statistical methods to analyse the data presented here. With larger sample sizes in future it will be possible to apply statistical analysis to determine the significance of results obtained and for quantitative conclusions to be drawn from the data.

The cell identity regulation that contributes to border sharpening may include both resolution of overlapping identity at segment borders and a complete switching of identity, which is likely to apply to misplaced cells within rhombomeres, rather than at segment borders. As I will discuss, it is currently not clear whether the contribution of cell identity regulation to border sharpening that I detect arises from identity resolution or identity switching, or both.

7.1.1 Resolution of overlapping identity at segment borders

At very early stages, cells at borders can be mis-specified and have an overlapping identity due to noise and stochasticity in RA signalling along the AP axis. These cells can resolve this overlapping identity through autoregulatory and cross-inhibitory interactions between conflicting transcription factors. This is thought to contribute to border sharpening, by some cells being able to select the appropriate identity for their AP position (Zhang *et al*, 2012). Prior to resolution of overlapping identity at segment borders, it is reasonable to assume that cells will also co-express conflicting Ephs and ephrins. It is not clear whether cells with overlapping Eph/ephrin expression will be capable of sorting until this dual identity has been resolved. As discussed in Chapter 5, when the extent of mis-specification along the AP axis is increased by reduction of Cyp26a1, Cyp26b1 and Cyp26c1 activity, I observe that some *egr2b*-expressing cells fail to completely segregate to borders; this failure to sort could be due to overlapping expression of Ephs and ephrins.

In contrast to other reporter lines used to monitor border sharpening, the new Tg[egr2b:H2B-Citrine] reporter line that I have created is expressed in r3 and r5 at the earliest possible stage, and is induced in parallel with *egr2b*. This has the advantage that in principle it may be possible to detect changes to cell identity that occur early, prior to cell segregation. However, I have not yet observed a contribution of identity resolution to border sharpening in Tg[egr2b:H2B-Citrine]; this is most likely due to identity resolution occurring prior to accumulation of sufficient reporter for detection.

In conclusion, it appears likely that resolution of overlapping identity contributes to border sharpening in zebrafish, but so far there is no direct evidence of this from the current reporter lines available. It is anticipated that future modifications to the existing Tg[egr2b:H2B-Citrine] reporter will improve its sensitivity to low levels of *egr2b* expression so that even cells that briefly express *egr2b* (co-expressed with *hoxb1a*) can be detected. In addition, combination with an additional, equally sensitive reporter of *hoxb1a* should indicate which cells initially co-express *egr2b* and *hoxb1a*.

7.1.2 Refinement of ectopic cells at segment borders

Resolution of overlapping identity alone is not sufficient to fully sharpen borders, and some dual-expressing cells will adopt the incorrect identity for their AP position, due to noise and stochasticity in RA signalling and downstream gene expression, while cell movements and divisions can also cause cells with a resolved identity to become misplaced. Ectopic cells that have adopted a particular identity may be refined through a combination of identity switching and cell segregation. It is clear from my results and those of others (Calzolari *et al*, 2014) that Eph/ephrin-mediated cell sorting does contribute to border sharpening. However, it is not clear whether regulation of identity also contributes to border sharpening at these later stages. The relative significance of these two sharpening mechanisms may depend on how much mixing occurs and how quickly cells are able to be sorted as opposed to switch their identity.

The fact that some ectopic H2B-Citrine-expressing cells are observed to sort, even in heterozygous Tg[egr2b:H2B-Citrine] embryos, indicates that these cells express fairly high levels of *egr2b* and have activated autoregulation of *egr2b* expression, suggesting that they do not have a dual identity; accordingly, these cells are not likely to express conflicting Ephs and ephrins. In addition, some of these ectopic cells are first observed outside r3 and r5, and not just at rhombomere borders, suggesting that they have arisen due to cell intermingling at earlier stages, rather than mis-specification at borders. I have shown in Chapter 4 that perturbation of Eph/ephrin signalling increases the amount of identity switching that can be detected in Tg[egr2b:H2B-Citrine], indicating that cell sorting does contribute to border sharpening.

Ectopic *egr2b*-expressing cells may also be refined by identity switching, but in Tg[egr2b:H2B-Citrine] embryos, reporter expression may not be detected in these cells if they become intermingled prior to accumulation of sufficient reporter for detection. This is supported by the observation that I can detect more ectopic cells containing H2B-Citrine outside r3 and r5 in homozygous Tg[egr2b:H2B-Citrine] embryos than in heterozygous embryos. Consistent with a need for identity switching of ectopic cells, I have found that knocking down Hoxb1 increases the

number of *egr2b*-expressing cells in r4. It is likely that these cells persist in r4 due to compromised switching, and an inability to downregulate *egr2b* expression, although these cells could also arise from a failure of co-expressing cells at the borders to downregulate *egr2b* and subsequently become intermingled with r4. As I will discuss shortly, the ability of cells to switch their identity depends on their AP position and the identity of their neighbours; mechanisms by which cells switch identity appear to be more effective when ectopic cells are completely surrounded by cells of an opposing identity at an incorrect AP position. These cells may also take longer to become correctly sorted, given the greater distance they have to travel, so could switch identity first.

In conclusion, the extent to which identity switching – as opposed to cell sorting – refines ectopic cells is still unclear, due to the possibility for some cells that have expressed *egr2b* to be undetected in the Tg[egr2b:H2B-Citrine] line.

7.2 Community effects and identity regulation

I have also attempted to improve our understanding of what mechanisms are involved in this regulation of identity. As I have already discussed, non cell-autonomous regulation of cell identity, via community effects, is an attractive mechanism by which ectopic cells may switch identity to sharpen rhombomere borders.

An important question is whether changes to cell identity are mediated via global signals that vary in strength along the AP axis, or via local interactions between cells. I have shown in cell transplantation experiments that isolated cells are capable of maintaining expression of *egr2b* at the correct AP position of r3, even when completely surrounded by cells that express *hoxb1a*. This indicates that when cells are at the correct AP position, they can maintain their identity via autoregulation, despite potential community effect signals from the surrounding cells. However, cells at the r2/4 border may receive local, graded signals from each adjacent territory, with the net effect of maintaining an r3 identity. In contrast, it has been found that when single cells from r5 are transplanted into r4, they

downregulate *egr2b* expression (Kemp *et al*, 2009). This implies that autoregulation of *egr2b* expression is insufficient to maintain identity of individual cells when cells are not at the correct AP position for their identity. This could be via global or local signals, and is in agreement with my observation that cells are capable of downregulating *egr2b* expression in Tg[egr2b:H2B-Citrine] when intermingling is increased by perturbation of Eph/ephrin signalling, causing cells to change their AP position.

However, I also observed that isolated *egr2b*-expressing EphA4 morphant cells are not capable of repressing *hoxb1a* expression if surrounded by *hoxb1a*-expressing cells. This supports my hypothesis that local, non cell-autonomous inductive signalling can also influence cell identity, but apparently not to a sufficient extent to repress expression of genes regulated by global signals and autoregulation. However, because of mutual inhibition and autoactivation between *egr2b* and *hoxb1a*, it is expected that this co-expressing state is not stable and will ultimately be resolved. It will be interesting to see whether at later stages, these cells are still capable of co-expressing both *egr2b* and *hoxb1a*, or whether one or other of these genes is downregulated.

I have also shown that wildtype cells, which form large clusters in r3* of Egr2 morphant hosts, are able to both maintain *egr2b* expression and prevent any non cell-autonomous induction of *hoxb1a*. This indicates that in sufficiently large groups of cells, mutually-inductive community effects are able to overcome the opposing non cell-autonomous inductive signals from neighbouring cells, which is in agreement with other cases of cell transplantation where large groups of cells can maintain an ectopic identity, even at the incorrect AP position for that identity, although some cells at the edges of the group do change identity (Schilling *et al*, 2001).

In summary, as illustrated in Figure 7-1, during border sharpening in normal development, both local community effects and global levels of signals may contribute to regulation of cell identity. Weaker local community effects (illustrated as pale dotted arrows) depend on the number of cells with a specific identity; for isolated ectopic cells in the middle of a segment (Figure 7-1 C), all neighbours have

a distinct identity, and community effects are sufficient to cause the isolated ectopic cell to switch identity. In contrast, for cells at a jagged border, where cells of opposing identities are intermingled but not completely isolated, it is less clear whether community effects will be able to contribute to identity switching. Misplaced cells are not completely surrounded by cells of a different identity and so experience a balance of different community effect signals here. It is therefore perhaps more likely that these cells are sharpened by Eph/ephrin-mediated sorting (Figure 7-1 B). Global AP signals also influence the ability of cells to switch identity, and are dominant over community effects. This is evident from the ability of isolated cells juxtaposed between r2 and r4 to maintain an r3 identity. A caveat of this is that a balance of opposing r2 and r4 community effects could also induce an r3 identity. The community effect is weaker than global signals that specify identity, but when there is a large enough group of ectopic cells, they can overcome global AP signals (Schilling *et al*, 2001)

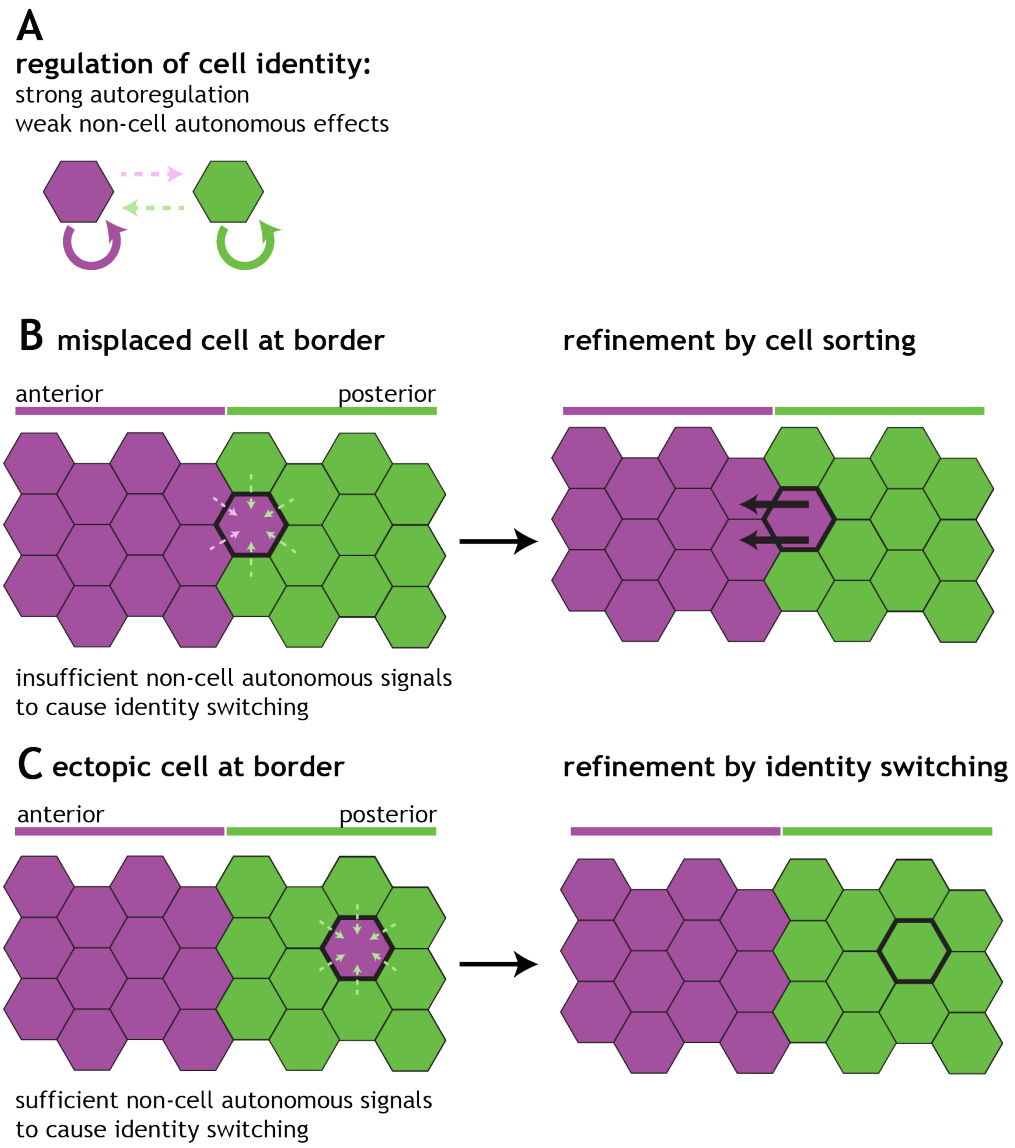

Figure 7-1 Proposed model for regulation of identity in the hindbrain through a combination of strong autoregulatory signals and weaker non cell-autonomous signals

A: The identity of cells is regulated by strong autoregulatory interactions (dark arrows), and weaker non cell-autonomous interactions (pale dotted arrows).

B: Misplaced cells at segment borders experience weak non cell-autonomous induction from fewer neighbouring cells of the opposing identity, in addition to non cell-autonomous inductive signals from neighbouring cells of its own identity. The strong autoregulatory regulation of this cell's identity, in combination with its AP position being close to that suitable for its identity, overcomes the non cell-autonomous effects from the neighbouring cells. These cells are refined by cell sorting rather than identity switching.

C: Completely ectopic cells experience a large number of weak non cell-autonomous inductive signals, due to being completely surrounded by cells of an opposing identity. No non-cell autonomous signals from cells of the same identity are received. The AP position of the cell is also not appropriate for its identity, and thus autoregulation is overcome and the cell switches its identity.

These interactions could explain why ectopic cells at the incorrect AP position during normal development change their identity. I have also investigated the mechanisms of how these cells may change their identity. Figure 7-2 shows a proposed model for how local regulation of RA signalling may contribute to identity regulation and refinement. This is consistent with a combination of local and global signals contributing to regulation of cell identity.

In this model, an initial gradient of RA is established and refined by feedback and feedforward mechanisms through Cyp26a1 and Fgf signalling, as proposed previously (White *et al*, 2007; Schilling *et al*, 2012). This gradient induces expression of different transcription factors along the AP axis that specify rhombomeric identity. These segmentally-expressed transcription factors can in turn regulate the level of RA signalling within rhombomeres, via regulation of the RA-degrading enzymes Cyp26b1 and Cyp26c1. These enzymes modify the pre-existing RA gradient, and regulate levels of RA within segments such that segmental identity is maintained. This model can also explain why groups of ectopic cells are able to maintain their identity, by an ability to sufficiently modify local levels of RA; in contrast, isolated cells do not significantly affect local RA levels, so the community effects from the surrounding cells dominate. Due to limitations in measuring RA within rhombomeres, it is not clear exactly what levels of RA signalling will be maintained within each rhombomere, but it is likely that neighbouring rhombomeres are thus able to maintain distinct levels of RA signalling from each other.

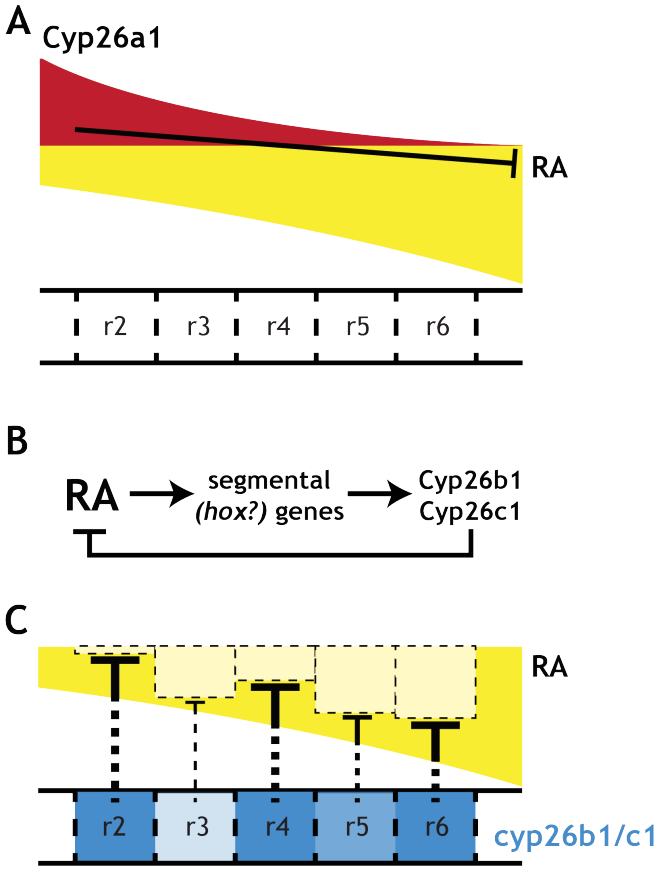

Figure 7-2 Model illustrating how segmental regulation of Cyp26 expression can regulate RA signalling within rhombomeres

A: An initial gradient of RA (yellow) is established across the AP axis of the hindbrain (rhombomeres 2-6 are shown only). This gradient is shaped through degradation mediated by an opposing gradient of Cyp26a1 (red), which is regulated by a combination of RA and Fgf signalling. At different positions along the AP axis, RA induces the expression of different segmentally-restricted genes

B: The segmentally expressed genes regulate segmental expression of Cyp26b1 and Cyp26c1, which, in turn, maintain an appropriate concentration of RA to reinforce segmental identity.

C: Segmentally-restricted Cyp26b1 and Cyp26c1 activity can influence the shape of the RA gradient through localised degradation. This may cause the RA gradient to become step-wise along the AP axis, as shown.

As previously discussed, consistent with this model, I have demonstrated that Egr2b can repress expression of Cyp26b1 and Cyp26c1 in r3 and r5. However, it is unclear whether segmental regulation of Cyp26b and Cyp26c1 contributes to regulation of identity in other rhombomeres. I have found that loss of Cyp26b1 and

Cyp26c1 has an impact on border sharpness, although it is likely that redundancy with alternative sharpening mechanisms, including Eph/ephrin signalling limits the extent to which sharpness is reduced here.

The proposed model implies that the interpretation of RA levels by cells is not based on a single assessment of RA levels at the time of their induction, but rather that cells are continuously monitoring and responding to changing levels of RA over time during patterning, which will improve robustness of patterning through spatial and temporal averaging, which has been previously described in alternative morphogen-induced patterning (Dessaud *et al*, 2010). Given how noisy the levels of RA are during the induction of segmentally-expressed genes (Sosnik *et al*, 2016), this additional temporal component is likely to improve the robustness and efficiency of hindbrain patterning. This concept of interpretation of RA levels over time is shared with several other models for RA-induced hindbrain patterning (Maves & Kimmel, 2005; Sirbu *et al*, 2005; Hernandez *et al*, 2007). However, the model that I propose here is different from these in that I also suggest that cells themselves are capable of modifying RA signalling, downstream of segmental identity, thereby helping to maintain the correct identity and contribute to sharpening of any mis-specified cells. I have suggested that this localised regulation of RA signalling is a form of community effect, similar to those involved in induction of progenitor cells via mutually-inductive signals (Bolouri & Davidson, 2010; Saka *et al*, 2011). However, there are two important differences in the model that I propose to canonical community effects. Firstly, this model involves localised destruction (or lack thereof) of the signalling factor within the community that regulates identity, as opposed to localised production of the signalling factor, as in canonical community effects. Secondly, my model concerns the maintenance of identity within communities of cells, rather than induction of identity. However, like canonical community effects, this model can explain how sufficient numbers of cells are capable of maintaining their identity downstream of inductive factors, in contrast to isolated cells.

I have described how the expression of the H2B-Citrine reporter in the Tg[egr2b:H2B-Citrine] line is more heterogeneous than expected, based on *egr2b* expression patterns. However, I have suggested that levels of H2B-Citrine

expression are still proportional to those of *egr2b*. It is not surprising that early *egr2b* expression is highly varied and heterogeneous based on high levels of noise in RA at the time of *egr2b* induction (Sosnik *et al*, 2016). The model for identity regulation that I propose, like canonical community effects, could explain how homogeneous gene expression within rhombomeres can be established through non cell-autonomous induction. However, as I and others have demonstrated, Egr2b can induce its own expression non cell-autonomously, which may occur though additional mechanisms to regulation of RA signalling, such as the production of an unknown signalling factor. These other non cell-autonomous mechanisms are perhaps more likely to contribute to the early non cell-autonomous induction of *egr2b* than modulation of RA.

It is possible that RA signalling is subject to segmental regulation by additional mechanisms than degradation by Cyp26 factors. Regulation of RA signalling can also involve cellular RA binding proteins. Crabp2a has been shown to modulate noise in RA at early patterning stages, and also regulates variation in *egr2b* expression and contributes to border sharpening (Sosnik *et al*, 2016). Crabp2a has also been shown to contribute to robustness of hindbrain patterning at later stages in zebrafish (Cai *et al*, 2012), but not in mouse (Lampron *et al*, 1995) where there could be redundancy with other binding proteins (Romand *et al*, 2000). *Crabp2a* is initially expressed in the posterior hindbrain up to r4, and is then further refined and expressed at higher levels in r4 and r6. Factors that regulate expression of *crabp2a* in the hindbrain are unclear, although it is known that *crabp2a* is inducible by RA. One of the known functions of Crabp2a is to transport RA to Cyp26 enzymes; segmental regulation of Crabp2a expression may therefore provide an additional level of regulation of RA signalling. It is likely that the level of RA signalling perceived by cells within a particular rhombomere depends on a combination of the cells' AP position within the RA gradient created via Cyp26a1, additional regulation by segmentally expressed Cyp26b1 and Cyp26c1, as well as the expression of Crabp2a, which may affect the extent to which any Cyp26 enzymes are capable of degrading RA. Binding of RA by Crabp2a will also reduce the distance over which RA may diffuse (White *et al*, 2007). This could have an impact on the strength of the non cell-autonomous effect of RA, such that territories where Crabp2a is expressed have weaker non cell-autonomous effects on adjacent areas.

An alternative mechanism of regulation of RA signalling that I have not addressed here is the regulation of RA synthesis across the hindbrain. *Raldh2* is under transcriptional control by Hox factors, for example, Hoxa1;Pbx1 mutant mice exhibit reduced mesodermal *Raldh2* expression (Vitobello *et al*, 2011). Localised regulation of RA production by Hox factors may therefore also contribute to shaping the RA gradient.

In conclusion, I have proposed a model by which segmental regulation of RA signalling can mediate identity switching and contributes to maintenance of rhombomeric identity. I have provided evidence that Cyp26 enzymes can regulate identity and may underlie community effects, but further work is needed to determine which Cyp26s contribute to border sharpening. The regulation of RA signalling throughout the hindbrain is complex and subject to multiple inputs, including feedforward and feedback regulation. There is also likely to be redundancy between factors that regulate RA signalling. It is therefore challenging to determine exactly which factors are important in the apparent RA-mediated switching of identity that I propose. This is impeded further by the technical limitations in quantifying levels of RA across the hindbrain, although new approaches, such as Phasor-FLIM, appear promising.

7.3 Contributions of Eph/ephrin signalling to identity regulation

The evidence that I have presented here also indicates that Eph/ephrin signalling, or at least EphA4, contributes to regulation of cell identity in the hindbrain. This effect could be exerted by EphA4-mediated clustering of cells into sufficiently sized groups to mediate identity regulation via community effects as previously described. Alternatively, or in addition, Eph/ephrin signalling may maintain discrete domains of identity within rhombomeres through repression of non cell-autonomous gene induction.

In several experiments I have shown that EphA4-mediated clustering of cells is important for maintaining their identity. Firstly, wildtype cells within r3* of Egr2

morphant hosts form clusters and repress induction of *hoxb1a*, via proposed community effects and local modulation of RA. However, EphA4 morphant cells no longer cluster and are unable to suppress expression of *hoxb1a*. Secondly, in Cyp26a1;Cyp26c1 double morphants, when EphA4 is initially knocked down, fewer cells maintain *egr2b* expression in r3 compared to when EphA4 is present. In addition, when EphA4 is knocked down in Tg[egr2b:H2B-Citrine] embryos, I observe increased numbers of cells that contain H2B-Citrine and co-express *egr2b* and *hoxb1a* at the interfaces of r3, r4 and r5, indicating that loss of EphA4 compromises the ability of cells to maintain a unique identity. It is possible that EphA4 contributes to regulation of cell identity in these cases by clustering sufficient numbers of cells for community effects to maintain identity. However, an additional explanation is that EphA4 may function at interfaces between different populations of cells to prevent non cell-autonomous gene induction across the interface.

One way in which EphA4 may reduce non cell-autonomous signalling is through Eph/ephrin-mediated reduction of gap junction communication (Mellitzer *et al*, 1999). Within the neuroepithelium, gap junctions connect the cytoplasm of adjacent cells and mediate the intercellular transfer of small molecules. These small molecules could include additional, as yet unidentified, mediators of the community effect. Gap junction communication is also reduced at boundary cells between rhombomeres, although this could also be mediated by increased Eph/ephrin signalling at these boundaries (Martinez *et al*, 1992).

It is possible that Eph/ephrin signalling at sharpened segment borders contributes to reduced cell-cell communication across borders. An alternative explanation for reduced non cell-autonomous induction across sharp borders could be that cells at borders experience a balance of community effects from the adjacent segments. I have shown that Egr2b-Myc no longer exerts a non cell-autonomous effect on adjacent territories when Egr2b-Myc-expressing cells are segregated to borders. It will be informative to see what impact knocking down EphA4 has on the ability of Egr2b-Myc to induce *egr2b* expression non cell-autonomously at later stages. However, this knockdown will prevent both the segregation of Egr2b-Myc-expressing cells to segment borders as well as any EphA4-dependent inhibition of

cell-cell communication, and it will be difficult to distinguish which of these two proposed mechanisms is responsible for EphA4 preventing non cell-autonomous induction.

Interestingly, boundary cells also show upregulation of Crabp2a and Cyp26c1, which could help prevent diffusion of RA between rhombomeres. This could enable boundary cells to help maintain rhombomeres as discrete compartments, with no ectopic gene induction occurring across them. Additional evidence that rhombomere boundaries may prevent non cell-autonomous gene expression across them comes from the observation that in chick, ablation of the r3/4 boundary by RA treatment causes expansion of EphA4 expression into r4 to a greater extent than expected from cell mixing alone (Nittenberg *et al*, 1997); it is possible that boundary loss permitted the ectopic induction of *epha4* in r4 via expansion of *egr2b* expression. In addition, non cell-autonomous induction of *Engrailed2* (*En2*) expression from *En2*-expressing neuroepithelium grafts in chick has been observed only when the donor graft did not contact rhombomere boundaries (Martínez *et al*, 1995), which is also consistent with the idea that rhombomere boundaries may function as barriers of non cell-autonomous gene induction. Since regulation of gap junction communication is a possible mechanism by which this could be achieved at rhombomere borders, in future experiments, it would be interesting to study whether chemical inhibitors of gap junctions have an impact on hindbrain patterning and non cell-autonomous gene induction.

Chapter 8. Appendix

8.1 Expression of *gfp* in pGFP5.3

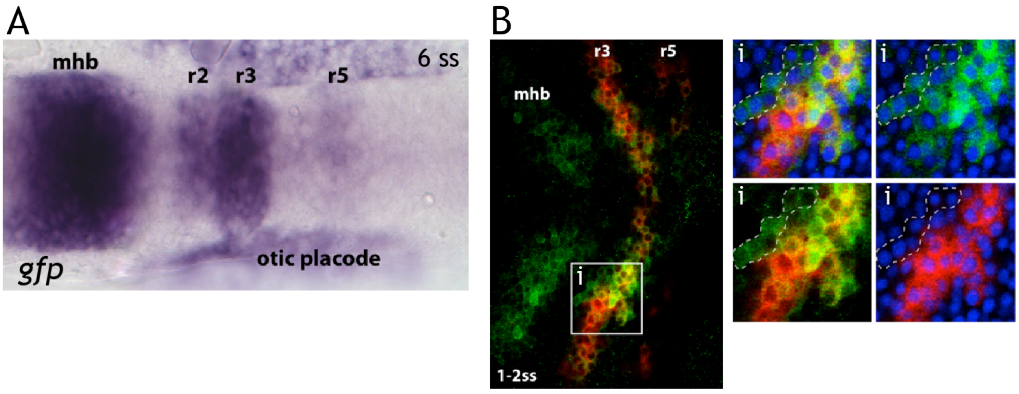

Figure 8-1 Expression of gfp in pGFP5.3

ISH for *gfp* expression (A) and double ISH for *gfp* (green) and *egr2b* (red) in pGFP5.3. At 1-2ss, *gfp* expression is broader than that of *egr2b* in r3 (B). At 6 ss, gfp is expressed in r2 and only weakly expressed in r5 (A). mhb, midbrain-hindbrain boundary.

8.2 mBait-cFos-H2B-Citrine Donor plasmid

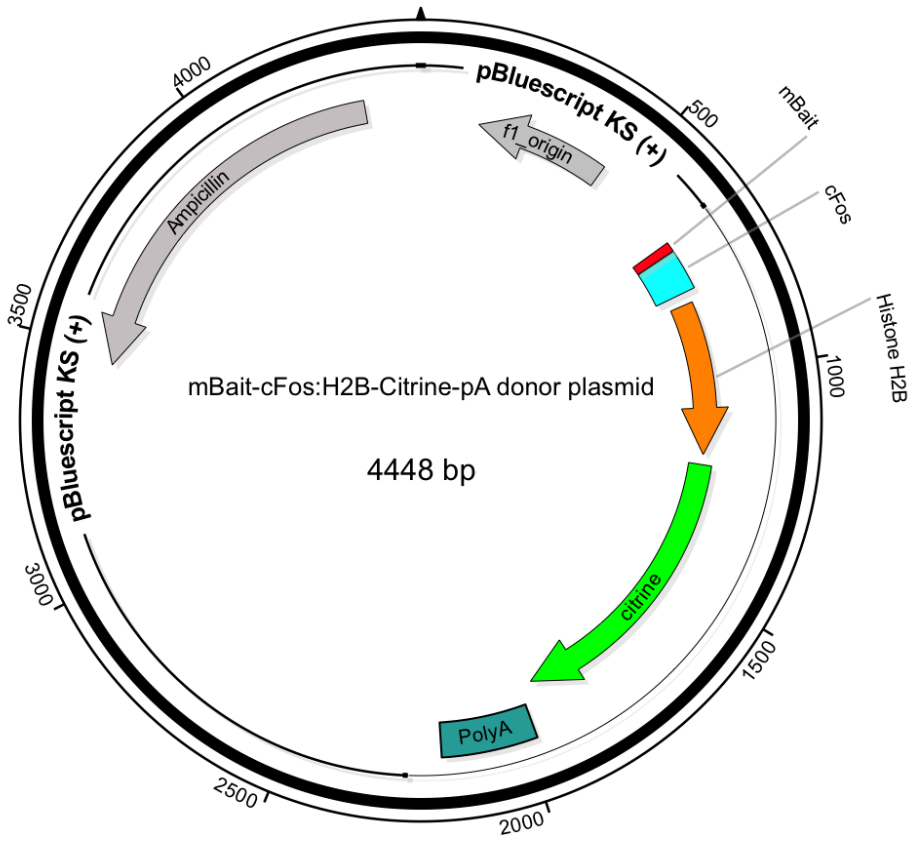

Figure 8-2 Map of mBait-cFos:H2B-Citrine-pA donor plasmid for CRISPR-mediated genome insertion

Reference List

Addison M & Wilkinson DG (2016) Segment Identity and Cell Segregation in the Vertebrate Hindbrain. *Essays Dev. Biol. Part A***:** 581–596

Aliee M, Röper J-C, Landsberg KP, Pentzold C, Widmann TJ, Jülicher F & Dahmann C (2012) Physical mechanisms shaping the Drosophila dorsoventral compartment boundary. *Curr. Biol.* **22:** 967–76

Aragón F, Vázquez-Echeverría C, Ulloa E, Reber M, Cereghini S, Alsina B, Giraldez F & Pujades C (2005) vHnf1 regulates specification of caudal rhombomere identity in the chick hindbrain. *Dev. Dyn.* **234:** 567–576

Auer TO, Duroure K, De Cian A, Concordet J-P & Del Bene F (2014a) Highly efficient CRISPR/Cas9-mediated knock-in in zebrafish by homology-independent DNA repair. *Genome Res.* **24:** 142–53

Auer TO, Duroure K, Concordet J-P & Del Bene F (2014b) CRISPR/Cas9-mediated conversion of eGFP- into Gal4-transgenic lines in zebrafish. *Nat. Protoc.* **9:** 2823–2840

Balciunas D, Wangensteen KJ, Wilber A, Bell J, Geurts A, Sivasubbu S, Wang X, Hackett PB, Largaespada D a, McIvor RS & Ekker SC (2006) Harnessing a high cargo-capacity transposon for genetic applications in vertebrates. *PLoS Genet.* **2:** 1715–1724

Bardine N, Lamers G, Wacker S, Donow C, Knoechel W & Durston A (2014) Vertical Signalling Involves Transmission of Hox Information from Gastrula Mesoderm to Neurectoderm. *PLoS One* **9:** e115208

Barrow JR, Stadler HS & Capecchi MR (2000) Roles of Hoxa1 and Hoxa2 in patterning the early hindbrain of the mouse. *Development* **127:** 933–44

Bedell VM, Wang Y, Campbell JM, Poshusta TL, Starker CG, Krug Ii RG, Tan W, Penheiter SG, Ma AC, Leung AYH, Fahrenkrug SC, Carlson DF, Voytas DF, Clark KJ, Essner JJ & Ekker SC (2012) In vivo genome editing using a high-efficiency TALEN system. *Nature*

Begemann G, Marx M, Mebus K, Meyer A & Bastmeyer M (2004) Beyond the neckless phenotype: Influence of reduced retinoic acid signaling on motor neuron development in the zebrafish hindbrain. *Dev. Biol.* **271:** 119–129

Begemann G, Schilling TF, Rauch GJ, Geisler R & Ingham PW (2001) The zebrafish neckless mutation reveals a requirement for raldh2 in mesodermal signals that pattern the hindbrain. *Development* **128:** 3081–3094

Beil J, Fairbairn L, Pelczar P & Buch T (2012) Is BAC transgenesis obsolete? State of the art in the era of designer nucleases. *J. Biomed. Biotechnol.* **2012:** 1–6

Bell E, Wingate R & Lumsden A (1999) Homeotic Transformation of Rhombomere Identity After Localized Hoxb1 Misexpression. *Science (80-.).* **284:** 2168–2171

Bielmeier C, Alt S, Weichselberger V, La Fortezza M, Harz H, Jülicher F, Salbreux G & Classen AK (2016) Interface Contractility between Differently Fated Cells Drives Cell Elimination and Cyst Formation. *Curr. Biol.* **26:** 563–574

Birgbauer E, Sechrist J, Bronner-Fraser M & Fraser S (1995) Rhombomeric origin and rostrocaudal reassortment of neural crest cells revealed by intravital microscopy. *Development* **121:** 935–45

Boch J, Scholze H, Schornack S, Landgraf A, Hahn S, Kay S, Lahaye T, Nickstadt A & Bonas U (2009) Breaking the code of DNA binding specificity of TAL-type III effectors. *Science* **326:** 1509–12

Bogdanove AJ & Voytas DF (2011) TAL Effectors: Customizable Proteins for DNA Targeting. *Science (80-.).* **333:** 1843–1846

Bolouri H & Davidson EH (2010) The gene regulatory network basis of the 'community effect,' and analysis of a sea urchin embryo example. *Dev. Biol.* **340:** 170–178

Bouchoucha YX, Reingruber J, Labalette C, Wassef M a, Thierion E, Desmarquet-Trin Dinh C, Holcman D, Gilardi-Hebenstreit P & Charnay P (2013) Dissection of a Krox20 positive feedback loop driving cell fate choices in hindbrain patterning. *Mol. Syst. Biol.* **9:** 690

Brennand K, Huangfu D & Melton D (2007) All beta cells contribute equally to islet growth and maintenance. *PLoS Biol.* **5:** e163

Cade L, Reyon D, Hwang WY, Tsai SQ, Patel S, Khayter C, Joung JK, Sander

JD, Peterson RT & Yeh J-RJ (2012) Highly efficient generation of heritable zebrafish gene mutations using homo- and heterodimeric TALENs. *Nucleic Acids Res.* **40:** 8001–10

Cai AQ, Radtke K, Linville A, Lander AD, Nie Q & Schilling TF (2012) Cellular retinoic acid-binding proteins are essential for hindbrain patterning and signal robustness in zebrafish. *Development* **139:** 2150–5

Calzolari S, Terriente J & Pujades C (2014) Cell segregation in the vertebrate hindbrain relies on actomyosin cables located at the interhombomeric boundaries. *EMBO J.* **33:** 686–701

Capecchi MR (2005) Gene targeting in mice: functional analysis of the mammalian genome for the twenty-first century. *Nat. Rev. Genet.* **6:** 507–512

Cavodeassi F, Ivanovitch K & Wilson SW (2013) Eph/Ephrin signalling maintains eye field segregation from adjacent neural plate territories during forebrain morphogenesis. *Development* **140:** 4193–202

Cayuso J, Xu Q & Wilkinson DG (2015) Mechanisms of boundary formation by Eph receptor and ephrin signaling. *Dev. Biol.* **401:** 122–131

Cermak T, Doyle EL, Christian M, Wang L, Zhang Y, Schmidt C, Baller J a, Somia N V, Bogdanove AJ & Voytas DF (2011) Efficient design and assembly of custom TALEN and other TAL effector-based constructs for DNA targeting. *Nucleic Acids Res.* **39:** e82

Chan J, Mably JD, Serluca FC, Chen JN, Goldstein NB, Thomas MC, Cleary J a, Brennan C, Fishman MC & Roberts TM (2001) Morphogenesis of prechordal plate and notochord requires intact Eph/ephrin B signaling. *Dev. Biol.* **234:** 470–82

Chen J & Ruley HE (1998) An enhancer element in the EphA2 (Eck) gene sufficient for rhombomere- specific expression is activated by HOXA1 and HOXB1 homeobox proteins. *J. Biol. Chem.* **273:** 24670–24675

Cheng YC, Amoyel M, Qiu X, Jiang YJ, Xu Q & Wilkinson DG (2004) Notch activation regulates the segregation and differentiation of rhombomere boundary cells in the zebrafish hindbrain. *Dev. Cell* **6:** 539–550

Choi HMT, Beck VA & Pierce NA (2014) Terms of Use Next-Generation in Situ

Hybridization Chain Reaction : Higher Gain , Lower Cost , Greater Durability. *ACS Nano***:** 4284–4294

Choi HMT, Chang JY, Trinh L a, Padilla JE, Fraser SE & Pierce N a (2010) Programmable in situ amplification for multiplexed imaging of mRNA expression. *Nat. Biotechnol.* **28:** 1208–12

Chomette D, Frain M, Cereghini S, Charnay P & Ghislain J (2006) Krox20 hindbrain cis-regulatory landscape: interplay between multiple long-range initiation and autoregulatory elements. *Development* **133:** 1253–62

Clay H & Ramakrishnan L (2005) Multiplex fluorescent in situ hybridisation in zebrafish embryos using tyramide signal amplification. *Zebrafish* **2:** 105–111

Cong L, Ran FA, Cox D, Lin S, Barretto R, Hsu PD, Wu X, Jiang W & Marraffini LA (2013) Multiplex Genome Engineering Using CRISPR/VCas Systems. *Science (80-.).* **339:** 819–823

Constable SCJ (2015) Investigating the role of Plzf in neural progenitors.

Cooke J, Moens C, Roth L, Durbin L, Shiomi K, Brennan C, Kimmel C, Wilson S & Holder N (2001) Eph signalling functions downstream of Val to regulate cell sorting and boundary formation in the caudal hindbrain. *Development* **128:** 571–80

Cooke JE, Kemp HA & Moens CB (2005) EphA4 is required for cell adhesion and rhombomere-boundary formation in the zebrafish. *Curr. Biol.* **15:** 536–42

Cooke JE & Moens CB (2002) Boundary formation in the hindbrain: Eph only it were simple... *Trends Neurosci.* **25:** 260–7

Cristea S, Freyvert Y, Santiago Y, Holmes MC, Urnov FD, Gregory PD & Cost GJ (2013) In vivo cleavage of transgene donors promotes nuclease-mediated targeted integration. *Biotechnol. Bioeng.* **110:** 871–80

D'Aniello E, Rydeen AB, Anderson JL, Mandal A & Waxman JS (2013) Depletion of retinoic acid receptors initiates a novel positive feedback mechanism that promotes teratogenic increases in retinoic acid. *PLoS Genet.* **9:** e1003689

Dahlem TJ, Hoshijima K, Jurynec MJ, Gunther D, Starker CG, Locke AS, Weis

AM, Voytas DF & Grunwald DJ (2012) Simple methods for generating and detecting locus-specific mutations induced with TALENs in the zebrafish genome. *PLoS Genet.* **8:** e1002861

Davenne M, Maconochie MK, Neun R, Pattyn A, Chambon P, Krumlauf R & Rijli FM (1999) Hoxa2 and Hoxb2 control dorsoventral patterns of neuronal development in the rostral hindbrain. *Neuron* **22:** 677–691

Davis S, Gale NW, Aldrich TH, Maisonpierre PC, Lhotak V, Pawson T, Goldfarb M & Yancopoulos GD (1994) Ligands for EPH-related receptor tyrosine kinases that require membrane attachment or clustering for activity. *Science* **266:** 816–819

Depaepe V, Suarez-Gonzalez N, Dufour A, Passante L, Gorski JA, Jones KR, Ledent C & Vanderhaeghen P (2005) Ephrin signalling controls brain size by regulating apoptosis of neural progenitors. *Nature* **435:** 1244–50

Dessaud E, Ribes V, Balaskas N, Yang LL, Pierani A, Kicheva A, Novitch BG, Briscoe J & Sasai N (2010) Dynamic assignment and maintenance of positional identity in the ventral neural tube by the morphogen sonic hedgehog. *PLoS Biol.* **8:**

Dessaud E, Yang LL, Hill K, Cox B, Ulloa F, Ribeiro A, Mynett A, Novitch BG & Briscoe J (2007) Interpretation of the sonic hedgehog morphogen gradient by a temporal adaptation mechanism. *Nature* **450:** 717–720

Distel M, Wullimann MF & Köster RW (2009) Optimized Gal4 genetics for permanent gene expression mapping in zebrafish. *Proc. Natl. Acad. Sci. U. S. A.* **106:** 13365–70

Dorsky RI, Sheldahl LC & Moon RT (2002) A transgenic Lef1/beta-catenin-dependent reporter is expressed in spatially restricted domains throughout zebrafish development. *Dev. Biol.* **241:** 229–37

Duester G (2007) Retinoic acid regulation of the somitogenesis clock. *Birth Defects Res. Part C - Embryo Today Rev.* **81:** 84–92

Dupé V & Lumsden A (2001) Hindbrain patterning involves graded responses to retinoic acid signalling. *Development* **128:** 2199–2208

Durai S, Mani M, Kandavelou K, Wu J, Porteus MH & Chandrasegaran S (2005) Zinc finger nucleases: Custom-designed molecular scissors for

genome engineering of plant and mammalian cells. *Nucleic Acids Res.* **33:** 5978–5990

Eisen JS & Smith JC (2008) Controlling morpholino experiments: don't stop making antisense. *Development* **135:** 1735–43

Elowitz MB, Levine AJ, Siggia ED & Swain PS (2002) Stochastic gene expression in a single cell. *Science (80-.).* **297:** 1183–1186

Emoto Y, Wada H, Okamoto H, Kudo A & Imai Y (2005) Retinoic acid-metabolizing enzyme Cyp26a1 is essential for determining territories of hindbrain and spinal cord in zebrafish. *Dev. Biol.* **278:** 415–27

Engler C, Gruetzner R, Kandzia R & Marillonnet S (2009) Golden gate shuffling: a one-pot DNA shuffling method based on type IIs restriction enzymes. *PLoS One* **4:** e5553

Fagotto F, Rohani N, Touret AS & Li R (2013) A Molecular Base for Cell Sorting at Embryonic Boundaries: Contact Inhibition of Cadherin Adhesion by Ephrin/Eph-Dependent Contractility. *Dev. Cell* **27:** 72–87

Fagotto F, Winklbauer R & Rohani N (2014) Ephrin-Eph signaling in embryonic tissue separation. *Cell Adhes. Migr.* **8:** 308–326

Fisher S, Grice E a, Vinton RM, Bessling SL, Urasaki A, Kawakami K & McCallion AS (2006) Evaluating the biological relevance of putative enhancers using Tol2 transposon-mediated transgenesis in zebrafish. *Nat. Protoc.* **1:** 1297–1305

Fraser S, Keynes R & Lumsden A (1990) Segmentation in the chick embryo hindbrain is defined by cell lineage restrictions. *Nature* **344:** 431–435

Gale E, Prince V, Lumsden A & Clarke J (1996a) Late effects of retinoic acid on neural crest and aspects of rhombomere. *Development* **793:** 783–793

Gale E, Zile M & Maden M (1999) Hindbrain respecification in the retinoid-deficient quail. *Mech. Dev.* **89:** 43–54

Gale NW, Holland SJ, Valenzuela DM, Flenniken A, Pan L, Ryan TE, Henkemeyer M, Strebhardt K, Hirai H, Wilkinson DG, Pawson T, Davis S, Yancopoulos GD, Pharmaceuticals R, Saw O, River M & York N (1996b) Eph receptors and ligands comprise two major specificity subclasses and are reciprocally compartmentalized during embryogenesis. *Neuron* **17:** 9–

19

Gavalas A, Davenne M, Lumsden A, Chambon P & Rijli FM (1997) Role of Hoxa-2 in axon pathfinding and rostral hindbrain patterning. *Development* **124:** 3693–3702

Gavalas A, Ruhrberg C, Livet J, Henderson CE & Krumlauf R (2003) Neuronal defects in the hindbrain of Hoxa1, Hoxb1 and Hoxb2 mutants reflect regulatory interactions among these Hox genes. *Development* **130:** 5663–5679

Geldmacher-Voss B, Reugels AM, Pauls S & Campos-Ortega J a (2003) A 90-degree rotation of the mitotic spindle changes the orientation of mitoses of zebrafish neuroepithelial cells. *Development* **130:** 3767–80

Genové G, Glick B & Barth A (2005) Brighter reporter genes from multimerized fluorescent proteins. *Biotechniques* **39:** 814–822

Gerety SS & Wilkinson DG (2011) Morpholino artifacts provide pitfalls and reveal a novel role for pro-apoptotic genes in hindbrain boundary development. *Dev. Biol.* **350:** 279–89

Giudicelli F, Taillebourg E, Charnay P & Gilardi-Hebenstreit P (2001) Krox-20 patterns the hindbrain through both cell-autonomous and non cell-autonomous mechanisms. *Genes Dev.* **15:** 567–80

Gonzalez-Quevedo R, Lee Y & Wilkinson DG (2011) Neuronal regulation of the spatial patterning of neurogenesis. *Dev Cell.* **18:** 1–23

Gould A, Itasaki N & Krumlauf R (1998) Initiation of rhombomeric Hoxb4 expression requires induction by somites and a retinoid pathway. *Neuron* **21:** 39–51

Grapin-Botton A, Bonnin MA, McNaughton LA, Krumlauf R & Le Douarin NM (1995) Plasticity of transposed rhombomeres: Hox gene induction is correlated with phenotypic modifications. *Development* **121:** 2707–21

Griesbeck O, Baird GS, Campbell RE, Zacharias DA & Tsien RY (2001) Reducing the environmental sensitivity of yellow fluorescent protein. Mechanism and applications. *J. Biol. Chem.* **276:** 29188–29194

Gu X, Xu F, Wang X, Gao X & Zhao Q (2005) Molecular cloning and expression of a novel CYP26 gene (cyp26d1) during zebrafish early development.

Gene Expr. Patterns **5:** 733–9

Gurdon JB (1988) A community effect in animal development. *Nature* **336:** 772–774

Gurdon JB, Lemaire P & Kato K (1993) Community effects and related phenomena in development. *Cell* **75:** 831–834

Guthrie S & Lumsden A (1991) Formation and regeneration of rhombomere boundaries in the developing chick hindbrain. *Development* **112:** 221–9

Hattori M, Osterfield M & Flanagan JG (2000) Regulated cleavage of a contact-mediated axon repellent. *Science (80-.).* **289:** 1360–1365

Heikal AA, Hess ST, Baird GS, Tsien RY & Webb WW (2000) Molecular spectroscopy and dynamics of intrinsically fluorescent proteins: Coral red (dsRed) and yellow (Citrine). *Proc. Natl. Acad. Sci. USA* **97:** 11996–12001

Hernandez RE, Putzke AP, Myers JP, Margaretha L & Moens CB (2007) Cyp26 enzymes generate the retinoic acid response pattern necessary for hindbrain development. *Development* **134:** 177–87

Hernandez RE, Rikhof H a, Bachmann R & Moens CB (2004) vhnf1 integrates global RA patterning and local FGF signals to direct posterior hindbrain development in zebrafish. *Development* **131:** 4511–20

Herrera SC & Morata G (2014) Transgressions of compartment boundaries and cell reprogramming during regeneration in *Drosophila*. *Elife* **3:** 1–15

Heyman I, Faissner a & Lumsden a (1995) Cell and matrix specialisations of rhombomere boundaries. *Dev. Dyn.* **204:** 301–15

Heyman I, Kent a & Lumsden a (1993) Cellular morphology and extracellular space at rhombomere boundaries in the chick embryo hindbrain. *Dev. Dyn.* **198:** 241–53

Higashijima SI (2008) Transgenic zebrafish expressing fluorescent proteins in central nervous system neurons. *Dev. Growth Differ.* **50:** 407–413

Holcman D, Kasatkin V & Prochiantz a (2007) Modeling homeoprotein intercellular transfer unveils a parsimonious mechanism for gradient and boundary formation in early brain development. *J. Theor. Biol.* **249:** 503–17

Hunt P, Whiting J, Muchamore I, Marshall H & Krumlauf R (1991) Homeobox genes and models for patterning the hindbrain and branchial arches. *Dev.*

Suppl. **1:** 187–96

Hunter MP & Prince VE (2002) Zebrafish hox paralogue group 2 genes function redundantly as selector genes to pattern the second pharyngeal arch. *Dev. Biol.* **247:** 367–389

Hwang WY, Fu Y, Reyon D, Maeder ML, Tsai SQ, Sander JD, Peterson RT, Yeh J-RJ & Joung JK (2013) Efficient genome editing in zebrafish using a CRISPR-Cas system. *Nat. Biotechnol.* **31:** 227–9

Irion U, Krauss J & Nusslein-Volhard C (2014) Precise and efficient genome editing in zebrafish using the CRISPR/Cas9 system. *Development* **141:** 4827–4830

Irvine KD & Rauskolb C (2001) Boundaries in Development: Formation and Function. *Annu. Rev. Cell Dev. Biol.* **17:** 189–214

Irving C, Nieto MA, DasGupta R, Charnay P & Wilkinson DG (1996) Progressive spatial restriction of Sek-1 and Krox-20 gene expression during hindbrain segmentation. *Dev. Biol.* **173:** 26–38

Itasaki N, Sharpe J, Morrison a & Krumlauf R (1996) Reprogramming Hox expression in the vertebrate hindbrain: influence of paraxial mesoderm and rhombomere transposition. *Neuron* **16:** 487–500

Jimenez-Guri E, Udina F, Colas J-F, Sharpe J, Padrón-Barthe L, Torres M & Pujades C (2010) Clonal analysis in mice underlines the importance of rhombomeric boundaries in cell movement restriction during hindbrain segmentation. *PLoS One* **5:** e10112

Jinek M, Chylinski K, Fonfara I, Hauer M, Doudna JA & Charpentier E (2012) A Programmable Dual-RNA – Guided DNA Endonuclease in Adaptive Bacterial Immunity. *Science (80-.).* **337:** 816–822

Joliot A & Prochiantz A (2004) Transduction peptides: from technology to physiology. *Nat. Cell Biol.* **6:** 189–96

Joliot A, Trembleau A, Raposo G, Calvet S, Volovitch M & Prochiantz A (1997) Association of Engrailed homeoproteins with vesicles presenting caveolae-like properties. **1875:** 1865–1875

Kaern M, Elston TC, Blake WJ & Collins JJ (2005) Stochasticity in gene expression: from theories to phenotypes. *Nat. Rev. Genet.* **6:** 451–464

Kawakami K (2007) Tol2: a versatile gene transfer vector in vertebrates. *Genome Biol.* **8:** S7

Kelly GM, Greenstein P, Erezyilmaz DF & Moon RT (1995) Zebrafish Wnt8 and Wnt8B share a common activity but are involved in distinct developmental pathways. *Development* **121:** 1787–1799

Kemp HA, Cooke JE & Moens CB (2009) EphA4 and EfnB2a maintain rhombomere coherence by independently regulating intercalation of progenitor cells in the zebrafish neural keel. *Dev Biol* **327:** 313–326

Kepler TB & Elston TC (2001) Stochasticity in Transcriptional Regulation: Origins, Consequences, and Mathematical Representations. *Biophys. J.* **81:** 3116–3136

Kiecker C & Lumsden A (2005) Compartments and their boundaries in vertebrate brain development. *Nat. Rev. Neurosci.* **6:** 553–64

Kimelman D & Martin BL (2012) Anterior-posterior patterning in early development: Three strategies. *Wiley Interdiscip. Rev. Dev. Biol.* **1:** 253–266

Kimmel CB, Ballard WW, Kimmel SR, Ullmann B & Schilling TF (1995) Stages of embryonic development of the zebrafish. *Dev. Dyn.* **203:** 253–310

Kimmel CB, Warga RM & Kane DA (1994) Cell cycles and clonal strings during formation of the zebrafish central nervous system. *Dev. {(Cambridge,} England)* **120:** 265–276

Kimura Y, Hisano Y, Kawahara A & Higashijima S (2014) Efficient generation of knock-in transgenic zebrafish carrying reporter/driver genes by CRISPR/Cas9-mediated genome engineering. *Sci. Rep.* **4:** 6545

Köntges G & Lumsden A (1996) Rhombencephalic neural crest segmentation is preserved throughout craniofacial ontogeny. *Development* **122:** 3229–42

Kozak M (1987) An analysis of 5'-noncoding sequences from 699 vertebrate messenger rNAS. *Nucleic Acids Res.* **15:** 8125–8148

Kudoh T, Wilson SW & Dawid IB (2002) Distinct roles for Fgf, Wnt and retinoic acid in posteriorizing the neural ectoderm. *Development* **129:** 4335–46

Kwan KM, Fujimoto E, Grabher C, Mangum BD, Hardy ME, Campbell DS, Parant JM, Yost HJ, Kanki JP & Chien C-B (2007) The Tol2kit: a multisite

gateway-based construction kit for Tol2 transposon transgenesis constructs. *Dev. Dyn.* **236:** 3088–99

Labalette C, Bouchoucha YX, Wassef MA, Gongal PA, Le Men J, Becker T, Gilardi-Hebenstreit P & Charnay P (2011) Hindbrain patterning requires fine-tuning of early krox20 transcription by Sprouty 4. *Development* **138:** 317–26

Labalette C, Wassef MA, Desmarquet-Trin Dinh C, Bouchoucha YX, Le Men J, Charnay P & Gilardi-Hebenstreit P (2015) Molecular dissection of segment formation in the developing hindbrain. *Development* **142:** 185–95

Lampron C, Rochette-Egly C, Gorry P, Dolle P, Mark M, Lufkin T, LeMeur M, Chambon P, Dollé P, Mark M, Lufkin T, LeMeur M & Chambon P (1995) Mice deficient in cellular retinoic acid binding protein II (CRABPII) or in both CRABPI and CRABPII are essentially normal. *Development* **121:** 539–548

Landsberg KP, Farhadifar R, Ranft J, Umetsu D, Widmann TJ, Bittig T, Said A, Jülicher F & Dahmann C (2009) Increased cell bond tension governs cell sorting at the Drosophila anteroposterior compartment boundary. *Curr. Biol.* **19:** 1950–5

Langheinrich U, Hennen E, Stott G & Vacun G (2002) Zebrafish as a model organism for the identification and characterization of drugs and genes affecting p53 signaling. *Curr. Biol.* **12:** 2023–8

Lauter G, Söll I & Hauptmann G (2011) Two-color fluorescent in situ hybridization in the embryonic zebrafish brain using differential detection systems. *BMC Dev. Biol.* **11:** 43

Lee K & Skromne I (2014) Retinoic acid regulates size, pattern and alignment of tissues at the head-trunk transition. *Development* **141:** 4375–4384

Linville A, Gumusaneli E, Chandraratna RAS & Schilling TF (2004) Independent roles for retinoic acid in segmentation and neuronal differentiation in the zebrafish hindbrain. *Dev. Biol.* **270:** 186–199

Lumsden A & Keynes R (1989) Segmental patterns of neuronal development in the chick hindbrain. *Nature* **337:** 424–428

Lumsden A, Sprawson N & Graham A (1991) Segmental origin and migration of neural crest cells in the hindbrain region of the chick embryo. *Development*

113: 1281–91

Major RJ & Irvine KD (2005) Influence of Notch on dorsoventral compartmentalization and actin organization in the Drosophila wing. *Development* **132:** 3823–3833

Major RJ & Irvine KD (2006) Localization and requirement for myosin II at the dorsal-ventral compartment boundary of the Drosophila wing. *Dev. Dyn.* **235:** 3051–3058

Makki N & Capecchi MR (2011) Identification of novel Hoxa1 downstream targets regulating hindbrain, neural crest and inner ear development. *Dev. Biol.* **357:** 295–304

Mali P, Yang L, Esvelt KM, Aach J, Guell M, DiCarlo JE, Norville JE & Church GM (2013) RNA-guided human genome engineering via Cas9. *Science* **339:** 823–6

Manzanares M, Trainor PA, Nonchev S, Ariza-McNaughton L, Brodie J, Gould A, Marshall H, Morrison A, Kwan CT, Sham MH, Wilkinson DG & Krumlauf R (1999) The role of kreisler in segmentation during hindbrain development. *Dev. Biol.* **211:** 220–237

Maresca M, Lin VG, Guo N & Yang Y (2013) Obligate Ligation-Gated Recombination (ObLiGaRe): Custom-designed nuclease-mediated targeted integration through nonhomologous end joining. **:** 539–546

Marshall H, Studer M, Pöpperl H, Aparicio S, Kuroiwa a, Brenner S & Krumlauf R (1994) A conserved retinoic acid response element required for early expression of the homeobox gene Hoxb-1. *Nature* **370:** 567–571

Marston DJ, Dickinson S & Nobes CD (2003) Rac-dependent trans-endocytosis of ephrinBs regulates Eph-ephrin contact repulsion. *Nat. Cell Biol.* **5:** 879–888

Martinez S, Geijo E, Sanchez-Vives M, Puelles L & Gallego R (1992) Reduced junctional permeability at interrhombomeric boundaries. *Development***:** 1069–1076

Martínez S, Marín F, Nieto MA & Puelles L (1995) Induction of ectopic engrailed expression and fate change in avian rhombomeres: intersegmental boundaries as barriers. *Mech. Dev.* **51:** 289–303

Martinez-Arias A & Lawrence PA (1985) Parasegments and compartments in the Drosophila embryo. *Nature* **313:** 639–642

Maves L, Jackman W & Kimmel CB (2002) FGF3 and FGF8 mediate a rhombomere 4 signaling activity in the zebrafish hindbrain. *Development* **129:** 3825–37

Maves L & Kimmel CB (2005) Dynamic and sequential patterning of the zebrafish posterior hindbrain by retinoic acid. *Dev. Biol.* **285:** 593–605

McCallum CM, Comai L, Greene EA & Henikoff S (2000) Targeting induced local lesions IN genomes (TILLING) for plant functional genomics. *Plant Physiol.* **123:** 439–442

McClintock JM, Carlson R, Mann DM & Prince VE (2001) Consequences of Hox gene duplication in the vertebrates: an investigation of the zebrafish Hox paralogue group 1 genes. *Development* **128:** 2471–84

McClintock JM, Kheirbek MA & Prince VE (2002) Knockdown of duplicated zebrafish hoxb1 genes reveals distinct roles in hindbrain patterning and a novel mechanism of duplicate gene retention. *Development* **129:** 2339–54

Megason SG (2009) In toto imaging of embryogenesis with confocal time-lapse microscopy. *Methods Mol. Biol.* **546:** 317–332

Mellitzer G, Xu Q & Wilkinson DG (1999) Eph receptors and ephrins restrict cell intermingling and communication. *Nature* **400:** 77–81

Miller JC, Tan S, Qiao G, Barlow KA, Wang J, Xia DF, Meng X, Paschon DE, Leung E, Hinkley SJ, Dulay GP, Hua KL, Ankoudinova I, Cost GJ, Urnov FD, Zhang HS, Holmes MC, Zhang L, Gregory PD & Rebar EJ (2011) A TALE nuclease architecture for efficient genome editing. *Nat. Biotechnol.* **29:** 143–8

Moens CB & Prince VE (2002) Constructing the hindbrain: insights from the zebrafish. *Dev. Dyn.* **224:** 1–17

Moens CB, Yan YL, Appel B, Force a G & Kimmel CB (1996) Valentino: a Zebrafish Gene Required for Normal Hindbrain Segmentation. *Development* **122:** 3981–3990

Monier B, Pélissier-Monier A, Brand AH & Sanson B (2010) An actomyosin-based barrier inhibits cell mixing at compartmental boundaries in

Drosophila embryos. *Nat. Cell Biol.* **12:** 60-65–9

Monk KR, Naylor SG, Glenn TD, Mercurio S, Perlin JR, Dominguez C, Moens CB & Talbot WS (2009) A G protein-coupled receptor is essential for Schwann cells to initiate myelination. *Science* **325:** 1402–5

Montague TG, Cruz JM, Gagnon JA, Church GM & Valen E (2014) CHOPCHOP: A CRISPR/Cas9 and TALEN web tool for genome editing. *Nucleic Acids Res.* **42:** 401–407

Moore S, Ribes V, Terriente J, Wilkinson D, Relaix F & Briscoe J (2013) Distinct Regulatory Mechanisms Act to Establish and Maintain Pax3 Expression in the Developing Neural Tube. *PLoS Genet.* **9:** e1003811

Morata G & Herrera SC (2016) Cell reprogramming during regeneration in Drosophila: Transgression of compartment boundaries. *Curr. Opin. Genet. Dev.* **40:** 11–16

Moscou MJ & Bogdanove AJ (2009) A simple cipher governs DNA recognition by TAL effectors. *Science* **326:** 1501

Nagai T, Ibata K, Park ES, Kubota M, Mikoshiba K & Miyawaki A (2002) A variant of yellow fluorescent protein with fast and efficient maturation for cell-biological applications. *Nat. Biotechnol.* **20:** 87–90

Neill AKO, Kindberg AA, Niethamer TK, Larson AR, Yi H, Ho H, Greenberg ME & Bush JO (2016) Unidirectional Eph / ephrin signaling creates a cortical actomyosin differential to drive cell segregation. **:** 217–229

Niederreither K, Vermot J, Schuhbaur B, Chambon P & Dollé P (2000) Retinoic acid synthesis and hindbrain patterning in the mouse embryo. *Development* **127:** 75–85

Ninov N, Borius M & Stainier DYR (2012) Different levels of Notch signaling regulate quiescence, renewal and differentiation in pancreatic endocrine progenitors. *Development* **139:** 1557–67

Nittenberg R, Patel K, Joshi Y, Krumlauf R, Wilkinson DG, Brickell PM, Tickle C & Clarke JD (1997) Cell movements, neuronal organisation and gene expression in hindbrains lacking morphological boundaries. *Development* **124:** 2297–306

Nolte C, Amores A, Nagy Kovács E, Postlethwait J & Featherstone M (2003)

The role of a retinoic acid response element in establishing the anterior neural expression border of Hoxd4 transgenes. *Mech. Dev.* **120:** 325–335

Nonchev S, Maconochie M, Vesque C, Aparicio S, Ariza-McNaughton L, Manzanares M, Maruthainar K, Kuroiwa a, Brenner S, Charnay P & Krumlauf R (1996a) The conserved role of Krox-20 in directing Hox gene expression during vertebrate hindbrain segmentation. *Proc. Natl. Acad. Sci. U. S. A.* **93:** 9339–45

Nonchev S, Vesque C, Maconochie M, Seitanidou T, Ariza-McNaughton L, Frain M, Marshall H, Sham MH, Krumlauf R & Charnay P (1996b) Segmental expression of Hoxa-2 in the hindbrain is directly regulated by Krox-20. *Development* **122:** 543–554

Ota S, Taimatsu K, Yanagi K, Namiki T, Ohga R, Higashijima S-I & Kawahara A (2016) Functional visualization and disruption of targeted genes using CRISPR/Cas9-mediated eGFP reporter integration in zebrafish. *Sci. Rep.* **6:** 34991

Oury F, Murakami Y, Renaud J, Pasqualetti M, Charnay P, Ren S & Rijli FM (2006) Somatosensory Map. *Science (80-.).*: 1408–1413

Oxtoby E & Jowett T (1993) Cloning of the zebrafish krox-20 gene (krx-20) and its expression during hindbrain development. *Nucleic Acids Res.* **21:** 1087–95

Packer AI, Crotty DA, Elwell VA & Wolgemuth DJ (1998) Expression of the murine Hoxa4 gene requires both autoregulation and a conserved retinoic acid response element. *Development* **125:** 1991–8

Papan C & Campos-Ortega J (1994) On the formation of the neural keel and neural tube in the zebrafish Danio (Brachydanio) rerio. *Roux's Arch. Dev. Biol.* **203:** 178–186

Parant JM, George SA, Pryor R, Wittwer CT & Yost HJ (2009) A rapid and efficient method of genotyping zebrafish mutants. *Dev. Dyn.* **238:** 3168–3174

Parker HJ, Piccinelli P, Sauka-Spengler T, Bronner M & Elgar G (2011) Ancient Pbx-Hox signatures define hundreds of vertebrate developmental enhancers. *BMC Genomics* **12:** 637

Parslow A, Cardona A & Bryson-Richardson RJ (2014) Sample drift correction following 4D confocal time-lapse imaging. *J. Vis. Exp.***:** e51086

Pasquale EB (2008) Eph-Ephrin Bidirectional Signaling in Physiology and Disease. *Cell* **133:** 38–52

Perz-Edwards a, Hardison NL & Linney E (2001) Retinoic acid-mediated gene expression in transgenic reporter zebrafish. *Dev. Biol.* **229:** 89–101

Pevny L & Placzek M (2005) SOX genes and neural progenitor identity. *Curr. Opin. Neurobiol.* **15:** 7–13

Picker A, Scholpp S, Böhli H, Takeda H & Brand M (2002) A novel positive transcriptional feedback loop in midbrain-hindbrain boundary development is revealed through analysis of the zebrafish pax2.1 promoter in transgenic lines. *Development* **129:** 3227–39

Poliakov A, Cotrina M & Wilkinson DG (2004) Diverse roles of eph receptors and ephrins in the regulation of cell migration and tissue assembly. *Dev. Cell* **7:** 465–80

Pöpperl H, Bienz M, Studer M, Chan SK, Aparicio S, Brenner S, Mann RS & Krumlauf R (1995) Segmental expression of Hoxb-1 is controlled by a highly conserved autoregulatory loop dependent upon exd/pbx. *Cell* **81:** 1031–1042

Pouilhe M, Gilardi-Hebenstreit P, Desmarquet-Trin Dinh C & Charnay P (2007) Direct regulation of vHnf1 by retinoic acid signaling and MAF-related factors in the neural tube. *Dev. Biol.* **309:** 344–357

Pourquié O (2003) Vertebrate somitogenesis: A novel paradigm for animal segmentation? *Int. J. Dev. Biol.* **47:** 597–603

Prin F, Serpente P, Itasaki N & Gould AP (2014) Hox proteins drive cell segregation and non-autonomous apical remodelling during hindbrain segmentation. *Development* **20:** 1492–1502

Prince VE, Moens CB, Kimmel CB & Ho RK (1998) Zebrafish hox genes: expression in the hindbrain region of wild-type and mutants of the segmentation gene, valentino. *Development* **125:** 393–406

Prochiantz A & Joliot A (2003) Can transcription factors function as cell-cell signalling molecules? *Nat. Rev. Mol. Cell Biol.* **4:** 814–9

Prochiantz A & Di Nardo AA (2015) Homeoprotein signaling in the developing and adult nervous system. *Neuron* **85:** 911–925

Rampon C, Gauron C, Lin T, Meda F, Dupont E, Cosson A, Ipendey E, Frerot A, Aujard I, Le Saux T, Bensimon D, Jullien L, Volovitch M, Vriz S & Joliot A (2015) Control of brain patterning by Engrailed paracrine transfer: a new function of the Pbx interaction domain. *Development* **142:** 1840–9

Reed GH, Kent JO & Wittwer CT (2007) High-resolution DNA melting analysis for simple and efficient molecular diagnostics. *Pharmacogenomics* **8:** 597–608

Riley BB, Chiang MY, Storch EM, Heck R, Buckles GR & Lekven AC (2004) Rhombomere boundaries are Wnt signaling centers that regulate metameric patterning in the zebrafish hindbrain. *Dev. Dyn.* **231:** 278–291

Robu ME, Larson JD, Nasevicius A, Beiraghi S, Brenner C, Farber S a & Ekker SC (2007) P53 Activation By Knockdown Technologies. *PLoS Genet.* **3:** e78

Rohrschneider MR, Elsen GE & Prince VE (2007) Zebrafish Hoxb1a regulates multiple downstream genes including prickle1b. *Dev. Biol.* **309:** 358–72

Romand R, Sapin V, Ghyselinck NB, Avan P, Le Calvez S, Dollé P, Chambon P & Mark M (2000) Spatio-temporal distribution of cellular retinoid binding protein gene transcripts in the developing and the adult cochlea. Morphological and functional consequences in CRABP- and CRBPI-null mutant mice. *Eur. J. Neurosci.* **12:** 2793–2804

Römer P, Hahn S, Jordan T, Strauss T, Bonas U & Lahaye T (2007) Plant pathogen recognition mediated by promoter activation of the pepper Bs3 resistance gene. *Science* **318:** 645–648

Rossant J, Zirngibl R & Cado D (1991) Expression of a retinoic acid response element-hsplacZ transgene defines specific domains of transcriptional activity during mouse embryogenesis. *Genes Dev.***:** 1333–1345

Rouet P, Smih F & Jasin M (1994) Introduction of double-strand breaks into the genome of mouse cells by expression of a rare-cutting endonuclease. *Mol. Cell. Biol.* **14:** 8096–106

Runko AP & Sagerström CG (2003) Nlz belongs to a family of zinc-finger-

containing repressors and controls segmental gene expression in the zebrafish hindbrain. *Dev. Biol.* **262:** 254–267

Rydeen A, Voisin N, D'Aniello E, Ravisankar P, Devignes C-S & Waxman JS (2015) Excessive feedback of Cyp26a1 promotes cell non-autonomous loss of retinoic acid signaling. *Dev. Biol.***:** 1–9

Saka Y, Lhoussaine C, Kuttler C, Ullner E & Thiel M (2011) Theoretical basis of the community effect in development. *BMC Syst. Biol.* **5:** 54

Sander JD, Maeder ML, Reyon D, Voytas DF, Joung JK & Dobbs D (2010) ZiFiT (Zinc Finger Targeter): An updated zinc finger engineering tool. *Nucleic Acids Res.* **38:** 462–468

Sander JD, Zaback P, Joung JK, Voytas DF & Dobbs D (2007) Zinc Finger Targeter (ZiFiT): An engineered zinc finger/target site design tool. *Nucleic Acids Res.* **35:** 599–605

Schilling TF, Nie Q & Lander AD (2012) Dynamics and precision in retinoic acid morphogen gradients. *Curr. Opin. Genet. Dev.* **22:** 1–8

Schilling TF, Prince V & Ingham PW (2001) Plasticity in zebrafish hox expression in the hindbrain and cranial neural crest. *Dev. Biol.* **231:** 201–16

Schilling TF, Sosnik J & Nie Q (2016) Visualizing retinoic acid morphogen gradients Elsevier Ltd

Schneider-Maunoury S, Seitanidou T, Charnay P & Lumsden A (1997) Segmental and neuronal architecture of the hindbrain of Krox-20 mouse mutants. *Development* **124:** 1215–26

Schneider-Maunoury S, Topilko P, Seitandou T, Levi G, Cohen-Tannoudji M, Pournin S, Babinet C, Charnay P, Seitanidou T, Giovanni L, Cohen-Tannoudji M, Pournin S, Babinet C & Charnay P (1993) Disruption of Krox-20 results in alteration of rhombomeres 3 and 5 in the developing hindbrain. *Cell* **75:** 1199–1214

Schulte-Merker S, Hammerschmidt M, Beuchle D, Cho KW, De Robertis EM & Nüsslein-Volhard C (1994) Expression of zebrafish goosecoid and no tail gene products in wild-type and mutant no tail embryos. *Development* **120:** 843–852

Schulte-Merker S & Stainier DYR (2014) Out with the old, in with the new:

reassessing morpholino knockdowns in light of genome editing technology. *Development* **141:** 3103–3104

Scott EK & Baier H (2009) The cellular architecture of the larval zebrafish tectum, as revealed by gal4 enhancer trap lines. *Front. Neural Circuits* **3:** 1–14

Seitanidou T, Schneider-Maunoury S, Desmarquet C, Wilkinson DG & Charnay P (1997) Krox-20 is a key regulator of rhombomere-specific gene expression in the developing hindbrain. *Mech. Dev.* **65:** 31–42

Sham MH, Vesque C, Nonchev S, Marshall H, Whiting J, Wilkinson D, Chamay P, Krumlauf R, Ridgeway T & Hill M (1993) The Zinc Finger Gene Krox20 in. *Cell* **72:** 183–196

Shimozono S, Iimura T, Kitaguchi T, Higashijima S-I & Miyawaki A (2013) Visualization of an endogenous retinoic acid gradient across embryonic development. *Nature* **496:** 363–6

Shin J, Chen J & Solnica-Krezel L (2014) Efficient homologous recombination-mediated genome engineering in zebrafish using TALE nucleases. *Development* **141:** 3807–18

Shizuya H, Birren B, Kim UJ, Mancino V, Slepak T, Tachiiri Y & Simon M (1992) Cloning and stable maintenance of 300-kilobase-pair fragments of human DNA in Escherichia coli using an F-factor-based vector. *Proc. Natl. Acad. Sci. U. S. A.* **89:** 8794–7

Sirbu IO, Gresh L, Barra J & Duester G (2005) Shifting boundaries of retinoic acid activity control hindbrain segmental gene expression. *Development* **132:** 2611–22

Sood R, English MA, Jones M, Mullikin J, Wang DM, Anderson M, Wu D, Chandrasekharappa SC, Yu J, Zhang J & Paul Liu P (2006) Methods for reverse genetic screening in zebrafish by resequencing and TILLING. *Methods* **39:** 220–227

Sosnik J, Zheng L, Rackauckas C V., Digman M, Gratton E, Nie Q & Schilling TF (2016) Noise modulation in retinoic acid signaling sharpens segmental boundaries of gene expression in the embryonic zebrafish hindbrain. *Elife* **5:** 1–14

Stedman A, Lecaudey V, Havis E, Anselme I, Wassef M, Gilardi-Hebenstreit P & Schneider-Maunoury S (2009) A functional interaction between Irx and Meis patterns the anterior hindbrain and activates krox20 expression in rhombomere 3. *Dev. Biol.* **327:** 566–77

Stoppie P, Borgers M, Borghgraef P, Dillen L, Goossens JAN, Sanz G, Szel H, Hove CVAN, Nyen GVAN, Nobels G, Bossche H Vanden, Venet M, Willemsens G & Wauwe JVAN (2000) R115866 Inhibits All- trans -Retinoic Acid Metabolism and Exerts Retinoidal Effects in Rodents. **293:** 304–312

Strate I, Min TH, Iliev D & Pera EM (2009) Retinol dehydrogenase 10 is a feedback regulator of retinoic acid signalling during axis formation and patterning of the central nervous system. *Development* **136:** 461–472

Streit A, Berliner AJ, Papanayotou C, Sirulnik A & Stern CD (2000) Initiation of neural induction by FGF signalling before gastrulation. *Nature* **406:** 74–78

Streubel J, Blücher C, Landgraf A & Boch J (2012) TAL effector RVD specificities and efficiencies. *Nat. Biotechnol.* **30:** 593–5

Stringari C, Cinquin A, Cinquin O, Digman MA, Donovan PJ & Gratton E (2011) Phasor approach to fluorescence lifetime microscopy distinguishes different metabolic states of germ cells in a live tissue. *Nat Acad Sci Proc* **108:** 13582–13587

Studer M, Gavalas A, Marshall H, Ariza-McNaughton L, Rijli FM, Chambon P & Krumlauf R (1998) Genetic interactions between Hoxa1 and Hoxb1 reveal new roles in regulation of early hindbrain patterning. *Development* **125:** 1025–1036

Studer M, Lumsden A, Ariza-McNaughton L, Bradley A & Krumlauf R (1996) Altered segmental identity and abnormal migration of motor neurons in mice lacking Hoxb-1. *Nature* **384:** 630–634

Stüttem I & Campos-Ortega J a (1991) Cell commitment and cell interactions in the ectoderm of Drosophila melanogaster. *Development* **Suppl 2:** 39–46

Sun Z, Shi K, Su Y & Meng A (2002) A novel zinc finger transcription factor resembles krox-20 in structure and in expression pattern in zebrafish. *Mech. Dev.* **114:** 133–5

Suster ML, Sumiyama K & Kawakami K (2009) Transposon-mediated BAC

transgenesis in zebrafish and mice. *BMC Genomics* **10:** 477

Swiatek PJ & Gridley T (1993) Perinatal lethality and defects in hindbrain development in mice homozygous for a targeted mutation of the zinc finger gene Krox20. *Genes Dev.* **7:** 2071–2084

Szymczak AL, Workman CJ, Wang Y, Vignali KM, Dilioglou S, Vanin EF & Vignali D a a (2004) Correction of multi-gene deficiency in vivo using a single 'self-cleaving' 2A peptide-based retroviral vector. *Nat. Biotechnol.* **22:** 589–94

Taneja R, Thisse B, Rijli FM, Thisse C, Bouillet P, Dollé P & Chambon P (1996) The expression pattern of the mouse receptor tyrosine kinase gene MDK1 is conserved through evolution and requires Hoxa-2 for rhombomere-specific expression in mouse embryos. *Dev. Biol.* **177:** 397–412

Terriente J, Gerety SS, Watanabe-Asaka T, Gonzalez-Quevedo R & Wilkinson DG (2012) Signalling from hindbrain boundaries regulates neuronal clustering that patterns neurogenesis. *Development* **139:** 2978–87

Theil T, Frain M, Gilardi-Hebenstreit P, Flenniken a, Charnay P & Wilkinson DG (1998) Segmental expression of the EphA4 (Sek-1) receptor tyrosine kinase in the hindbrain is under direct transcriptional control of Krox-20. *Development* **125:** 443–52

Trainor P a & Krumlauf R (2000a) Patterning the cranial neural crest: hindbrain segmentation and Hox gene plasticity. *Nat. Rev. Neurosci.* **1:** 116–24

Trainor P & Krumlauf R (2000b) Plasticity in mouse neural crest cells reveals a new patterning role for cranial mesoderm. *Nat. Cell Biol.* **2:** 96–102

Tümpel S, Cambronero F, Ferretti E, Blasi F, Wiedemann LM & Krumlauf R (2007) Expression of Hoxa2 in rhombomere 4 is regulated by a conserved cross-regulatory mechanism dependent upon Hoxb1. *Dev. Biol.* **302:** 646–660

Tümpel S, Wiedemann LM & Krumlauf R (2009) Hox genes and segmentation of the vertebrate hindbrain. *Curr. Top. Dev. Biol.* **88:** 103–37

Turing AM (1952) The Chemical Basis of Morphogenesis. *Philos. Trans. R. Soc. Lond. B. Biol. Sci.* **237:** 37–72

Vesque C, Maconochie M, Nonchev S, Ariza-McNaughton L, Kuroiwa a,

Charnay P & Krumlauf R (1996) Hoxb-2 transcriptional activation in rhombomeres 3 and 5 requires an evolutionarily conserved cis-acting element in addition to the Krox-20 binding site. *EMBO J.* **15:** 5383–5396

Vitobello A, Ferretti E, Lampe X, Vilain N, Ducret S, Ori M, Spetz J-F, Selleri L & Rijli FM (2011) Hox and Pbx Factors Control Retinoic Acid Synthesis during Hindbrain Segmentation. *Dev Cell.* **20:** 469–482

Voiculescu O, Taillebourg E, Pujades C, Kress C, Buart S, Charnay P & Schneider-Maunoury S (2001) Hindbrain patterning: Krox20 couples segmentation and specification of regional identity. *Development* **128:** 4967–78

Waskiewicz AJ, Rikhof HA & Moens CB (2002) Eliminating zebrafish Pbx proteins reveals a hindbrain ground state. *Dev. Cell* **3:** 723–733

Wassef M a, Chomette D, Pouilhe M, Stedman A, Havis E, Desmarquet-Trin Dinh C, Schneider-Maunoury S, Gilardi-Hebenstreit P, Charnay P & Ghislain J (2008) Rostral hindbrain patterning involves the direct activation of a Krox20 transcriptional enhancer by Hox/Pbx and Meis factors. *Development* **135:** 3369–78

Westerfield M (1993) The zebrafish book 4th ed. Oregon: University of Oregon Press

White RJ, Nie Q, Lander AD & Schilling TF (2007) Complex regulation of cyp26a1 creates a robust retinoic acid gradient in the zebrafish embryo. *PLoS Biol.* **5:** e304

White RJ & Schilling TF (2008) How degrading: Cyp26s in hindbrain development. *Dev. Dyn.* **237:** 2775–90

Wiellette EL & Sive H (2003) vhnf1 and Fgf signals synergize to specify rhombomere identity in the zebrafish hindbrain. *Development* **130:** 3821–3829

Wienholds E, van Eeden F, Kosters M, Mudde J, Plasterk RHA & Cuppen E (2003) Efficient target-selected mutagenesis in zebrafish. *Genome Res.* **13:** 2700–2707

Wilkinson DG, Bhatt S, Chavrier P, Bravo R & Charnay P (1989a) Segment-specific expression of a zinc-finger gene in the developing nervous system

of the mouse. *Nature* **337:** 461–4

Wilkinson DG, Bhatt S, Cook M, Boncinelli E & Krumlauf R (1989b) Segmental expression of Hox-2 homoeobox-containing genes in the developing mouse hindbrain. *Nature* **341:** 405–409

Wilson SI, Rydström A, Trimborn T, Willert K, Nusse R, Jessell TM & Edlund T (2001) The status of Wnt signalling regulates neural and epidermal fates in the chick embryo. *Nature* **411:** 325–330

Wolpert L (1969) Positional information and the spatial pattern of cellular differentiation. *J. Theor. Biol.* **25:** 1–47

Xu Q, Alldus G, Holder N & Wilkinson DG (1995) Expression of truncated Sek-1 receptor tyrosine kinase disrupts the segmental restriction of gene expression in the Xenopus and zebrafish hindbrain. *Development* **121:** 4005–16

Xu Q, Holder N, Patient R & Wilson SW (1994) Spatially regulated expression of three receptor tyrosine kinase genes during gastrulation in the zebrafish. *Development* **120:** 287–99

Xu Q, Mellitzer G, Robinson V & Wilkinson DG (1999) In vivo cell sorting in complementary segmental domains mediated by Eph receptors and ephrins cells . We report here that mosaic activation of Eph receptors leads. *Nature* **399:** 267–271

Yang Z, Jiang H, Chachainasakul T, Gong S, Yang XW, Heintz N & Lin S (2006) Modified bacterial artificial chromosomes for zebrafish transgenesis. *Methods* **39:** 183–188

Zhang F, Nagy Kovács E & Featherstone MS (2000) Murine Hoxd4 expression in the CNS requires multiple elements including a retinoic acid response element. *Mech. Dev.* **96:** 79–89

Zhang L, Radtke K, Zheng L, Cai AQ, Schilling TF & Nie Q (2012) Noise drives sharpening of gene expression boundaries in the zebrafish hindbrain. *Mol. Syst. Biol.* **8:** 613

Zhang M, Kim HJ, Marshall H, Gendron-Maguire M, Lucas D a, Baron a, Gudas LJ, Gridley T, Krumlauf R & Grippo JF (1994) Ectopic Hoxa-1 induces rhombomere transformation in mouse hindbrain. *Development*

120: 2431–2442

Zhao Q, Dobbs-McAuliffe B & Linney E (2005) Expression of cyp26b1 during zebrafish early development. *Gene Expr. Patterns* **5:** 363–9

Zigman M, Laumann-Lipp N, Titus T, Postlethwait J & Moens CB (2014) Hoxb1b controls oriented cell division, cell shape and microtubule dynamics in neural tube morphogenesis. *Development* **141:** 639–49

Zimmer M (2003) Mechanisms of Eph/ephrin mediated cell-cell communication.

Zu Y, Tong X, Wang Z, Liu D, Pan R, Li Z, Hu Y, Luo Z, Huang P, Wu Q, Zhu Z, Zhang B & Lin S (2013) TALEN-mediated precise genome modification by homologous recombination in zebrafish. **:** 1–4